Universitat Jaume I

Departamento de Química Física y Analítica

Instituto Universitario de Plaguicidas y Aguas

EVALUACIÓN DE NUEVAS HERRAMIENTAS ANALÍTICAS PARA MEJORAR LA CAPACIDAD DE DETECCIÓN EN EL CONTROL DEL DOPAJE

Tesis Doctoral

MONTSERRAT RARO MACIÁN

2016

La Dra. **Elena Pitarch Arquimbau**, Profesora Titular de Química Analítica de la Universitat Jaume I de Castellón, el Dr. **Óscar J. Pozo Mendoza**, Investigador del grupo de bioanálisis de la Fundación IMIM y Dr. **Juan Vicente Sancho Llopis**, Catedrático de Química Analítica de la Universitat Jaume I de Castellón,

CERTIFICAN QUE: la **Tesis Doctoral** "Evaluación de nuevas herramientas analíticas para mejorar la capacidad de detección en el control del dopaje" ha sido desarrollada bajo su dirección, en el área de Química Analítica del Departamento de Química Física y Analítica de la Universitat Jaume I de Castellón, por **Montserrat Raro Macián.**

Lo que certificamos para los efectos oportunos en Castellón de la plana, a 5 de febrero de 2016.

Fdo. Dra. Elena Pitarch Arquimbau **Fdo. Dr. Óscar J. Pozo Mendoza**

Fdo. Dr. Juan Vicente Sancho Llopis

Este trabajo responde al compromiso adquirido con el Ministerio de Economía y Competitividad del Gobierno de España, por la concesión de una ayuda para la formación de personal investigador (FPI-MICINN) desde el 1 de noviembre de 2010 (BES-2010-035846).

Montserrat Raro Macián ha sido beneficiaria de dos ayudas concedidas por el Ministerio de Economía y Competitividad del Gobierno de España, para realizar estancias en centros extranjeros (Subprograma FPI-MICINN).

La primera fue llevada a cabo en el *Centre for Research into Atmospheric Chemistry (CRAC)*, en Cork, Irlanda, desde el 9 de enero hasta el 9 de abril de 2012. El trabajo realizado llevaba por título: "Estudios de formación de aerosoles orgánicos secundarios (SOA) de la degradación atmosférica de compuestos orgánicos seleccionados". La segunda estancia de investigación, dentro del programa de la presente Tesis, fue en el *Doping Control Laboratory* (DoCoLab) de la *Universiteit Gent* en Bélgica, desde el 23 de septiembre hasta el 17 de diciembre de 2013. El trabajo realizado: "Estrategias metabolómicas para la detección de marcadores que faciliten el cribado del abuso a esteroides endógenos", fue llevado a cabo bajo la supervisión del Prof. Dr. Peter Van Eenoo.

Los trabajos realizados en la presente memoria han sido en parte financiados por los proyectos del Ministerio de Economía y Ciencia (DEP2011-28573-C02-01/02), de la Generalitat Valenciana (PROMETEO/2009/054; ISIC 2012/016) y de la Generalitat de Catalunya (Consell Català d'Esport y DIUE 2009SGR4929).

Esta Tesis ha sido realizada y será defendida de acuerdo con los requisitos exigidos para la obtención del título de Doctorado Internacional.

Previamente a la defensa de la Tesis Doctoral, este trabajo ha sido evaluado por dos censores extranjeros independientes directamente relacionados con el área de investigación, Dr. Alexander L. N. van Nuijs (*Researcher of Toxicological Center, University of Antwerp, Belgium)* and Dr. Koen Deventer (*Researcher of Doping Control Laboratory, Ghent University, Belgium*).

"Lo importante en los Juegos Olímpicos no es ganar, sino participar.
Igual que en la vida, el objetivo no es conquistar, sino luchar bien".

Barón Pierre de Coubertin,

Inauguración Juegos Olímpicos de Berlín, 1936

A Vicente Raro y Alberto Macián,

AGRADECIMIENTOS

No es fácil resumir lo que me ha aportado esta etapa de crecimiento personal y profesional. Me siento afortunada ya que, de principio a fin, he estado muy bien acompañada. Por ello ha llegado el momento de dar gracias.

Para empezar, quiero dar las gracias a mis directores. A Elena, gracias por ser mi directora desde antes de llegar al IUPA, por darme la oportunidad de venir y empezar de nuevo, por sus consejos y preocupación. A Juanvi, por tener siempre abierta la puerta de su despacho. Gracias por enseñarme tantas cosas y por ese buen humor constante. Gracias a Óscar por su supervisión en la distancia, vía email, llamada, whatsapp... Gracias por enseñarme lo que sé acerca del mundo del dopaje y por animarme siempre a esforzarme por hacerlo mejor. A los tres muchas gracias, he tenido mucha suerte. También me gustaría dar las gracias a Félix, por transmitirnos siempre buenos consejos desde su experiencia, por su interés y su ayuda.

Gracias a **todos** los compañeros que he conocido en el IUPA, porque con todos he pasado muy buenos momentos. A los que me han acompañado los 4 años, a los que se fueron en algún momento (pero nunca del todo), a los que vinieron de visita y a las recientes incorporaciones. Ha sido un placer conoceros a todos y cada uno.

Agradezco a Ramon por mi primer año en el IUPA, por introducirme en el mundo de la metabolómica y la LC, transmitirme su entusiasmo por la investigación y seguir preocupándose por mí en la distancia.

A Tania, mi guía GC, siempre dispuesta a ayudarme en cualquier crisis, he aprendido y disfrutado mucho trabajando contigo. Gracias!

A María, profesora, tutora de prácticas, compañera de congresos etc., por su ayuda siempre que he necesitado algo.

A Mercedes por ser siempre un encanto y por preocuparse por mí.

A Leticia, por su entusiasmo y ganas de aprender y ayudar.

A Rubén. Llevamos casi el mismo tiempo en el IUPA y me ha ayudado tanto que un gracias me parece poco. Así que, gracias, gracias, mil gracias...

A Inés y Laura, a las que he echado mucho de menos en la etapa final, por el año en el que compartimos "despatxet". Gracias por hacer que mire a Dani Martín con otros ojos...

A Edu (*IUPA community manager*), por su ayuda desde el principio pero, sobre todo, en la etapa final donde hemos estado más cerca.

Gracias de forma especial a Clara, compañera de carrera, de tesis, de bodas.... Has sido un apoyo muy importante.

A los compañeros del IMIM, por hacer que me sintiera como en casa en cada visita a Barcelona. Gracias Andreu, Josep, Lorena, Rosa, Jordi, Giorgina, Argi...

Thanks to Peter Van Eenoo for allowing me to stay in his group, to Koen for supervising my work and also thanks to Eva, for teaching me about the work in the lab and about the life in Belgium. Thanks to all the colleagues of DoCoLab, because my stay in Ghent was really a very nice experience.

Gracias a mis compañeras/os de la licenciatura, por hacer lo posible por mantener el contacto. Gracias por tantos y tan buenos momentos. También a mis compañeros del máster, por ese año del que guardo tan buen recuerdo y a Jordi por seguir estando ahí.

Gracias a mis amigos por acompañarme en este camino, por venir a visitarme donde fuera, por aguantar mis historias sin fin y porque, sin ellos, la vida sería más triste y aburrida. En especial a mis chicas, a las que quiero muchísimo, con sus defectos y virtudes, porque así me quieren ellas.

Gracias a mi abuela Pilar, ejemplo de fortaleza. A mis tíos por estar siempre presentes, como segundos padres y madres, hermanos mayores y amigos. A mis primos pequeños de los que me siento tan orgullosa y a mis primas mayores, primas hermanas en el sentido literal de la palabra. A Cristina, porque estando con ella me olvido de los problemas, disfrutando como si también tuviera dos años. También gracias a mi familia política, por su preocupación y por ser un ejemplo de trabajo en equipo y de trabajo duro.

Gracias a mi hermana y mis padres por su apoyo incondicional. A mi hermana por estar siempre a mi lado, su ayuda me da la seguridad que tanta falta hace en momentos como este. A mi madre, por ser el pilar de la familia y enseñarme la importancia de trabajar (también por esos *tuppers* sin los que muchos días no hubiera tenido las fuerzas necesarias...). A mi padre, por consentirme, protegerme y enseñarme que con sentido del humor, todo es más fácil. Es un alivio saber que estáis conmigo tanto si tengo éxito como si no.

Termino dando las gracias a Nacho por haber estado conmigo a cada paso, triste cuando yo estaba triste, feliz cuando yo estaba feliz. Gracias por quererme tantísimo. Parte del mérito de esta Tesis es también tuyo.

Montse

Resumen

La competición deportiva es uno de los ámbitos donde más notorio se muestra el afán del ser humano de superar a sus rivales. En el esfuerzo de conseguir ventaja frente al resto de participantes podemos encontrar técnicas de entrenamiento, nutrición, motivación personal… aunque también son frecuentes otros procedimientos ilegales, como la ingesta de sustancias que ayuden a mejorar el rendimiento mental o físico de un deportista, dando lugar a lo que se conoce como *Dopaje*. La lucha contra estas prácticas se ha convertido en una preocupación permanente, por lo que se realizan controles, por parte de organismos deportivos, desde hace décadas, con el fin de garantizar la legalidad y la buena salud de los deportistas.

La Agencia Mundial Antidopaje (AMA) fue creada en 1999 con el objetivo de cooperar por un deporte libre de dopaje. Surge de la necesidad de tener un órgano independiente ya que, anteriormente, las federaciones que se encargaban de la organización de los deportistas eran las mismas responsables de los controles de dopaje, lo que llevaba a conflictos de intereses. La AMA publica, desde el 2004, una lista de sustancias prohibidas, dentro y fuera de competición, entre los que se encuentran: esteroides anabolizantes androgénicos, hormonas, beta-2-agonistas, diuréticos, estimulantes, narcóticos, cannabinoides, glucocorticosteroides, beta-bloqueantes etc. Los laboratorios para el control del dopaje deben desarrollar metodologías analíticas para detectar estas sustancias a las concentraciones requeridas.

En la presente Tesis Doctoral se han evaluado nuevas herramientas analíticas; instrumentales, metodológicas y de tratamiento de datos, para mejorar la detección del consumo de sustancias dopantes en el deporte. Se trata, con todo esto, de reducir los límites de cuantificación, aumentar el tiempo de detección posible o del descubrimiento de nuevos metabolitos o marcadores del abuso de una sustancia en concreto.

El control del dopaje, la cromatografía, la espectrometría de masas, las aproximaciones non-target para detección de compuestos desconocidos y las nuevas técnicas metabolómicas, resumen los hilos conductores a lo largo de esta tesis.

El trabajo realizado se divide en dos partes diferenciadas:

En la **primera parte**, se trabajó en la puesta a punto de metodología analítica para la determinación de esteroides anabolizantes androgénicos (AAS) y metabolitos seleccionados mediante Cromatografía de Gases - Espectrometría de Masas en tándem con analizador híbrido Cuadrupolo-Tiempo de Vuelo (CG-QTOF MS/MS) y la nueva fuente de ionización a presión atmosférica (APCI). Se llevó a cabo un estudio de ionización y se compararon los resultados con los obtenidos mediante los métodos de rutina que emplean analizador de Cuadrupolo sencillo (Q) trabajando en modo Selected Ion Monitoring (SIM) con fuente de ionización electrónica (EI). Este estudio evidencia los beneficios de emplear la nueva interfase a presión atmosférica para cromatografía de gases, la cual promueve una ionización con baja fragmentación, que permite conservar $[M+H]^+$, $[M+H\text{-}xTMSOH]^+$ o $M^{+\cdot}$, en la mayoría de casos, como pico base del espectro; con las ventajas que esto supone a la hora de elegir transiciones más específicas en experiencias de MS/MS. Posteriormente, se llevó a cabo un estudio de fragmentación de los iones obtenidos mediante esta interfase para los AAS seleccionados, con el fin de establecer relaciones entre los iones presentes en los espectros MS/MS y la estructura de los esteroides. El hecho de que el pico base obtenido mediante la interfase APCI, fuera $[M+H]^+$ o $M^{+\cdot}$, permitió, a continuación, la selección de iones más específicos como iones precursores en métodos target. Con esto, se desarrolló y validó cualitativamente un método Selected Reaction Monitoring (SRM) para la detección de esteroides anabolizantes androgénicos en orina mediante (CG-(APCI)-QqQ MS/MS).

La **segunda parte** de la tesis ha consistido en la aplicación de técnicas metabolómicas y análisis multivariante a estudios de excreción para la búsqueda de marcadores del abuso de sustancias dopantes, analizando las muestras en equipos de Cromatografía de Líquidos (LC) acoplado a analizadores de alta resolución (HR). El primer estudio fue desarrollado para la búsqueda de marcadores del abuso de la *hormona del crecimiento* (rhGH). Las muestras fueron inyectadas tanto en una columna de fase inversa (RP) como en una de interacción hidrofílica (HILIC), resultando para cada caso un marcador destacable del abuso de esta sustancia. Por otra parte, se aplicaron las mismas técnicas metabolómicas para un estudio de excreción de *testosterona*. En este caso, las muestras fueron inyectadas en un instrumento UHPLC-QTOF MS, así como en un UHPLC-QOrbitrap, resultando el mismo marcador del abuso en ambos casos.

Summary

Competitive sport is one of the areas where humans show their ambition to lead their opponents. In the effort to surpass their rivals, some techniques can be carried out, such as training, nutrition, personal motivation… although another illegal procedures are also frequent, like the ingestion of substances that can help athletes to improve their mental or physical conditions. That practice is well known as *Doping*. The fight against these procedures has become an issue that concerns everyone so; different controls have been carried out by sports organizations for decades, to ensure legality and the good health of athletes.

The World Anti Doping Agency (WADA) was created in 1999 with the objective of guarantee a doping-free sport. It was the result of the necessity to have an independent anti-doping organ, because before WADA was introduced, the federations which organized the athletes were also responsible for the doping controls and created some conflicts of interest. WADA publishes, since 2004, a list of banned substances, in and out of competition, where we can find, among others: anabolic androgenic steroids, hormones, beta-2-agonists, diuretics, stimulants, narcotics, cannabinoids, glucocorticosteroids, beta-blockers etc. Doping control laboratories have to develop analytical methodologies to detect all these substances at the required concentration levels.

In the present Doctoral Thesis, new analytical tools have been evaluated; instrumental, methodological and referent to data treatment, in order to improve the detection of the misuse of doping products. This is, trying to reduce the detection limits, to increase the time of detection or to discover new metabolites or markers of misuse for a specific substance.

Doping control, chromatography, mass spectrometry, non-target approaches for the detection of unknown compounds and metabolomic techniques define the common topics along this Thesis.

The work has been clearly divided into two parts:

In the **first part**, the work was focused in the study of anabolic androgenic steroids (AAS) and selected metabolites by means of Gas Chromatography coupled to Mass Spectrometry with hybrid Quadrupole-Time of flight analyzer (GC-QTOF MS/MS) and the new ionization source at atmospheric pressure (APCI). An ionization study was performed and results

were compared with the ones obtained by routine methods working with a single quadrupole analyzer (Q) in Selected Ion Monitoring (SIM) mode and electron ionization source (EI). This study has demonstrated the benefits of the new interface at atmospheric pressure for gas chromatography that promotes ionization with very low fragmentation. In most cases $[M+H]^+$, $[M+H-xTMSOH]^+$ o $M^{+\cdot}$ are present as the base peak of the spectrum, which implies an advantage for the selection of more specific precursor ions for MS/MS experiences. Afterwards, a fragmentation study was carried out using this new interface for the selected AAS in order to establish relationships between the ions present in the MS/MS spectra and the structure of the steroids. Thanks to the low fragmentation achieved in the APCI source, more specific precursor ions could be selected for target methods. A Selected Reaction Monitoring (SRM) method was developed and qualitatively validated for the detection of selected AAS in urine by (GC-(APCI)-QqQ MS/MS).

The **second part** of the Thesis has consisted in the application of metabolomic techniques and multivariate analysis to excretion studies for the search of markers of the misuse of doping substances, analyzing the samples by Liquid Chromatography (LC) coupled to High Resolution (HR) mass analyzers. The first study was developed for the search of markers of *recombinant human growth hormone* (rhGH). Samples were injected with a reverse phase (RP) column as well as with and hydrophilic interaction (HILIC) one, resulting a different misuse marker for each case. Moreover, the same metabolomic techniques were applied to an excretion study of *Testosterone*. In this case, samples were analyzed by Liquid Chromatography coupled to QTOF MS and Q-Orbitrap MS analyzers, giving as a result the same marker of abuse in both cases.

ÍNDICE GENERAL

ÍNDICE DE ACRÓNIMOS

AAS	Anabolic Androgenic Steroids
ACN	Acetonitrile
AIF	All Ion Fragmentation
APCI	Atmospheric Pressure Chemical Ionization
BPI	Base Peak Ion chromatogram
CE	Collision Energy
CI	Chemical Ionization
DS	Dilute and Shoot
EAAS	Endogenous Anabolic Androgenic Steroids
EI	Electron Ionization
EPO	Erythropoietin
FT	Fourier Transform
FWHM	Full Width at Half Maximum
GC	Gas Chromatography
GC/C/IRMS	Gas Chromatography Combustion Isotope Ratio Mass Spectrometry
GH	Growth Hormone
CWT	Continuous Wavelet Transform
HE	High Energy
HILIC	Hydrophilic Interaction Liquid Chromatography
HPLC	High Performance Liquid Chromatography
HR	High Resolution
IGF-I	Insuline-like Growth Factor I
IOC	International Olympic Commitee
IS	Internal Standard
IRMS	Isotope Ratio Mass Spectrometry
IT	Ion Trap

LC	Liquid Chromatography
LE	Low Energy
LLE	Liquid liquid extraction
LOD	Limit of Detection
LOQ	Limit of Quantification
LRMS	Low Resolution Mass Spectrometry
LTM	Long-Term Metabolite
m/z	Mass to charge ratio
MeOH	Methanol
MRPL	Minimum Required Performance Level
MS	Mass Spectrometry
MS/MS	Tandem mass spectrometry
MSTFA	N-Methyl-N-(trimethylsilyl)trifluoroacetamide
NPLC	Normal Phase Liquid Chromatography
OPLS-DA	Orthogonal Partial Least Square-Discriminant Analysis
P-III-NP	Amino-terminal pro-peptide of type III collagen
PCA	Principal Component Analysis
PLS-DA	Partial Least Square-Discriminant Analysis
ppm	Part Per Million
ppb	Part Per Billion
PTV	Programmable Temperature Vaporization
Q	Quadrupole
QC	Quality Control
QqQ	Triple quadrupole
QTOF	Quadrupole-time of flight
Q-Orbitrap	Quadrupole-orbitrap
reGH	Recombinant Equine Growth Hormone
rhGH	Recombinant Human Growth Hormone
RIA	Radioimmunoassay

ROI	Region of Interest
RPLC	Reverse Phase Liquid Chromatography
RSD	Relative Standard Deviation
RT	Retention Time
S/N	Signal to noise
SIM	Selected Ion Monitoring
SPE	Solid Phase Extraction
SPME	Solid Phase Micro-Extraction
SRM	Selected Reaction Monitoring
SFC	Supercritical Fluid Chromatography
T	Testosterone
TBME	Tert-Butyl Methyl Ether
THG	Tetrahidrogestrinone
TMS	TriMethylSilyl
TOF	Time-of-flight
UHPLC	Ultra High Pressure Liquid Chromatography
vDIA	variable Data Independent Analysis
XIC	eXtracted Ion Chromatogram
WADA	World Anti-Doping Agency

ÍNDICE DE FIGURAS

ÍNDICE DE TABLAS

OBJETIVOS

OBJECTIVES

Objetivos

Este trabajo ha sido llevado a cabo gracias a la sinergia de dos grupos de investigación. Mientras uno de ellos ha aportado el conocimiento sobre la problemática, el *know-how* del control del dopaje, el otro ha contribuido con su conocimiento y experiencia en instrumentación analítica. De esta colaboración surgen los **objetivos generales** de la presente Tesis Doctoral, que son los siguientes:

- Evaluación de nuevas técnicas analíticas (GC(APCI)-QqQ, GC(APCI)-QTOF o UHPLC-QTOF con MS^E) que permitan avanzar en la mejora de la detección de sustancias dopantes siendo, en mayor medida, los esteroides anabolizantes androgénicos el caso de estudio.

- Estudio de herramientas útiles en el campo del control del dopaje como son, la búsqueda de nuevos metabolitos o el uso de nuevas metodologías que permitan incrementar el tiempo en el que el abuso de una determinada sustancia dopante se puede detectar.

- Evaluación del potencial de las técnicas metabolómicas, empleadas en distintos campos de aplicación y que se prevé resulten de gran utilidad en la selección de marcadores adecuados para detectar el abuso sustancias dopantes.

Siguiendo estos objetivos globales, una serie de **objetivos específicos** han guiado el trabajo que será expuesto en esta Tesis. Se resumen en los siguientes puntos:

- Estudio del comportamiento de ionización de esteroides anabolizantes androgénicos conocidos mediante cromatografía de gases con la nueva fuente de ionización a presión atmosférica (APCI) y analizador QTOF, con el fin de evaluar la idoneidad de esta nueva fuente en comparación a los métodos rutinarios (GC-EI-

MS/MS QqQ) y ser capaces de establecer relaciones entre el comportamiento de ionización y la estructura de los esteroides.

- Estudio del comportamiento de fragmentación de esteroides anabolizantes androgénicos conocidos mediante cromatografía de gases con la nueva fuente de ionización a presión atmosférica (APCI) y analizador QTOF.

- Desarrollo y validación de un método target para la detección de esteroides anabolizantes androgénicos mediante GC-APCI-MS/MS con analizador QqQ en modo SRM, teniendo en cuenta, en este punto, la importancia que presentan los esteroides endógenos.

- Evaluación de estrategias metabolómicas para la detección de nuevos marcadores de abuso de esteroides anabolizantes androgénicos y otras sustancias dopantes como la hormona del crecimiento, mediante cromatografía de líquidos, con distintas condiciones cromatográficas y diferentes analizadores de alta resolución.

Objectives

The present work has been carried out thanks to the fusion of two research groups; one of them has provided their knowledge about the doping control field and, the other, has provided its experience in the analytical instrumentation. From this collaboration, some **general objectives** are detailed for the present Doctoral Thesis:

- Evaluation of new analytical techniques (GC(APCI)-QqQ, GC(APCI)-QTOF o UHPLC-QTOF con MS^E), that permit to move forward in the detection of doping substances; being, in most cases, anabolic androgenic steroids, the case of study.

- Study of useful tools in the doping control field such as, the search of new metabolites or the use of new methodologies that allow the increase of the detection time of a specific doping substance misuse.

- Evaluation of the potential of metabolomic techniques that are expected to be very useful for the selection of adequate markers of the misuse of doping substances.

Having into account those general goals, some **specific objectives** have guided the work that will be exposed in this Thesis. They are summarized as follows:

- Study of the ionization behaviour of known anabolic androgenic steroids by means of gas chromatography with the new atmospheric pressure chemical ionization source (APCI) and QTOF analyzer, to study the suitability of this source in comparison with the routine methods (GC-EI-MS/MS QqQ) and try to establish connections between ionization behaviour and the structure of the steroids.

- Study of fragmentation behaviour of known anabolic androgenic steroids by means of gas chromatography with the new atmospheric pressure chemical ionization source (APCI) and QTOF analyzer.

- Development and validation of a target method by GC-APCI-MS/MS and QqQ analyzer in SRM mode, paying special attention to the endogenous steroids present in urine at the moment of the transitions selection.

- Evaluation of metabolomic strategies for the detection of new markers of AAS misuse or other doping substances such as Growth Hormone, by means of liquid chromatography, using different chromatographic conditions and different high resolution mass analyzers.

CAPÍTULO I

INTRODUCCIÓN GENERAL

I.1. Control del dopaje

I.1.1 Antecedentes

El uso de sustancias farmacológicamente activas para mejorar el rendimiento deportivo por parte de los atletas es tan antiguo como la propia competición deportiva. Son numerosas las anécdotas conocidas a lo largo de la historia sobre estas prácticas. Ya en el siglo III a.c., los atletas griegos que participaban en los Juegos Olímpicos en la antigüedad tomaban algunos tipos de setas alucinógenas para prepararse mentalmente para la competición. También los gladiadores romanos tomaban pociones especiales, con raíces u otros extractos de plantas con el objetivo de mejorar su rendimiento (Botrè & Pavan, 2008). Otro ejemplo es el de los guerreros escandinavos que pensaban que su fuerza en combate aumentaba ingiriendo una seta psicoactiva llamada *amanita muscaria* (Delbeke, 2000).

La primera noticia sobre dopaje en atletas es de 1865 en Ámsterdam, cuando varios nadadores fueron acusados de consumir drogas durante la competición a través de los canales de la ciudad. A medida que el ciclismo tomaba importancia, tanto en Europa como en América, se conocen algunos casos de ciclistas que consumían heroína o cocaína para incrementar su resistencia. El primer caso de un deportista que falleciera por estas prácticas data de 1886 (Todd, 1987).

Ya en el siglo XX, son numerosos los casos documentados de atletas y entrenadores que admitieron el uso de drogas, sin que estos hechos tuvieran consecuencias. El primero ocurrió en 1904 en los Juegos Olímpicos de Verano de San Luis (Misuri, Estados Unidos), donde el maratoniano Thomas Hicks se desmayó al llegar a la meta tras mezclar sulfato de estricnina con unos vasos

de coñac. Al no existir leyes que lo prohibieran, subió al escalón más alto del podio.

La elaboración de otras drogas como las anfetaminas en los años 30 o el aislamiento y síntesis de testosterona dentro del campo de la investigación científica, han sido algunos de los hitos más importantes en la historia del dopaje en el deporte hasta aproximadamente mediados de siglo XX. Posteriormente, ha habido otros como la síntesis recombinante de hormona del crecimiento (GH) o la eritropoietina (EPO), así como el dopaje genético ya en el siglo XXI.

Debido a la necesidad de un control en el abuso de estas sustancias, en 1968, el Comité Olímpico Internacional (*International Olympic Commitee*, IOC) realizó el primer control antidopaje oficial en los Juegos Olímpicos de México (Kremenik *et al.*, 2006). Entonces, se consideraban sustancias prohibidas, aquellas capaces de producir efectos significativos en el rendimiento deportivo justo antes o durante la competición. Periódicamente, se publicaba una lista con los compuestos prohibidos por parte del Comité Médico del IOC hasta la creación, en 1999, de la Agencia Mundial Antidopaje (*World Anti-Doping Agency*, WADA). Desde 2004 y según el mandato del Código Mundial Antidopaje (WADA, *The Code*), la WADA es responsable de la preparación y la publicación de la lista de sustancias prohibidas (WADA *Prohibited List,* 2016). Esta lista se actualiza anualmente e identifica sustancias y métodos prohibidos dentro y fuera de competición, clasificándolos por categorías (**Tabla I.1**).

Tabla I.1. Clasificación de sustancias y métodos prohibidos por la WADA, dentro y fuera de competición, en 2016.

	Código AMA	Sustancia	Ejemplos
Sustancias prohibidas dentro y fuera de competición	**S1**	Agentes anabolizantes	Testosterona, Dehidroepiandrosterona(DHEA), 19-Norandrosterona, Clenbuterol
	S2	Hormonas peptídicas, factores de crecimiento y sustancias afines	Eritropoyetina (EPO), Hormona del crecimiento (GH)
	S3	Agonistas Beta-2	Salbutamol, Formoterol
	S4	Moduladores hormonales y metabólicos	Anastrozol, Tamoxifeno, Insulinas
	S5	Diuréticos y otros agentes enmascarantes	Desmopresina, Tiazidas, Vaptanes
Métodos prohibidos	**M1**	Manipulación de sangre y componentes sanguíneos	
	M2	Manipulación química y física	
	M3	Dopaje genético	
Sustancias prohibidas en competición	**S6**	Estimulantes	Anfetamina, Cocaína, Catinonas, Estricnina
	S7	Narcóticos	Morfina, Diamorfina, Metadona
	S8	Cannabinoides	Hachís, Marihuana
	S9	Glucocorticosteroides	Prednisona, Triamcinolona
Sustancias prohibidas en ciertos deportes	**P1**	Alcohol	
	P2	Betabloqueantes	Betaxolol, Levobunolol, Sotalol

Las sustancias y métodos prohibidos por la WADA se clasifican en varios grupos, según si están prohibidos en todo momento (dentro y fuera de competición) (S1-S5, M1-M3) o sólo durante la competición (S6-S9). P1 y P2 son sustancias prohibidas en determinados deportes, como automovilismo, karate o tiro con arco.

El uso de sustancias dopantes suele llevar asociado efectos secundarios que ponen en riesgo la salud del atleta. Así, algunas de las sustancias prohibidas (p. ej. EPO) incrementan la cantidad de oxígeno en los músculos, aumentando la resistencia, pero pueden acarrear principalmente problemas cardiovasculares; otras que incrementan la masa muscular como los **esteroides anabolizantes androgénicos** (*Anabolic Androgenic Steroids*, AAS), pueden derivar en problemas de hígado o desordenes sexuales; sustancias estimulantes como la cocaína crean adicción, agresividad, taquicardia… (Sjöqvist *et al.*, 2008). Por todo esto, la realización de controles del dopaje tiene dos objetivos principales: por un lado asegurar una competición limpia y justa y, por otro, y quizás más importante, velar por la salud de los atletas. La prevención frente al abuso de sustancias dopantes debe incluir controles y seguimientos médicos, intervenciones pedagógicas, duras legislaciones frente a la posesión de sustancias prohibidas y serias descalificaciones a los atletas.

En este contexto, la detección en fluidos biológicos de marcadores del abuso de sustancias prohibidas es la herramienta más habitual en el control del dopaje. Tanto los marcadores utilizados como los métodos analíticos para su detección están en constante desarrollo con el fin de velar tanto por la salud de los atletas como por la limpieza de la competición. La presente Tesis Doctoral se enmarca en el uso de nuevas estrategias analíticas para mejorar los controles del dopaje.

I.1.2 Retos analíticos actuales del control del dopaje

La comunidad de laboratorios de control del dopaje ha desarrollado una importante labor de investigación en la detección de sustancias dopantes en las últimas décadas, haciendo que hoy en día sea posible aplicar protocolos de detección a cientos de sustancias diferentes. No obstante, al mismo tiempo, también el desarrollo de nuevas sustancias ilegales está en continuo desarrollo.

Históricamente, las sustancias más empleadas por parte de los atletas para aumentar su rendimiento deportivo, eran moléculas exógenas de bajo peso molecular desarrolladas por compañías farmacéuticas. Con el fin de demostrar su consumo, era suficiente con demostrar la presencia de esta sustancia en el organismo. Así que, mayoritariamente, se desarrollan métodos analíticos para la detección directa o *target* de agentes dopantes o sus metabolitos en orina.

En los últimos años, se ha producido una evolución en las sustancias dopantes que dificulta su detección. Por una parte, ha aumentado el número de sustancias endógenas, proteínas, sustancias no registradas y métodos/sustancias diseñadas específicamente para evadir los controles. Por otra, se han perfeccionado los métodos de administración con el fin de dificultar la tarea de los laboratorios. Así, en la actualidad el campo del control del dopaje presenta importantes retos analíticos. Algunos de los cuales son:

(i) Aumentar la ventana de detección de AAS. Puesto que los AAS están prohibidos tanto durante como fuera de la competición, es importante disponer de marcadores que puedan detectar el abuso durante el periodo de tiempo más

largo posible. El aumento de la ventana de detección de AAS se puede conseguir mediante la detección de metabolitos de larga duración (*long term metabolites*, LTM) o bien tratando de aumentar la sensibilidad de las técnicas analíticas.

(ii) *Screening* de administración exógena de AAS endógenos. Es el caso de la detección del abuso a testosterona. En el caso de los AAS endógenos, los laboratorios tienen que diferenciar la sustancia que se ha administrado de forma exógena de la correspondiente endógena presente en el cuerpo humano. Se necesitan desarrollar métodos de *screening* que puedan ser aplicados a todas las muestras y que diferencien aquellas que sean sospechosas de las negativas.

(iii) *Screening* de sustancias peptídicas en orina. Es el caso de la detección del abuso a la EPO o la hormona del crecimiento recombinante humana (rhGH). La problemática en su detección radica en que muchas de estas sustancias metabolizan para dar lugar a péptidos endógenos y además, la sensibilidad de las técnicas analíticas para su detección en orina es baja. Aunque existen métodos para su detección, éstos suelen ser tediosos y no se pueden aplicar a todas las muestras. La detección de marcadores urinarios de abuso que puedan ser utilizados como *screening* en todas las muestras supondría un gran avance.

(iv) Detección de sustancias diseñadas para eludir los controles de dopaje, como la tetrahidrogestrinona (THG). Pequeñas modificaciones en sustancias ya existentes dan lugar a otras que nunca se han comercializado y que pueden mantener la función del compuesto original. Estas sustancias

permanecen invisibles por los métodos *target* clásicos. El reto en estos casos consiste en detectar estas sustancias mediante métodos de detección abierta de compuestos de similar estructura o mediante marcadores de su efecto.

En la presente Tesis se evaluará el avance de la química analítica y su aportación en tres retos de actualidad en el control del dopaje, como son (i) ampliación de la ventana de tiempo en la detección de AAS exógenos, (ii) detección de marcadores alternativos del abuso de AAS endógenos (testosterona) y (iii) detección de marcadores alternativos del abuso de rhGH.

A continuación, se explicarán los métodos actuales de detección de AAS, tanto exógenos como endógenos, así como de la rhGH. Para cada uno de ellos, se tratará sobre los métodos por los que son detectados hoy en día, las dificultades que surgen en el *screening* y la necesidad del descubrimiento de nuevos marcadores de abuso.

I.1.3 Métodos actuales y detección de nuevos marcadores

I.1.3.1 Esteroides anabolizantes androgénicos (AAS)

Los AAS son derivados de la testosterona (T), la principal hormona masculina. La T se produce en los testículos de los machos (células de Leydig) y en los ovarios de las hembras y, en pequeñas cantidades, se secreta en las glándulas suprarrenales.

Los AAS componen el grupo de sustancias dopantes detectado con mayor frecuencia por los laboratorios de control del dopaje (WADA *Statistics*,

2014). Reciben esta denominación debido a sus efectos androgénicos o virilizantes y por sus efectos anabolizantes o de crecimiento de la masa muscular y la fuerza (Kochakian, 1976; Geraline & Erinoff, 1990), siendo estos últimos los efectos deseados por aquellos atletas que los consumen. Por otro lado, son numerosos los efectos adversos asociados a su abuso (Maravelias *et al.,* 2005; Hartgens & Kuipers, 2004), tales como problemas cardiovasculares, de conducta (irritabilidad, agresividad…), hepáticos, reproductivos, etc. Por estos motivos, el uso de AAS está prohibido tanto durante la competición como fuera de ella.

La estructura general de los AAS se basa en modificaciones del ciclopentanoperhidrofenantreno (**Figura I.1)**, una estructura de cuatro anillos condensados, tres de ellos (A, B, C) de seis carbonos y otro (anillo D) de cinco carbonos.

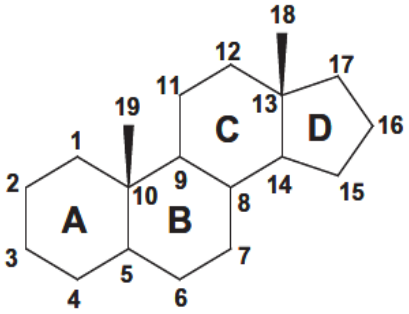

Figura I.1. Estructura general de los esteroides anabolizantes androgénicos.

Hoy en día, el método más utilizado para la detección de AAS engloba una hidrólisis enzimática, una extracción líquido-líquido (*liquid-liquid extraction*, LLE) y una derivatización, previos al análisis por cromatografía de gases acoplado a espectrometría de masas (GC-MS) (Pozo *et al.*, 2008a), tal como se muestra en la **Figura I.2**. En dicha figura se muestra un esquema del procedimiento de tratamiento de muestra llevado a cabo para la detección de

AAS por cromatografía de gases acoplado a espectrometría de masas en tándem (GC-MS(/MS)), que ha sido el aplicado a lo largo de la presente Tesis Doctoral.

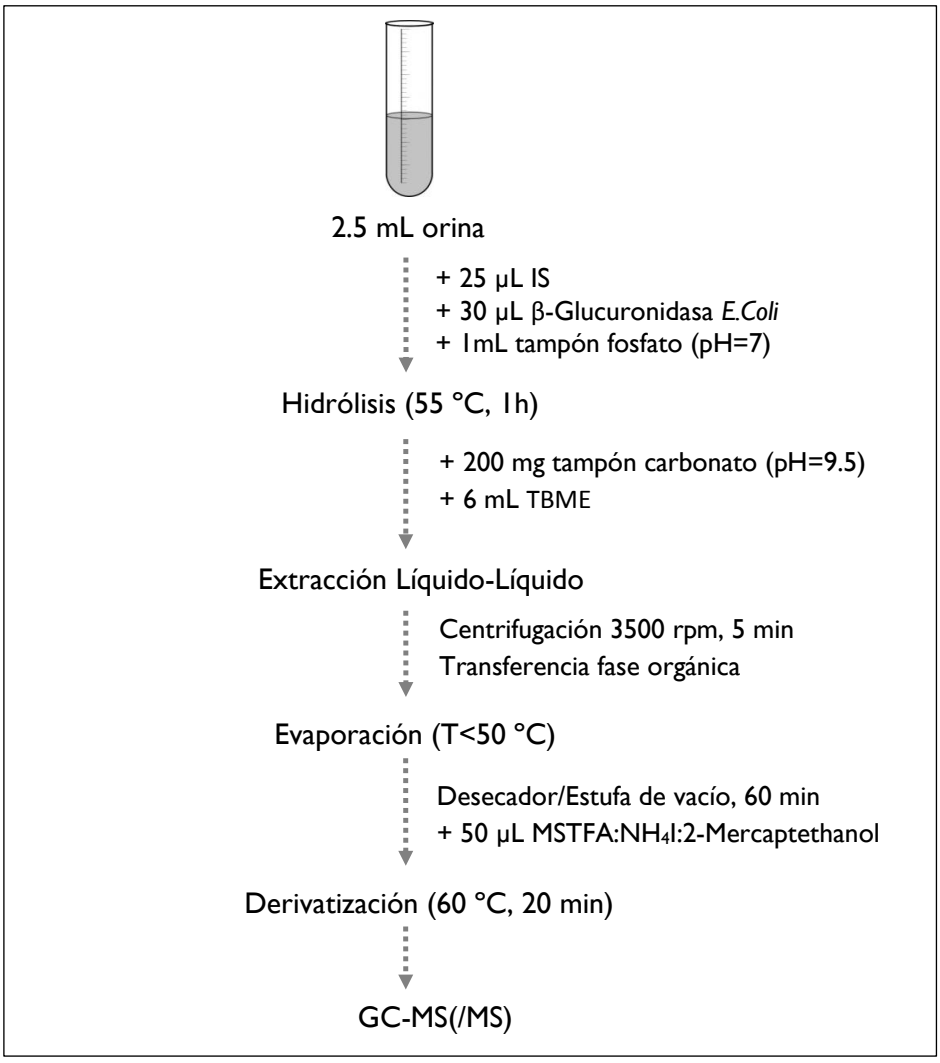

Figura I.2. Esquema del procedimiento analítico para la determinación de AAS por GC-MS(/MS)

La etapa adicional de derivatización se ha aplicado tradicionalmente para mejorar la forma cromatográfica en GC, permitiendo la determinación de AAS polares y no polares. La derivatización consiste en una trimetilsililación donde los grupos hidroxilo o enol son reemplazados por grupos TMS (*TriMethylSilyl*) (**Figura I.3**). Esta metodología se basa en la desarrollada por el grupo del Profesor Donike en 1969 (Donike, 1969). Las desventajas asociadas a la derivatización son el tiempo requerido en preparar las muestras y las dificultades que presenta para algunos compuestos como el stanozolol y aquellos AAS que contienen un núcleo 4,9,11-trieno es su estructura, como por ejemplo el THG (Brun *et al*., 2011).

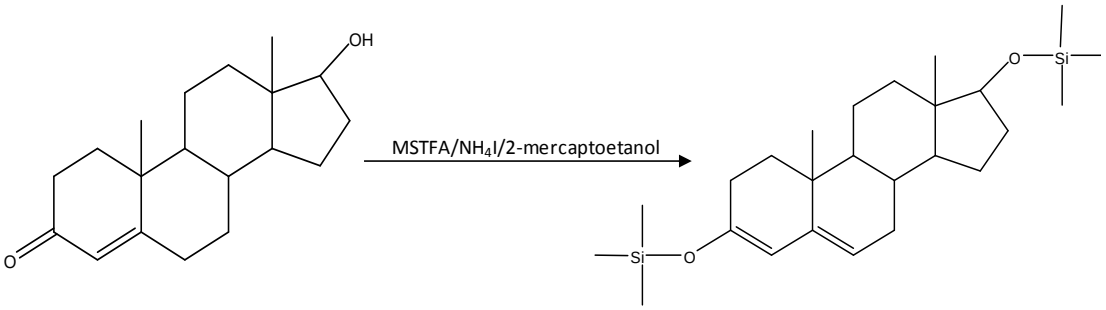

Figura I.3. Reacción de TMS-derivatización de la testosterona

El análisis se realiza habitualmente por GC-MS en modo *Selected Ion Monitoring* (SIM) o por GC-MS/MS en modo *Selected Reaction Monitoring* (SRM). Estos métodos permiten detectar un gran número de compuestos con una adecuada sensibilidad y especificidad. Desde hace relativamente poco tiempo, se han empezado a desarrollar métodos de cromatografía de líquidos acoplada a espectrometría de masas en tándem (LC-MS/MS) en modo SRM como alternativa o como complemento a los métodos GC (Pozo *et al.*, 2008b; Ma & Kim, 1997). La metodología LC-MS/MS ha permitido la detección de compuestos termolábiles o compuestos de alta polaridad evitando etapas adicionales de derivatización, así como la detección directa de metabolitos

en Fase II (principalmente glucurónidos o sulfatos). De esta manera, se han identificado algunos metabolitos que no se detectaban por el método tradicional, como sulfatos (Gómez *et al.*, 2013) o glucurónidos resistentes a la hidrólisis enzimática (Fabregat *et al*., 2013).

Desde el punto de vista del control del dopaje, los AAS pueden dividirse en (i) naturales o endógenos, es decir, que pueden ser producidos por el organismo humano y en (ii) sintéticos o exógenos, que no son producidos por el organismo humano. Entre los AAS exógenos se encuentran algunos como danazol, fluoximesterona, metenolona, estanozolol o trenbolona. La simple detección e identificación del compuesto y/o sus metabolitos en orina es suficiente para reportar un resultado analítico adverso. La detección de AAS endógenos es más compleja ya que se requiere demostrar que los niveles anómalos se deben al consumo de sustancias dopantes y no a una síntesis endógena anormal. Dentro de este grupo se incluyen compuestos como androstenediol, androstendiona, dehidroepiandrosterona (DHEA), dihidrotestosterona (DHT) o testosterona.

La problemática analítica de ambos grupos de AAS es totalmente distinta y, por lo tanto, debe tratarse por separado. A continuación se explicarán los métodos actuales de detección de AAS exógenos y endógenos.

Esteroides exógenos

Inicialmente, los AAS exógenos eran detectados mediante técnicas de Radioinmunoensayo (*Radioimmunoassay*, RIA), las cuales presentaban notables limitaciones en sensibilidad y selectividad (Brooks *et al.*, 1975). Durante los Juegos Olímpicos de 1976 en Montreal se empezó a utilizar la técnica de GC-MS, lo cual mejoró notablemente la detección e identificación

de estos compuestos (Thevis, 2005). A partir de ese momento, los esteroides exógenos se han determinado principalmente mediante técnicas de GC-MS(/MS) o mediante la complementaria LC-MS(/MS) (Parr & Schänzer, 2010), la mayoría tras la hidrólisis de los glucurónidos, siguiendo el procedimiento expuesto anteriormente.

Como se ha comentado anteriormente, en el caso de AAS exógenos, la detección del compuesto y/o alguno de sus metabolitos es suficiente para reportar un resultado adverso. Por este motivo, es necesario conocer minuciosamente el metabolismo de estos compuestos. Las rutas metabólicas descritas para AAS (Pozo *et al.*, 2010; Schänzer, 1996) se dividen en las conocidas como metabolismo en Fase I y en Fase II, donde los esteroides derivan en compuestos con una polaridad mayor que facilita su eliminación. Las reacciones de Fase I son catalizadas enzimáticamente e incluyen oxidaciones y reducciones en varias posiciones del anillo esteroidal. Las reacciones en Fase II engloban la formación de conjugados, mayoritariamente glucurónidos o sulfatos.

La WADA establece unos niveles mínimos requeridos, los MRPL (*Minimun Required Performance Level*), para asegurar la detección de una sustancia prohibida o sus metabolitos, por un laboratorio acreditado. Para el caso particular de los AAS, se establece en 5 ng/mL en orina, y para algún compuesto en concreto, como el Estanozolol o la Metiltestosterona, de 2 ng/mL. En el caso de la validación analítica, el nivel requerido es el 50 % del MRPL (WADA MRPL, 2014). Consecuentemente, los laboratorios necesitan desarrollar métodos analíticos lo suficientemente sensibles para detectar estos compuestos en orina.

El MRPL de una sustancia no tiene que ser considerado ni como un umbral de detección ni como un límite de detección. Así, se pueden reportar resultados adversos para una sustancia por debajo de su MRPL. Esto es especialmente relevante para aquellas sustancias (como los AAS) que están prohibidas tanto durante la competición como fuera de ella. Como se ha comentado anteriormente, el aumento de la ventana de detección del abuso a estas sustancias es uno de los retos actuales de la comunidad antidopaje. La búsqueda de LTM así como el estudio de nuevas técnicas analíticas (cromatográficas/espectrométricas) que permitan un aumento en la sensibilidad, son dos vías de trabajo actuales en la mejora de la detección de los AAS exógenos.

Esteroides endógenos

En el caso de AAS endógenos, no es suficiente con la mera presencia de la sustancia para reportar un resultado adverso. Los laboratorios deben poder diferenciar la administración exógena de los niveles endógenos del compuesto.

La administración de testosterona provoca cambios en el perfil esteroidal de la orina, por ello, la relación testosterona/epitestosterona excretados como glucurónidos (T/E) es el indicador que se usa normalmente para detectar el abuso. En 1983, Donike *et al.* introdujeron esta relación (Donike *et al*., 1983) aprovechando que la epitestosterona, un epímero 17α de la testosterona, permanece relativamente inalterado tras la administración mientras que la testosterona aumenta significativamente. Desde entonces, la detección del abuso de testosterona ha estado directamente vinculada a la determinación del valor T/E.

Como una primera aproximación, tras el estudio de un numeroso grupo de casos, el IOC estableció una relación T/E por encima de 6 para calificar una muestra como positiva. Posteriormente este valor se amplió a 10 al encontrarse individuos con T/E naturales elevadas (Aguilera *et al.*, 1999). Otra limitación que presenta el uso de T/E con un valor de corte reside en las diferencias entre los niveles basales encontrados entre diferentes grupos de población, puesto que pueden diferenciarse en más de un orden de magnitud. Por este motivo, los individuos con valores basales de T/E bajos no excedían el umbral tras la administración de T, dificultando la detección del abuso en estos individuos (Ayotte *et al.*, 1996).

La introducción de una técnica específica de confirmación facilitó que la medida de T/E pasara a ser usada como *screening* permitiendo bajar su umbral a un valor de 4. Este método de confirmación se basa en la medida de los isótopos $^{13}C/^{12}C$ mediante espectrometría de masas de relaciones isotópicas (IRMS) (Meier-Augenstein, 1999; Van Renterghem *et al.*, 2012; Cawley *et al.*, 2009). Ésta técnica (GC/C/IRMS, *Gas Chromatography Combustion Isotope Ratio Mass Spectrometry*) permite diferenciar los esteroides administrados de forma exógena de los producidos naturalmente por el cuerpo humano. Las desventajas radican en la cantidad de orina que se necesita y en el aumento del tiempo de análisis, por lo que resulta imposible aplicarlo a todas las muestras que deben ser analizadas por un laboratorio. Por ello, sólo se utiliza como técnica de confirmación en muestras sospechosas.

A pesar de los avances conseguidos, el uso de T/E > 4 como *screening* y posterior confirmación por GC/C/IRMS presenta como principal limitación la dificultad para detectar el abuso en atletas con T/E basal extremadamente bajo. Las grandes diferencias inter-individuo de la concentración urinaria de esteroides hace que ciertas concentraciones bajas de AAS endógenos pueden

pasar desapercibidas en un test anti dopaje usando umbrales obtenidos por estadísticas poblacionales (Van Renterghem *et al.*, 2010). Para minimizar esta limitación, en 2014 entró en vigencia el módulo esteroidal del pasaporte biológico del atleta (ABP). A mediados de 2006 se introduce el ABP como un seguimiento de los valores hematológicos y urinarios de cada atleta de forma individual, permitiendo detectar cambios eventuales que puedan ser causados por el consumo de sustancias dopantes (Robinson *et al.*, 2011). El documento de WADA de 2014 sobre los AAS endógenos (WADA, TD2014-EAAS), trata sobre la medida del "perfil esteroidal" dentro del ABP. Cada orina se analiza para determinar, además del valor T/E, su contenido en los siguientes esteroides libres:

- Testosterona
- Epitestosterona
- Androsterona
- Etiocolanolona
- 5α-androstane-3α, 17β-diol
- 5β-androstane-3α, 17β-diol

El módulo esteroidal del ABP permite comparar los valores obtenidos en una muestra puntual con los de referencia de un determinado atleta siendo capaz de detectar pequeñas variaciones en el perfil esteroidal. El ABP no se tiene que considerar como una herramienta estática ya que la inclusión de nuevos marcadores puede mejorar su eficiencia en el *screening* del abuso de AAS endógenos.

I.1.3.2 Hormona del crecimiento

La hormona del crecimiento (*Growth Hormone*, GH) es una hormona peptídica natural segregada por la hipófisis o glándula pituitaria del cerebro. Está formada por 191 aminoácidos y tiene un peso molecular de unos 22.000 Da. Su estructura consta de cuatro hélices y dos puentes disulfuro. La GH es responsable del crecimiento de huesos y tejidos y está también asociada a efectos en las funciones reproductivas (Kieken *et al.*, 2011).

La primera fuente para la obtención de la GH eran cadáveres humanos, práctica que quedó obsoleta por el alto riesgo de contraer la enfermedad de Creutzfeldt-Jacob (Rahmanian *et al.*, 1997; Saugy *et al.*, 2006). A finales de la década de los 80 se desarrolla, mediante ingeniería genética, la hormona de crecimiento recombinante (*recombinant human Growth Hormone*, rhGH), para ser aplicada a pacientes con deficiencia en esta hormona. Se sospechó de su uso en el deporte por sus propiedades anabólicas. Su abuso por parte de atletas y culturistas se debe a sus efectos en el aumento de la masa corporal magra y disminución de la adiposa o grasa. El abuso de rhGH a largo plazo presenta serios problemas como, por ejemplo, el aumento del riesgo de diabetes, hipertensión, problemas cardíacos, osteoporosis etc. El uso de la rhGH en el deporte se basa, no sólo en sus propiedades anabólicas, sino también en su efecto sobre el metabolismo de los carbohidratos y la grasa.

El método directo pare la detección de rhGH en sangre se basa en el hecho de que la hormona se encuentra en una sola isoforma nativa (22 kDa), mientras que la hGH (*human Growth Hormone*) en circulación se encuentra en varias formas (mezcla de 22, 20 y 18 kDa, dímeros, etc.). Por tanto, cuando se inyecta rhGH en el cuerpo humano, aumenta la proporción de esta isoforma respecto de todas las otras formas en circulación. En los Juegos Olímpicos de Atenas de 2004, se implementó por primera vez este método de

detección directa de hGH (Kniess *et al.*, 2013). Ya que la detección de esta hormona presenta una vida media corta (24-36 h tras la administración), estudios posteriores han demostrado el potencial de monitorizar marcadores secundarios como las proteínas factor de crecimiento similar a la insulina I (IGF-I) y propéptido aminoterminal de procolágeno de tipo III (P-III-NP) (Bosch *et al.*, 2012), marcadores sensibles al tratamiento con rhGH, pero relativamente inalterados con el tiempo o en respuesta al ejercicio. El método conocido como GH-2000 (Erotokritou-Mulligan *et al.*, 2012), se basa en la medida de estos biomarcadores, cuya sensibilidad se puede ver aumentada gracias al ABP, ya que no sólo se aplicarían umbrales basados en test poblacionales sino también individuales.

Resumiendo, la detección de rhGH presenta varias limitaciones: una vida media corta, su concentración en el cuerpo humano es baja, no se puede detectar con los métodos de análisis clásicos por su peso molecular elevado y la secuencia de aminoácidos de la molécula recombinante es idéntica a la natural. Otra de las desventajas de los métodos actuales radica en que la matriz empleada para su detección es sangre. La recolección, transporte y almacenaje son mucho más complicados e invasivos que para la matriz estándar, orina. Mayoritariamente, el número de muestras que se analizan son de orina, por lo que el abuso de esta sustancia no se puede controlar por completo mediante métodos actuales. La caracterización de marcadores urinarios para el *screening* de rhGH puede suponer un paso muy importante en la lucha contra el dopaje.

I.2. Cromatografía acoplada a Espectrometría de Masas

I.2.1 Técnicas cromatográficas

La cromatografía se define como el proceso de separación que se consigue tras la distribución de los componentes de una mezcla en dos fases, una estacionaria y una móvil. Los compuestos que se retienen preferentemente en la fase estacionaria, permanecen más tiempo en el sistema. Consecuentemente, los analitos son eluidos del sistema como concentraciones locales en la fase móvil en orden dependiente de los coeficientes de distribución respecto a la fase estacionaria, consiguiéndose así, la separación (Scott, 2003).

La principal clasificación de las técnicas cromatográficas se basa en la naturaleza física de la fase móvil, siendo un gas en la cromatografía de gases (GC), un líquido en la cromatografía de líquidos (LC) y un fluido supercrítico en la cromatografía de fluidos supercríticos (SFC). Puesto que las primeras han sido utilizadas en la realización de esta Tesis Doctoral, serán explicadas a continuación.

Cromatografía de gases

La cromatografía de gases es una técnica de separación que se aplica especialmente para compuestos volátiles, apolares y termoestables. Se basa en el equilibrio del analito entre una fase estacionaria y una fase móvil gas.

El elemento fundamental de la cromatografía de gases para conseguir una buena separación es la fase estacionaria o ***columna cromatográfica***. La gran mayoría de las aplicaciones utilizan columnas capilares de sílice fundida debido a su alta eficacia de separación, consiguiendo reducir el tiempo de análisis y el volumen de muestra. Estas columnas consisten en unos tubos revestidos en su pared interior con una fina película de fase estacionaria polimérica y recubiertas por un polímero de poliamida en el exterior (Grob & Barry, 2004).

La etapa de la inyección de la muestra en GC debe realizarse adecuadamente para asegurar una correcta transferencia de los analitos a la columna. Existen diferentes ***técnicas de inyección*** para columnas capilares (Hübschmann, 2001), entre las más utilizadas se encuentran las siguientes:

- Inyección con división de muestra o *split*: Se basa en la división del flujo de la muestra entrante según una relación de división previamente establecida. La cantidad de analito que llega al detector en este tipo de inyección es más baja que si no hubiera separación disminuyendo de esta manera la sensibilidad del método. Por tanto puede ser un inconveniente para analitos que se encuentren a muy bajas concentraciones. Uno de los motivos principales de su uso es en casos donde la muestra está concentrada de analito, con el fin de no saturar la fase estacionaria, así como en casos de muestras complejas o sucias. Debido a este último motivo, ha sido el modo de inyección seleccionado en el tercer trabajo del Capítulo II de la presente Tesis Doctoral.

- Inyección sin división de muestra o *splitless*: En este caso, la totalidad de la muestra inyectada es dirigida a la columna, utilizando el mismo sistema que para el modo *split*, pero con la válvula de purga

completamente cerrada. Este modo es más adecuado para análisis de trazas, en muestras limpias, ya que permite un aumento de la sensibilidad.

- Inyección en columna: En estos sistemas la muestra se introduce directamente en el interior de la columna sin previa vaporización. Con ellos se evitan los problemas de discriminación y posible degradación térmica. Por el contrario, los compuestos de baja volatilidad pueden quedar retenidos en la cabeza de la columna, promoviendo su deterioro, con lo que este modo de inyección queda limitado a muestras limpias.

- Inyector de vaporizador con temperatura programada (PTV): La muestra se introduce a baja temperatura en un inyector tipo *split/splitless* en el que se aplica un programa de temperaturas. Presenta la ventaja de poder realizar inyección de grandes volúmenes de muestra, aunque la optimización de todas las variables presentes dificulta el proceso.

Debido a las características de la técnica GC, los analitos a separar deben presentar propiedades como (i) ser volátiles a la temperatura de trabajo o (ii) ser estables térmicamente. Si estos requisitos no se cumplieran existen técnicas auxiliares como la conocida como ***derivatización***. Mediante este proceso se modifica químicamente un compuesto generando un derivado con nuevas propiedades que facilitan su análisis, pudiéndose mejorar su volatilidad, su estabilidad térmica o su detección. Hay diversos tipos como alquilación, acilación o sililación; siendo este último el aplicado a lo largo de los trabajos de GC de la presente Tesis.

En el Capítulo II de la presente Tesis Doctoral se emplea la cromatografía de gases. A lo largo de los tres trabajos científicos que se presentan se describe el tipo de columnas, modo de inyecciones utilizadas, derivatización, etc.

Cromatografía de líquidos

La cromatografía de líquidos es una técnica de separación que se emplea para el análisis de compuestos con carácter polar de baja volatilidad y termolábiles.

La ***fase móvil*** juega un papel principal ya que es una de las variables que permite más juego a la hora de conseguir una buena separación. La selección se lleva a cabo teniendo en cuenta la fuerza eluotrópica de los disolventes, pudiéndose elegir disolventes de un amplio rango de polaridades o efectuar mezclas.

La separación tiene lugar por la diferencia de coeficientes de distribución entre los compuestos de una muestra, que atraviesa sucesivas etapas de adsorción/desorción a lo largo de la ***fase estacionaria*** (Ardrey, 2003).

Existen varios tipos de cromatografía de líquidos dependiendo de la fase estacionaria, seleccionada en función de la naturaleza de los analitos a separar.

- **Fase inversa (RPLC)**: la fase estacionaria es no polar, frecuentemente un hidrocarburo alifático y se emplean solventes polares (agua, metanol, acetonitrilo) como fase móvil. En este caso,

las sustancias más polares eluyen primero mientras que las apolares o hidrofóbicas quedan más retenidas.

Es la técnica más utilizada debido a su robustez y universalidad, ya que permite separar un gran número de compuestos orgánicos. Además, la volatilidad de los disolventes orgánicos utilizados hace posible el acoplamiento LC-MS.

- **Fase normal (NPLC)**: la fase estacionaria es polar (como por ejemplo sílice) y la fase móvil es poco polar (hexano, diclorometano, cloroformo). En esta modalidad los compuestos más polares quedan más retenidos mientras que los menos polares eluyen primero. Es menos empleada con detectores de masas debido a la incompatibilidad de los solventes apolares con la fuente electrospray (ESI), de la que se hablará más adelante en el punto I.2.2.1.
- **De interacción hidrofílica (HILIC)**: variante de NPLC donde la fase estacionaria es polar y la fase móvil acuosa. Se utiliza para la separación de analitos muy polares. La mayor diferencia entre HILIC y NPLC reside en las distintas fases móviles utilizadas. Mientras NPLC utiliza solventes 100% orgánicos o mezclas miscibles de ellos, HILIC usa fases móviles orgánicas miscibles en agua. Así pues, la HILIC salva los problemas de solubilidad normalmente encontrados en NPLC en muestras acuosas.

La LC también se puede clasificar teniendo en cuenta el tamaño de partícula de la fase estacionaria. En HPLC (*High Performance Liquid Chromatography*) el diámetro de partícula suele ser igual o inferior a 5 μm. Se considera ultra alta resolución (UHPLC) cuando se trabaja con partículas de diámetro inferior a 2 μm. La selección de columnas con estas características presenta una mayor eficiencia de separación cromatográfica y la posibilidad

de separaciones más rápidas gracias a flujos más elevados sin pérdida de eficiencia cromatográfica.

En los dos trabajos científicos presentados dentro del Capítulo III se ha hecho uso de la cromatografía de líquidos, tanto en fase inversa como de interacción hidrofílica con columnas UHPLC. Gracias al uso de este tipo de columnas complementarias se amplía el rango de compuestos de estudio, aspecto importante en trabajos metabolómicos no dirigidos como los presentados en dicho capítulo.

I.2.2 Espectrometría de masas

La espectrometría de masas (MS) es una técnica en la que los átomos o moléculas de una muestra son ionizados, separados por su relación masa/carga (*m/z*) y, posteriormente, detectados. Es una técnica muy versátil ya que permite determinar la estructura de compuestos muy diversos y es aplicable a todo tipo de muestras, volátiles, no volátiles, polares y apolares, sólidos, líquidos y gases. En combinación con técnicas de separación de alta resolución, es la más cualificada para analizar muestras complejas reales. Por todo esto, la espectrometría de masas es una de las técnicas de referencia en el control del dopaje (Thevis *et al.*, 2013), como se tratará en el punto I.2.3, y es la técnica empleada a lo largo de los trabajos presentados en esta Tesis.

A continuación, se comentan algunas características básicas de las fuentes de ionización y de los analizadores de masas más empleados.

I.2.2.1 Fuentes de ionización

La ionización de los analitos es un paso crucial en el análisis por espectrometría de masas puesto que permite la obtención de especies iónicas en fase gas a partir de compuestos neutros. Hay una amplia variedad de técnicas de ionización, aunque ninguna es universal (Dass, 2007). A continuación, se explican las fuentes de ionización más utilizadas en instrumentos de espectrometría de masas, acoplados a GC y LC.

Ionización en GC

Las fuentes de ionización más comunes en GC son aquellas que trabajan en condiciones de vacío, como la ionización electrónica (EI) y la ionización química (CI), aunque avances en los últimos años han permitido acoplar la cromatografía de gases a fuentes a presión atmosférica (APCI).

- Ionización electrónica (EI). Es el modo de ionización clásico más empleado debido a su universalidad, reproducibilidad y robustez. El proceso de ionización se produce a través de un bombardeo de la muestra vaporizada mediante un haz de electrones acelerados a alta energía (70 eV, superior a la energía de ionización de la mayoría de moléculas). Un electrón de la molécula (M) es expulsado convirtiéndose en un ión positivo, quedando el ión molecular resultante en forma ($M^{+\cdot}$). Se trata de una ionización que genera espectros comparables a los disponibles en las librerías comerciales de espectros. Por otra parte, al tratarse de una ionización fuerte, en muchos casos se genera una fragmentación excesiva, e incluso la ausencia del ión molecular.

- Ionización química (CI). En este caso, las moléculas del compuesto en fase gaseosa se ionizan al colisionar con los iones producidos al bombardear un gas reactivo (metano, isobutano o amoniaco) con electrones. La transferencia de energía generalmente no supera los 5 eV, por lo que se considera una técnica de ionización suave, mediante la cual es más fácil determinar el peso molecular aunque ofrece menor información estructural. No es una técnica universal ya que no es efectiva para todas las familias de compuestos, pero ofrece una elevada sensibilidad y selectividad, sobre todo en modo negativo en compuestos con elevada electronegatividad.

- Ionización química a presión atmosférica (APCI). Combinando la universalidad de la EI con el carácter de ionización suave de la CI, surge la fuente de ionización química a presión atmosférica compatible con GC. En este caso, de la misma forma que en CI, la ionización ocurre por reacción con los iones de un gas reactivo, dando lugar a los iones $[M+H]^+$ o $M^{+\cdot}$ como pico base del espectro (Portolés *et al*, 2010; Horning *et al.*, 1977). El esquema de la fuente y los mecanismos de reacción que en ella ocurren se explican con más detalle en la introducción del Capítulo II.

  Debido a la baja fragmentación obtenida con la fuente APCI, ésta presenta un alto potencial en aplicaciones de análisis de trazas (aplicaciones medioambientales, de seguridad alimentaria, etc.) (Li *et al.*, 2015). El potencial de esta nueva técnica de ionización ha sido evaluado en los trabajos de esta Tesis Doctoral basados en la determinación de sustancias dopantes mediante GC-MS y que se explican en el Capítulo II.

Ionización en LC

La incompatibilidad entre el caudal líquido proveniente del LC y el elevado vacío de MS, genera la necesidad de utilizar interfaces adecuadas en el acoplamiento LC-MS. Estas interfases deben ser, por tanto, capaces de eliminar el disolvente e ionizar los compuestos, para ser introducidos en el analizador de masas. Las más utilizadas en la actualidad son las interfases/fuentes de ionización a presión atmosférica que se explican a continuación:

- Interfase electrospray (ESI). Consiste en un capilar al que se le aplica un elevado potencial (3.500 V) junto con un flujo de gas de manera concéntrica, lo que genera un spray de gotas cargadas. Estas gotas van reduciendo su tamaño a medida que avanzan por la cámara de desolvatación hasta que, por fuerzas de repulsión entre cargas, pasan a estado gaseoso. Estos iones en fase gaseosa pueden ser con carga positiva (moléculas protonadas o aductos de sodio, potasio o amonio) o con carga negativa (moléculas desprotonadas o aductos de formato o acetato) y entran al analizador de masas a través de lentes focalizadas (Ardrey, 2003; Dass, 2007). Esta fuente ha sido la elegida en los trabajos de LC-MS de esta Tesis Doctoral y que se explican en el Capítulo III.

- Interfase de ionización química a presión atmosférica (APCI): Esta técnica de ionización suave presenta una ionización eficiente para compuestos más apolares que en el caso de ESI. Consiste en una sonda de entrada de muestra que introduce el eluato del LC a una cámara de nebulización caliente gracias a un gas inerte que consigue la desolvatación. Por acción de una aguja corona, se

genera un plasma de iones de la fase móvil que, por transferencia de carga, ionizan la muestra (Barceló, 1996; Ardrey, 2003).

I.2.2.2 Analizadores

El analizador de masas es el núcleo central del espectrómetro de masas que se encarga de separar los iones según su relación masa/carga. Existen diferentes tipos de analizadores con diferentes características en cuanto a sensibilidad, rango de masas o poder de resolución (Dass, 2007). Algunos de los más empleados y que serán explicados en más detalle a continuación son: cuadrupolo simple (Q), trampa de iones (IT), tiempo de vuelo (TOF), triple cuadrupolo (QqQ), Orbitrap y los híbridos cuadrupolo-tiempo de vuelo (QTOF) y cuadrupolo-Orbitrap (Q-Orbitrap).

- **ANALIZADORES DE BAJA RESOLUCIÓN**

Cuadrupolo simple (Q)

El analizador cuadrupolar está compuesto de cuatro barras metálicas cilíndricas dispuestas en paralelo dos a dos a las que se les aplica una corriente continua y un voltaje de radiofrecuencia. La aplicación de estos potenciales permite determinar aquellos iones con una determinada relación *m/z* que son capaces de describir trayectorias estables desde el interior del cuadrupolo hasta llegar al detector. El cuadrupolo permite realizar barridos completos de iones, *Full Scan*, así como seleccionar una determinada masa/carga en análisis dirigidos o tipo *target* para trabajar en modo *Selected Ion Monitoring* (SIM).

Trampa de iones (IT)

La trampa de iones consiste en tres electrodos, dos terminales enfrentados y un anillo situado entre ellos. Potenciales de corriente continua y radiofrecuencia son aplicados entre ellos, lo que permite almacenar aquellos iones que describen trayectorias estables y separar aquellos iones con *m/z* concretas que no sean estables. Se puede trabajar en modo *Full Scan*, haciendo un barrido de todos los iones, o también trabajar en modo masas en tándem (MS/MS), desestabilizando todos los iones excepto el que se quiere fragmentar, para realizar posteriormente un barrido de sus iones producto.

Triple cuadrupolo (QqQ)

Este analizador está compuesto por tres cuadrupolos sencillos en serie, actuando el cuadrupolo central como celda de colisión (ver **Figura I.4**). La fragmentación de los iones se produce por disociación inducida por colisión con las moléculas de un gas inerte (nitrógeno o argón). Dependiendo de la finalidad, se pueden llevar a cabo análisis MS, como si se tratara de un cuadrupolo simple, o MS/MS, que es el modo utilizado más frecuentemente en este tipo de analizadores. El uso de un QqQ en MS/MS permite la monitorización de una transición concreta (*Selected Reaction Monitoring*, SRM), realizar barrido de iones producto (*Product Ion Scan*), búsqueda de iones precursores (*Precursor Ion Scan*) y pérdidas neutras (*Neutral Loss Scan*). El modo de trabajo SRM es uno de los más utilizados en el análisis *target*. En el primer cuadrupolo se selecciona un ión precursor que es fragmentado en el segundo cuadrupolo a una determinada energía de colisión (CE), por último, el tercer cuadrupolo selecciona un determinado ión

producto, con lo que se consigue monitorizar transiciones específicas que mejoran la sensibilidad y selectividad del método (Niessen, 2007).

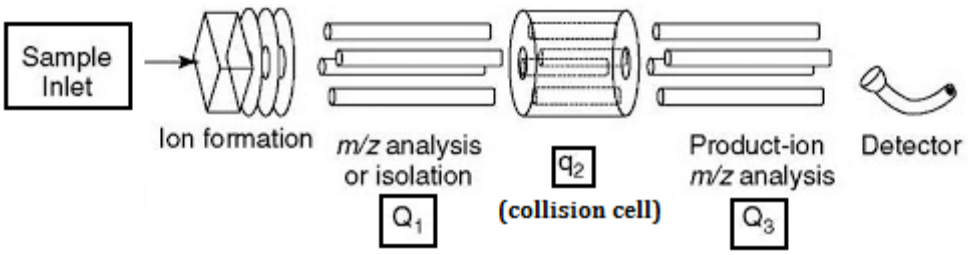

Figura I.4. Esquema de un analizador de triple cuadrupolo

El analizador de triple cuadrupolo ha sido empleado en el *artículo científico 3* dentro del Capítulo II de la presente Tesis Doctoral.

◈ ANALIZADORES DE ALTA RESOLUCIÓN

Tiempo de vuelo (TOF)

El analizador de tiempo de vuelo consiste en un tubo de vuelo donde los iones se separan en función del tiempo que tardan en atravesarlo. Así, los menos pesados tardarán menos tiempo (menor *m/z*, mayor velocidad) y los más pesados más tiempo en llegar al detector (mayor *m/z*, menor velocidad). Alcanza una elevada resolución, por lo que el analizador TOF tiene la ventaja de medir la *m/z* de los iones con exactitud, es decir, asignando valores de masas a los iones muy próximas al valor verdadero. Su alta resolución y elevada sensibilidad en modo *Full Scan*, hace que sea un analizador muy utilizado en el análisis no dirigido o *non target*. Al trabajar con masa exacta se requiere una calibración diaria mediante la adición de un compuesto

conocido como *lock mass*. Las masas se corregirán respecto a la de este compuesto generalmente con errores bajos.

Cuadrupolo Tiempo de vuelo (QTOF)

El analizador híbrido QTOF consiste en el acoplamiento de un analizador cuadrupolar y uno de tiempo de vuelo por medio de una celda de colisión, tal y como se observa en la **Figura I.5**. Existe la posibilidad de trabajar en modo *Full Scan* o en modo *Product Ion Scan* o MS/MS. En el modo MS/MS, un ión precursor de una determinada *m/z* es seleccionado en el cuadrupolo, que será fragmentado en la celda de colisión localizada entre el cuadrupolo y el TOF. A continuación, en el TOF se realiza un barrido de iones producto con alta resolución, exactitud de masa y sensibilidad, lo cual aporta información estructural altamente fiable. También es posible trabajar en modo MS^E, donde se adquieren simultáneamente dos funciones, una a baja energía (LE, *Low Energy*) y otra a alta energía (HE, *High Energy*). En el primer caso, la fragmentación es baja y en el espectro predominan los iones de las moléculas o sus aductos (similar a un *Full Scan*), mientras que en el segundo caso, a alta energía de colisión, se obtiene información de los iones producto.

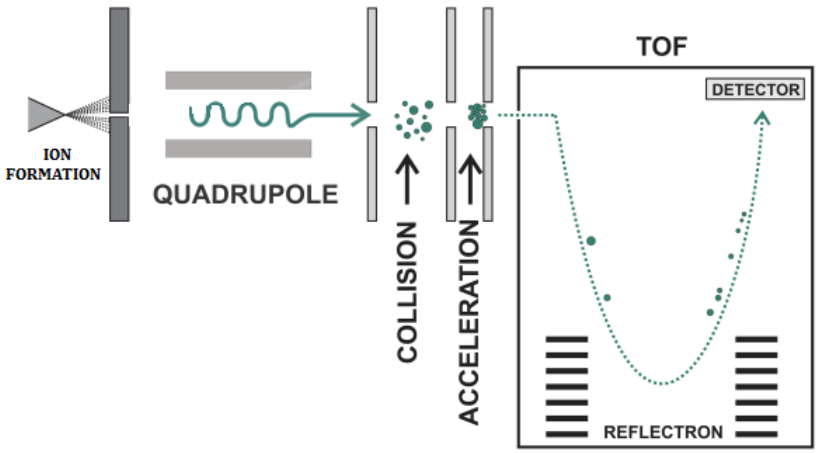

Figura I.5. Esquema de un analizador híbrido Cuadrupolo-Tiempo de vuelo

El analizador QTOF, ha sido utilizado en los *artículos científicos 1 y 2* del Capítulo II acoplado a GC, así como en los *artículos científicos 4 y 5* del Capítulo III acoplado a LC.

Orbitrap

El analizador de masas Orbitrap fue desarrollado por Alexander Makarov a principios de los años 2000 (Makarov, 2000; Makarov *et al.*, 2006) como una modificación de la trampa de iones desarrollada por K. H. Kingdon en 1923. Consta de dos electrodos, uno tubular externo y un filamento interno coaxial donde se forma un campo electrostático que atrapa los iones. En el orbitrap, el filamento interno es una barra en forma de huso y las paredes que lo contienen presentan forma de barril. Los iones de la fuente son dirigidos hacia el C-trap, donde se "atrapan" los iones y son transferidos al orbitrap mediante pulsos cortos, donde cada población de *m/z* forma un pulso de microsegundos. Una vez dentro del orbitrap, los iones adquieren un movimiento radial alrededor del huso combinado con un movimiento axial periódico cuya frecuencia es una función de su *m/z*. Éste movimiento es medido en el electrodo externo que registra todas las señales conjuntas, que transformadas mediante la Transformada de Fourier (FT) permite obtener el espectro de masas final con una elevadísima resolución a expensas del tiempo de medida.

En un Orbitrap, el modo de trabajo principal sería el modo *Full Scan*, pudiendo seleccionar diferentes resoluciones en función del tiempo de *Scan*. Para mejorar las capacidades identificativas, se añadió posteriormente una celda de colisión junto al C-trap, donde los iones son fragmentados y medidos

posteriormente en el orbitrap. Este modo de trabajo se conoce como *All Ion Fragmentation* (AIF) y sería equivalente al modo MS^E del TOF.

(Cuadrupolo) Orbitrap

A semejanza del QTOF, el analizador híbrido Q-Orbitrap como el que se observa en la **Figura I.6**, permite trabajar tanto en modo *Full Scan*, haciendo un barrido de todos los iones, como en modo MS/MS. Para ello, se selecciona un determinado *m/z* en el cuadrupolo, estos iones son fragmentados en la celda de colisión e introducidos mediante la C-Trap al Orbitrap donde se llevaría a cabo el barrido de iones producto. Además, este sistema híbrido, permite un modo de trabajo similar al AIF anterior, pero mejorado, ya que podemos, mediante el filtro cuadrupolar, aislar un rango de *m/z* de interés y no fragmentar todos los potenciales iones precursores, como ocurre en AIF. Este rango puede abarcar desde todo el rango de masas hasta ventanas estrechas, reduciendo así la complejidad de los datos y aumentando la selectividad. Este modo, conocido como vDIA (*variable Data Independent Analysis*) permite obtener espectros de fragmentación más limpios y sencillos (Pong Law & Pin Lim, 2013).

En esta Tesis se ha hecho uso de este analizador durante la estancia de investigación realizada en el laboratorio antidopaje *Docolab* (*Doping Control Laboratory*) en Gante, Bélgica. Su uso queda plasmado en el *trabajo científico 4* del Capítulo III.

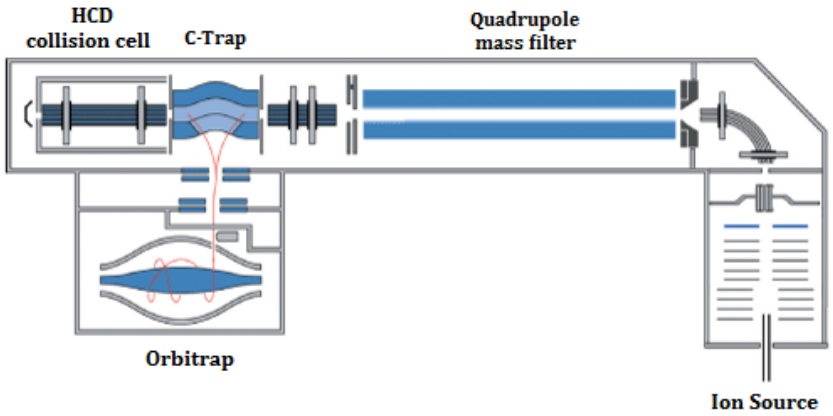

Figura I.6. Esquema de un analizador híbrido Cuadrupolo-Orbitrap

I.2.3 Espectrometría de masas en el control del dopaje

La espectrometría de masas se ha convertido en los últimos 40 años en la técnica más utilizada en el análisis de control del dopaje para identificar sustancias prohibidas debido a sus características en cuanto a sensibilidad y selectividad. Acoplada a cromatografía de gases o de líquidos, empleando diversos métodos de ionización y haciendo uso de diferentes analizadores de masas, se han establecido numerosas aplicaciones que han permitido la detección de sustancias prohibidas en diversas matrices como orina, sangre o pelo (Thieme *et al.*, 2003).

Fue en los Juegos Olímpicos de Múnich de 1972, conocidos como los Juegos de la XX Olimpiada, cuando la espectrometría de masas fue introducida como herramienta para identificar sustancias prohibidas. Desde entonces, ha sido una parte fundamental en la lucha contra el dopaje. El profesor Manfred Donike, del Instituto de Bioquímica de la Universidad de Colonia (Alemania) fue pionero en la introducción del MS en el análisis del dopaje, trabajando en este objetivo desde 1977 hasta 1995 y sembrando las

bases para el desarrollo de ésta técnica en todos los laboratorios acreditados del mundo (Hemmersbach, 2008).

Durante los Juegos Olímpicos de Montreal en 1976 y los posteriores de Moscú (1980) y Los Ángeles (1984), empezó a hacerse obvio que el método definitivo para el estudio de agentes dopantes en orina implicaba hacer uso de la espectrometría de masas, tal como se puede comprobar en la literatura científica de la época (Beckett & Cowan, 1976; Catlin *et al.*, 1987). Este desarrollo se va acentuando a lo largo de la década de los 80, siendo en los juegos de Seúl de 1988 donde se emplean activamente la técnica GC-MS para detectar estimulantes, narcóticos o AAS, y LC-MS para la investigación de corticosteroides (Park *et al.*, 1990). Durante los Juegos de invierno de 1994, se empezaron a analizar muestras haciendo uso de GC-MS con analizadores de alta resolución con el objetivo de disminuir los límites de detección de algunas sustancias con el fin de poder detectarlas durante más tiempo.

El desarrollo de la espectrometría de masas de relaciones isotópicas (IRMS) coincide con los juegos de Atlanta de 1996, por lo que todavía no pudo ser aplicada para diferenciar la testosterona endógena de la administrada. Ya durante los siguientes en Sidney (2000), toda la tecnología desarrollada en torno a la espectrometría de masas pudo ser utilizada.

Tras los Juegos de Atenas de 2004, la técnica LC-MS/MS empieza a adquirir relevancia, a la hora de determinar algunos AAS que no se detectaban adecuadamente por GC-MS por problemas en la derivatización como la Trenbolona, la Gestrinona o el THG, así como para la detección de corticosteroides (Spyridaki *et al.*, 2006; Thevis & Schänzer, 2007a; Pozo *et al.*, 2007). Finalmente, en los juegos más recientes, la espectrometría de masas fue empleada tanto para los test iniciales como para las confirmaciones. A partir de 2006 se empezaron a detectar nuevos marcadores que se

analizaron por primera vez en los juegos de Beijing (2008). Más adelante, los juegos de Londres (2012) fueron los primeros donde se empleó el TOF para análisis retrospectivo.

La complementariedad de las técnicas GC-MS(/MS) y LC-MS(/MS) resulta altamente necesaria para la determinación de un amplio abanico de sustancias prohibidas en el deporte, debido a su robustez, sensibilidad y selectividad, tanto en *screening* como en los procesos específicos de confirmación, siendo, hoy en día, la base del control del dopaje (Thevis & Schänzer, 2007b). En la presente Tesis Doctoral se ha hecho uso de estas técnicas cromatográficas complementarias, GC y LC, acopladas a distintos analizadores de baja y alta resolución, como se tratará a lo largo de los Capítulos II y III y como se discutirá, posteriormente, en el Capítulo IV.

I.3. Estrategias Metabolómicas

I.3.1 Definición

Los subproductos del metabolismo, conocidos como metabolitos, son moléculas transformadas durante los procesos celulares, que sirven, por tanto, como medida indirecta de su actividad bioquímica. La metabolómica engloba el estudio de la composición metabólica de un organismo o sistema biológico, describiendo tanto los metabolitos primarios como secundarios (Moco *et al.*, 2007). Esta disciplina es la más reciente de las llamadas técnicas *ómicas* primarias y, a día de hoy, está adquiriendo un interés similar al alcanzado por la genómica, la transcriptómica o la proteómica, debido a su relevancia en el contexto biológico. Todas estas técnicas aportan grandes avances en el conocimiento básico de los temas biológicos suponiendo además un enorme desarrollo en el campo del análisis de la funcionalidad celular y en sus aplicaciones biotecnológicas. Las ciencias ómicas tienen en común el elevado volumen de datos requerido para su análisis, lo que hace necesario el uso de la bioinformática en la interpretación de los mismos.

La identificación mediante la aproximación de huella metabólica o *metabolic fingerprinting* no tiene como objetivo identificar cada metabolito observado, sino comparar patrones (o *fingerprints*) de metabolitos que sufren cambios en respuesta a enfermedades, tóxicos, factores ambientales o alteraciones genéticas con el objetivo de identificar metabolitos significativos (Dettmer *et al.*, 2007). La ausencia o presencia de algunos de estos metabolitos, así como la concentración relativa entre ellos, puede ser un indicador, por ejemplo, de estados de enfermedad o de factores de predisposición a ella.

I.3.2 Procedimiento y tratamiento de datos

En el procedimiento de evaluación por perfil metabólico o *metabolic fingerprinting* para la búsqueda de nuevos biomarcadores, no sólo la elección de la técnica analítica requiere especial atención, sino todo el diseño experimental en su conjunto, desde el muestreo hasta el proceso de elucidación de los potenciales marcadores. En la **Figura I.7** se presenta un esquema general simplificado de un procedimiento metabolómico *non target* o no dirigido, que ha sido el llevado a cabo durante los estudios desarrollados en esta Tesis Doctoral.

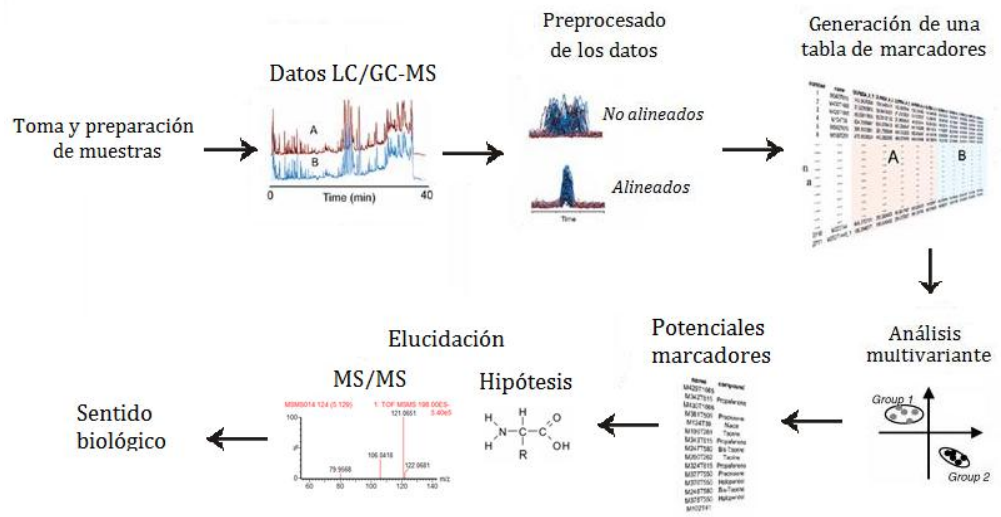

Figura I.7 Esquema simplificado del trabajo llevado a cabo durante un estudio metabolómico no dirigido

A continuación se describen detalladamente las siguientes etapas que se suelen incluir en el desarrollo de un procedimiento metabolómico:

1) ***Diseño experimental*.** El primer paso consiste en exponer el planteamiento del trabajo. Si se trata, por ejemplo, de una comparación entre tejidos normales y tejidos enfermos o tratados, si se trata de un "time course" o variación de actividad tras una administración a lo largo del tiempo... En función de la información disponible acerca del problema biológico, se puede optar por llevar a cabo una estrategia dirigida o no-dirigida. Puesto que la estrategia seguida en los trabajos expuestos en esta Tesis es la no dirigida, la explicación se centrará en esta opción, en la cual no se dispone de información previa sobre los metabolitos de interés.

   En este caso, el diseño experimental debe ser lo más detallado posible para detectar el mayor número de metabolitos y variará en función del problema analítico que se plantee en cada caso. Es importante conocer el número de muestras, voluntarios, dosis, tipo de matriz, etc. Además, resulta también crítico el planteamiento de los requisitos mediante los cuales un compuesto será considerado como marcador. Éste aspecto se explica en detalle en los trabajos presentados dentro de este capítulo.

2) ***Toma y preparación de muestras***. La toma de muestras debe realizarse bajo las mismas condiciones (envases, ciclos congelación/descongelación, etc.) para las muestras de un mismo estudio. Una vez que se dispone de todas las muestras, se les aplica el tratamiento adecuado teniendo en cuenta el tipo de matriz, tipo de análisis... Este tratamiento consiste en extraer los analitos de las matrices complejas para hacerlos compatibles con las técnicas

analíticas. En el caso de estudios no-dirigidos, se pretende llevar a cabo el menor tratamiento de muestra posible para maximizar el número de compuestos a detectar. Para ello, una técnica muy empleada en muestras líquidas como la orina (matriz de estudio en los trabajos que nos ocupan) es la conocida como *Dilute-and-shoot* para LC-MS (DS-LC-MS), que consiste, simplemente, en diluir las muestras en un disolvente adecuado para el análisis. Se trata de una técnica sencilla y rápida que minimiza efectos matriz así como potenciales pérdidas de compuestos de interés (Deventer *et al.*, 2014).

Para análisis por GC-MS, se requieren otras técnicas de preparación de muestra, tales como SPE o SPME, en algunas ocasiones, previos al análisis.

Al mismo tiempo que las muestras, se preparan también unas muestras control o Quality Control (QC) que actuarán como representativas del procedimiento global. Los QC están formados por una mezcla del mismo volumen de todos los extractos de muestra. Se inyectan 10 QC al principio de la secuencia para estabilizar el sistema cromatográfico y, después, uno cada diez muestras con el fin de comprobar la estabilidad y robustez del análisis.

3) ***Análisis de las muestras***. El objetivo principal de un análisis metabolómico es la detección del mayor número posible de compuestos, por tanto, en cada caso, se seleccionarán las condiciones que maximicen dicho número. Las técnicas más utilizadas para el *screening* e identificación de compuestos desconocidos son las técnicas cromatográficas acopladas a detectores de masas, GC-MS(/MS) y LC-MS(/MS). Concretamente, la técnica empleada en los trabajos reflejados en esta Tesis es la cromatografía de líquidos, por lo

que, en los siguientes puntos, se hará únicamente referencia a dicha técnica en estudios metabolómicos.

Mediante LC, el tratamiento de muestra para estudios metabolómicos es más sencillo, evitando por ejemplo, derivatizar las muestras y, al tratarse de una inyección directa de la muestra, se evita la posible pérdida de ciertos compuestos. La cromatografía en fase inversa (RP) usando columnas C_{18} con tamaños de partícula inferiores a 2 μm es muy empleada en metabolómica, debido a que genera picos cromatográficos estrechos que mejoran la resolución. Una alternativa para separación de compuestos polares es la cromatografía HILIC (Cubbon *et al*., 2010), como ya se mencionó en el punto anterior **I.2**.

Los analizadores más empleados, sobre todo en metabolómica no dirigida, son los de alta resolución (HR) como el Cuadrupolo-Tiempo de vuelo (Regal *et al*., 2011; Díaz *et al.,* 2014), ya que permiten la medida de la masa exacta y la posterior identificación de los metabolitos. También han sido reportadas, investigaciones en las que se utilizan otros analizadores como trampa de iones (Tolstikov & Fiehn, 2002) o triple cuadrupolo (Idborg-Bjorkman *et al*., 2003) en aplicaciones de metabolómica dirigida y no dirigida, respectivamente.

La técnica de ionización ESI es la más utilizada en estudios metabolómicos debido a su universalidad, en modo positivo y negativo, pudiéndose llevar a cabo simultáneamente en algunos instrumentos, con lo que se amplía el número de compuestos posibles a detectar.

El modo de trabajo seleccionado en metabolómica no dirigida es el de *Full Scan*, ya que en la búsqueda de marcadores desconocidos se necesita una detección abierta. Es el modo de trabajo seleccionado en los artículos científicos presentados en el Capítulo III de la presente

Tesis Doctoral, junto con la información estructural que aporta el modo de trabajo MS^E (Sección I.2.2.2) en los análisis por QTOF.

4) ***Tratamiento de datos***. Ya que el conjunto de datos obtenido del sistema LC/GC-MS en estudios metabolómicos es voluminoso, éstos son exportados a software específicos como MetAlign, MZmine o XCMS, especializados en tratamiento de datos y manipulación de cromatogramas. Para ello, primero los datos son convertidos a formatos de acceso abierto como netCDF. En la presente Tesis, el software empleado fue el XCMS (XCMS software, enlace; Smith *et al.*, 2006) de acceso libre, el cual está integrado dentro del software estadístico R (Paquete estadístico R, enlace). Después, con ayuda del software EZinfo (Umetrics, Umea, Sweeden), se lleva a cabo el análisis estadístico (punto e.), donde se buscarán diferencias significativas a la hora de encontrar un potencial marcador. A continuación se explican, en más detalle, las diferentes etapas dentro del procedimiento de tratamiento de datos.

    a. Peak Picking. Una vez los datos se transforman al formato adecuado, el programa extrae los iones que generan picos cromatográficos (XIC), mediante el proceso conocido como *peak picking*. El método utilizado en los trabajos presentados en la Tesis es el *Centwave*, que funciona buscando unas regiones de interés (ROI), siguiendo una aproximación llamada *Continuous Wavelet Transform* (CWT) (Tautenhahn *et al.*, 2008). Consiste en buscar para cada *m/z* diferentes ROI dentro de un error fijado, por lo que, generalmente, cada pico creará una ROI a la que se le asignará un descriptor de masa y tiempo de retención (MxxxTyyy) y se integran, tal como está representado en la **Figura I.8.a**.

b. Alineación de tiempos de retención o *retention time alignment*. El tiempo de retención al que aparece un mismo compuesto puede variar ligeramente a lo largo de las secuencias, ya que son generalmente largas. Si un pico se repite en las muestras, el programa le asigna el mismo descriptor. Para ello, el programa selecciona picos con tiempo de retención (RT) y masa exacta similares en diferentes muestras y los agrupa, utilizándolos después para alinear el resto. Finalmente, se asigna como descriptor de un pico la masa (M) en masa nominal seguido del tiempo (T) en segundos (*MxxxTyyy*), (**Figura I.8.b**).

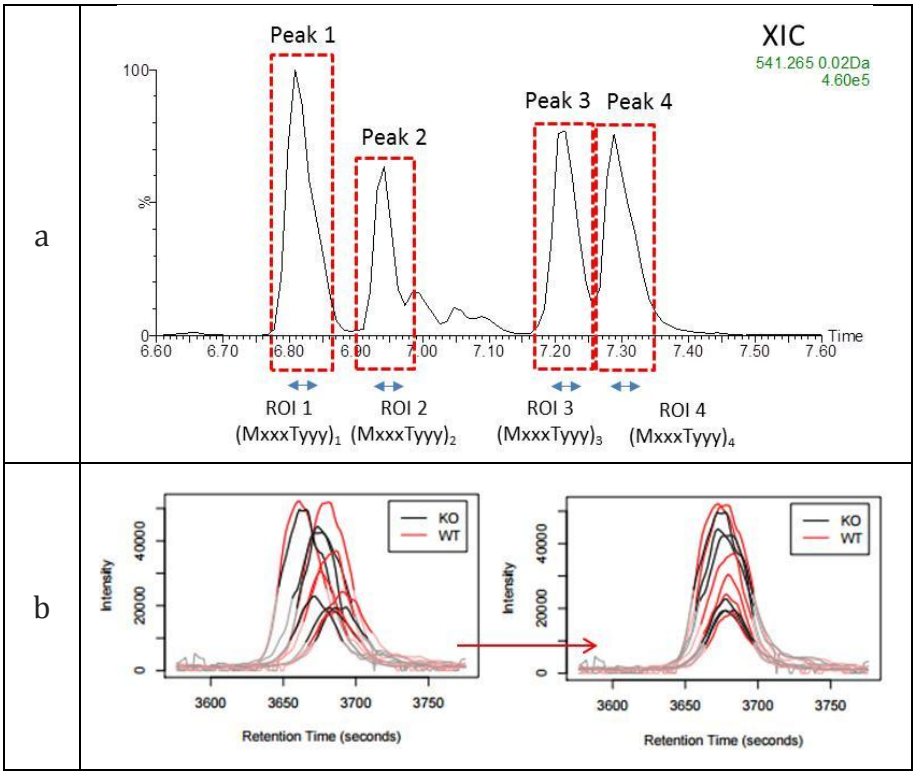

Figura I.8 Procesos ocurridos durante a) *Peak Picking* y b) *Retention time alignment.*

c. Integración. A continuación, se integran los picos en todas las muestras en las que no esté presente para evitar ceros, con lo que se genera una tabla de áreas de cada pico (filas) en cada muestra (columnas), además de la información de masa exacta.

d. Normalización. Es recomendable, en la mayoría de los casos, aplicar una normalización de las áreas de pico debido a la deriva del instrumento a lo largo de la secuencia o bien para tener en cuenta las diferencias de concentración de la orina por las diferencias en el volumen excretado en cada caso. Esto se lleva a cabo mediante un *script* de R, diseñado para corregir la respuesta de las muestras. En la **Figura I.9** se muestra gráficamente cómo afecta este proceso a las muestras. Si nos fijamos en las muestras QC que aparecen al final, se observa la deriva del instrumento a lo largo de la secuencia, hecho que se corrige tras la normalizalización.

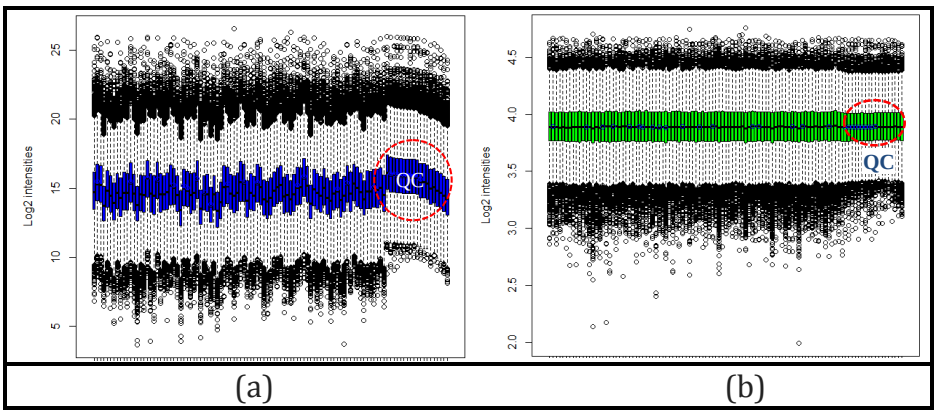

Figura I.9 Representación gráfica de las intensidades de los componentes de diferentes muestras: a) Datos antes de normalizar, b) Datos después de normalizar. Las muestras QC se muestran destacadas.

e. Análisis multivariante. La primera herramienta estadística que se aplica es un PCA (*Principal Component Analysis*), que trabaja generando unas matrices a partir de las tablas de datos (Brereton, 2003). Su principal característica es que no es dirigido. La estadística aplicada busca diferencias numéricas significativas, pero sin ninguna información sobre las muestras. El objetivo de realizar este gráfico es comprobar que el análisis se ha realizado correctamente y esto es gracias a las muestras QC, que deben aparecer lo más juntas y centradas posibles en el PCA, tal como vemos en la **Figura I.10 a**, donde los QC corresponden con las muestras en verde. El siguiente paso es aplicar un PLS-DA (*Partial Least Square- Discriminant Analysis*) (**Figura I.10 b**). Se genera de la misma forma que el PCA pero con información previa sobre los grupos en los que se encuentran las muestras. Con esta información, el método crea componentes principales maximizando la separación de los grupos. Por último, el OPLS-DA *(Orthogonal Partial Least Square- Discriminant Analysis*) (Boccard & Rutledge, 2013), que enfrenta únicamente dos grupos, se basa en todas las muestras de los grupos escogidos e intenta diferenciarlas en conjunto. En este punto, mediante una representación gráfica conocida como "S-Plot", se pueden obtener los compuestos que el método utiliza para explicar el modelo. El S-Plot representa con un punto cada uno de los marcadores e indica su validez para separar los grupos. Los compuestos que mejor explican diferencias se sitúan en los extremos superior derecho o inferior izquierdo (**Fig I.10 c**).

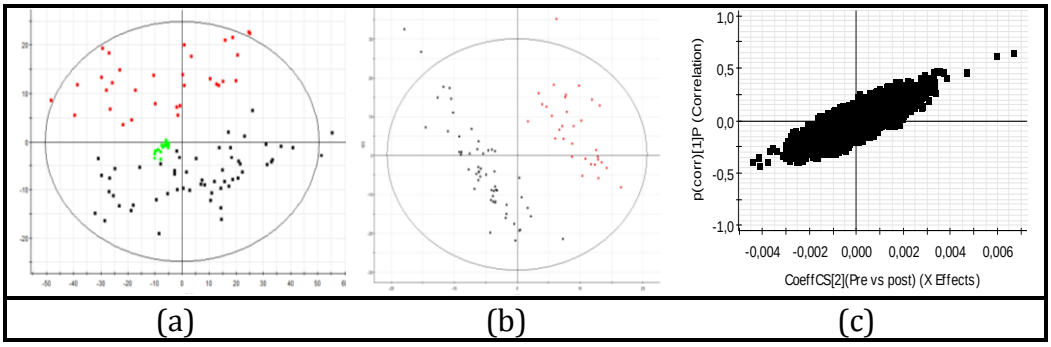

Figura I.10 Ejemplos de representaciones gráficas: a) PCA, b) PLS-DA, c) S-Plot

5) ***Identificación de marcadores.*** La última etapa dentro del esquema analítico de trabajo en metabolómica es la elucidación del compuesto o compuestos desconocidos con función discriminante. Si los análisis son realizados en instrumentos de alta resolución, como es el caso de la presente Tesis, se dispone de la masa exacta del marcador como punto de partida. Con ello, se puede determinar la composición elemental y realizar búsquedas en librerías comerciales. En este punto, resulta fundamental la realización de experiencias MS/MS a distintas energías de colisión, ya que aportan información de los fragmentos en masa exacta.

   Con toda la información adquirida, espectral (MS y MS/MS), posibles fórmulas, patrones de fragmentación, búsqueda en librerías… se plantea una hipótesis y se procede a comparar (tiempo de retención, fragmentos e intensidades) con un patrón, que puede estar disponible comercialmente o, en otros casos, es necesario sintetizar, tal como se explica en los trabajos desarrollados en el Capítulo III de la Tesis.

El estudio analítico desarrollado a lo largo de esa sección debe considerarse como una primera etapa el estudio metabolómico global. Una vez encontrado un potencial marcador, se debería llevar a cabo una validación del mismo así como estudiar su explicación biológica dentro del planteamiento del problema inicial.

I.3.3 Espectrometría de masas y metabolómica

Las técnicas metabolómicas engloban la detección de un amplio número de metabolitos en diversos tipos de muestras, por ejemplo, biológicas. Estos compuestos presentan diferentes propiedades químicas (peso molecular, polaridad o solubilidad) y físicas (volatilidad), además de estar presentes en diferentes niveles de abundancia (pmol-mmol). Por todo ello, la metabolómica resulta un reto importante para los investigadores.

La espectrometría de masas resulta ser una herramienta potente en el campo de la metabolómica, ya que es capaz de proporcionar análisis rápidos, sensibles y selectivos, por su alta resolución y amplio rango dinámico, así como por su viabilidad para llevar a cabo la elucidación estructural de los metabolitos (Dunn & Ellis, 2005; Armitage *et al*., 2013, Lu *et al*., 2008). Se puede utilizar directamente o acoplada a técnicas de separación, obteniéndose una mejora sustancial. Las técnicas GC-MS y LC-MS permiten analizar una gran cantidad de metabolitos a sensibilidades muy superiores a las de la RMN. Como también se ha mencionado en el apartado anterior, es de gran importancia la elección del analizador de masas, siendo los de alta resolución los más empleados en metabolómica no dirigida, por su alta sensibilidad en modo *Full Scan* y la posibilidad de diferenciar entre metabolitos con idéntica *m/z* nominal.

I.3.4 Metabolómica en el control del dopaje

Desde principios de la década de los 80, empiezan a aparecer investigaciones donde se aplica la metabolómica no dirigida en matrices biológicas, siendo muy valiosa en aplicaciones como el descubrimiento de nuevas drogas, búsqueda de nuevos metabolitos, confirmación de rutas metabólicas, etc. dentro de campos como el clínico o el toxicológico.

Como se comentó en el apartado I.1, la demanda de investigación analítica en el campo de control del dopaje ha ido en aumento, investigación capaz de ayudar a detectar con claridad el abuso de sustancias prohibidas. Ya que en este campo se asumen también cambios a nivel molecular debidos a la ingesta de sustancias, las técnicas "ómicas" han sido también investigadas (Reichel, 2011).

En la introducción del Capítulo III de la presente Tesis, se exponen, más en detalle algunos de los trabajos reportados sobre metabolómica aplicada al control del dopaje, tanto en animales como en humanos. En estos trabajos, se empieza a poner de manifiesto el potencial de las estrategias metabolómicas, aunque las aplicaciones reportadas totalmente no dirigidas, son todavía escasas. Los trabajos presentados en el Capítulo III abren nuevas vías de investigación en este campo.

CAPÍTULO II

POTENCIAL DE LA FUENTE DE IONIZACIÓN APCI ACOPLADA A GC-MS PARA EL ESTUDIO DEL COMPORTAMIENTO DE LOS ESTEROIDES ANABOLIZANTES ANDROGÉNICOS Y SU POSTERIOR DETECCIÓN EN ORINA MEDIANTE GC-MS/MS

II.1. Introducción

De acuerdo con la lista de sustancias prohibidas por la WADA (WADA *Prohibited List,* 2015), los agentes anabolizantes pueden ser tanto AAS (exógenos o endógenos) u otros como el clenbuterol o los moduladores selectivos de los receptores de andrógenos. Los AAS comprenden un grupo de compuestos derivados de la testosterona que son utilizados clínicamente o por deportistas debido a sus propiedades anabólicas. Todos los esteroides presentan tanto efectos anabolizantes o de estimulación del crecimiento, como androgénicos o virilizantes. Ninguna sustancia derivada de la testosterona es puramente anabolizante.

Las estrategias empleadas para mejorar su detección incluyen estrategias no dirigidas para la detección de esteroides de diseño o modificados, el ABP o técnicas IRMS para la detección del abuso de endógenos y la prolongación de la ventana de detección para los exógenos, (Geyer *et al*., 2014). Una de las posibles maneras de prolongar la ventana de detección es el aumento de sensibilidad del método analítico utilizado.

Los AAS han sido tradicionalmente analizados en orina mediante técnicas GC-MS tras una etapa de hidrólisis y otra de derivatización. Pese a las ventajas de la cada vez más utilizada LC-MS, mediante la cual no se requiere de dichas etapas previas, la GC todavía sigue teniendo mucha presencia en el análisis de estos compuestos. Por lo general, la fuente de EI es la más utilizada, aunque la elevada fragmentación del $M^{+\cdot}$ puede acarrear problemas de especificidad y sensibilidad en modo MS/MS, ya que se seleccionan precursores de menor *m/z* y/o poco intensos. La especificidad es un aspecto crítico en el análisis de orina al tratarse de una matriz compleja con presencia de numerosos compuestos de estructuras similares. Además, la

alta fragmentación generada en esta fuente, genera espectros similares en familias de compuestos como los que se estudian en este capítulo, pudiendo dificultar, en algunas ocasiones, su identificación.

En los trabajos presentados en el Capítulo II, se ha evaluado el potencial de la fuente de APCI comercializada para GC, presentándose como una alternativa interesante. Los problemas de la elevada fragmentación de la EI y el carácter selectivo de la CI, vendrían paliados por esta fuente de ionización suave y universal. En la **figura II.1** se muestra un esquema de la fuente de APCI.

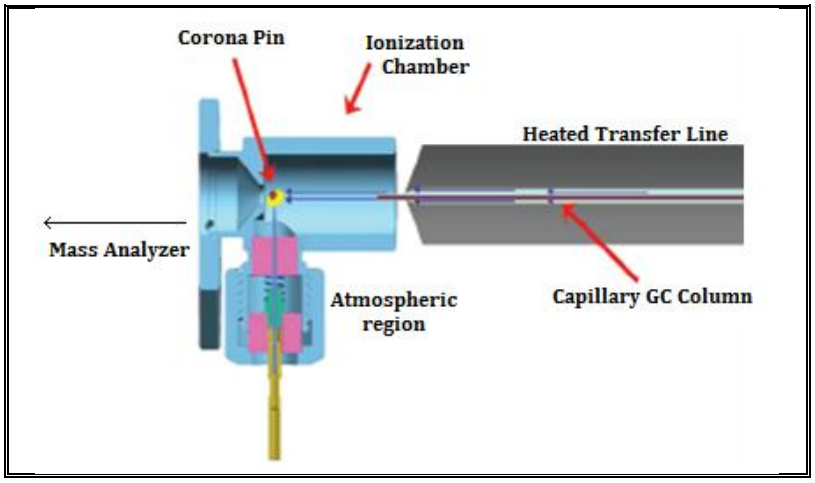

Figura II.1. Esquema de la fuente de ionización química a presión atmosférica (*Waters Corporation*).

El mecanismo de ionización que tiene lugar en la fuente de APCI es la utilización del N_2 como gas reactivo dando lugar a procesos de ***transferencia de carga*** (**figura II.2.a**) desde el plasma generado ($N_2^{\cdot+}$ y $N_4^{\cdot+}$) a las moléculas de analito generando el $M^{\cdot+}$. Otro proceso simultáneo que tiene lugar es el de ***protonación***, donde se genera la molécula protonada $[M+H]^+$ a

partir del ión $[H_3O]^{+\cdot}$ debido a las trazas de vapor de agua que siempre están presentes en la fuente (**figura II.2.b**) (Portolés *et al*., 2012). La adición de agua o metanol en la fuente como modificadores favorece este segundo mecanismo haciendo aumentar la intensidad de $[M+H]^+$.

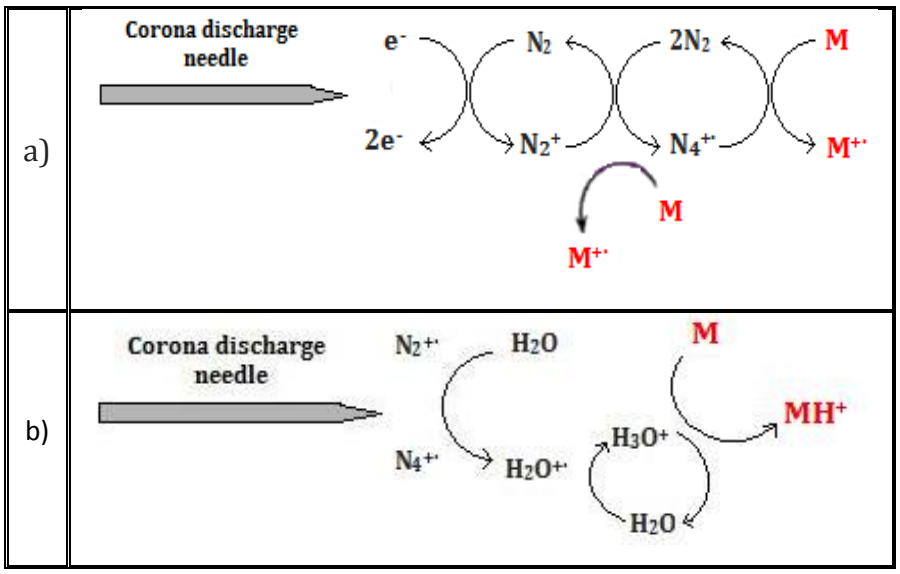

Figura II.2. Ionización mediante a) transferencia de carga b) transferencia de protón

En el presente capítulo, se han evaluado las capacidades de la fuente de APCI para GC para la detección de AAS. Por una parte, como se detalla en los *artículos científicos 1 y 2*, acoplada a un analizador de alta resolución (QTOF) para estudiar el comportamiento de ionización y fragmentación de 60 AAS modelo. El principal objetivo de ambos trabajos fue el encontrar relaciones entre dicho comportamiento y la estructura de los AAS. Para ello, fue crítica la división de los AAS modelo en distintos grupos según su estructura. Las relaciones Comportamiento-Estructura encontradas pueden ayudar en la elucidación de metabolitos desconocidos de AAS. Por otra parte, una vez recopilada y estudiada dicha información, se validó un método de *screening* de esteroides en orina mediante GC(APCI)-QqQ (*artículo científico*

3). En este trabajo, se validó la detección de 16 AAS en orina, presentando así a la fuente de APCI como alternativa válida a la tradicional EI, en términos de sensibilidad, especificidad y precisión. La optimización de transiciones para el método SRM fue crítica en este trabajo debido, como se ha comentado previamente, a la presencia de esteroides endógenos en la orina. La mejora en sensibilidad en algunos casos, quedó demostrada tras la aplicación del método validado en muestras de un estudio de excreción del esteroide 4-Cloro-Metandienona, donde la ventana de detección se vio ampliada respecto a la detección por EI.

II.2. Artículo científico 1

Research article

Journal of MASS SPECTROMETRY

Received: 20 January 2014 Revised: 13 March 2014 Accepted: 14 March 2014 Published online in Wiley Online Library

(wileyonlinelibrary.com) DOI 10.1002/jms.3367

Mass spectrometric behavior of anabolic androgenic steroids using gas chromatography coupled to atmospheric pressure chemical ionization source. Part I: Ionization

M. Raro,[a] T. Portolés,[a] J. V. Sancho,[a] E. Pitarch,[a] F. Hernández,[a] J. Marcos,[b,c] R. Ventura,[b,c] C. Gómez,[b] J. Segura[b,c] and O. J. Pozo[b]*

The detection of anabolic androgenic steroids (AAS) is one of the most important topics in doping control analysis. Gas chromatography coupled to (tandem) mass spectrometry (GC–MS(/MS)) with electron ionization and liquid chromatography coupled to tandem mass spectrometry have been traditionally applied for this purpose. However, both approaches still have important limitations, and, therefore, detection of all AAS is currently afforded by the combination of these strategies. Alternative ionization techniques can minimize these drawbacks and help in the implementation of a single method for the detection of AAS. In the present work, a new atmospheric pressure chemical ionization (APCI) source commercialized for gas chromatography coupled to a quadrupole time-of-flight analyzer has been tested to evaluate the ionization of 60 model AAS. Underivatized and trimethylsylil (TMS)-derivatized compounds have been investigated. The use of GC–APCI–MS allowed for the ionization of all AAS assayed irrespective of their structure. The presence of water in the source as modifier promoted the formation of protonated molecules ($[M+H]^+$), becoming the base peak of the spectrum for the majority of studied compounds. Under these conditions, $[M+H]^+$, $[M+H-H_2O]^+$ and $[M+H-2\cdot H_2O]^+$ for underivatized AAS and $[M+H]^+$, $[M+H-TMSOH]^+$ and $[M+H-2\cdot TMSOH]^+$ for TMS-derivatized AAS were observed as main ions in the spectra. The formed ions preserve the intact steroid skeleton, and, therefore, they might be used as specific precursors in MS/MS-based methods. Additionally, a relationship between the relative abundance of these ions and the AAS structure has been established. This relationship might be useful in the structural elucidation of unknown metabolites. Copyright © 2014 John Wiley & Sons, Ltd.

Keywords: anabolic androgenic steroids (AAS); atmospheric pressure chemical ionization (APCI); gas chromatography (GC); mass spectrometry (MS); doping control analysis

Mass spectrometric behavior of anabolic androgenic steroids using gas chromatography coupled to atmospheric pressure chemical ionization source. Part I: Ionization.

Montse Raro[a], Tania Portolés[a], Juan Vicente Sancho[a], Elena Pitarch[a], Félix Hernández[a], Josep Marcos[b,c], Rosa Ventura[b,c], Cristina Gómez[b], Jordi Segura[b,c], Óscar. J. Pozo[b]

a) Research Institute for Pesticides and Water, University Jaume i, E-12071 Castellõn, Spain

b) Bioanalysis Research Group, IMIM, Hospital Del Mar Medical Research Institute, Doctor Aiguader 88, 08003 Barcelona, Spain

c) Department of Experimental and Health Sciences, Universitat Pompeu Fabra, Doctor Aiguader 88, 08003 Barcelona, Spain

Abstract

The detection of anabolic androgenic steroids (AAS) is one of the most important topics in doping control analysis. Gas chromatography coupled to (tandem) mass spectrometry (GC–MS(/MS)) with electron ionization and liquid chromatography coupled to tandem mass spectrometry have been traditionally applied for this purpose. However, both approaches still have important limitations and, therefore, detection of all AAS is currently afforded by the combination of these strategies. Alternative ionization techniques can minimize these drawbacks and help in the implementation of a single method for the detection of AAS. In the present work, a new atmospheric pressure chemical ionization (APCI) source commercialized for gas chromatography coupled to a quadrupole time-of-flight analyzer has been tested to evaluate the ionization of 60 model AAS. Underivatized and trimethylsylil (TMS)-derivatized compounds have been investigated. The use

of GC–APCI–MS allowed for the ionization of all AAS assayed irrespective of their structure. The presence of water in the source as modifier promoted the formation of protonated molecules ($[M+H]^+$), becoming the base peak of the spectrum for the majority of studied compounds. Under these conditions, $[M+H]^+$, $[M+H-H_2O]^+$ and $[M+H-2\cdot H_2O]^+$ for underivatized AAS and $[M+H]^+$, $[M+H-TMSOH]^+$ and $[M+H-2\cdot TMSOH]^+$ for TMS-derivatized AAS were observed as main ions in the spectra. The formed ions preserve the intact steroid skeleton, and, therefore, they might be used as specific precursors in MS/MS-based methods. Additionally, a relationship between the relative abundance of these ions and the AAS structure has been established. This relationship might be useful in the structural elucidation of unknown metabolites.

Introduction

Anabolic androgenic steroids (AAS) are synthetic derivatives of testosterone with a common cyclopentaneperhydrophenanthrene structure (inserted in Table 1). Their use can stimulate the formation of muscle cells, increasing the muscle growth, so they are widely used to improve athletic performance. Since their first prohibition in sports in 1976 [1], AAS are the most frequently detected group of prohibited substances by World Antidoping Agency (WADA) Accredited Laboratories in doping control analyses [2]. Moreover, the number of illegal steroids is constantly increasing; thus, the detection of AAS is a continuous challenge for doping control laboratories.

AAS are prohibited by WADA at all times, in and out of competition. Any trace of these substances or their metabolites is sufficient to report an

adverse analytical finding. Therefore, it is important to apply the most sensitive methods and to keep working on the discovery of new metabolites that can be detected for a longer time after the administration of the drug, the so-called long-term metabolites.

Routine methods for the detection of AAS have been mostly based on GC–MS operating in selected ion monitoring mode [3]. The use of GC–MS/MS methods in selected reaction monitoring (SRM) mode is gradually becoming more popular due to the improvement in sensitivity and selectivity [4, 5].

However, the high fragmentation of the compounds in the electron ionization (EI) source can hamper the selection of an adequate precursor ion in these strategies, because quite often, the molecular ion shows a very low relative abundance or it is even absent. For these reason, it cannot be used as precursor ion.

Moreover, the low abundance of the molecular ion when using EI sources also hampers the detection and elucidation of new metabolites. Several approaches have been described for the detection of unknown metabolites based either on the acquisition of open scan methods [6, 7] or on the selection of theoretical transitions for expected metabolites [3, 8]. GC–EI–MS methods show some limitations for this purpose like (1) the difficulties in establishing the molecular formula for a new metabolite due to the common absence of the molecular ion and (2) the difficulties to predict a theoretical transition for a previously unknown but expected metabolites. For these reasons, the study of AAS ionization and fragmentation using alternatives interfaces can be very useful.

Liquid chromatography coupled to mass spectrometry (LC–MS) with atmospheric pressure interfaces (API) has proved to be an excellent

complement to GC–MS in the detection of AAS [9], particularly for those compounds with low thermal stability that present problems in derivatization, e.g. steroids bearing a 4-9-11-triene nucleus [9-11]. Additionally, the soft ionization of API sources generates adequate/abundant precursor ions, which facilitates the development of sensitive SRM methods for AAS using LC–MS/MS [12]. Together with the generation of adequate precursor ions, the established relationship between API ionization and structure is a useful tool for the elucidation of new metabolites [13, 14]. However, AAS ionization by API is not universal, and only those compounds with an ionizable center can be detected. The consequence is that important AAS biomarkers, such as the totally reduced metabolites, are missed by this technique [13, 14]. The appearance of commercial atmospheric pressure chemical ionization (APCI) interfaces for GC opened new lines of research for improving the detection of known steroids/metabolites and the discovery of new ones. Since the introduction of the APCI interface to a GC instrument by Horning *et al*. in 1977 [15], this interface has undergone several modifications over the years.

Several works have been carried out using GC–API–MS for the analysis of steroids [16, 17]. These articles show the high potential of microchip atmospheric pressure photoionization combined with GC–MS for the detection of AAS. However, up to our knowledge, the relationship between steroid atmospheric pressure ionization and its structure has not been studied. Recently, a new APCI source using a purge of nitrogen gas has been commercialized [18, 19]. This interface promotes ionization with very little fragmentation resulting in the formation of $[M+H]^+$ or $M^{+\bullet}$ ions as the base peaks of the mass spectrum, as occurs in LC–MS. Figure 1a and 1b shows common reactions that take place in the source. Ionization presents two possible mechanisms, charge transfer (in which the principal ion is $M^{+\bullet}$) or

protonation (in which the principal ion is $[M+H]^+$). Using modifiers such as water or methanol, protonation can be forced in order to enhance the presence of $[M+H]^+$. Water molecules react with the nitrogen plasma ions generating H_3O^+ which in turn produces analyte ions such as $[M+H]^+$ by proton transfer reactions. The reduced fragmentation observed by using this new source can have a significant impact on target analysis at trace levels.

Since its first application for metabolic profiling in 2009 [20], the usefulness of this interface has been demonstrated in several fields [21-26] but, up to our knowledge, it has not been applied yet to the doping control analysis.

The main aim of this work is the study of the AAS ionization with the recently commercialized APCI interface by GC–MS using a quadrupole time of flight (QTOF) analyzer in order to establish relationships between the ionization behavior and the AAS structure. For this purpose, 60 AAS with different chemical structures and their derivatized compounds have been selected, and their ionization behavior has been studied.

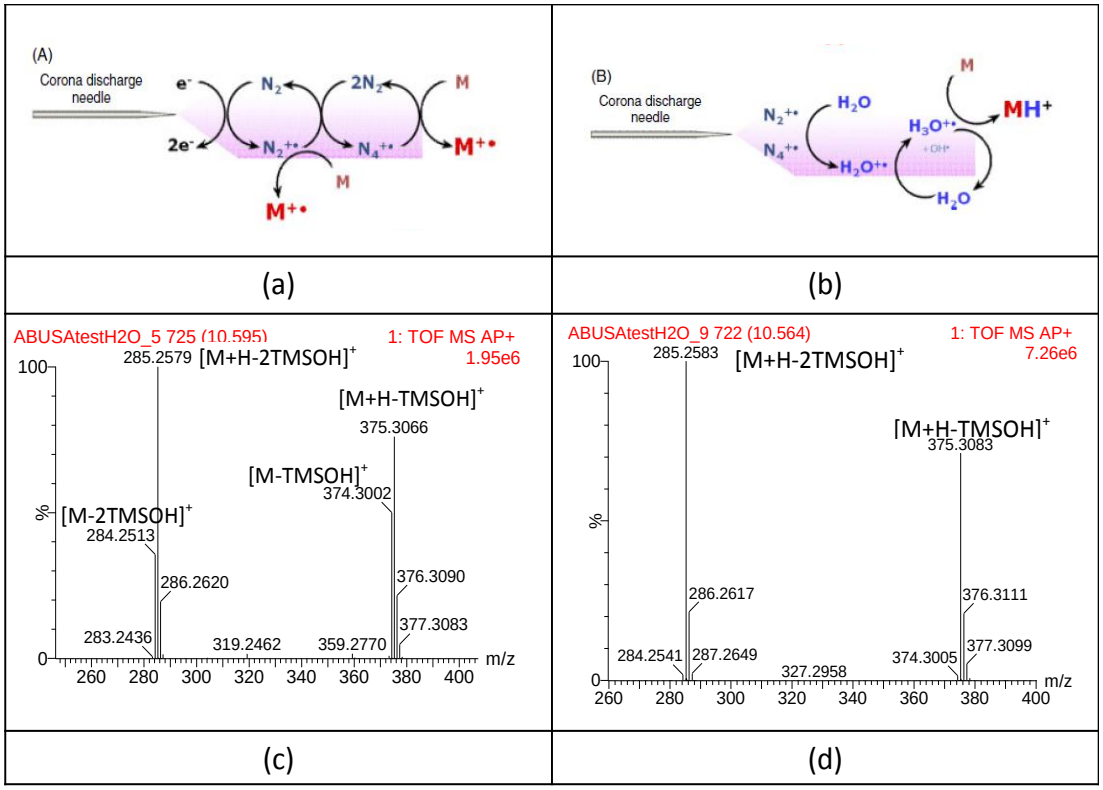

Figure 1. Ionization reactions in APGC source: (a) N_2 transfer conditions, (b) proton transfer conditions, (c) full-scan TOFMS spectra for TMS-derivatized BOLASmet under N_2 transfer conditions and (d) full-scan TOFMS spectra for TMS-derivatized BOLASmet under proton transfer conditions.

Experimental

Chemical and reagents

Structure information of the selected steroids is shown in Table 1. Androstenedione (AED), ethisterone (DANmet), testosterone (T), methandienone (MTD), boldenone (BD) and 11β-hydroxy-etiocholanolone (11OH-Etio) were obtained from Sigma (St. Louis, MO, USA). 1-Androstenedione (1-AED), 6α-hydroxy-androstenedione (6OH-AED),

fluoxymesterone (FLU), methenolone (METH), mibolerone (MIB), 4,6-androstadien-3,17-dione (4,6-AD), 6-dehydrotestosterone (6-T), androstatrienedione (ATD), trenbolone (TREN), 11β-hydroxy-androsterone (11OH-Andros), oxandrolone (OXA), 16-androstenol (16AOL) were obtained from Steraloids (Newport, RI, USA). 4-hydroxy-androstenedione (4OH-AED), 4-hydroxy-nandrolone (4OH-NAN), 4-hydroxy-testosterone (4OH-T), 17β-hydroxy-5β-androstan-1-ene-3-one (BDmet), 1-testosterone (1-T), epitestosterone (E), 9α-fluoro-11β-hydroxy-17,17-dimethyl-18-norandrosta-4,13-diene-3-one (FLUmet), 17α-metyl-1-testosterone (1-MeT), 1,4-androstadien-3,17-dione (1,4-AD), 6β-hydroxy-4-chloromethandienone (6OH-4Cl-MTD), epimethandienone (epiMTD), 6β-hydroxy-methandienone (6OH-MTD), methyldienolone (MDONE), tetrahydrogestrinone (THG), androsterone (Andros), Etiocholanolone (Etio), 4-chloro-3α-hydroxy-androst-4-en-17-one (CLOSmet), dehydroepiandrosterone (DHEA), dihydrotestosterone (DHT), 3α-hydroxy-2α-methyl-5α-androstan-17-one (DROSmet), 3α-hydroxy-1α-methyl-5α-androstan-17-one (MESTmet), 3α-hydroxy-1-methylen-5α-androstan-17-one (METHmet), 3α-hydroxy-5α-estran-17-one (NANmet1), 3α-hydroxy-5β-estran-17-one (NANmet2), 5α-androstane-3α,17β-diol (5α3α-DIOL), 5α-androstane-3β,17β-diol (5α3β-DIOL), 5β-androstane-3α,17β-diol (5β3α-DIOL), 5β-androstan-7α,17α-dimethyl-3α,17β-diol (BOLASmet), 5β-androstan-7β,17α-dimethyl-3α,17β-diol (CALUSmet), 17β-methyl-5β-androst-1-en-3α,17α-diol (MTDmet3), 17,17-dimethyl-18-nor-5β-androsta-1,13-dien-3α-ol (MTDmet4), 5α-androstan-17α-methyl-3α,17β-diol (MeTmet1), 5β-androstan-17α-methyl-3α,17β-diol (MeTmet2), 13β,17α-diethyl-5α-gonane-3α,17β-diol (NORBOLmet1), 13β,17α-diethyl-5β-gonane-3α,17β-diol (NORBOLmet2) and 17α-ethyl-5β-estrane-3α,17β-diol (NORETHANmet1) were purchased from NMI (Pymble, Australia). 6-Oxo-androstenedione (6OXO-AED), oxymesterone (OXY), methyltestosterone (MeT), stenbolone (STEN) and madol (MADOL)

were provided by the Toronto Research Chemicals (Toronto, Canada). 5α-Androstan-2α, 17α-dimethyl-3α, 17β-diol (METHASmet1) was a kind gift from the World Association of Anti-Doping Scientists (WAADS).

For underivatized AAS, stock standard solutions at 10 and 100 µg/mL were prepared by dissolving reference standards in methanol and they were stored at –20 °C. Working AAS standard solutions at 1 µg/mL were prepared by dilution of stock solution in acetone. Derivatized compounds were prepared from stock solutions in order to obtain a final concentration of 10 µg/mL.

Reagents, N-methyl-N-trimethylsilyltrifluoracetamide (MSTFA), ammonium iodide (NH_4I) and 2-mercaptoethanol were purchased from Sigma-Aldrich Química SA (Madrid, Spain). Acetone and methanol were purchased form Scharlab (Barcelona, Spain).

Table 1. Structural information of the groups of steroids investigated

Compound	Ring A	Ring B	Ring C	Ring D
General Steroid Structure 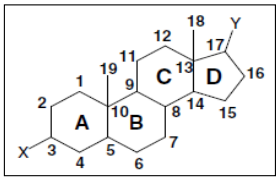				
Group I.				
AED	Δ^4 ^{3}CO	-	-	^{17}CO
1-AED	Δ^1 ^{3}CO	-	-	^{17}CO
1-T	Δ^1 ^{3}CO	-	-	^{17}OH
4OH-AED	Δ^4 ^{3}CO ^{4}OH	-	-	^{17}CO
4OH-NAN	Δ^4 ^{3}CO ^{4}OH nor $^{19}CH_3$	-	-	^{17}CO
4OH-T	Δ^4 ^{3}CO ^{4}OH	-	-	^{17}OH
6OH-AED	Δ^4 ^{3}CO	^{6}OH	-	^{17}CO
6oxo-AED	Δ^4 ^{3}CO	^{6}CO	-	^{17}CO
BDmet	Δ^1 ^{3}CO	-	-	^{17}OH
DANmet	Δ^4 ^{3}CO	-	-	^{17}OH ^{17}C≡C
E	Δ^4 ^{3}CO	-	-	^{17}OH
FLU	Δ^4 ^{3}CO	^{9}F	^{11}OH	^{17}OH $^{17}CH_3$
FLUmet	Δ^4 ^{3}CO	^{9}F	^{11}OH nor $^{19}CH_3$	^{17} CH_3 $^{17}CH_3$
METH	Δ^1 ^{3}CO $^1CH_3$	-	-	^{17}OH
M-1-T	Δ^1 ^{3}CO	-	-	^{17}OH $^{17}CH_3$
MeT	Δ^4 ^{3}CO	-	-	^{17}OH $^{17}CH_3$
MIB	Δ^4 ^{3}CO nor $^{19}CH_3$	$^7CH_3$	-	^{17}OH $^{17}CH_3$
OXY	Δ^4 ^{3}CO ^{4}OH	-	-	^{17}OH $^{17}CH_3$
STEN	Δ^1 $^2CH_3$ ^{3}CO	-	-	^{17}OH
T	Δ^4 ^{3}CO	-	-	^{17}OH

Table 1. (Cont.)

Compound	Ring A	Ring B	Ring C	Ring D
Group II.				
1,4-AD	$\Delta^{1,4}$ ^{3}CO	-	-	^{17}CO
4,6-AD	Δ^{4} ^{3}CO	Δ^{6}	-	^{17}CO
6OH-4Cl-MTD	$\Delta^{1,4}$ ^{3}CO ^{4}Cl	^{6}OH	-	^{17}OH ^{17}CH$_3$
6-T	Δ^{4} ^{3}CO	Δ^{6}	-	^{17}OH
ATD	$\Delta^{1,4}$ ^{3}CO	Δ^{6}	-	^{17}CO
BD	$\Delta^{1,4}$ ^{3}CO	-	-	^{17}OH
epiMTD	$\Delta^{1,4}$ ^{3}CO	-	-	^{17}OH ^{17}CH$_3$
MTD	$\Delta^{1,4}$ ^{3}CO	-	-	^{17}OH ^{17}CH$_3$
MTDmet1	$\Delta^{1,4}$ ^{3}CO	^{6}OH	-	^{17}OH ^{17}CH$_3$
MDONE	Δ^{4} ^{3}CO nor ^{19}CH$_3$	Δ^{9}	-	^{17}OH ^{17}CH$_3$
THG	Δ^{4} ^{3}CO	Δ^{9}	Δ^{11} ^{13}CH$_2$CH$_3$	^{17}OH ^{17}CH$_2$CH$_3$
TREN	Δ^{4} ^{3}CO nor ^{19}CH$_3$	Δ^{9}	Δ^{11}	^{17}OH
Group III.				
11OH-Andros	^{3}OH 5αH	-	^{11}OH	^{17}CO
11OH-Etio	^{3}OH 5βH	-	^{11}OH	^{17}CO
Andros	^{3}OH 5αH	-	-	^{17}CO
CLOSmet	Δ^{4} ^{3}OH ^{4}Cl	-	-	^{17}CO
DHEA	^{3}OH	Δ^{5}	-	^{17}CO
DHT	^{3}CO 5αH	-	-	^{17}OH
DROSmet	^{2}CH$_3$ ^{3}OH 5αH	-	-	^{17}CO
Etio	^{3}OH 5βH	-	-	^{17}CO
MESTmet	^{1}CH$_3$ ^{3}OH 5αH	-	-	^{17}CO
METHmet	^{1}C=CH$_2$ ^{3}OH 5αH	-	-	^{17}CO
NANmet1	^{3}OH 5αH nor ^{19}CH$_3$	-	-	^{17}CO
NANmet2	^{3}OH 5βH nor ^{19}CH$_3$	-	-	^{17}CO
OXA	^{3}CO ^{2} –O– 5αH	-	-	^{17}OH ^{17}CH$_3$

Table 1. (Cont.)

Compound	Ring A	Ring B	Ring C	Ring D
Group IV.				
16-AOL	^{3}OH 5αH	-	-	Δ^{16}
5a3a-DIOL	^{3}OH 5αH	-	-	^{17}OH
5a3b-DIOL	^{3}OH 5αH	-	-	^{17}OH
5b3aDIOL	^{3}OH 5βH	-	-	^{17}OH
BOLASmet	^{3}OH 5βH	$^{7}CH_3$	-	^{17}OH $^{17}CH_3$
CALUSmet	^{3}OH 5βH	$^{7}CH_3$	-	^{17}OH $^{17}CH_3$
MADOL	Δ^{2} 5αH	-	-	^{17}OH $^{17}CH_3$
MTDmet3	Δ^{1} ^{3}OH 5βH	-	-	^{17}OH $^{17}CH_3$
MTDmet4	Δ^{1} ^{3}OH 5βH	-	Δ^{13} nor$^{18}CH_3$	$^{17}CH_3$ $^{17}CH_3$
METHASmet1	$^{2}CH_3$ ^{3}OH 5αH	-	-	^{17}OH $^{17}CH_3$
MeTmet1	^{3}OH 5αH	-	-	^{17}OH $^{17}CH_3$
MeTmet2	^{3}OH 5βH	-	-	^{17}OH $^{17}CH_3$
NORBOLmet1	^{3}OH 5αH nor $^{19}CH_3$	-	$^{13}CH_2CH_3$	^{17}OH ^{17} CH_2CH_3
NORBOLmet2	^{3}OH 5βH nor $^{19}CH_3$	-	$^{13}CH_2CH_3$	^{17}OH ^{17} CH_2CH_3
NORETHANmet1	^{3}OH 5βH nor $^{19}CH_3$	-	-	^{17}OH $^{17}CH_2CH_3$

Derivatization method

The derivatization protocol employed in this study is based on the use of a mixture of MSTFA/NH_4I/2-mercaptoethanol in order to obtain the enol-trimethylsylil (TMS) derivatives of the analytes. Derivatized standards were prepared by adding 100 µL MSTFA/NH_4I/2-mercaptoethanol (1000/2/6; *v/w/v*) and heating at 60 °C for 20 min.

Instrumentation

A GC system (Agilent 7890A, Palo Alto, CA, USA) equipped with an Agilent 7693 autosampler and a split/splitless injector port was coupled to a QTOF mass spectrometer Xevo G2 QTOF (Waters Corporation, Manchester, UK) by means of an APCI source, commercialized as APGC source.

For derivatized compounds, an HP Ultra 1 capillary column (length 16.5 m × I.D. 0.25 mm × 0.11 µm of film thickness) was used for the chromatographic separation. The oven program was: 90 °C, 20 °C/min to 300 °C (5 min). Split injections (ratio 1:10) of a 1µL sample were carried out having the injector port at 280 °C. For underivatized compounds, an HP Ultra 2 column (length 12 m × I.D. 0.2 mm × 0.33 µm of film thickness) was used. The oven program in this case was: 90 °C (1 min), 20 °C/min to 300 °C (3 min). Splitless injections of 1 µL of the sample were carried out having the injector port at 280 °C. For both, derivatized and underivatized compound analyses, constant pressure mode was used at 25.8 psi.

The temperature in the source was set to 150 °C. Nitrogen was used as auxiliary gas at 150 L/h, make-up gas at 18L/h and cone gas at 16 L/h. APCI corona pin was fixed at 1 µA for underivatized and 1.6 µA for derivatized compounds, and cone voltage was 30 V, in both cases. APCI positive polarity

was selected. The ionization process occurred within an enclosed chamber, which enabled control over the protonation/charge transfer processes.

Xevo G2 QTOF was operated at a scan time of 0.3 s acquiring in a mass range of *m/z* 50–650 using a multi-channel plate voltage of 3350 V. TOF MS resolution mass was approximately 18 000 (FWHM) at *m/z* 614. Heptacosa (Sigma-Aldrich, Madrid, Spain), was used for the daily mass calibration. Internal calibration was performed using a background ion coming from the GC-column bleed as lock mass (protonated molecule of octamethylcyclotetrasiloxane, *m/z* 297.0830).

Results and discussion

Selection of model compounds

Sixty AAS including both parent steroids and metabolites were selected on the basis of their structural differences (Table 1). AAS structures share a common cyclopentaneperhydrophenantrene skeleton with normally between one and three oxygen atoms. These atoms are the only structural features in AAS with lone pairs, and, therefore, they are the most feasible ionization centers. Taking into account the proton affinity of the oxygen containing moieties [28], the expected order for AAS protonation would be: AAS containing a conjugated carbonyl > AAS with unconjugated carbonyl > AAS with hydroxyl functions. For this reason and, in order to make the study more comprehensive, model AAS was divided into four groups attending to their chemical structures:

- Group I. Compounds containing a mono-conjugated carbonyl. Testosterone and steroids with similar structure are included in this group.
- Group II. Compounds containing a poly-conjugated carbonyl function. Boldenone and Trenbolone are included in this group.
- Group III. Compounds containing an unconjugated keto function in their structure. Most of compounds included in this group presented the carbonyl function in C17, with the exceptions of DHT and OXA in which the carbonyl function was in C3.
- Group IV. Compounds with no-keto function in their structure. Androstanediols are included in this group.

Derivatization process

As mentioned in the introduction section, steroid analysis by GC–MS usually requires a previous derivatization step. Although it is a time-consuming procedure, it improves the chromatographic behavior of hydroxylated AAS allowing the profiling of both polar and non-polar AAS [10, 29]. The most common derivatization reaction for steroids is the trimethylsilylation, where active hydrogens on hydroxyl or enol groups are replaced with TMS groups [30]. In the doping control field, this derivatization process is based on the methodology developed by Donike in 1969 which consist on the use of N-methyl-N-trimethylsilyltrifluoracetamide in conjunction with NH_4I as a derivatization reagent for those compounds containing hydroxyl and ketone groups [31]. 2-Mercaptoethanol is added as a reducing agent to minimize the formation of iodine; which can degrade the mixture. This approach is the most widely used in the field [32], and it has shown excellent results in doping control screening, allowing the detection of

a large number of steroids, β2 agonists and other substances like endogenous glucocorticosteroids [27].

However, it is possible to analyze steroids by GC–MS without derivatization at higher concentration, as, for example, in the identification of some endogenous steroids [33, 34], or in the structural elucidation of AAS metabolites [35, 36].

For these reasons, the ionization behavior of both underivatized AAS and TMS AAS derivatives by APCI–GC–MS was investigated. Relationships between APCI ionization and structure were studied separately since complementary information can be obtained when analyzing underivatized and TMS-derivatized analytes.

Optimization of the ionization parameters

The 'soft' ionization behavior of the APCI interface was tested using AAS standards underivatized and TMS derivatized. As mentioned in the introduction (Figs. 1a and 1b), two ionization mechanisms can take place in the source: (1) charge transfer reaction from nitrogen make up gas or proton transfer reaction and (2) promotion of protonation reaction with the addition of water in the source as a modifier. In some occasions, protonation produced by only the water vapor traces present in ambient air of the ion chamber can also be observed.

Some preliminary experiments regarding the analyte ionization were made in order to evaluate the effect of water in the ion chamber. A subset of two analytes belonging to the different groups was selected for analysis with

and without the presence of water. Both underivatized and derivatized steroids were tested.

In experiments without water, we observed that, together with the expected molecular ion $M^{+\cdot}/[M\text{-}H_2O]^{+\cdot}$, considerable amounts of the $[M+H]^+/[M+H\text{-}H_2O]^+$ ions in the charge transfer spectrum were also formed. Similar results (showing the $[M+H\text{-}TMSOH]^+$ and the $[M\text{-}TMSOH]^{+\cdot}$ instead the $[M+H\text{-}H_2O]^+$ and the $[M\text{-}H_2O]^{+\cdot}$, respectively) were obtained for derivatized AAS (see Fig. 1c). The simultaneous occurrence of the two mentioned mechanisms, i.e. charge transfer and proton transfer from water vapor traces, seemed to show a tendency of steroids to be protonated. Taking into account this consideration, similar experiments were repeated but adding water as a modifier in the source. In this way, the proton transfer mechanism was enhanced, causing an increase in the relative abundance of $[M+H]^+$ (see Fig. 1d).

Therefore, we decided to use water as modifier for further experiments. This fact should be taken into account for the following discussion of the results.

Group I: AAS containing mono-conjugated keto function

Table 2 shows the ions for derivatized and underivatized steroids from Group I observed with APCI. A summary on the ionization behavior for these compounds is described below.

When underivatized, all analytes belonging to this group exhibited a prominent $[M+H]^+$ due to the protonation of the keto function. A less

abundant $[M+H-H_2O]^+$ was also observed with relative abundances lower than 30%. No relationship could be established between the presence/relative abundance of $[M+H-H_2O]^+$ and additional structural features. Any attempt to determine a relationship between structure and the number of observed losses of water was also unsuccessful.

Enol-TMS derivatization of AAS from group I followed the expected behavior, and all oxygen atoms of the molecule were derivatized. Similarly to their underivatized counterparts, TMS derivatives from group I showed the $[M+H]^+$ as the base peak of the spectrum. A $[M+H-TMSOH]^+$ ion was also observed in most cases. The relative abundance of this ion (normally above 40%) was higher than the corresponding $[M+H-H_2O]^+$ shown in underivatized AAS. The neutral loss of TMSOH can be generated either after protonation of the TMS ether or by remote loss of TMSOH after protonation of the enol-TMS ether (Fig. 2a). The high proton affinity of the TMS ether compared with the hydroxyl group can explain the differences in relative abundance observed for this loss between TMS derivatives and underivatized analytes.

The occurrence of abundant $[M+H-TMSOH]^+$ could be linked to the structure of the D ring of the AAS. Thus, those analytes with a hydroxyl group in the D ring exhibited an abundant $[M+H-TMSOH]^+$, whereas this ion was absent (or with a relative abundance lower than 10%) in those AAS having a carbonyl (AED, 1-AED, 4OH-AED, 6OH-AED and 6OXO-AED) or a 17,17-dimethyl (FLUmet) functions. A feasible explanation for this observation is the formation of a keto-enol equilibrium when a keto function is derivatized and subsequently protonated (Fig. 2b). The formation of this equilibrium would increase stability and avoid the neutral loss of TMSOH observed after protonation of a derivatized hydroxyl group (Fig. 2a).

4OH-T is shown as an illustrative example of this group in Fig. 3. The spectra of both underivatized (Fig. 3a) and TMS-derivatized 4OH-T (Fig. 3b) showed the $[M+H]^+$ as the base peak. In the case of the TMS derivatized, the $[M+H\text{-}TMSOH]^+$ ion was also relatively abundant.

Group II: AAS containing poly-conjugated keto function

Similar to Group I, the ionization of underivatized steroids from Group II in APCI source generated mainly $[M+H]^+$ being $[M+H\text{-}H_2O]^+$ also present with relative abundances normally lower than 30% (see Table 3). The main exception for this common behavior was 6OH-4Cl-MTD and MTDmet1 in which the $[M+H\text{-}H_2O]^+$ had 50% and 95% relative abundance, respectively. The presence of the hydroxyl group in C6 can be the driving force for this behavior. However, this abundant $[M+H\text{-}H_2O]^+$ was not observed in 6-hydroxy analytes belonging to group I like 6OH-AED. This fact suggests that either the extra conjugation of the keto function or the configuration of the hydroxyl group in C6 can also play an important role in this behavior.

The number of water losses observed for underivatized analytes from group II was always one less than the sum of hydroxyl and carbonyl functions of the molecule. This result can be due to the extra conjugation of the keto function, which might difficult the loss of the CO oxygen as water.

Enol-TMS derivatization is problematic for polyconjugated carbonyl functions [10, 11]. This limiting factor was also observed in our study. On one hand, incomplete derivatization was obtained for some compounds as ATD and 6OH-4Cl-MTD in which the most abundant peaks corresponded to species containing one underivatized oxygen (Table 3). On the other hand, compounds with the polyconjugation extended to A, B and C rings showed

several peaks in the chromatogram, some of them coming from derivatization artefacts. This was the case of THG where the most abundant peak corresponded to $[M+H-2Da]^+$ probably arising from the protonated molecule of an oxidation product formed during derivatization.

Steroids with satisfactory derivatization properties followed the ionization behavior described for Group I and summarized in Fig. 2a and 2b. Thus, those analytes with a carbonyl moiety in C17 did not show an abundant $[M+H-TMSOH]^+$, whereas those with a hydroxyl function in C17 commonly presented a relative abundance for this ion higher than 40%.

BD is shown as an illustrative example for AAS from Group II (Fig. 3). Similar to Group I, $[M+H]^+$ was found to be the main peak in the underivatized spectra (Fig. 3c), whereas both $[M+H]^+$ and $[M+H-TMSOH]^+$ were observed in the TMS-derivatized one (Fig. 3d).

Group III: AAS containing unconjugated keto function

Compounds included in this group (Table 4) contain an unconjugated keto function in their structures. This keto function is normally present in C17 although two compounds (DHT and OXA) have it in C3. The position of the keto function seems to guide the ionization behavior of underivatized analytes from Group III. Similar to Groups I and II, the $[M+H]^+$ was the base peak for analytes with the carbonyl in C3, whereas the $[M+H]^+$ relative abundance was less than 30% for 17-oxo compounds (Table 4). Analytes with the keto function in C17 showed a prominent $[M+H-H_2O]^+$ (relative abundances higher than 60%) being in most cases the base peak of the spectrum.

Contrary to Groups I and II, an abundant $[M+H-2H_2O]^+$ was found in the spectra of underivatized compounds with unconjugated keto functions. The relative abundance of the $[M+H-2H_2O]^+$ was found to be dependent of the structural properties of C5. Thus, 5α-steroids exhibited $[M+H-2H_2O]^+$ions with relative abundances lower than 50%. On the other hand, 5β-steroids and steroids having a double bond in C5 (either Δ^5 or Δ^4) showed relative abundances for $[M+H-2H_2O]^+$ higher than 65%, being in some cases the base peak of the spectrum.

Finally, the number of water losses observed for this group was always the sum of hydroxyl and carbonyl functions present in the molecule.

The absence of any conjugated carbonyl moiety facilitated the derivatization of this group of analytes, and all hydroxyl and keto functions were converted to TMS groups. Similarly to the behavior observed for underivatized analytes, TMS-derivatives of compounds with a carbonyl group in C3 exhibited a $[M+H]^+$ as base peak of the spectrum. Regarding those analytes with a keto function in C17, different ionization behavior was observed depending on the structure at C5. Thus, 5α-analytes showed an abundant $[M+H]^+$ which was the base peak of the spectrum in all cases except for 11OH-Andros (70%). The relative abundance of the $[M+H]^+$ for TMS-derivatives of 5β-analytes and compounds with a double bond in C5 (either Δ^5 or Δ^4) was found to be approximately 50% with the main exception of 11OH-Etio (20%). In these analytes, the base peak of the spectrum was $[M+H-TMSOH]^+$.

An additional relationship between structure and ionization for TMS-derivatives was found in the study of the number of neutral losses of TMSOH. Similar to the behavior observed for Groups I and II, analytes with the carbonyl in C3 only exhibited the TMSOH loss coming from the hydroxyl group. However, steroids with a keto function in C17 showed as many TMSOH losses as oxygen atoms present in the molecule. This fact indicates that, although with low relative abundance (5–20%), the derivatizated keto function in C17 can be also lost as TMSOH.

In Fig. 3, an example of this group is displayed. Andros shows a minor peak at $[M+H]^+$ being the $[M+H-H_2O]^+$ the base peak of the mass spectrum. A $[M+H-2H_2O]^+$ was also observed (Fig. 3e). In the TMS derivatized, the $[M+H]^+$ becomes the base peak with an abundant $[M+H-TMSOH]^+$ also present in the spectrum (Fig. 3f).

Group IV: AAS with no-keto function in their structure

The last group contains compounds with no keto function in their structures, like hydroxyandrostanes and hydroxyandrostenes (Table 5). The main characteristic of the APCI spectrum for underivatized analytes from this group was the total absence of the $[M+H]^+$ (only a small $[M+H]^+$ signal representing a 5% was found for MADOL). This might be explained because protonation of the hydroxyl groups would facilitate the loss of water. The maximum possible number of losses of water was observed, i.e. a $[M+H-zH_2O]^+$ was detected for $C_xH_yO_z$ steroids. This $[M+H-zH_2O]^+$ ion was found to be the base peak of the spectrum.

No differences were observed in the spectra obtained for 5α and 5β-metabolites. However, a relationship was found between ionization behavior and the structural characteristics of the hydroxyl at C17. Analytes with a tertiary hydroxyl in C17 (17-alkyl-17-hydroxy steroids) exhibited lower relative abundances of $[M+H-H_2O]^+$ (<30%) than those containing a secondary alcohol in C17 ($[M+H-H_2O]^+$ relative abundances >60%).

Due to the absence of any keto function, the TMS derivatization of the analytes belonging to this group provided suitable derivatives. Contrary to the behavior observed for other groups, ionization of TMS derivatives from Group IV did not substantially differ from their underivatized counterparts (Table 5). Thus, similar structural considerations could be extracted from this study, for instance, the absence of $[M+H]^+$ which can be explained by the easy loss of TMSOH after the protonation of the TMS-ether function (Fig. 2c).

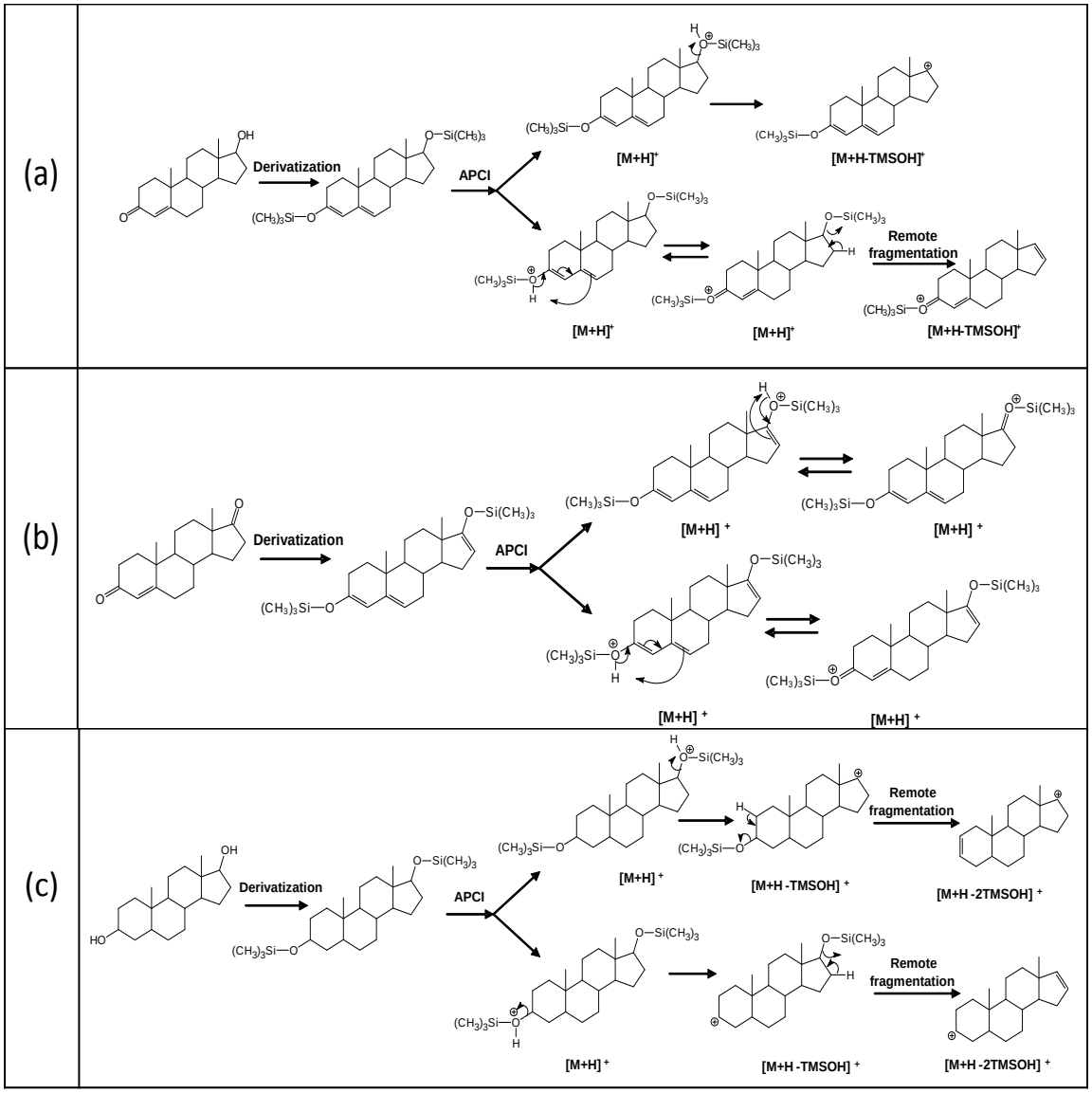

Figure 2. Ionization and in-source fragmentat ion pathways under proton transfer conditions for a) steroids with carbonyl function in C3 and hydroxyl function in C17, b) steroids with carbonyl functions in both C3 and C17, c) steroids with hydroxyl functions in both C3 and C17

In Fig. 3, the MS spectrum for MeTmet1 is shown as an example. In this case, $[M+H-2H_2O]^+$ appears as the base peak of the spectrum for the underivatized compound (Fig. 3g), whereas a prominent [M+H-2TMSOH]$^+$ was observed for the enol-TMS derivative (Fig. 3h). In both cases, minor ions corresponding to single losses of water or TMSOH were also observed.

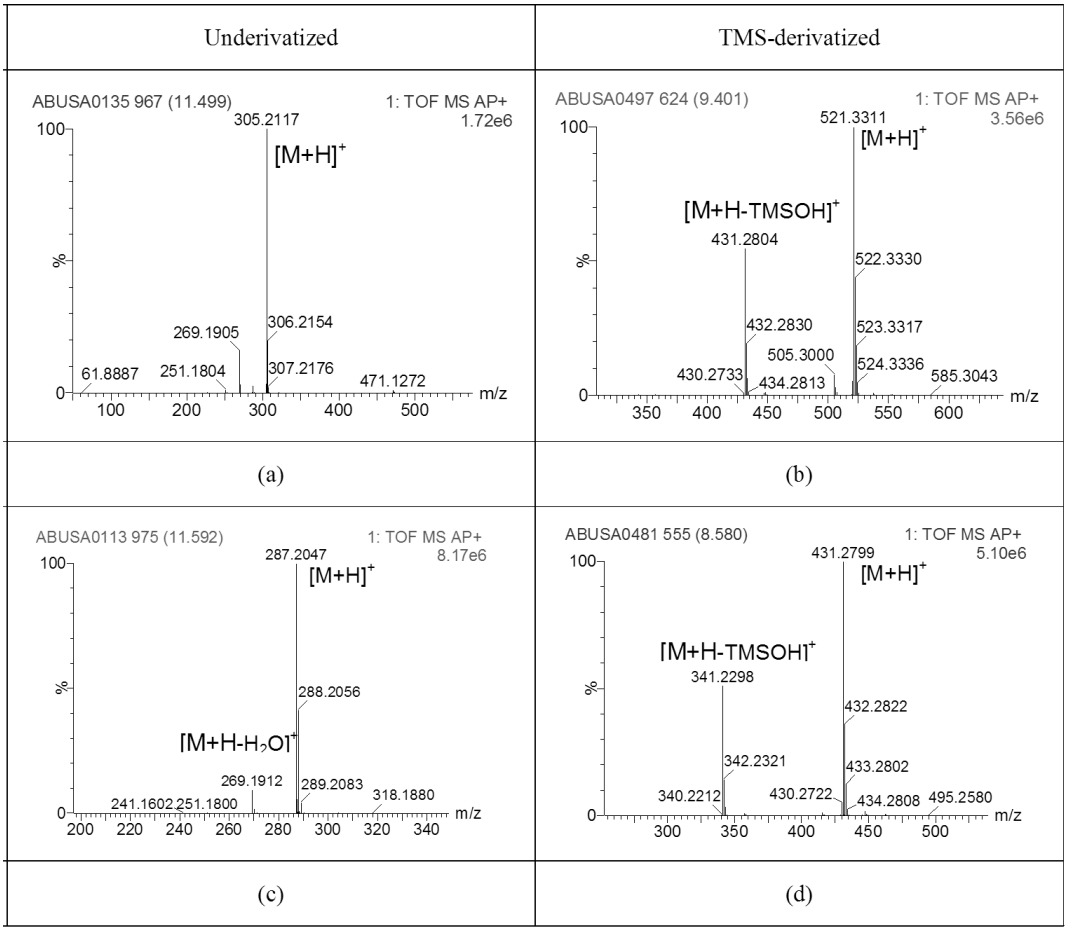

Figure 3. Full-scan TOFMS spectra, proton transfer conditions for selected compounds belonging to Group I: (a) Underiv. 4OH-T, (b) TMS- 4OH-T, Group II: (c) Underiv. BD, (d) TMS- BD, Group III: (e) Underiv. ANDROS, (f) TMS- ANDROS and Group IV: (g) Underiv. MeTmet1, (h) TMS- MeTmet1.

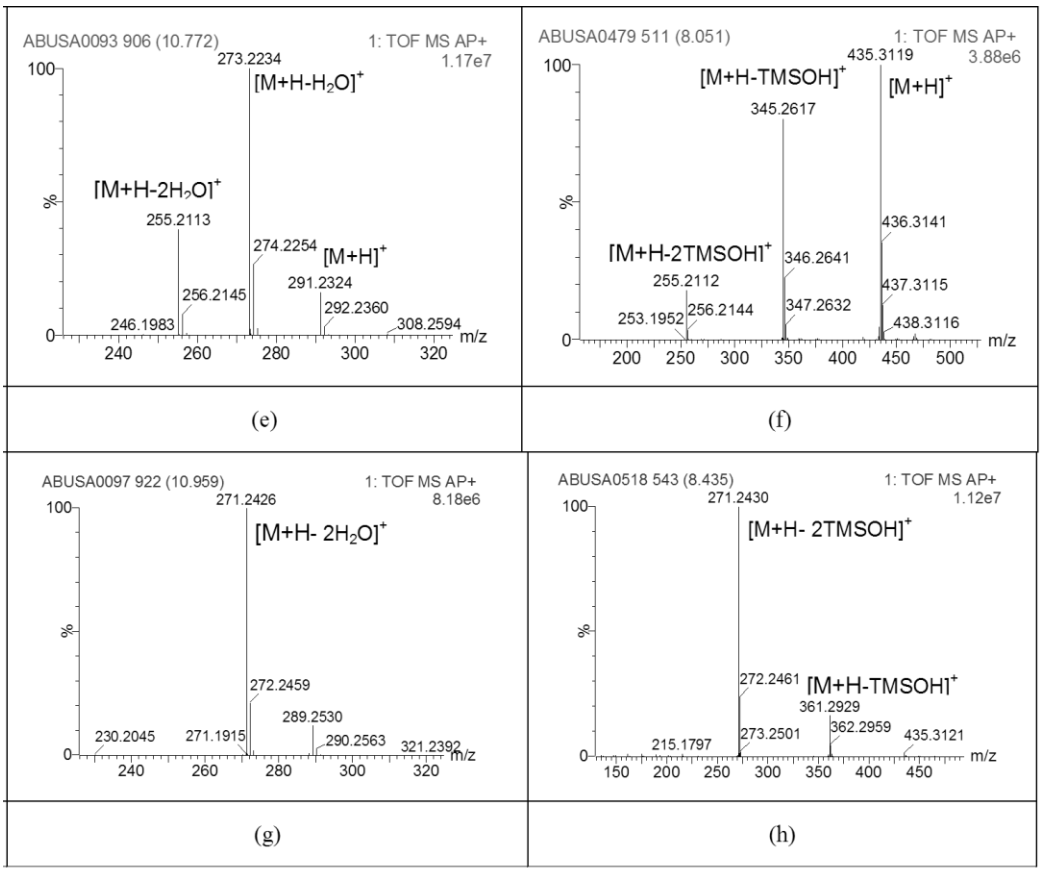

Figure 3 (Cont.)

Table 2. Group I. Retention times (RT) and *m/z* ions and relative abundances (in brackets) obtained for underivatized and TMS-derivatized steroids by GC-(APCI)(QTOF)-MS/MS

	Underivatized					TMS-derivatized				
Compound	Formula	RT (min)	$[M+H]^+$	$[M+H-H_2O]^+$	$[M+H-2H_2O]^+$	Derivative	RT (min)	$[M+H]^+$	$[M+H-TMSOH]^+$	$[M+H-2TMSOH]^+$
Group I.										
AED	$C_{19}H_{26}O_2$	11.34	287.2030 (100)	269.1910 (7)	-	bis-O-TMS	8.57	431.2884 (100)	-	-
1-AED	$C_{19}H_{26}O_2$	11.02	287.2012 (100)	269.1905 (30)	-	bis-O-TMS	8.33	431.2811 (100)	341.2310 (5)	-
1-T	$C_{19}H_{28}O_2$	11.10	289.2171 (100)	271.2060 (12)		bis-O-TMS	8.40	433.2953 (100)	343.2457 (50)	-
4OH-AED	$C_{19}H_{26}O_3$	11.35	303.1963 (100)	285.1853 (25)	267.1750 (15)	tris-O-TMS	9.32	519.3167 (100)	-	-
4OH-NAN	$C_{18}H_{26}O_3$	11.23	291.1958 (100)	273.1848 (10)	255.1747 (5)	tris-O-TMS	9.15	507.3155 (100)	417.2650 (50)	-
4OH-T	$C_{19}H_{28}O_3$	11.48	305.2117 (100)	-	269.1904 (18)	tris-O-TMS	9.40	521.3310 (100)	431.2805 (50)	-
6OH-AED	$C_{19}H_{26}O_3$	12.06	303.1957 (100)	285.1852 (22)	-	tris-O-TMS	9.18	519.3194 (100)	-	-
6OXO-AED	$C_{19}H_{24}O_3$	12.00	301.1822 (100)	283.1700 (18)	-	tris-O-TMS	9.08	517.3012 (100)	-	-
BDmet	$C_{19}H_{28}O_2$	11.00	289.2168 (100)	271.2061 (26)	253.1957 (5)	bis-O-TMS	7.76	433.2979 (100)	343.2472 (70)	-
DANmet	$C_{21}H_{28}O_2$	11.70	313.2187 (100)	295.2067 (20)	-	bis-O-TMS	9.07	457.2977 (100)	367.2473 (70)	-
E	$C_{19}H_{28}O_2$	11.37	289.2171 (100)		-	bis-O-TMS	8.45	433.2985 (100)	343.2479 (55)	-
FLU	$C_{20}H_{29}FO_3$	13.21	337.2195 (100)	319.2075 (5)	301.1969 (10)	tris-O-TMS	9.68	553.3389 (100)	463.2884 (45)	353.2300 (3)
FLUmet	$C_{20}H_{27}FO_2$	11.08	319.2081 (100)		-	bis-O-TMS	8.38	463.2930 (100)	373.2373 (5)	-
METH	$C_{20}H_{30}O_2$	12.01	303.2373 (100)	285.2229 (30)	-	bis-O-TMS	8.76	447.3133 (100)	357.2628 (60)	267.2113 (5)
1-MeT	$C_{20}H_{30}O_2$	11.23	303.2335 (100)	285.2221 (12)	-	bis-O-TMS	8.76	447.3143 (100)	357.2635 (60)	-
MeT	$C_{20}H_{30}O_2$	11.40	303.2324 (100)	285.2214 (12)	-	bis-O-TMS	9.01	447.3163 (100)	357.2648 (70)	-
MIB	$C_{20}H_{30}O_2$	11.40	303.2332 (100)	285.2219 (22)	-	bis-O-TMS	8.82	447.3153 (100)	357.2639 (60)	-
OXY	$C_{20}H_{30}O_3$	11.61	319.2276 (100)	301.2168 (6)	283.2064 (15)	tris-O-TMS	9.73	535.3494 (100)	445.2978 (55)	-
STEN	$C_{20}H_{30}O_2$	11.18	303.2336 (100)	285.2219 (12)	-	bis-O-TMS	8.60	447.3102 (100)	357.2606 (35)	-
T	$C_{19}H_{28}O_2$	11.40	289.2215 (100)	271.2072 (18)	253.1955 (5)	bis-O-TMS	8.63	433.2973 (100)	343.2472 (70)	-

Table 3. Group II. Retention times (RT) and *m/z* ions and relative abundances (in brackets) obtained for underivatized and TMS-derivatized steroids by GC-(APCI)(QTOF)-MS/MS

	Underivatized					TMS-derivatized				
Compound	Formula	RT (min)	$[M+H]^+$	$[M+H-H_2O]^+$	$[M+H-2H_2O]^+$	Derivative	RT (min)	$[M+H]^+$	$[M+H-TMSOH]^+$	$[M+H-2TMSOH]^+$
Group II.										
1,4-AD	$C_{19}H_{24}O_2$	11.46	285.1853 (100)	267.1753 (18)	-	bis-O-TMS	8.51	429.2664 (100)		-
4,6-AD	$C_{19}H_{24}O_2$	11.36	285.1853 (100)	267.1749 (8)	-	bis-O-TMS	8.51	429.2676 (100)	-	-
6OH-4Cl-MTD	$C_{20}H_{27}O_3Cl$	14.28	351.1732 (100)	333.1625 (50)	315.1521 (55)	bis-O-TMS	9.95	495.2533 (100)	405.2029 (10)	315.1521 (10)
6-T	$C_{19}H_{26}O_2$	11.55	287.2016 (100)	269.1905 (8)	-	bis-O-TMS	8.60	431.2825 (100)	341.2314 (45)	-
ATD	$C_{19}H_{22}O_2$	11.40	283.1711 (100)	265.1592 (25)		mono-O-TMS	8.50	355.2113 (100)	-	-
BD	$C_{19}H_{26}O_2$	11.59	287.2051 (100)	269.1910 (40)	-	bis-O-TMS	8.58	431.2799 (100)	341.2298 (50)	-
EpiMTD	$C_{20}H_{28}O_2$	11.73	301.2168 (100)	283.2061 (55)	-	bis-O-TMS	8.54	445.2991 (100)	355.2474 (40)	-
MTD	$C_{20}H_{28}O_2$	11.73	301.2161 (100)	283.2073 (5)	-	bis-O-TMS	8.93	445.2966 (100)	355.2462 (55)	-
MTDmet1	$C_{20}H_{28}O_3$	12.41	317.2115 (45)	299.2007 (95)	281.1902(100)	tris-O-TMS	9.50	533.3318 (100)	443.2812 (40)	-
MDONE	$C_{19}H_{26}O_2$	11.75	287.2012 (100)	269.1904 (10)	-	bis-O-TMS	8.96	431.2828 (100)	341.2317 (50)	-
THG	$C_{21}H_{28}O_2$	12.92	313.2168 (100)	295.2061 (12)	-	bis-O-TMS	9.55	[a]455.2823 (100)	[a]365.2319 (35)	-
TREN	$C_{18}H_{22}O_2$	11.67	271.1716 (100)	253.1590 (12)	-	bis-O-TMS	8.72	415.2472 (100)	325.1969 (45)	-

[a]Derivatized THG is detected as $[M+H-2Da]+$ probably coming from the $[M+H]^+$ of an oxidation product produced during derivatization

Table 4. Group III. Retention times (RT) and *m/z* ions and relative abundances (in brackets) obtained for underivatized and TMS-derivatized steroids by GC-(APCI)(QTOF)-MS/MS

	Underivatized						TMS-Derivatized				
Compound	Formula	RT (min)	$[M+H]^+$	$[M+H-H_2O]^+$	$[M+H-2H_2O]^+$	$[M+H-3H_2O]^+$	Derivative	RT (min)	$[M+H]^+$	$[M+H-TMSOH]^+$	$[M+H-2TMSOH]^+$
Group III.											
11OH-Andros	$C_{19}H_{30}O_3$	11.87	307.2276 (20)	289.2174 (65)	271.2076 (100)	253.1968 (30)	tris-O-TMS	8.66	523.3489 (70)	433.2981 (50)	343.24089 (100)
11OH-Etio	$C_{19}H_{30}O_3$	11.63	307.2279 (22)	289.2179 (100)	271.2070 (98)	253.1961 (43)	tris-O-TMS	8.69	523.3468 (20)	433.2982 (100)	343.2453 (70)
Andros	$C_{19}H_{30}O_2$	10.76	291.2333 (20)	273.2219 (100)	255.2111 (50)	-	bis-O-TMS	8.05	435.3119 (100)	345.2617 (80)	255.2112 (20)
CLOSmet	$C_{19}H_{27}ClO_2$	11.53	323.1775 (7)	305.1677 (62)	287.1570 (100)	-	bis-O-TMS	8.75	467.2578 (40)	377.2081 (100)	287.1574 (5)
DHEA	$C_{19}H_{28}O_2$	10.72	289.2177 (20)	271.2111 (100)	253.1974 (65)	-	bis-O-TMS	8.35	433.2980 (65)	343.2485 (100)	253.1962 (10)
DHT	$C_{19}H_{30}O_2$	11.03	291.2353 (100)	273.2219 (30)	255.2113 (22)	-	bis-O-TMS	8.53	435.3166 (100)	345.2656 (85)	-
DROSmet	$C_{20}H_{32}O_2$	10.89	305.2484 (10)	287.2383 (100)	269.2273 (30)	-	bis-O-TMS	8.21	449.3333 (100)	359.2816 (80)	269.2278 (5)
Etio	$C_{19}H_{30}O_2$	10.62	291.2328 (23)	273.2221 (100)	255.2114 (85)	-	bis-O-TMS	8.08	435.3128 (50)	345.2669 (100)	255.2115 (10)
MESTmet1	$C_{20}H_{32}O_2$	11.15	305.2475(7)	287.2375 (100)	269.2265 (20)	-	bis-O-TMS	8.41	449.3315 (100)	359.2800 (65)	269.2281 (10)
METHmet 1	$C_{20}H_{32}O_2$	11.02	305.2481 (33)	287.2375 (100)	269.2269 (25)	-	bis-O-TMS	8.33	447.3140 (100)	357.2633 (55)	267.2119 (5)
NANmet1	$C_{18}H_{28}O_2$	10.22	277.2168 (22)	259.2061 (100)	241.1955 (35)	-	bis-O-TMS	7.71	421.3008 (100)	331.2498 (80)	241.1968 (20)
NANmet2	$C_{18}H_{28}O_2$	10.35	277.2167 (22)	259.2060 (85)	241.1955 (100)	-	bis-O-TMS	7.92	421.2978 (50)	331.2482 (100)	241.1964 (13)
OXA	$C_{19}H_{30}O_3$	12.05	307.2300 (100)	289.2193 (95)	271.2070 (20)	-	mono-O-TMS	9.13	379.2668 (100)	289.2167 (40)	-

Table 5. Group IV. Retention times (RT) and *m/z* ions and relative abundances (in brackets) obtained for underivatized and TMS-derivatized steroids by GC-(APCI)(QTOF)-MS/MS

	Underivatized					TMS-Derivatized				
Compound	Formula	RT (min)	$[M+H]^+$	$[M+H-H_2O]^+$	$[M+H-2H_2O]^+$	Derivative	RT (min)	$[M+H]^+$	$[M+H-TMSOH]^+$	$[M+H-2TMSOH]^+$
Group IV.										
16-AOL	$C_{19}H_{30}O$	9.32	-	257.2223 (100)	-	mono-O-TMS	6.60	-	257.2334 (100)	-
5a3aDIOL	$C_{19}H_{32}O_2$	10.81	-	275.2391 (60)	257.2300 (100)	bis-O-TMS	8.13	-	347.2773 (20)	257.2272 (100)
5a3bDIOL	$C_{19}H_{32}O_2$	10.87	-	275.2369 (90)	257.2284 (100)	bis-O-TMS	8.47	-	347.2776 (50)	257.2279 (100)
5b3aDIOL	$C_{19}H_{32}O_2$	10.67	-	275.2376 (60)	257.2274 (100)	bis-O-TMS	8.16	-	347.2771 (70)	257.2268 (100)
BOLASmet	$C_{21}H_{36}O_2$	11.17	-	303.2690 (20)	285.2585 (100)	bis-O-TMS	8.75	-	375.3105 (70)	285.2620 (100)
CALUSmet	$C_{21}H_{36}O_2$	11.04	-	303.2697 (25)	285.2590 (100)	bis-O-TMS	8.65	-	375.3093 (15)	285.2629 (100)
MADOL	$C_{20}H_{32}O$	9.72	289.2531 (5)	271.2492 (100)	-	mono-O-TMS	7.47	361.2943 (5)	271.2440 (100)	-
MTDmet3	$C_{20}H_{32}O_2$	10.7	-	-	269.2271 (100)	bis-O-TMS	7.78	-	359.2781 (5)	269.2334 (100)
MTDmet4	$C_{20}H_{30}O$	9.36	-	269.2270 (100)	-	mono-O-TMS	6.83	-	269.2328 (100)	-
METHASmet1	$C_{21}H_{36}O_2$	11.09	-	303.2685 (18)	285.2583 (100)	bis-O-TMS	8.58	-	375.3116 (45)	285.2653 (100)
MeTmet1	$C_{20}H_{34}O_2$	10.97	-	289.2530 (12)	271.2426 (100)	bis-O-TMS	8.43	-	361.2929 (15)	271.2430 (100)
MeTmet2	$C_{20}H_{34}O_2$	10.75	-	289.2531 (20)	271.2429 (100)	bis-O-TMS	8.45	-	361.2962 (50)	271.2521 (100)
NORBOLmet1	$C_{21}H_{36}O_2$	11.43	-	303.2689 (15)	285.2584 (100)	bis-O-TMS	9.10	-	375.3097 (20)	285.2605 (100)
NORBOLmet2	$C_{21}H_{36}O_2$	11.51	-	303.2690 (20)	285.2590 (100)	bis-O-TMS	8.99	-	375.3102 (10)	285.2601 (100)
NORETHANmet1	$C_{20}H_{34}O_2$	11.09	-	289.2528 (20)	271.2423 (100)	bis-O-TMS	8.76	-	361.2946 (40)	271.2460 (100)

Conclusions

The use of a new APCI interface coupled to GC–QTOF has been investigated for the ionization of model AAS. The addition of water in the interface promoted the proton transfer reaction producing mainly protonated species, i.e. $[M+H]^+$ and $[M+H-H2O]^+$ (or $[M+H-TMSOH]^+$ for TMS derivatives). A relationship between ionization behavior and structure has been established. The main conclusions are summarized in Table 6.

Table 6. Summary of the relationships found between ionization behavior and structure for the different groups of compounds

Underivatized						
Group	**Primary structural feature**	**Secondary structural feature**	**$[M+H]^+$**	**$[M+H-H_2O]^+$**	**$[M+H-2H_2O]^+$**	**Water losses from $C_xH_yO_z$**
I	Mono-conjugated CO	-	100%	0-30%	0-15%	Variable
II	Poly-conjugated CO	^{6}H	100%	5-25%	*n.d.*	z-1
		^{6}OH	45-100%	50-95%	55-100%	z-1
III	Unconjugated CO	^{3}CO	100%	30-95%	~20%	z
		^{17}CO, 5α	7-33%	100%	20-50%	z
		^{17}CO, 5β/5ene	7-23%	62-100%	65-100%	z
IV	Hydroxylated	Secondary ^{17}OH	*n.d.*	60-90%	100%	z
		Tertiary ^{17}OH	0-5%	12-25%	100%	z

Table 6. (Cont.)

TMS-derivatized						
Group	**Primary structural feature**	**Secondary structural feature**	**$[M+H]^+$**	**$[M+H-TMSOH]^+$**	**$[M+H-2TMSOH]^+$**	**TMSOH losses from $C_xH_yO_z$**
I	Mono-conjugated CO	^{17}OH	100%	35-70%	0-5%	Variable (normally z-1)
		^{17}CO/ ^{17,17}diCH$_3$	100%	0-5%	*n.d.*	0
II	Poly-conjugated CO [a]	^{17}OH	100%	10-55%	*n.d.*	z-1
		^{17}CO	100%	*n.d.*	*n.d.*	0
III	Unconjugated CO	^{3}CO	100%	40-85%	*n.d.*	z-1
		^{17}CO, 5α	70-100%	50-80%	5-20% [b]	z
		^{17}CO, 5β/5ene	20-65%	100%	5-20% [b]	z
IV	Hydroxylated	Secondary ^{17}OH	*n.d.*	20-70% [c]	100%	z
		Tertiary ^{17}OH	0-5%	5-70% [c]	100%	z

[a] Results obtained for properly derivatized analytes
[b] Larger abundances for analytes with an extra hydroxyl group
[c] 100% for compounds with only one oxygen
***n.d.* not detected**

The low fragmentation observed in the APCI spectra (all ions contained the intact steroid skeleton) would facilitate the selection of abundant and/or more specific precursor ions in tandem MS experiments. Theoretically, this fact would lead to a neat sensitivity and selectivity improvement in SRM-based methods. The effect of this improvement in the control of the abuse of steroids in sports should be investigated.

Furthermore, the knowledge gained regarding the behavior of AAS ionization in the APCI source might be helpful in the identification and elucidation of unknown metabolites of steroids in urine. Thus, based on the information depicted in Table 6, a theoretical ion for a predicted metabolite can be postulated. This can help in the target detection of potential metabolites by GC–APCI–MS. Additionally, if an unknown steroid is detected

by untargeted methods, some valuable structural information can be obtained based on the results showed in this work.

Acknowledgements

The authors acknowledge the financial support of the Ministry of Education and Science, Spain, in the project DEP2011-28573-C02-01/02. The authors from University Jaume I also acknowledge the support from Generalitat Valenciana (Research Group of Excellence Prometeo/2009/054). The authors from IMIM acknowledge the support from Generalitat de Catalunya (Consell Català de l'Esport and DIUE 2009SGR4929).

M. Raro is also grateful to the Ministry of Education and Science for her predoctoral grant.

References

[1] P. Hemmersbach. History of mass spectrometry at the Olympic Games. J. Mass Spectrom. 2008, 43, 839.

[2] Anti-Doping Testing Figures Report. 2012. http://www.wada-ama.org/Documents/Resources/Testing-Figures/WADA-2012-Anti-Doping-Testing-Figures-Report-EN.pdf released April 2014

[3] C. Gómez, A. Fabregat, O. J. Pozo, J. Marcos, J. Segura, R. Ventura. Analytical strategies based on mass spectrometric techniques for the study of steroid metabolism. TrAC. Trends Anal. Chem. 2014, 53, 106.

[4] P. Van Eenoo, W. Van Gansbeke, N. De Brabanter, K. Deventer, F. T. Delbeke. A fast, comprehensive screening method for doping agents in urine by gas chromatography-triple quadrupole mass spectrometry. J. Chromatogr. A 2011, 1218, 3306.

[5] M. A. Delgadillo, L. Garrostas, O. J. Pozo, R. Ventura, B. Velasco, J. Segura, J. Marcos. Sensitive and robust method for anabolic agents in human urine by gas chromatography-triple quadrupole mass spectrometry. J. Chromatogr. B 2012, 897, 85.

[6] O. J. Pozo, K. Deventer, P. Van Eenoo, F. Delbeke. Efficient approach for the comprehensive detection of unknown anabolic steroids andmetabolites in human urine by liquid chromatography-electrospray-tandem mass spectrometry. Anal. Chem. 2008, 80, 1709.

[7] M. Thevis, H. Geyer, U. Mareck, W. Schänzer. Screening for unknown steroids in human urine by liquid chromatography-tandem mass spectrometry. J. Mass Spectrom. 2005, 40, 955.

[8] C. Gómez, O. J. Pozo, J. Marcos, J. Segura, R. Ventura. Alternative long-term markers for the detection of methyltestosterone misuse. Steroids 2013, 78, 44.

[9] O. J. Pozo, P. Van Eenoo, K. Deventer, F. T. Delbeke. Detection and characterization of anabolic steroids in doping analysis by LC-MS. TrAC Trends Anal. Chem. 2008, 27, 657.

[10] M. Galesio, R. Rial-Otero, J. Simal-Gándara, X. de la Torre, F. Botrè, J. L. Capelo-Martínez. Improved ultrasonic-based sample treatment for the screening of anabolic steroids by gas chromatography/mass spectrometry. Rapid Commun. Mass Spectrom. 2010, 24, 2375.

[11] E. M. Brun, R. Puchades, Á. Maquieira. Analytical methods for anti-doping control in sport: anabolic steroids with 4,9,11-triene structure in urine. TrAC Trends in Anal. Chem. 2011, 30, 771.

[12] O. J. Pozo, P. Van Eenoo, K. Deventer. Development and validation of qualitative screening method for the detection of exogenous anabolic steroids in urine by liquid chromatography-tandem mass spectrometry. Anal. Bioanal. Chem. 2007, 389, 1209.

[13] O. J. Pozo, P. Van Eenoo, K. Deventer, F. T. Delbeke. Ionization of anabolic steroids by adduct formation in liquid chromatography electrospray mass spectrometry. J. Mass Spectrom. 2007, 42, 467.

[14] Y.-C. Ma, H.-Y. Kim. Determination of steroids by liquid chromatography/Mass spectrometry. J. Am. Soc. Mass Spectrom. 1997, 8, 1010.

[15] E. C. Horning, D.I. Carroll, I. Dzidic, K. D. Haegele, S. Lin, C. U. Oertli, R. N. Stillwell. Development and use of analytical systems based on mass spectrometry. Clin. Chem. 1977, 23, 13.

[16] L. Hintikka, M. Haapala, T. Kuuranne, A. Leinonen, R. Kostiainen. Analysis of anabolic steroids in urine by gas chromatography-microchip atmospheric pressure photoionization-mass spectrometry with chlorobenzene as dopant. J. Chromatogr. A 2013, 1312, 111.

[17] L. Hintikka, M. Haapala, S. Franssila, T. Kuuranne, A. Leinonen, R. Kostiainen. Feasibility of gas chromatography-microchip atmospheric pressure photoionization-mass spectrometry in analysis of anabolic steroids. J. Chromatogr. A 2010, 1217, 8290.

[18] C. N. McEwen, R. G. McKay. A Combination Atmospheric Pressure LC/MS:GC/MS Ion Source: Advantages of Dual AP-LC/MS:GC/MS Instrumentation. J. Am. Soc. Mass Spectrom. 2005, 16, 1730.

[19] R. Schiewek, M. Lorenz, R. Giese, K. Brockmann, T. Benter, S. Gäb, O. J. Schmitz. Development of a multipurpose ion source for LC-MS and GC-API MS. Anal. Bioanal. Chem. 2008, 392, 87.

[20] A. Carrasco-Pancorbo, E. Nevedomskaya, T. Arthen-Engeland, T. Zey, G. Zurek, C. Baessmann, A. M. Deelder, O. A. Mayboroda. Gas chromatography/Atmospheric Pressure Chemical Ionization-time of flight mass spectrometry: Analytical validation and applicability to metabolic profiling. Anal. Chem. 2009, 81,10071.

[21] T. Portolés, J. V. Sancho, F. Hernández, A. Newton, P. Hancock. Potential of atmospheric pressure chemical ionization source in GC-QTOF MS for pesticide residue analysis. J. Mass Spectrom. 2010, 45, 926.

[22] T. Portolés, L. Cherta, J. Beltran, F. Hernández. Improved gas chromatography-tandem mass spectrometry determination of pesticide residues making use of atmospheric pressure chemical ionization. J. Chromatogr. A 2012, 1260, 183.

[23] T. Portolés, J. G. J. Mol, J. V. Sancho, F. Hernández. Advantages of atmospheric pressure chemical ionization in gas chromatography tandem mass spectrometry: Pyrethroid insecticides as a case study. Anal. Chem. 2012, 84, 9802.

[24] T. Bristowm M. Harrison, M. Sims. The application of gas chromatography/atmospheric pressure chemical ionisation time-of-flight mass spectrometry to impurity identification in Pharmaceutical Development. Rapid Commun. Mass Spectrom. 2010, 24, 1673.

[25] R. García-Villalba, T. Pacchiariotta, A. Carrasco-Pancorbo, A. Segura-Carretero, A. Fernández-Gutiérrez, A. M. Deelder, O. A. Mayboroda. Gas chromatography-atmospheric pressure chemical ionization-time of flight mass spectrometry for profiling of phenolic compounds in extra virgin olive oil. J. Chromatogr. A 2011, 1218, 959.

[26] C. Domeño, E. Canellas, P. Alfaro, A. Rodríguez-Lafuente, C. Nerin. Atmospheric pressure gas chromatography with quadrupole time of flight mass spectrometry for simultaneous detection and quantification of polycyclic aromatic hydrocarons and nitro-polycyclic aromatic hydrocarbons in mosses. J. Chromatogr. A 2012, 1252, 146.

[27] M. A. Sípoli, H. M. Gualberto, M. Costa, F. R. de Aquino. Analysis of synthetic 19-norsteroids trenbolone, tetrahdrogestrinone and gestrinone by gas chromatography-mass spectrometry. J. Chromatogr. A 2007, 1150, 215.

[28] E.P. Hunter, S.G. Lias. NIST Chemistry WebBook. National Institute of Standards and Technology (NIST): Gaithersburg, MD, 2005 URL: http://webbook.nist.gov/chemistry/

[29] J. A. Bowden, D. M. Colosi, D. C. Mora-Montero, T. J. Garrett, R. A. Yost. Enhancement of chemical derivatization of steroids by gas chromatography/mass spectrometry (GC/MS). J. Chromatogr. B 2009, 877, 3237.

[30] J. M. Halket, D. Waterman, A. M. Przyboroska, R. K. P. Patel, P. D. Fraser, P. M. Bramley. Chemical derivatization and mass spectral libraries in metabolic profiling by GC/MS and LC/MS/MS. J. Exper. Bot. 2005, 56, 219.

[31] Donike, M., N-Methyl-N-trimethylsilyl-trifluoracetamid, ein neues Silylierungs mittel aus der Reihe der silylierten Amide, J. Chromatogr. 1969, 42, 103.

[32] W. Schänzer. Detection of exogenous anabolic steroids in Drug Abuse Handbook. B. Steven, M.D. Karch (Eds). CRC Press: San Francisco, California, 1998, 671–688.

[33] P. Van Renterghem, M. Polet, L. Brooker, W. Van Gansbeke, P. Van Eenoo. Development of a GC/C/IRMS method. Confirmation of a novel steroid profiling approach in doping control. Steroids 2012, 77, 1050.

[34] X. de la Torre, C. Colamonici, D. Curcio, F. Molaioni, F. Botrè. A comprehensive procedure based on gas chromatography-isotope ratio mass spectrometry following high performance liquid chromatography purification for the analysis s of underivatized testosterone and its analogues in human urine. Anal. Chim. Acta 2012, 756, 23.

[35] M. K. Parr, G. Fubhöller, N. Schlörer, G. Opfermann, T. Piper, G. Rodchenkov, W. Schänzer. Metabolism of androsta-1,4,6-triene-3,17-dioneand detection by gas chromatography/mass spectrometry in doping control. Rapid Commun. Mass Spectrom. 2009, 23, 207.

[36] W. Schänzer, H. Geyer, G. Fubhöller, N. Halatcheva, M. Kohler, M.-K. Parr, S. Guddat, A. Thomas, M. Thevis. Mass spectrometric identification and characterization of a new long-term metabolite of metandienone in human urine. Rapid Commun. Mass Spectrom. 2006, 20, 2252.

II.3. Artículo científico 2

Mass spectrometric behavior of anabolic androgenic steroids using gas chromatography coupled to atmospheric pressure chemical ionization source. Part II: Collision Induced Dissociation.

Montse Raro[a], Tania Portolés[a], Rubén Gil[a], Juan Vicente Sancho[a], Elena Pitarch[a], Félix Hernández[a], Josep Marcos[b,c], Rosa Ventura[b,c], Jordi Segura[b,c], Óscar J. Pozo[b]

[a]Research Institute for Pesticides and Water, University Jaume I, E-12071, Castellón, Spain

[b] Bioanalysis Research Group, IMIM, Hospital del Mar Medical Research Institute, Doctor Aiguader 88, 08003 Barcelona, Spain

[c] Department of Experimental and Health Sciencies, Universitat Pompeu Fabra, Doctor Aiguader 88, 08003 Barcelona, Spain

Abstract

The atmospheric pressure chemical ionization (APCI) source, recently available for gas chromatography, coupled to quadrupole time-of-flight analyzer, was employed to make a complete study of the CID of a list of 60 anabolic androgenic steroids (AAS), both underivatized and trimethylsylil (TMS)-derivatized. Compounds belonging to this group are prohibited by the World Anti-Doping Agency (WADA) at all times, in an out of competition, being their misuse the most detected in athletes.

As previously stated in the first part of this study [1], the low fragmentation achieved in the APCI source and the addition of water in the interface as a modifier, promotes the formation of mainly $[M+H]^+$ or $[M+H-nH_2O]^+$ (or –nTMSOH). Based on this information four main groups were selected. The CID of the model AAS was studied at different collision energies. A relationship between CID behavior and AAS structure has been evaluated. Based on their CID behavior several subclasses in each selected group could be identified. A similar CID behavior was detected for each subclass of compounds. This fact was illustrated by the presence of several product ions and neutral losses common to the AAS belonging to each subclass. The combination of the results presented here and the conclusions about ionization behavior extracted in the first part of this paper could be helpful in the search of new steroids or metabolites in the doping control field.

Keywords: Anabolic androgenic steroids (AAS), Atmospheric pressure chemical ionization (APCI), Gas chromatography (GC), Mass Spectrometry (MS), Quadrupole Time-of-flight (QTOF), Doping control analysis

Introduction

The World Anti-Doping Agency (WADA) reports an annual list of banned substances and methods in sport [2]. Anabolic androgenic steroids (AAS) are included in this list because of their anabolic effects of muscle growth and their negative effects to athlete's health. AAS are among the most frequently detected groups by doping control laboratories [3]. For these reasons, researchers working on this field have the continuous challenge of developing specific and sensitive methods to detect AAS.

Nowadays, chromatographic techniques coupled to different mass spectrometric (MS) analyzers are the most established strategies to detect AAS in urine samples [4]. By one hand, gas chromatography couple to MS (GC-MS) is the traditional technique for AAS detection, working in selected ion monitoring (SIM) mode or, preferably, in selected reaction monitoring (SRM) mode to achieve the required sensitivity in tandem MS experiments (GC-MS/MS) [5,6]. Most recently, as complementary technique to GC, liquid chromatography tandem MS (LC-MS/MS) has become a good alternative to GC-MS [7], for example in the case of steroids bearing a 4-9-11-triene nucleus that present problems in derivatization [8].

The common analytical procedure for the analysis of AAS previous to GC, consists of an enzymatic hydrolysis, followed by a liquid-liquid extraction (LLE) and then, a derivatization step [9]. Derivatization is carried out to improve chromatographic and spectrometric behavior of the steroids. The reaction with N-methyl-N-trimethylsilyltrifluoroacetamide (MSTFA) to generate trimethylsilyl derivatives (TMS) is the most common derivatization reaction in case of AAS [10].

The number of AAS occurring in the black market is continuously increasing. These designer steroids are synthesized with the main objectives of evading doping controls. Therefore, advances in target analysis remains as important as the untarget studies. A correct understanding of the fragmentation patterns of the AAS and their metabolites is one of the main tools available in order to improve the detection of these designer steroids [11].

Additionally, a comprehensive study of fragmentation pathways can be also useful in the detection of unreported metabolites. The most common metabolic pathways for AAS include phase I (normally oxidations or reductions) and phase II reactions (glucuronidation or sulfonations) [12]. The selection of common ions/losses for known metabolites can be useful for the detection of the unexpected ones [13].

Studies of fragmentation patterns after electrospray (ESI) ionization by LC-MS/MS have been reported [14, 15]. Moreover, different studies have been performed for trimethylsilyl derivatized (TMS) steroids by GC-MS/MS making use, in occasions, of statistical tools to estimate fragmentation pathways of unknown steroids [16, 17].

Electron ionization source (EI) has been employed in the mentioned works of GC, although "soft" ionization sources recently tested for AAS [18, 19] could be a suitable alternative in this kind of studies. One of these soft ionization sources is the atmospheric pressure chemical ionization (APCI) source, a commercialized source for GC that works at atmospheric pressure [20]. By means of mechanisms of protonation or charge transfer, this soft source generates mainly $[M+H]^+$ or $M^{+\cdot}$ ions as the base peak of the spectrum [21]. In the first part of this work [1], the ionization behavior of underivatized and TMS-derivatized AAS was studied by using this source.

The results, in terms of relative abundance of the main ions, allowed for the establishment of a relationship between ionization and structure. The formed ions maintained the intact steroid skeleton, which is an advantage for the selection of specific precursor ions for tandem MS methods [18].

In this work, a full overview of the fragmentation patterns of 60 AAS is presented. For this purpose, an approach based on APCI source for GC coupled to QTOF high resolution mass spectrometer has been applied to both underivatized and TMS-derivatized AAS. Afterwards, data have been evaluated in order to establish relationships between fragmentation behavior and the structure of the steroids.

2. Experimental

2.1. Chemical and reagents

Sixty AAS were selected as model compounds. They were obtained from Sigma (St. Louis, MO, USA), Steraloids (Newport, RI, USA), NMI (Pymble, Australia), Toronto Research Chemicals (Toronto, Canada) and the World Association of Anti-Doping Scientists (WAADS). Detailed information about the individual suppliers of the AAS and their structural information are summarized in Supplementary Information Table 1SI.

N-methyl-N-trimethylsilyltrifluoracetamide (MSTFA), ammonium iodide (NH_4I) and 2-mercaptoethanol used in the dervatization were purchased from Sigma-Aldrich Química SA (Madrid, Spain). Acetone and methanol were purchased from Scharlab (Barcelona, Spain).

2.2. Derivatization method

The standard procedure for the formation of trimethylsylil (TMS) and enol-TMS derivatives was applied [22]. Briefly, TMS-derivatized standards were prepared by adding a volume of 100 µL of the mixture MSTFA/ NH_4I/2-mercaptoethanol (1000/2/6; v/w/v) and then heating at 60 °C during 20 min.

2.3. Instrumentation

Same instrumentation as in the Part I was used [1]. Briefly, a GC system (Agilent 7890A, Palo Alto, CA, USA) was coupled to a QTOF mass spectrometer Xevo G2 QTOF (Waters Corporation, Manchester, UK) equipped with an APCI source.

For the chromatographic separation in case of TMS-derivatized compounds, an HP Ultra 1 capillary column (16.5m×0.25mm×0.11µm) was used. The oven program was set as follows: 90 °C, 20 °C/min to 300 °C (5 min). 1µL of sample was injected in split mode (ratio 1:10) with the injector port at 280 °C. For underivatized compounds, an HP Ultra 2 column (12m×0.2mm×0.33 µm) was used. The oven program was: 90 °C (1 min), 20 °C/min to 300 °C (3 min). Splitless injections of 1 µL were carried out with the injector port at 280 °C. Constant pressure mode at 25.8 psi was used. The temperature in the source was set to 150 °C. Cone voltage was 30 V in both cases. APCI positive polarity was selected adding water as modifier in the enclosed chamber.

For CID study, product ion scan at different collision energies (20, 30 and 50 eV) were acquired. Precursor ions selected for underivatized AAS

were $[M+H]^+$, $[M+H-H_2O]^+$ or $[M+H-2H_2O]^+$ and, for TMS-derivatized AAS, $[M+H]^+$, $[M+H-TMSOH]^+$ or $[M+H-2TMSOH]^+$ were selected, depending on the ionization behavior observed for each group of compounds [1].

For more instrumental details see Supplementary Information.

3. Results and discussion

3.1. Classification of model compounds

The 60 AAS selected as model compounds were divided in structural groups in order to facilitate the comprehensive study of their CID behavior. As starting point, they were divided in the four groups previously reported for ionization behavior [1]:

Group I: AAS containing mono-conjugated keto function. $[M+H]^+$ was used as main precursor ion in MS/MS experiments, for both underivatized and TMS-derivatized. This group contained 20 of the selected AAS.

Group II: AAS containing poly-conjugated keto function. $[M+H]^+$ was used as main precursor ion in MS/MS experiments, for both underivatized and TMS-derivatized. This group contained 12 of the selected AAS.

Group III: AAS containing unconjugated keto function. $[M+H-H_2O]^+$ for underivatized and $[M+H-TMSOH]^+$ for TMS-derivatized were used as main precursor ions in MS/MS experiments. This group contained 13 of the selected AAS.

Group IV: AAS with no keto function in their structure. $[M+H-2H_2O]^+$ and $[M+H-2TMSOH]^+$ were used for both underivatized and TMS-derivatized, respectively, as main precursor ions in MS/MS experiments. It is remarkable that these species corresponded to the same ion. This group contained 15 of the selected AAS.

Thus, the most abundant ion generated in the APCI ionization process was selected as precursor ion for each group. This fact provided the first behavioral difference between groups and for this reason each group was studied separately.

For the CID study, product ion scan spectra were acquired at three collision energies (20, 30 and 50 eV) for both underivatized and TMS-derivatized AAS. Examples of CID spectra at different collision energies are shown in figures F1SI and F2SI of Supplementary Information. Three main zones of the acquired spectra were selected for the study. A graphical visualization of the three zones is displayed in Figure 1. These zones can be described as follows:

Zone 1: Relevant ions at $m/z > 220$. This region provides information about common neutral losses of the AAS normally produced without alteration of the steroid skeleton. This zone was evaluated at all collision energies tested. Ions with relative abundance higher than 10 % were considered as relevant.

Zone 2: Relevant ions at $90 < m/z < 220$. This region provides information about the primary fragmentation of the steroid skeleton. This zone was evaluated at all collision energies tested. Ions with relative abundance higher than 10 % were considered as relevant.

Zone 3: Relevant ions at $50 < m/z < 115$ after molecular explosion of the AAS. This region was studied at high collision energy (50 eV) in order to promote

the complete fragmentation of the steroid skeleton. Common ions of this skeleton were evaluated in this zone. Ions with relative abundance higher than 10 % were considered as relevant.

The product ions and the correspondent neutral losses appearing in the selected zones of the AAS belonging to a specific group were evaluated. The analytes were classified based on common ions and losses. On the basis of this information, several subclasses could be identified in each group allowing for the establishment of several structural-CID behavior relationships.

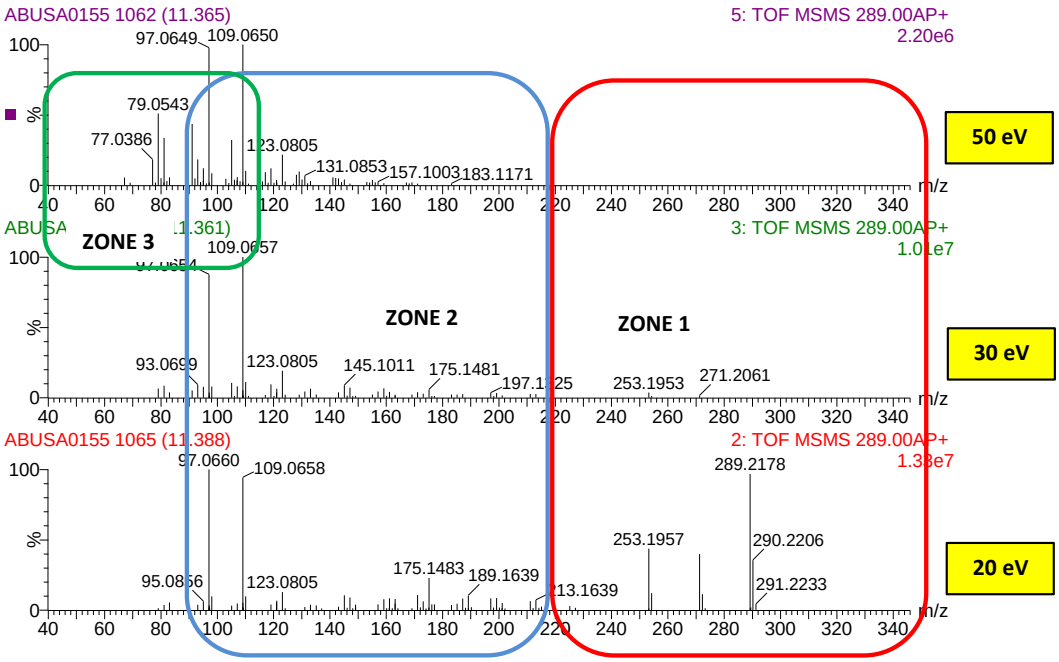

Figure 1. Scheme of the different zones of study on the MS/MS spectra at different collision energies. Example of Epitestosterone.

3.2. CID information

Group I

Among the model AAS, 20 analytes belonged to the Group I. The high proton affinity provided by the conjugated keto function facilitated that the analytes for Group I were mainly ionized as $[M+H]^+$. Thus, this ion was selected as precursor ion for the study of the CID behavior of both underivatized and TMS-derivatived AAS. Based on this behavior, AAS from this group could be divided into three subclasses.

Group Ia: Δ^4 ^{3}CO

Compounds belonging to the group Ia contained a carbonyl function in C3 conjugated with a double bond in position 4. Nine AAS were included in this class (Table 1).

When underivatized, the zone 1 of the CID spectra for Δ^4 ^{3}CO-AAS was dominated by several losses of water. For 17-hydroxy-AAS, the number of the losses of water detected was identical to the number of oxygen atoms in the molecule. Thus, whereas T showed two losses of water and contained tow oxygen atoms, three losses of water were observed in those AAS containing three oxygen atoms e.g. OXY and 4OH-T. In the case of 17-keto-AAS, the number of losses of water detected was one less than the number of oxygen atoms in the molecule.

The zone 2 in the spectra of underivatized AAS belonging to this group was clearly dominated by the ions at *m/z* 109.0649 and *m/z* 97.0650 corresponding to the formula C_7H_9O and C_6H_9O, respectively. These ions have been already reported for the fragmentation of the $[M+H]^+$ after ESI

ionization and have been explained by fragmentation of the A ring [15, 23]. In the case of 4-hydroxy-AAS of this group, the analogue oxygen containing product ions at *m/z* 125.0599 and *m/z* 113.0600 were observed.

At high collision energy, the zone 3 of the spectra of the AAS of this class were similar and contained, mainly, hydrocarbon ions coming from the fragmentation of the cyclopentaneperhydrophenanthrene structure of the AAS. Thus, ions at *m/z* 77.0386, 79.0544, 81.0700, 91.0545 and 105.0701 were observed. Some of these ions have been reported also after CID of the $[M+H]^+$ generated by ESI ionization [24].

The spectra observed after TMS-derivatization showed some similarities and some differences with the behavior of the underivatized molecules. Thus, also some neutral losses of TMSOH (90.0501 Da) were observed for some compounds, they were only clear for those AAS without any modification neither in the A nor in the D ring. As an example, neutral losses of TMSOH were not observed for 4-hydroxy-AAS like 4OH-T or 4OH-NAN. A relationship between the ions present in this zone and the substitution at C17 could be established. Thus, 17-methylated AAS showed a neutral loss of 130.0815 Da corresponding to $C_6H_{14}SiO$, whereas AAS substituted with ethylene like DANmet showed a neutral loss of 140.0660 Da corresponding to $C_7H_{12}SiO$. This behavior has been also observed in the CID spectra of the $[M+H]^+$ of TMS-AAS derivative generated after CI [19]. A feasible explanation for the occurrence of this neutral loss is the charge remote fragmentation shown in Figure 2.

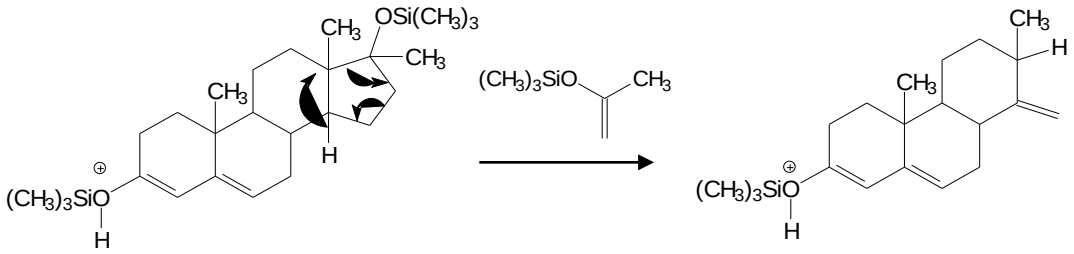

Figure 2. Proposed fragmentation pathway for the neutral loss of 130.0815 Da ($C_6H_{14}SiO$)

Similarly to the underivatized compounds, the zone 2 of the TMS-derivatized AAS was dominated for two ions. In the case of non-hydroxylated AAS, these ions (*m/z* 181.1044 and *m/z* 169.1042) corresponded to the mono-TMS derivatives of the ions at *m/z* 109.0649 and *m/z* 97.0650 previously described. Remarkably, abundant ions at *m/z* 181 and 169 were also observed for 4-hydroxy-AAS. However, the accurate mass measurements revealed that these ions had a different *m/z* and, therefore, a different origin.

Finally, although ions coming to the AAS skeleton could be also observed after TMS derivatization, in some cases part of these ions were underdetected due to the presence of an abundant *m/z* 73.0477 corresponding to the ion TMS^+ coming from the derivatizating agent.

Group Ib: Δ¹ 3CO

Compounds belonging to this group contain a carbonyl function in C3 conjugated with a double bond in position 1. Six AAS were included in this class (Table 2).

Regarding the CID spectra from underivatized compounds of group Ib, several water losses were observed in the zone 1. Contrarily to group Ia, both 17-hydroxy-AAS and 17-keto-AAS showed a number of water losses identical to the number of oxygen atoms in the molecule.

In the zone 2 of the spectra, abundant ions at *m/z* 187, 145 and 131 were observed for 17-hydroxy-AAS. Analogous ions were observed at 183, 143 and 129 for 17-keto-AAS (e.g. 1-AED) and at 145, 159 and 201 (+ 14 Da) for 17-methyl-AAS (e.g. Me-1-T). This information suggests that D ring is part of these ions. Their presence has been reported after ESI ionization [22]. The ion at *m/z* 187.1505 ($C_{14}H_{19}$) consists of the BCD rings whereas the ions at *m/z* 145.1023 ($C_{11}H_{13}$) and *m/z* 131.0858 ($C_{10}H_{11}$) contain BC rings. Thus, contrarily to Δ^4 ^{3}CO, the double bond in C1 promotes the loss of the A ring, followed by the loss of the B one.

In the zone 3, at higher collision energy, the spectra of the AAS were similar for all the compounds showing the same ions as the ones observed in the previous group explained. That is, the ions at *m/z* 77.0386, 79.0544, 81.0700, 91.0545 and 105.0701, from AAS skeleton, were observed.

Regarding TMS-derivatized compounds, the zone 1 of the spectra shows TMSOH losses of 90.0501 Da. In that case, the number of losses was identical to the number of oxygen atoms present in the structures, for both 17-keto-AAS and for 17-hydroxy-AAS. In the same way as described for the

group Ia, the 17-methylated AAS, Me-1-T showed a neutral loss of 130.0815 ($C_6H_{14}SiO$) instead of the second loss of 90 [19]. Remarkably, significant ions at *m/z* 415, 417 or 431, for 17-keto-AAS (1-AED), 17-hydroxy-AAS (1-T and BDmet) and 17-hydroxy-17-methyl-AAS (METH, Me-1-T and STEN), respectively, were observed in this zone. These ions are generated after a neutral loss of 16.0313 (CH_4). Differently from the group Ia, the existence of a double bond in position C1 favored the neutral loss of a CH_4. This fact can be explained by the formation of an aromatic stable A ring. An example of that process is shown for 1-AED in Figure 3. This loss does not occur when the double bond is on position C4 because the derivatization process do not favor the resonance of the A ring. This loss is not observed for underivatized fragmentation, probably because it is a consequence of the enolization produced in the derivatization of the 3-carbonyl group.

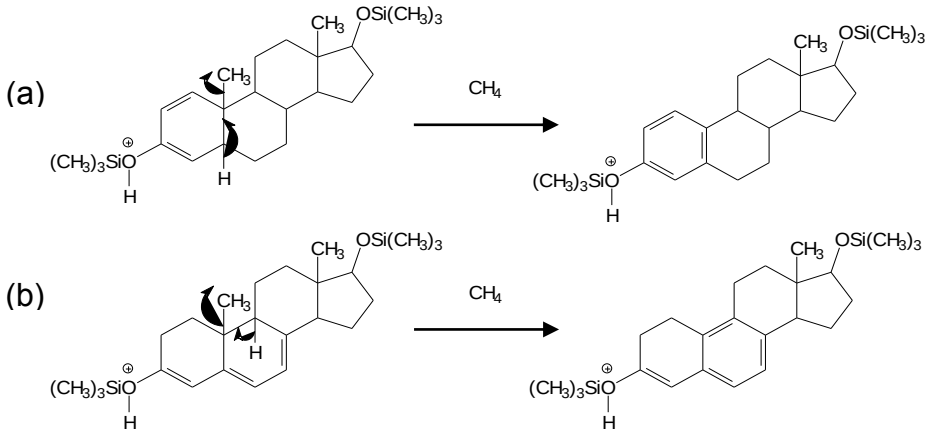

Figure 3. Proposed fragmentation pathway explaining the CH_4 loss showed in (a) Group Ib and (b) Group IIa

The zone 2 of the TMS-derivatized presented, for Me-1-T, 1-AED and 1-T, the ions of *m/z* 181.1044 and *m/z* 169.1042, although their corresponding *m/z* 109.0649 and *m/z* 97.0650 were not observed in underivatized. Besides, abundant ion of *m/z* 187.1505 ($C_{14}H_{19}$) from the BCD rings, previously described, was also observed for all the compounds of this group; for 1-AED (17-keto-AAS) *m/z* 185 was observed and for Me-1-T the analogue *m/z* 201 was found, due to the extra methyl group.

Similar to group group Ia, ions *m/z* 91.0545 and 105.0701 from the AAS skeleton could be observed in zone 3, together with the abundant ion *m/z* 73.0477 from the derivatizating agent.

Group Ic: Δ^4 3CO, ring B modification

Compounds belonging to this group contained a carbonyl function in C3 conjugated with a double bond in position 4. The difference with the group Ia is that these compounds present a modification in the B ring. Several modifications were considered including 6-hydroxy, 6-oxo, 9-fluorine or 7-methyl AAS. Five compounds were included in this class (Table 3).

The zone 1 of the CID spectra from underivatized compounds also showed several water losses. Similar to other groups, the number of losses of water was normally equivalent to the number of oxygen atoms of the molecule (except for 6OH and 6-CO metabolites) However, this behavior was not followed after derivatization. For fluorine containing AAS (FLU and FLU met), these water (or TMSOH) losses are combined with the loss of HF. Other remarkable ion of this zone, when underivatized, was *m/z* 255/257 which comes from a neutral loss of 46.0055 corresponding to the combination of a water loss and a loss of CO. This neutral loss was observed in those AAS for which the modification in the B ring contained an oxygen atom.

Contrarily to other groups, the zone 2 of the CID spectra for underivatized compounds showed several abundant ions. Most of them showed a *m/z* in the area 120-180 and corresponded basically to hydrocarbons. This behaviour was observed irrespective of the modification introduced in the B ring. A similar behaviour was observed when studying the zone 2 of the TMS derivatized analytes belonging to this group.

In the zone 3, the behaviour described for the other classes was also observed in this group. Thus, the ions at *m/z* 77.0386, 79.0544, 81.0700, 91.0545 and 105.0701 were observed in both underivatized and TMS-derivatized analytes.

Group II

This group contained 12 analytes. The high proton affinity provided by the polyconjugated keto function facilitated these compounds were mainly ionized as $[M+H]^+$. Thus, this ion was selected as precursor ion for the study of the CID behavior of both underivatized and TMS-derivatived AAS. Depending on the position of the double bonds conjugated with the carbonyl group, AAS from this group could be divided into two subclasses.

Group IIa: polyconjugated-3CO, polyconjugation exclusively located in A ring

In this group, compounds contained a carbonyl function in C3 polyconjugated with double bonds in position 1 and 4. Six AAS were included in this class (Table 4).

As previously described for $\Delta^{1,4}$ 3CO AAS after ESI ionization [14, 15], only one water loss was detected for these compounds with two oxygen atoms on their structures, whereas two losses were observed for those containing three oxygen atoms (6OH-4Cl-MTD and MTDmet1). A different behaviour was observed when studying the TMS derivatives. In this case, the number of losses of TMSOH was guided by the C17 substituent. Thus, the number of TMSOH losses was coincident with the number of oxygen atoms for most of the AAS of this group (17-hydroxy-AAS). 17-keto-AAS (1,4-AED) only showed one TMSOH loss and the neutral loss of 130, previously described. Moreover, the previously mentioned loss of CH_4 was also observed for compounds in this group probably due to the stability of the formation of an aromatic A ring. This loss was observed in all cases except for 6OH-4Cl-MTD, possibly due to the presence of a chlorine atom in C4.

The zone 2 of the CID spectra for underivatized compounds was dominated by only one abundant characteristic ion at *m/z* 121.0653 (C_8H_9O). This ion has been previously observed after CID of the $[M+H]^+$ generated by ESI ionization [15]. For TMS derivatized AAS, the analogous ion at *m/z* 193.1049 was observed. This ion was also reported for the $[M+H]^+$ of TMS-AAS generated after CI [19]. In the case of 6OH-4Cl-MTD the corresponding detected ion was *m/z* 155.0264 (C_8H_8OCl), for both the underivatized and the TMS-derivatives.

The same behaviour described for the other groups in the third zone was also observed for group IIa.

Group IIb: polyconjugated-3CO, polyconjugation exceeding A ring

Compounds belonging to this group contain a carbonyl function in C3 polyconjugated, where the conjugation reaches either B or both B and C rings. $\Delta^{4,6}$, $\Delta^{4,9}$ and $\Delta^{4,9,11}$ AAS are part of this subclass. Six compounds were included in this group (Table 5).

Similar to AAS from group IIa, the first zone of the CID spectra when underivatized, showed only one water loss, although they contain two oxygen atoms on their structures.

In zone 2, underivatized compounds belonging to this group showed several abundant ions with *m/z* ranging 130 to 200. Similar to the group Ic, the variations on the B ring can be behind the relative large number of abundant ions in this area. Although it was difficult to establish a common trend, it could be concluded that AAs with double bonds reaching only the B ring showed abundant ions containing two rings. Thus, 4,6-AED and 6-T showed abundant ions containing both C and D rings (*m/z* 149.0966/131.0861 and *m/z* 151.1123/133.1017, respectively) whereas MDONE and ATD showed ions containing both A and B rings (*m/z* 159.0810/135.0810 and *m/z* 147.0810/171.0810/173.0964 respectively). On the other hand, those AAS in which the conjugation reached the C ring (4,9,11-triene-3-keto-AAS like TREN and THG) presented common fragment ions of *m/z* 241.1602 and 199.1123 which contain three rings (A, B and C), as previously described in literature [14, 15].

Regarding TMS-derivatized, the structure of 4,9,11-triene-3-keto-AAS (TREN and THG) made their TMS-derivatization difficult [8]. For this reason, we could not evaluate the behavior of these compounds after derivatization. For the rest, one TMSOH loss was observed in the CID spectra in zone 1,

except for MDONE which presented two TMSOH loss. In this group, CH_4 losses were observed for 4,6-AED and 6-T, due to the presence of a double bond in C6 which makes it possible to generate an aromatic B ring (Figure 3). In case of MDONE, with a double bond in C9, that loss is not observed because the methyl group at C19 is absent in this compound.

In zone 2, ion with *m/z* 195.1174 was observed for all the compounds ($C_{11}H_{19}SiO$). It is similar to the ion at *m/z* 193.1049 described in the previous group but without the double bond in position 1. Based on these results, it seems that the TMS-derivatization helps the fragmentation of the B ring even though it is modified with extra double bonds.

The same behaviour described previously for the zone 3 was also observed in the present group.

Group III

The main difference between groups the two first groups and the two last ones is the selected precursor. Contrarily to groups I and II the main ion formed in group III was the $[M+H-H_2O]^+$ (or the analogous $[M+H-TMSOH]^+$ for TMS derivatized). That means that for mono-TMS compounds like OXA the precursor ion selected correspond to the same molecule. The selected precursor together with the absence of double bonds guided the fragmentation of this group.

Group IIIa: unconjugated 3CO

Group III consists of steroids with unconjugated keto function. Among them, only OXA and DHT presented unconjugated CO on C3. They form the subclass IIIa (Table 6).

Compounds from group IIIa lost all their oxygen atoms as water (or TMSOH when derivatized). Thus, DHT showed a neutral loss of water whereas OXA showed two. Since the lactone moiety in OXA is not derivatized, these two neutral losses of water are also observed after TMS derivatization.

In zone 2, a remarkable behaviour was observed. After the first loss of water, the A ring was fragmented showing a neutral loss of their atoms at positions C2-C3-C4 (Figure 4). Thus, in the case of DHT, an ion at *m/z* 215.1800 corresponding to a loss of water followed by a loss of acetone (-18.0106 and -58.0419 Da) from the A ring was observed. In the case of OXA which contained an oxygen atom in position C2, an ion of experimental *m/z* 229.1958 was observed as the base peak of the spectrum at 20 eV, corresponding to a water plus an acetic acid loss (-18.0106 and -60.0211). After this fragmentation, the product ions observed were basically the same, but with a methyl group in 17 for OXA.

TMS-derivatized spectra of this group were comparable to the underivatized ones. One TMSOH loss was observed for DHT and, in case of OXA, a mono-O-TMS AAS, two water losses were observed because the precursor ion selected was the same as for underivatized $[M+H\text{-}TMSOH]^+$. Also, the same ion of *m/z* 229 was observed for OXA in zone 2.

In zone 3, for underivatized and TMS-derivatized AAS, the common fragments *m/z* 77.0386, 91.0545 and 105.0701 were mainly observed. Also the ion *m/z* 73 was present in the case of TMS- derivatized.

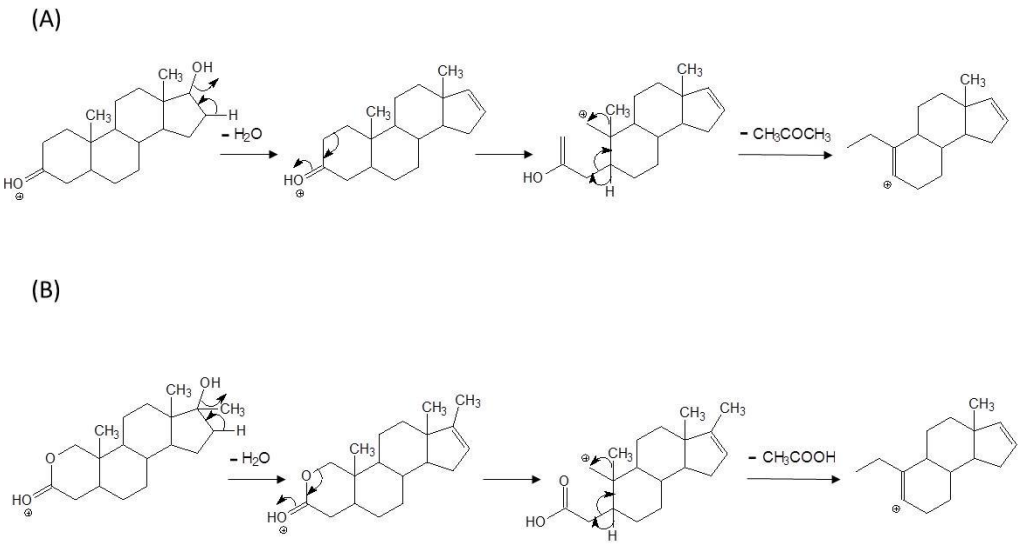

Figure 4. Tentative fragment ions of underivatized a) DHT and b) OXA. (Group IIIa)

Group IIIb: unconjugated 17CO

Compounds belonging to this group IIIb, present an unconjugated 17CO. Eleven AAS are included in this class (Table 7).

The precursor ion selected in this case was $[M+H-H_2O]^+$ or [M+H-TMSOH]$^+$. All the oxygen atoms remaining in the molecule were lost as water or TMSOH for underivatized and derivatized AAS respectively. As an example, the zone 1 of the CID spectra of 11OH-Andros showed two losses of water since it contains three oxygen atoms. Similarly, two TMSOH losses were observed in the spectra of the TMS derivatized 11OH-Andros.

In zone 2, underivatized AAS of this group showed a common fragment ion of *m/z* 213.1643 ($C_{16}H_{21}$) from an acetone loss. This loss is analogous to the *m/z* 215 explained in the previous group for DHT (17-hydroxyl-AAS) but coming from the D ring (Figure 4). From this fragment, a neutral loss of CH_2 results in the common ion at *m/z* 199.1487 ($C_{15}H_{19}$). Afterwards, ions differing from a methylen group were commonly observed. Thus ions at m/z 185.1330, 161.1329, 147.1169, 133.1016, 119.0857 or 105.0699 are common in this group. In the particular case of CLOSmet which contains a chlorine atom in C4, the observed ions in zone 2 were a water loss, a hydrochloric acid loss and the combination of both. Besides, analogous loss of acetone, in the same way as the rest of the components of the group was observed, although in CLOSmet, the chlorine atom was still present: *m/z* 247.1254 ($C_{16}H_{20}Cl$).

In zone 2 for TMS-derivatized compounds, an extensive fragmentation was observed, as well as in the underivatized spectra. Common ions *m/z* 145, 169, 181 and 195 were observed, they were previously explained in group Ia.

In zone 3, for underivatized and TMS-derivatized AAS, the common fragments explained for the previous groups were also detected.

Group IV

Group IV consists of steroids with no keto function present in their structures. Fifteen AAS are included in this class (Table 8). In this case, precursor ions selected for the MS/MS experiments were $[M+H-2H_2O]^+$ for underivatized and $[M+H-2TMSOH]^+$ for TMS-derivatized. Thus, precursor

ions coincide in both derivatized and undervatized forms, being the product ion spectra equivalents.

Since all the oxygen atoms were absent in the precursor ion due to their loss by in-source fragmentation, water or TMSOH losses were not expected in zone 1. In fact, few ions were found in this area of the spectra. One of them was the ion at *m/z* 241.1956 ($C_{18}H_{25}$) observed in MTDmet3 and METDmet4. This ion corresponds to a neutral loss of C_2H_4 and can be generated by the presence of a double bond in position 1 for these AAS. Additionally, the ion at *m/z* 229.1956 ($C_{17}H_{25}$), corresponding with a neutral loss of 56.0626 (C_4H_8), was observed for compounds with extra methyl groups in C7/C2 and C17 (CALUSmet, BOLASmet or METHASmet) or for those with nor $18CH_3$ but extra $17CH_2CH_3$ (NORBOLmet1 and NORBOLmet2). This neutral loss was also observed in zone 2 for most of the compounds producing the ion at *m/z* 215.1800 ($C_{15}H_{19}$) analogous to the ion at *m/z* 213, previously explained in the group IIIb. Therefore, although it is commonly produced, the loss of C_4H_8 seems to have different origin since it is present irrespective of the variations in A, B or D rings. Moreover, for derivatized 16-AOL and MTDmet4, mono-TMS AAS, a loss of CH_4 is observed, these compounds present double bonds in C16 and C13, respectively and absent 17OH group, so, this loss could be due to the loss of C18 in case of 16-AOL or C17 in case of MTDmet4.

Similar to group IIIb, the fragmentation of the ion at *m/z* 215 provides several hydrocarbon ions at differences of methylen group. Thus ions at *m/z* 119.0861, 133.1017, 145.1017, 161.1330, 175.1487, and 189.1311 coming from the fragmentation of the steroid skeleton were observed.

In the same way of the rest of the groups, in zone 3 the common fragments previously detailed, were also observed.

4. Conclusions

A CID study of 60 model AAS has been carried out in order to establish relationships between fragmentation patters and structure. For this purpose, the soft APCI source coupled to GC-QTOF has been employed. The low in-source fragmentation assessed by this source allows for the selection of abundant and specific precursor ions, which maintain the skeleton of the steroid. Thus, by means of proton transfer reactions either $[M+H]^+$ or $[M+H-nH_2O]^+$ were selected as precursor ions. For TMS-derivatized AAS, either $[M+H]^+$ or $[M+H-nTMSOH]^+$ were used. Based on the differences and similarities in the CID behavior a relationship between structure and fragmentation could be established. Thus, AAS could be divided into 8 classes depending on their CID behavior. The main conclusions extracted from this work are summarized in Table 9. It can be concluded that the presence and the nature of conjugated carbonyls are guiding the fragmentation of AAS. Among the different modifications, alterations at the B ring seem to be more important for the fragmentation pathway than the observed in other rings.

The reported data about similarities and differences of the fragmentation patterns between groups, depending on the structure, can be a valuable tool for future understanding of fragmentation pathways of the AAS. Additionally, it can be the basis for developing analytical strategies for the elucidation of unknown AAS and metabolites. Finally, the knowledge of common fragmentation pathway is relevant for the adequate selection of specific transitions for SRM methods. This fact has been already reported for Selected Reaction Monitoring (SRM)-based methods [18] in which the specificity of the neutral loss detailed for group Ib was useful for the selection of specific transitions for BDmet or 1-T.

5. Acknowledgements

The authors acknowledge the financial support of the Ministry of Economy and Competitivity, Spain, in the project DEP2011-28573-C02-01/02. The authors from University Jaume I also acknowledge the support from Generalitat Valenciana (Research Group of Excellence Prometeo II/2014/023; ISIC EnviFood 2012/016). The authors from IMIM acknowledge the support from Generalitat de Catalunya (Consell Català de l'Esport and DIUE 2009SGR4929). Spanish Health National System is acknowledged for O. J. Pozo contract (MS10/00576). M. Raro is also grateful to the Ministry of Economy and Competitivity for her predoctoral grant.

6. References

[1] M. Raro, T. Portolés, J. V. Sancho, E. Pitarch, F. Hernández, J. Marcos, R. Ventura, C. Gómez, J. Segura, O. J. Pozo. Mass spectrometric behavior of anabolic androgenic steroids using gas chromatography coupled to atmospheric pressure chemical ionization source. Part I: Ionization. *J. Mass Spectrom*. **2014**, 49, 509–521

[2] World Anti-Doping Agency. Prohibited List **2015**. https://wada-main-prod.s3.amazonaws.com/resources/files/wada-2015-prohibited-list-en.pdf Last accesed 07.10.2015

[3] World Anti-Doping Agency. Testing figures report **2013**. https://wada-main-prod.s3.amazonaws.com/resources/files/WADA-2013-Anti-Doping-Testing-Figures-LABORATORY-REPORT.pdf Last accessed 07.10.2015.

[4] C. Gomez, A. Fabregat, O. J. Pozo, J. Marcos, J. Segura, R. Ventura. Analytical strategies based on mass spectrometric techniques for the study of steroid metabolism. *TrAC-Trend Anal Chem*. **2014**, 53, 106–116

[5] G. de Albuquerque Cavalcanti, F. Dias Leal, B. Carius Garrido, M. Costa Padilha, F. Radler de Aquino Neto. Detection of designer steroid methylstenbolone in 'nutritional supplement' using gas chromatography and tandem mass spectrometry: Elucidation of its urinary metabolites. *Steroids*. **2013**, 78, 228–233

[6] M. A. Delgadillo, L. Garrostas, O. J. Pozo, R. Ventura, B. Velasco, J. Segura, J. Marcos. Sensitive and robust method for anabolic agents in human urine by gas chromatography–triple quadrupole mass spectrometry. *J.Chromatogr. B*. **2012**, 897, 85– 89

[7] O. J. Pozo, P.Van Eenoo, K. Deventer, F. T. Delbeke. Development and validation of a qualitative screening method for the detection of exogenous anabolic steroids in urine by liquid chromatography-tandem mass spectrometry. *Anal Bioanal Chem*. **2007**, 389, 1209–1224

[8] E. M. Brun, R. Puchades, A. Maquieira, Analytical methods for anti-doping control in sport: anabolic steroids with 4,9,11-triene structure in urine, *TrAC-Trend Anal Chem*. **2011**, 30:5, 771-783.

[9] P. Van Eenoo, W. Van Gansbeke, N. De Brabanter, K. Deventer, F. T. Delbeke . A fast, comprehensive screening method for doping agents in urine by gas chromatography–triple quadrupole mass spectrometry. *J. Chromatogr. A*. **2011,** 1218, 3306–3316

[10] J. Segura, R. Ventura, C. Jurado. Derivatization procedures for gas chromatographic–mass spectrometric determination of xenobiotics in biological samples, with special attention to drugs of abuse and doping agents. *J.Chromatogr. B*. **1998**, 713, 61–90

[11] O. J. Pozo, N. De Brabanter, A. Fabregat, J. Segura, R. Ventura, P. Van Eenoo, K. Deventer. Current status and bioanalytical challenges in the detection of unknown anabolic androgenic steroids in doping control analysis. *Bioanalysis*. **2013**, 5(21), 2661–2677

[12] Schänzer W. Metabolism of anabolic androgenic steroids. *Clin. Chem*. **1996**, 42(7), 1001-1020

[13] J. Marcos, O. J. Pozo. Current LC–MS methods and procedures applied to the identification of new steroid metabolites. *J. Steroid Biochem. Mol. Biol*. **2015**, http://dx.doi.org/10.1016/j.jsbmb.2015.12.012

[14] F. Guan, L. R. Soma, Y. Luo. Collision-Induced dissociation pathways of anabolic steroids by electrospray ionization tandem mass spectrometry. *J. Am. Soc. Mass Spectrom.* **2006**, 17(4), 477–489

[15] O. J. Pozo, P. Van Eenoo, K. Deventer, S. Grimalt, J. V. Sancho, F. Hernández, F. T. Delbeke. Collision-induced dissociation of 3-keto anabolic steroids and related compounds after electrospray ionization. Considerations for structural elucidation. *Rapid Commun. Mass Spectrom*. **2008**, 22, 4009-4024

[16] M. Thevis, W. Schänzer. Mass spectrometry in sports drug testing: structure characterization and analytical assays. *Mass Spectrom. Rev.* **2007**, 26, 79– 107

[17] A.G. Fragkaki, Y.S. Angelis, A. Tsantili-Kakoulidou, M. Koupparis, C. Georgakopoulos. Statistical analysis of fragmentation patterns of electron ionization mass spectra of enolized-trimethylsilylated anabolic androgenic steroids. *Int. J. Mass Spectrom.*. **2009**, 285, 58–69

[18] M. Raro, T. Portolés, E. Pitarch, J.V. Sancho, F. Hernández, L. Garrostas, J. Marcos, R. Ventura, J. Segura, O. J. Pozo. Potential of atmospheric pressure chemical ionization source in gas chromatography tandem mass spectrometry for the screening of urinary exogenous androgenic anabolic steroids. *Anal. Chim. Acta*. **2016**, 906, 128-138

[19] M. Polet, W. Van Gansbeke, P. Van Eenoo, K. Deventer. Gas chromatography/chemical ionization triple quadrupole mass spectrometry analysis of anabolic steroids: ionization and collision-induced dissociation behavior. *Rapid Commun. Mass Spectrom*. **2016**, 30, 511–522

[20] T. Portolés, J. V. Sancho, F. Hernández, A. Newton, P. Hancock. Potential of atmospheric pressure chemical ionization source in GC-QTOF MS for pesticide residue analysis. *J. Mass. Spectrom.* **2010**, 45, 926–936

[21] D-X. Li, L. Gan, A. Bronja, O. J. Schmitz. Gas chromatography coupled to atmospheric pressure ionization mass spectrometry (GC-API-MS): Review. *Anal Chim Acta*. **2015**, 891, 43-61

[22] J. Marcos, O. J. Pozo. Derivatization of steroids in biological samples for GC–MS and LC–MS analyses. *Bioanalysis*. **2015**, 7(19), 2515-2536

[23] T. M. Williams, A. J. Kind, E. Houghton, D. W. Hill. Electrospray collision-induced dissociation of testosterone and testosterone hydroxy analogs. *J. Mass Spectrom*. **1999**, 34, 206-216

[24] O. J. Pozo, K. Deventer, P. Van Eenoo, F. T. Delbeke. Efficient approach for the comprehensive detection of unknown anabolic steroids and metabolites in human urine by liquid chromatography-electrospray-tandem mass spectrometry. *Anal. Chem*. **2008**, 80, 1709-1720

TABLES

Table 1. Group Ia: Δ^4 3CO. *m/z* ions and optimized CE (eV) obtained for underivatized and TMS-derivatized steroids

			Underivatized					TMS- derivatized				
Compound	**X**	**Y**	**Zone1**	**CE**	**Zone2**	**CE**	**Zone3 (50)**	**Zone1**	**CE**	**Zone2**	**CE**	**Zone3 (50)**
AED	H	17 CO	269.1905	20	211.1482	20	105.0701	341.2283	20	211.1471	30	105.0709
			229.1589	20	123.0808	30	79.0544	251.1792	20	195.1186	30	91.0555
					109.0649*	20	77.0387			181.1044*	30	73.0482
$[M+H]^+_{und}$	287.2030				97.0650*	20				169.1042*	30	
$[M+H]^+_{TMS}$	431.2884									155.0881	30	
4OH-AED*	4 OH	17 CO	285.1861	20	173.1331*	20	105.0700	429.2643	30	181.0900*	50	73.0478
			267.1754	20	145.1013	20	91.0545	269.1389	30	169.0915*	50	
					125.0602*	30	79.0544	257.1390	30	155.0673	50	
$[M+H]^+_{und}$	303.1963				113.0604*	30	77.0386	243.1236	30			
$[M+H]^+_{TMS}$	519.3167						67.0543					
4OH-NAN*	4 OH	17β OH	273.1853	20	213.1645	20	105.0702	419.2457	30	181.0901*	50	105.0699
			255.1751	20	145.1013*	30	91.0545	391.2488	30	169.0913	50	91.0516
			237.1643	20	131.0857*	30	79.0545	269.1395	30	155.0673*	50	73.0477
$[M+H]^+_{und}$	291.1958				125.0599*	30	77.0388	243.1242	30			
$[M+H]^+_{TMS}$	507.3155				105.0702*	30	67.0542					
4OH-T*	4 OH	17β OH	269.1906	20	175.1485	20	113.0600	269.1399	30	181.0901*	50	73.0480
			241.1957	20	163.1485	20	105.0700	257.1400	30	169.0913*	50	
					139.0757	30	91.0544					
					125.0601*	30	79.0544					
$[M+H]^+_{und}$	305.2117				113.0600*	30	77.0390					
$[M+H]^+_{TMS}$	521.3311				105.0700	30	67.0542					
DANmet	H	17β OH	295.2065	20	123.0806	20	109.0650	317.2290	30	195.1193	30	105.0705
		17C≡C	277.1959	20	109.0650*	20	105.0709	227.1793	30	181.1049*	30	91.0552
					97.0650*	20	97.0650			169.1046*	30	73.0477
							91.0543			119.0862	30	
							81.0702					
$[M+H]^+_{und}$	313.2187						79.0544					
$[M+H]^+_{TMS}$	457.2977						77.0386					
E	H	17β OH	271.2099	20	189.1643	20	109.0651	343.2536	20	181.1091*	30	105.0702
			253.1960	20	175.1486	20	105.0708	253.2011	20	169.1086*	30	91.0549
					159.1169	30	97.0650			155.0888	30	73.0494
					123.0807	30	91.0548			145.1052	30	
					109.0651*	30	81.0703					
$[M+H]^+_{und}$	289.2171				97.0650*	30	79.0544					
$[M+H]^+_{TMS}$	433.2985						77.0386					
MeT	H	17βOH	285.2225	20	189.1642	20	109.0654	317.2295	30	195.1204	30	105.0704
		17CH3	267.2117	20	177.1643	20	105.0701	267.2121	30	181.1050*	30	91.0547
			245.1906	20	133.1014	30	97.0654	227.1799	30	169.1048*	30	73.0479
			227.1800	20	123.0806	30	91.0545			155.0889	30	
					109.0654*	30	81.0700			119.0871	30	
$[M+H]^+_{und}$	303.2324				97.0654*	30	79.0544					

OXY*	4 OH	17β OH	301.2178	20	189.1646	20	105.0702	519.3118	20	181.0714*	30	73.0474
			283.2070	20	159.1173	30	91.0545	445.2920	20	147.0989	30	
			265.1964	20	133.1016	30	81.0701	405.2524	20			
			255.2118	20	125.0602*	30	79.0545	389.2416	30			
					113.0603*	30	77.0389	355.2522	30			
$[M+H]^+_{und}$	319.2276				107.0859	30	67.0543	321.1822	30			
$[M+H]^+_{TMS}$	535.3494							269.1456	30			
					105.0702	30		257.1398	30			
T	H	17β OH	271.2060	20	123.0804	20	109.0649	343.2449	20	181.1048*	30	105.0706
			253.1951	20	109.0666*	20	105.0703	253.1961	20	169.1042*	30	91.0557
					97.0659*	20	97.0649			155.0887	30	73.0485
							91.0545			119.0863	30	
							81.0701					
$[M+H]^+_{und}$	289.2215						79.0543					
$[M+H]^+_{TMS}$	433.2973						77.0386					

*tris-O-TMS compounds

Table 2. Group Ib: Δ^1 3CO. *m/z* ions and optimized CE (eV) obtained for underivatized and TMS-derivatized steroids

			Underivatized					TMS- derivatized				
Compound	**X**	**Y**	**Zone1**	**CE**	**Zone2**	**CE**	**Zone3 (50)**	**Zone1**	**CE**	**Zone2**	**CE**	**Zone3 (50)**
1-AED	H	17 CO	269.1908	20	203.1439	20	105.0700	415.2500	20	193.1054	30	105.0706
			251.1801	20	185.134*	20	97.0651	341.2300	20	185.1326	30	91.0549
					143.0857	30	91.0544	275.1836	30	181.1055*	30	73.0478
					129.0697	30	79.0543	231.1205	30	169.1054*	30	
$[M+H]^+_{und}$	287.203				121.1014	30	77.0388			143.0880	30	
$[M+H]^+_{TMS}$	431.2884				97.0649	30						
1-T	H	17β OH	271.2059	20	205.1597*	20	105.0701	417.2652	20	195.1183	30	105.0703
			253.1961	20	187.1516*	20	91.0545	343.2454	30	187.1479*	30	91.0547
					159.1169	30	79.0543	317.2304	30	181.1040*	30	73.0470
					145.1012*	30	77.0382	277.1981	30	169.1040*	30	
					131.0857*	30		253.1949	30			
$[M+H]^+_{und}$	289.2171				117.0700	30						
$[M+H]^+_{TMS}$	433.2953				105.0700*	30						
BDmet	H	17β OH	271.2062	20	213.1643	20	105.0699	417.2598	20	201.1648*	30	105.0702
			253.1954	20	201.1641	20	91.0546	343.2450	20	193.1051*	30	91.0541
					187.1487*	20	79.0545	317.2304	30	187.1488*	30	73.0477
					159.1168	30	69.0335	289.1985	30	157.1005	30	
					145.1012*	30		253.1964	30	145.1011	30	
$[M+H]^+_{und}$	289.2168				131.0861*	30				119.0858	30	
$[M+H]^+_{TMS}$	433.2979				105.0700*	30						
METH	H	17β OH	285.2214	20	187.1486*	20	105.0700	431.2777	20	209.135*		105.0704
			267.2111	20	161.1326	20	91.0543	357.2587	20	187.1478*		91.0505
			205.1589	20	159.1167	30	83.0492	331.2448	30	173.1322*		73.0479
					145.1011*	30	79.0543	267.2097	30	145.1015		
					131.0854	30	77.0386			133.1013		
$[M+H]^+_{und}$	303.2373				119.0859	30				119.0859		
$[M+H]^+_{TMS}$	447.3133				105.0699	30				105.0701		
Me-1-T	H	17βOH	285.2238	20	219.1750	20	105.0700	431.2812	20	201.1648	30	105.0702
		17CH3	267.2116	20	201.1674*	20	91.0544	357.2601	30	181.1053*	30	91.0504
					161.1329	30	79.0544	317.2296	30	169.1052*	30	73.0479
					159.1171*	30	77.0386	301.1994	30	143.089	30	67.0546
					145.1018*	30		227.1798	30	131.0879	30	
					131.0856	30						
$[M+H]^+_{und}$	303.2335				119.0857	30						
$[M+H]^+_{TMS}$	447.3143				105.0700	30						
STEN	H	17β OH	285.2226	20	205.1596	20	105.0700	431.2803	20	195.1210*	30	105.0701
			267.2118	20	187.1495*	20	91.0543	357.2615	20	187.1478*	30	91.0545
					159.1171	30	81.0703	267.2114	20	183.1210*	30	73.0476
					145.1014*	30	79.0543			169.1045	30	
					131.0856	30	77.0379					
					119.0858	30	67.0543					
$[M+H]^+_{und}$	303.2336				105.0701*	30						
$[M+H]^+_{TMS}$	447.3102				95.0857	30						

Table 3. Group Ic: Δ^4 3CO ring B variation. *m/z* ions and optimized CE (eV) obtained for underivatized and TMS-derivatized steroids

			Underivatized					TMS- derivatized				
Compound	**X**	**Y**	**Zone1**	**CE**	**Zone2**	**CE**	**Zone3 (50)**	**Zone1**	**CE**	**Zone2**	**CE**	**Zone3 (50)**
6OH-AED*	H	17 CO	285.1860	20	209.1331	20	105.0700	429.2646	20	181.1044	30	105.0701
(6OH)			267.1752	20	189.1280	20	91.0545	375.2163	30	169.1041*	30	73.0475
			257.1907	20	183.1171	30	79.0544	339.2142	30	155.0885	30	
			227.1438	20	157.1011	30	77.0388	299.1826	30	143.0877	30	
					145.1015	30	67.0539	247.1514	30			
					131.0856	30						
$[M+H]^+_{und}$	303.1957				105.0701	30						
$[M+H]^+_{TMS}$	519.3194				97.0650*	30						
6OXO-AED*	H	17 CO	283.1704	20	213.1280	20	105.0701	427.2467	30	193.1027	30	105.0700
(6CO)			265.1595	20	187.1124	20	91.0544	387.2160	30	181.1044	30	73.0481
			255.1754	20	171.0806*	30	79.0545	333.1693	30	169.1040	30	
			225.1282	20	145.1013*	30	77.0390	245.1342	30	155.0894	30	
					131.0858*	30	81.0692	221.1355	30	131.0860	50	
					121.0653*	30	67.0541			105.0700	50	
					107.0856*	30						
$[M+H]^+_{und}$	301.1822				105.0701*	30						
$[M+H]^+_{TMS}$	517.3012				97.0649*	30						
FLU*	H	17βOH	299.2015	20	183.1171*	30	105.0700	533.2935	20	217.1062	30	105.0707
(9F)		17CH3	281.1910	20	181.1025*	30	91.0544	462.2781	20	193.0987	30	91.0530
			255.1750	30	145.1014*	30	81.0697	407.2393	20	169.1062	30	73.0457
			241.1592	30	131.0858*	30	79.0544	353.2236	30	143.0883	30	
$[M+H]^+_{und}$	337.2195		223.1486	30	119.0859	30	67.0542	319.1877	30	121.0966	30	
$[M+H]^+_{TMS}$	553.3389				109.1014	30						
FLUmet	H	17CH_3	299.2024	20	207.1174	30	105.0700	443.2813	30	207.1178*	30	105.0715
(9F)		17CH3	281.1917	20	183.1165	30	91.0543	353.2290	30	195.1192	30	73.0482
			255.1755	20	175.1123*	30	79.0543	297.1671	30	193.1021	30	
			225.1286	20	159.1172*	30	77.038	263.1792	30	155.0903	30	
					143.0858	30	67.0541	247.1494	30			
					123.0807*	30						
					121.0652	30						
$[M+H]^+_{und}$	319.2081				105.0699	30						
$[M+H]^+_{TMS}$	463.293				95.0857	30						
MIB	H	17βOH	285.2218	20	189.1269	30	105.0696	431.2802	20	227.1810	30	105.0708
(7CH_3)		17CH3	267.2111	20	177.1271	30	91.0541	373.2569	20	211.1493	30	91.0553
			245.1902	20	133.1009	30	81.0702	357.2618	30	185.1331	30	73.0478
			227.1796	20	121.1011*	30	79.0541	317.2307	30	171.1179	30	
					107.0854*	30	77.0386	301.1992	30	157.1017	30	
$[M+H]^+_{und}$	303.2332				95.0854*	30		267.2124	30	133.1018	30	
$[M+H]^+_{TMS}$	447.3153									119.0869	30	

*tris-O-TMS compounds

Table 4. Group IIa: polyconjugated-3CO, polyconjugation exclusively located in A ring. *m/z* ions and optimized CE (eV) obtained for underivatized and TMS-derivatized steroids

			Underivatized					TMS- derivatized				
Compound	**X**	**Y**	**Zone1**	**CE**	**Zone2**	**CE**	**Zone3 (50)**	**Zone1**	**CE**	**Zone2**	**CE**	**Zone3 (50)**
1,4-AED	H	17CO	267.1765	20	151.1120	20	91.0543	413.2390	20	219.1200	30	105.0701
					121.0681*	20	77.0386	339.2127	20	207.1190	30	91.0555
								299.1805	30	195.1187	30	73.0476
								243.1201	30	193.1042	20	
										181.1041	30	
$[M+H]^+_{und}$	285.1853									169.1047	30	
$[M+H]^+_{TMS}$	429.2664									133.1017	30	
6OH-4Cl-MTD	Cl	17βOH	333.1623	20	181.0414	30	105.0700	405.2014	20	207.0580	30	105.0695
		17CH3	315.1518	20	155.0262*	30	91.0545	315.1516	20	193.0451	30	91.0544
			209.1540	20	147.1170*	30	79.0540	289.1354	20	155.0272*	30	73.0474
					133.1013	30		279.1742	20	147.1156	30	
$[M+H]^+_{und}$	351.1732							243.0625	30	107.0861	30	
$[M+H]^+_{TMS}$	495.2533							233.0735	30			
ATD*	H	17CO	265.1590	20	187.1118	20	105.0701	265.1593	20	209.1058	30	105.0706
			223.1120	20	173.0964*	20	91.0543	221.1353	20	195.1123	30	91.0554
					171.0806*	20	77.0387			193.1048	30	73.0479
					147.0808*	20				173.0963*	30	
					121.0650	20				147.0816*	30	
$[M+H]^+_{und}$	283.1711				105.0701					121.0658*	30	
$[M+H]^+_{TMS}$	355.2113				97.0649							
BD	H	17βOH	269.1922	20	173.0966	20	105.0702	415.2478	20	207.1176	20	105.0705
					135.1172*	20	91.0544	341.2287	20	193.1038*	20	91.0553
					121.0658*	20	77.0387	251.1797	20	181.1035	30	73.0478
								245.1361	20	169.1023	30	
$[M+H]^+_{und}$	287.2047									135.1178	30	
$[M+H]^+_{TMS}$	431.2799									119.0856	50	
epiMTD	H	17βOH	283.2095	20	173.0965	20	105.0701	355.2449	20	193.1046*	20	105.0701
		17CH3			149.1332*	20	91.0543	339.2137	20	149.1327*	20	91.0549
					121.0659*	20	77.0387	281.1898	20	119.0865	50	73.0476
$[M+H]^+_{und}$	301.2168							265.1950	20			
$[M+H]^+_{TMS}$	445.2991							225.1636	20			
MTD	H	17βOH	283.2093	20	187.1119	20	91.0544	429.2650	20	207.1195	20	105.0704
		17CH3			173.0964	20	77.0387	355.245	20	193.1051*	20	91.0542
$[M+H]^+_{und}$	301.2209				149.1335*	20		315.2138	20	149.1324	20	73.0476
$[M+H]^+_{TMS}$	445.2976				121.0662*	30		265.1950	20	109.1017	20	
MTDmet1*	H	17βOH	299.2016	20	173.0961	30	105.0701	-				
		17CH3	281.1910	20	147.0806*	30	91.0543					
$[M+H]^+_{und}$	317.2115		241.1593	20	121.0649*	30	77.0389					
$[M+H]^+_{TMS}$	533.3318		225.1278	20								

*MTD: tris-O-TMS compound, ATD: mono-O-TMS compound
*Not reliable data available for TMS- derivatized MTDmet1

Table 5. Group IIb: polyconjugated-3CO, polyconjugation exceeding A ring. *m/z* ions and optimized CE (eV) obtained for underivatized and TMS-derivatized steroids

			Underivatized					TMS- derivatized				
Compound	**X**	**Y**	**Zone1**	**CE**	**Zone2**	**CE**	**Zone3 (50)**	**Zone1**	**CE**	**Zone2**	**CE**	**Zone3 (50)**
4,6-AED	H	17CO	267.1751	20	183.1172	30	105.0699	413.2306	20	195.1198	30	105.0701
$\Delta^{4,6}$			227.1437	20	149.0985*	30	97.0650	339.2119	20	169.1044*	30	91.0581
					131.0856	30	91.0543	245.1353	20	131.0859	30	73.0469
					107.0492*	30	79.0542	221.1347	30			
$[M+H]^+_{und}$	285.1853				105.0698*	30	77.0386					
$[M+H]^+_{TMS}$	429.2676				97.0650*	30						
6-T	H	17βOH	269.1910	20	151.1129*	20	105.0701	415.2495	20	223.1516	30	105.0707
$\Delta^{4,6}$			229.1595	20	133.1024*	30	97.0649	341.2303	30	195.1181	30	91.0554
					107.0857	30	91.0544	315.2147	30	169.1040	30	79.0549
$[M+H]^+_{und}$	287.2016				105.0702	30	79.0544			155.0872	30	73.0479
$[M+H]^+_{TMS}$	431.2825				97.0650	30	77.0388			133.1018*	30	
MDONE	H	17βOH	269.1909	20	173.0964	20	105.0700	341.2297	20	209.1320	30	105.0700
$\Delta^{4,9}$		17CH3	213.1277	20	159.0809*	30	91.0543	267.1740	20	195.1165	30	91.0584
					135.0809*	30	79.0543	251.1800	20	159.1108	30	73.0467
$[M+H]^+_{und}$	287.2012				107.0857	30	77.0387	231.1198	30			
$[M+H]^+_{TMS}$	431.2828				95.0857	30						
ATD	H	17CO	265.1590	20	187.1118	20	105.0701	265.1593	20	209.1058	30	105.0706
$\Delta^{1,4,6}$			223.1120	20	173.0964*	20	91.0543	221.1353	20	195.1123	30	91.0554
					171.0806*	20	77.0387			193.1048	30	73.0479
					147.0808*	20				173.0963*	30	
					121.0650	20				147.0816*	30	
$[M+H]^+_{und}$	283.1711				105.0701	20				121.0658*	30	
$[M+H]^+_{TMS}$	355.2113				97.0649	20						
THG	H	17βOH	295.2069	20	199.1118*	30	107.0493	-		-		-
$\Delta^{4,9,11}$		17CH2CH3	266.1674	20	159.0809*	30	105.0700					
			241.1595	20	133.0652	30	91.0545					
$[M+H]^+_{und}$	313.2168				107.0493	30	79.0545					
$[M+H]^+_{TMS}$	455.2823						77.0385					
TREN	H	17βOH	253.1600	20	199.1124	20	107.0490	-		-		-
$\Delta^{4,9,11}$			227.1435	20	157.0645	30	105.0700					
					133.0647	30	91.0543					
$[M+H]^+_{und}$	271.1716				117.0698	30	79.0545					
$[M+H]^+_{TMS}$	415.2472				107.0490	30	77.0385					

*Not reliable data available for TMS- derivatized THG and TREN

Table 6. Group IIIa: Unconjugated 3CO. *m/z* ions and optimized CE (eV) obtained for underivatized and TMS-derivatized steroids

			Underivatized					TMS- derivatized				
Compound	**X**	**Y**	**Zone1**	**CE**	**Zone2**	**CE**	**Zone3 (50)**	**Zone1**	**CE**	**Zone2**	**CE**	**Zone3 (50)**
DHT	H	17βOH	255.2114	20	215.1800	20	105.0701	255.2117	20	203.1800	20	105.0704
					199.1485	20	91.0545			195.1199	30	91.0558
					185.1326	30	81.0701			181.1045*	30	81.0702
					173.1326	30	79.0543			169.1045	30	79.0544
					159.1167	30	77.0388			159.1170*	30	77.0400
					147.1172	30	67.0543			147.117*	30	73.0476
					145.1012	30				133.1015	30	
					133.1018	30				121.1014	30	
					131.0856*	30				119.0858	30	
$[M+H-H_2O]^+$	273.2219				119.0857*	30				109.1013	30	
$[M+H-TMSOH]^+$	345.2656				107.0856*	30				107.086*	30	
					105.0701*	30				95.0857*	30	
OXA*	H	17βOH	271.2078	20	213.1645	20	105.0701	271.2072	20	213.1646	30	105.0706
		17CH3	253.1960	20	173.1329	30	91.0545	253.1958	20	187.1491	30	91.0554
			229.1958	20	159.1172	30	81.0702	229.1956	20	173.1322	30	81.0705
					149.1328	30	79.0544			159.1172	30	79.0540
					147.1173	30	77.0388			147.1157*	30	77.0389
					135.1172	30	67.0544			133.1008*	30	67.0541
$[M+H-H_2O]^+$	289.2193				133.1010*	30				121.1011*	30	
					121.1012	30				119.0859*	30	
$[M+H-TMSOH]^+$	289.2167				119.0858*	30				107.0857*	30	
					107.0856*	30				105.0707*	30	
					105.0701*	30						

*mono-O-TMS

Table 7. Group IIIb: Unconjugated 17CO. *m/z* ions and optimized CE (eV) obtained for underivatized and TMS-derivatized steroids

			Underivatized					TMS- derivatized				
Compound	**X**	**Y**	**Zone1**	**CE**	**Zone2**	**CE**	**Zone3 (50)**	**Zone1**	**CE**	**Zone2**	**CE**	**Zone3 (50)**
11OH-Andros*	H	17CO	271.2063	20	213.1604*	20	105.0699	343.2474	20	197.1382	30	105.0713
			253.1958	20	197.1328	20	91.0543	253.1965	20	171.1201	30	91.0532
					171.1168	30	79.0543	238.1731	30	169.1035	30	73.0457
					163.1121	30	77.0388			159.1172	30	
					157.1014*	30	67.0541			145.1039	30	
					145.1013*	30						
					133.1013*	30						
$[M+H-H_2O]^+$	289.2174				131.0857*	30						
$[M+H-TMSOH]^+$	433.2981				119.0857	30						
					105.0701*	30						
11OH-Etio*	H	17CO	271.2068	20	213.1641*	20	105.0700	343.2448	20	195.1210*	30	105.0633
			253.1962	20	197.1326	30	91.0545	253.1762	20	181.1021	30	95.0864
					171.1170*	30	79.0546	233.1372	30	169.1048	30	93.0708
					159.1171*	30	77.0388			143.0873	30	91.0555
					145.1015*	30	67.0542					73.0424
					143.0857*	30						
$[M+H-H_2O]^+$	289.2179				131.0856*	30						
$[M+H-TMSOH]^+$	433.2982				129.0698	30						
					119.0858	30						
					105.0702*	30						
Andros	H	17CO	255.2121	20	213.1639	20	105.0700	255.2123	20	199.1499	30	105.0716
			185.1324	20	199.1481	20	91.0545			181.1062	30	91.0554
					161.1323	20	79.0545			161.1337	30	73.0484
					159.1171	20	77.0391			159.119*	30	
					147.1168*	30				147.1188*	30	
					131.0858	30				145.1025*	30	
					119.0858	30				131.0860	30	
$[M+H-H_2O]^+$	273.2234				105.0701*	30				119.0858	30	
$[M+H-TMSOH]^+$	345.2617									107.0856*	30	
										105.0703*	30	
CLOSmet	H	17CO	287.1576	20	211.1486*	30	105.0702	287.1533	20	195.1165*	30	105.0691
			269.1912	20	195.1172*	30	91.0544	251.1777	20	181.1021*	30	91.0420
			251.1801	20	181.1009*	30	79.0543			169.1016*	30	73.0469
			247.1252	20	173.1329*	30	77.0386			145.1010	30	
			231.0937	20	157.1012*	30	67.0542					
					155.0855*	30						
					145.1013*	30						
$[M+H-H_2O]^+$	305.1677				131.0856*	30						
$[M+H-TMSOH]^+$	377.2081				115.0311	30						
					105.0701	30						

DHEA	H	17CO	253.1976	20	213.1643*	20	105.0701	253.1950	20	211.1483	30	105.0700
			227.1801	20	197.1331*	20	91.0545	238.1718	30	195.1192	30	95.0856
					171.1171	30	81.0701			181.1042	30	91.0545
					157.1014*	30	79.0544			169.1032	30	81.0696
					145.1015*	30	77.0388			159.1166	30	73.0468
					131.0856*	30	67.0542			145.1011	30	
$[M+H-H_2O]^+$	271.2111				129.0699	30				131.0853	30	
$[M+H-TMSOH]^+$	343.2485				119.0858*	30				119.0858	30	
					105.0700*	30				105.0700	30	
DROSmet	H	17CO	269.2294	20	213.1643	20	105.0699	269.1865	20	195.0925	30	105.0547
			229.1954	20	199.1487	20	91.0542			181.0779*	30	91.0414
					173.1328	30	81.0701			169.0803*	30	73.0372
					161.1327	30	79.0543			145.0797	30	
					145.1011*	30	77.0387			121.0839	30	
					133.1011	30	67.0545					
					121.1016*	30						
$[M+H-H_2O]^+$	287.2383				119.0859*	30						
$[M+H-TMSOH]^+$	359.2861				107.0856*	30						
					105.0703*	30						
Etio	H	17CO	255.2138	20	213.1639	20	105.0700	255.2107	20	195.1200*	30	105.0702
					215.1797	20	91.0544			181.1042*	30	91.0548
					199.1483	20	81.0700			169.1043*	30	73.0470
					173.1326	20	79.0543			159.1171*	30	
					159.1169*	20	77.0387			145.1013*	30	
					147.1169*	20	67.0544			131.0855	30	
					133.1014	20				119.0860	30	
$[M+H-H_2O]^+$	273.2221				119.0857*	30				109.1010	30	
$[M+H-TMSOH]^+$	345.2669				107.0856*	30				107.0856*	30	
					105.0699*	30				105.0703*	30	
MESTmet	H	17CO	269.2269	20	213.1641	20	105.0701	269.2299	20	199.1492	20	105.0709
			229.1954	20	199.1488	20	91.0545			195.1209	30	91.0553
					173.1328	30	81.0701			181.1050	30	73.0477
					161.1329*	30	79.0544			161.1335	30	
					147.1169*	30	77.0387			145.1017*	30	
$[M+H-H_2O]^+$	287.2375				131.0854	30	67.0546			121.1020*	30	
$[M+H-TMSOH]^+$	359.28				119.0858*	30						
					105.0701*	30						
METHmet	H	17CO	267.2097	20	211.1538	30	105.0701	267.2097	20	195.1218	30	105.0713
			227.1770	20	285.1256	30	91.0545	225.1593	30	181.1044*	30	91.0551
					159.1172	30	81.0701			169.1035*	30	81.0697
$[M+H-H_2O]^+$	287.2375				145.1039*	30	79.0544			145.1039	30	73.0457
$[M+H-TMSOH]^+$	359.2800				131.0870	30	77.0387			119.0863	30	
					119.0863*	30						
					105.0713*	30	67.0545			105.0713	30	

NANmet1	H	17CO	241.1962	20	213.1648	20	105.0700	241.1953	20	185.1343	20	105.0704
					199.1487	20	91.0544			181.1045	30	91.0548
					185.1330	20	79.0545			157.1008	30	73.0471
					159.1169	20	77.0388			147.1179	30	
					147.1168	20	67.0544			145.1023*	30	
					145.1017*	30				133.1021*	30	
					133.1016	20						
					131.0855	30						
$[M+H-H_2O]^+$	259.2061				121.1016	30						
$[M+H-TMSOH]^+$	331.2498				119.0857	30						
					105.0699*	30						
NANmet2	H	17CO	241.1978	20	213.1646	20	105.0700	241.1962	20	195.1204	30	105.0713
					199.1487	20	91.0544			181.1045*	30	91.0556
					185.1330	20	79.0545			159.1171	30	73.0466
					159.1169	20	77.0388			145.1014*	30	
					147.1173	20	67.0544					
					145.1017*	20						
					133.1016	20						
					131.0855*	30						
$[M+H-H_2O]^+$	259.2060				121.1016	30						
$[M+H-TMSOH]^+$	331.2482				119.0857	30						
					105.0699*	30						

* tris-O-TMS compounds

Table 8. Group IV. *m/z* ions and optimized CE (eV) obtained for underivatized and TMS-derivatized steroids

			Underivatized					TMS- derivatized				
Compound	**X**	**Y**	**Zone1**	**CE**	**Zone2**	**CE**	**Zone3 (50)**	**Zone1**	**CE**	**Zone2**	**CE**	**Zone3 (50)**
16 AOL	H	H			201.1641	20	105.0853	241.1938	20	201.1673	20	105.0713
					175.1484	20	91.0542			175.1486	20	91.0532
					161.1327*	20	81.0703			161.1333*	20	79.0551
					147.1170*	20	79.0544			147.1187*	20	77.0405
					135.1169	20	77.0387			135.1170*	20	67.0559
					133.1016*	30	67.0542			133.1015	30	
$[M+H-H_2O]^+$	257.2223				119.0855*	30				119.0863*	30	
$[M+H-TMSOH]^+$	257.2334				107.0853*	30				107.0872*	30	
					105.0700*	30				105.0713*	30	
5a3a-DIOL	H	17βOH	229.1933	20	201.1637	20	105.0700			201.1631*	20	105.0701
					175.1483*	20	91.0543			175.1476*	20	91.0554
					161.1329	20	81.0702			161.1328*	20	81.0702
					147.1170	20	79.0543			147.1169*	20	79.0546
					135.1177	20	77.0391			135.1165*	20	77.0403
					133.1012	30	67.0545			133.1012	30	67.0544
					119.0858*	30				119.0855*	30	
$[M+H-2H_2O]^+$	257.2300				109.1012*	30				109.1009*	30	
$[M+H-2TMSOH]^+$	257.2272				107.0856*	30				107.0854*	30	
					105.0701*	30				105.0701*	30	
5a3b-DIOL	H	17βOH			201.1643	20	105.0703			201.1631	20	105.0702
					175.1485	20	91.0547			175.1476*	20	91.0546
					161.1330*	20	81.0701			161.1319*	20	81.0703
					147.1173*	20	79.0546			147.1169*	20	79.0546
					135.1173	20	77.0388			135.1169*	20	77.0388
					133.1015	30	67.0543			133.1012*	30	67.0544
					119.0858*	30				119.0855*	30	
$[M+H-2H_2O]^+$	257.2284				109.1011*	30				109.1009*	30	
$[M+H-2TMSOH]^+$	257.2279				107.0855*	30				107.0854*	30	
					105.0701*	30				105.0701*	30	
5b3a-DIOL	H	17βOH			201.1644	20	105.0697			201.1638	20	105.0706
					175.1486	20	91.0545			175.1487*	20	91.0551
					161.1329*	20	81.0701			161.1324*	20	81.0701
					147.1173*	20	79.0543			147.1174*	20	79.0543
					135.1171*	20	77.0383			135.1172	20	77.0400
					133.1013*	30	67.0541			133.0865	30	67.0549
					119.0858*	30				119.0871*	30	
$[M+H-2H_2O]^+$	257.2274				109.1011*	30				109.1010*	30	
$[M+H-2TMSOH]^+$	257.2268				107.0856*	30				107.0854*	30	
					105.0699*	30				105.0703*	30	

BOLASmet	H	17βOH	229.1953	20	215.1799	20	105.0700	229.1964	20	215.1794	20	105.0704
		17CH3			203.1797*	20	91.0544			203.1811	20	91.0555
					189.1640	20	81.0701			189.1665	20	81.0706
					175.1484*	20	79.0543			175.149*	20	77.0384
					161.1310	30	77.0385			161.1309	20	67.0558
					159.1162	30	67.0541			159.1164	20	
					147.1170	30				147.1188	30	
					133.1012	30				133.1025	30	
					119.0856*	30				119.087*	30	
$[M+H-2H_2O]^+$	285.2585				109.1009*	30				109.1010*	30	
$[M+H-2TMSOH]^+$	285.2583				107.0856*	30				107.0855*	30	
					105.0701*	30				105.0701	30	
CALUSmet	H	17βOH	229.1958	20	215.1801	20	105.0701	229.1958	20	215.1801	20	105.0707
		17CH3			203.1800	20	91.0545			203.1802	20	91.0554
					189.1643	20	81.0700			189.1644	20	81.0713
					175.1488	20	79.0545			175.1488*	20	67.0549
					161.1330	30	77.0388			161.1325	30	
					147.1171*	30	67.0543			147.1172	30	
					133.1015*	30				133.1021	30	
					119.0859*	30				119.0864*	30	
$[M+H-2H_2O]^+$	285.2590				109.1014*	30				109.1010*	30	
$[M+H-2TMSOH]^+$	285.2629				107.0850*	30				107.0855*	30	
					105.0700*	30				105.0701*	30	
MADOL*	H	17βOH			215.1797	20	105.0698			215.1785	20	105.0696
		17CH3			201.1693	20	91.0542			201.1629	20	91.0541
					189.1640	20	81.0699			189.1627	20	81.0701
					175.1484	20	79.0542			175.1570	20	79.0539
					161.1328*	20	77.0386			161.1319	20	77.0385
					147.1169	30	67.0543			147.1172	20	67.0542
					135.1171	30				145.1009	30	
					133.1010*	30				133.1009*	30	
					119.0856*	30				119.0854*	30	
$[M+H-H_2O]^+$	271.2492				109.1015*	30				109.1010*	30	
$[M+H-TMSOH]^+$	271.2440				107.0855*	30				107.0855*	30	
					105.0701*	30				105.0701*	30	
MTDmet3	H	17βOH	241.1957	20	213.1647	20	105.0700			213.1306	20	105.0521
		17CH3			201.1644	20	91.0543			201.1646	20	91.0385
					185.1325	20	79.0543			185.132	30	79.0437
					171.1169	30	77.0387			171.1170	30	77.0263
					161.1324	30				161.1058	30	
					145.1011	30				145.0784	30	
					131.0856	30				131.0634	30	
$[M+H-2H_2O]^+$	269.2271				119.0856	30				119.0678	30	
$[M+H-2TMSOH]^+$	269.2334				107.0855*	30				107.0853*	30	
					105.0701*	30				105.0539*	30	

MTDmet4	H	$17CH_3$	241.1961	20	213.1647	20	105.0701	253.1998	20	213.1646	20	105.0692
		17CH3			201.1645	20	91.0544			201.1645	20	91.0551
					175.1487	30	79.0543			175.1459	20	79.0533
					161.1332	30	81.0702			161.1333	30	77.0387
					145.1012	30	77.0386			145.1015	30	67.0542
					131.0856	30	67.0544			131.0855	30	
$[M+H-H_2O]^+$	269.2270				119.0856*	30				119.0863	30	
$[M+H-TMSOH]^+$	269.2328				107.0856*	30				107.0850	30	
					105.0701*	30				105.0692*	30	
METHASmet	H	17βOH	229.1959	20	215.1802	20	105.0702	229.1947	20	215.1774	20	105.0703
		17CH3			189.1644	20	91.0544			189.1635	20	91.0574
					175.1489*	20	81.0701			175.1488	20	79.0536
					161.1332*	20	79.0543			161.1339	20	77.0427
					149.1326	20	77.0386			149.1325	30	67.0542
					135.1173	20	67.0542			135.1172	30	
					133.1014	30				133.1012	30	
					121.1015	30				131.0871	30	
$[M+H-2H_2O]^+$	285.2583				119.0858*	30				121.1022*	30	
$[M+H-2TMSOH]^+$	285.2653				107.0850*	30				107.0858*	30	
					105.0700*	30				105.0707	30	
MeTmet1	H	17βOH			215.1802	20	105.0703			215.1806	20	105.0706
		17CH3			201.1646	20	91.0544			201.1644	20	91.0534
					189.1645	20	81.0699			189.1624	20	81.0702
					175.1486	20	79.0542			175.1492	20	79.0516
					161.1330*	20	77.0387			161.1326*	20	77.0432
					145.1015	20	67.0545			145.1011*	30	67.0539
					135.1173*	20				135.1172*	30	
					133.1017*	30				133.1005*	30	
					119.0859*	30				119.0864*	30	
$[M+H-2H_2O]^+$	271.2430				109.1015*	30				109.1013*	30	
$[M+H-2TMSOH]^+$	271.2430				107.0855*	30				107.0853*	30	
					105.0701*	30				105.0701*	30	
MeTmet2	H	17βOH			215.1799	20	105.0702			215.1808	20	105.0710
		17CH3			201.1643	20	91.0546			201.1642	20	91.0553
					189.1644	20	81.0701			189.1662	20	81.0702
					175.1485*	20	79.0544			175.1492	20	79.0546
					161.1328*	20	77.0386			161.134*	30	77.0408
					145.1013	20	67.0543			145.1015	30	67.0554
					135.1173*	20				135.1171*		
					133.1015*	30				133.1024*	30	
					119.0858*	30				119.0864*	30	
$[M+H-2H_2O]^+$	271.2429				109.1015*	30				109.1012*	30	
$[M+H-2TMSOH]^+$	271.2521				107.0855*	30				107.0854*	30	
					105.0701*	30				105.0701*	30	

NORBOLmet1	H	17βOH	229.1956	20	215.1799	20	105.0702	229.1960	20	215.1802	20	105.0706
		17CH2CH3			201.1649	20	91.0544			201.1648	20	91.0550
					189.1641*	20	81.0700			189.1645	20	81.0702
					175.1486	20	79.0544			175.1481	20	79.0551
					161.1330	20	77.0388			161.1329	30	77.0397
					147.1171*	30	67.0544			147.1176*	30	67.0556
					133.1014*	30				133.1015*	30	
					121.1014*	30				121.1015*	30	
					119.0858*	30				119.0863*	30	
$[M+H-2H_2O]^+$	285.2584				109.1011	30				109.1012*	30	
$[M+H-2TMSOH]^+$	285.2605				107.0855	30				107.0854*	30	
					105.0702*	30				105.0701*	30	
					95.0857*	30				95.0861*	30	
NORBOLmet2	H	17βOH	229.1958	20	215.1803	20	105.0701	229.1958		215.1799	20	105.0704
		17CH2CH3			201.1642	20	91.0545			201.1641	20	91.0547
					189.1645*	20	81.0700			189.1641	20	79.0546
					175.1487	20	79.0544			175.1475	20	77.0389
					161.1328	20	77.0387			161.1327	30	67.0544
					147.1170	30	67.0543			147.1171	30	
					133.1014*	30				133.1015*	30	
					121.1015*	30				121.1014*	30	
					119.0858*	30				119.0860*	30	
$[M+H-2H_2O]^+$	285.2590				109.1011	30				109.1012*	30	
$[M+H-2TMSOH]^+$	285.2601				107.0855	30				107.0854*	30	
					105.0702*	30				105.0701*	30	
					95.0857*	30				95.0861*	30	
NORETHANmet1	H	17βOH			215.1798	20	105.0701			215.1802	20	105.0705
		17CH2CH3			201.1643	20	91.0543			201.1641	20	91.0549
					187.1484	20	81.0700			187.1488	20	81.0701
					175.1487*	20	79.0544			175.1484*	20	79.0552
					149.1328	20	77.0386			149.1329	20	77.0394
					147.1169	20	67.0543			133.1019*	30	67.0553
					133.1013	20				121.1015*	30	
					121.1014	20				119.0861*	30	
$[M+H-2H_2O]^+$	271.2423				119.0857*	30				109.1012*	30	
$[M+H-2TMSOH]^+$	271.2460				107.0855*	30				107.0854*	30	
					105.0701*	30				105.0699*	30	
					95.0858	30				95.0860*	30	

* mono-O-TMS compounds

Table 9. Summary of neutral losses and fragment ions observed in CID fragmentation of AAS in Zones 1, 2 and 3(CxHyOz). **a) Underivatized, b) Derivatized**

(a)			Zone 1	Zone 2		Zone 3
Group	**Structural feature**		Losses	Losses	Ions	Ions
Ia	General		H_2O (n=z)		97.0650 (C_6H_9O) 109.0649 (C_7H_9O)	105.0704 (C_8H_9) 91.0548 (C_7H_7) 81.0700 (C_6H_9) 79.0544 (C_6H_7) 77.0386 (C_6H_5) 67.0548 (C_5H_7)
	Specific	17CO	H_2O (n=z-1)			
		4OH			113.0600 ($C_6H_9O_2$) 125.0599 ($C_7H_9O_2$)	
Ib	General		H_2O (n=z)	$H_2O + C_5H_8O$ $H_2O + C_5H_8O + C_3H_6$ $H_2O + C_5H_8O + C_4H_8$		
Ic	General		H_2O (n=z)		Ions containing A-B rings	
	Specific	17CO	H_2O (n=z-1)			
		9F	$HF + H_2O$ (n=z)			
IIa	General		H_2O (n=z-1)		121.0653 (C_8H_9O)	
	Specific	4Cl			155.0264 (C_8H_8OCl)	
IIb	General		H_2O (n=z-1)			
	Specific	$\Delta^{4,6}$		$C_9H_{12}O$ (A-B rings) $H_2O + C_9H_{12}O$ (A-B rings)		
		$\Delta^{4,9}$			159.0810 ($C_{11}H_{11}O$) 135.0810 ($C_9H_{11}O$)	
		$\Delta^{1,4,6}$			171.0810 ($C_{12}H_{11}O$) 147.0810 ($C_{10}H_{11}O$)	
		$\Delta^{4,9,11}$			199.1123 ($C_{14}H_{15}O$)	

Table 9. (Cont)

IIIa	General		H_2O (n=z)* CH_3COCH_3	199.1487 ($C_{15}H_{19}$) and subsequent – CH_2- losses	
	Specific	2O	CH_3COOH		
IIIb	General		H_2O (n=z-1)*	199.1487 ($C_{15}H_{19}$) and subsequent – CH_2- losses	
	Specific	4Cl	HCl + H_2O (n=z)*		
IV	General		C_4H_8	189.1311 and subsequent – CH_2- losses	
	Specific	$^1\Delta$	C_2H_4		

* $[M+H-H_2O]^+$ selected as precursor ion, i.e. one oxygen already lost by in source fragmentation

Table 9. (Cont. TMS-Derivatized)

(b)			Zone 1		Zone 2		Zone 3
Group	**Structural feature**		Losses		Losses	Ions	Ions
Ia	General		TMSOH (n=z)			169.1042 ($C_9H_{17}SiO$) 181.1044 ($C_{10}H_{17}SiO$)	105.0704 (C_8H_9) 91.0548 (C_7H_7)
	Specific	17OH 17 CH_3	130 (TMSOH + D ring) TMSOH				81.0700 (C_6H_9)
Ib	General		H_2O (n=z)	CH_4	TMSOH + C_5H_8O-TMS		79.0544 (C_6H_7)
	Specific	1-T, 1-AED, Me-1-T				169.1042 ($C_9H_{17}SiO$) 181.1044 ($C_{10}H_{17}SiO$)	77.0386 (C_6H_5) 73.0477 (TMS^+)
Ic	General		TMSOH (n=z)		Ions containing A-B rings	169.1042 ($C_9H_{17}SiO$)	
	Specific	17CO	TMSOH (n=z-1) 130 (TMSOH+D ring)			181.1044 ($C_{10}H_{17}SiO$)	
		9F	HF + TMSOH (n=z)				
IIa	General		TMSOH (n=z)	CH_4		193.1049 ($C_{11}H_{17}SiO$)	
	Specific	17CO	TMSOH (n=z-1) 130 (TMSOH+D ring)				
		4Cl	TMSOH (n=z-1)				
IIb	General		-			195.1174 ($C_{11}H_{19}SiO$)	
	Specific	$\Delta^{4,6}$	TMSOH (n=z-1)	CH_4		169.1042 ($C_9H_{17}SiO$)	
		$\Delta^{4,9}$	TMSOH (n=z)				
		$\Delta^{1,4,6}$	TMSOH (n=z-1)				
IIIa	General		TMSOH (n=z) CH_3COCH_3				
	Specific	2O	CH_3COOH				
IIIb	General		TMSOH (n=z-1)			169.1042 ($C_9H_{17}SiO$) 181.1044 ($C_{10}H_{17}SiO$)	

SUPPLEMENTARY INFORMATION

2.3. Instrumental information

Nitrogen was used as auxiliary gas at 150 L/h, make-up gas at 18 L/h and cone gas at 16 L/h. APCI corona pin used was 1 µA for underivatized and 1.6 µA for TMS-derivatized.

Xevo G2 QTOF operated at a scan time of 0.3 s in a mass range of *m/z* 50–650. TOF MS resolution mass was approximately 18 000 (FWHM) at *m/z* 614.

Heptacosa (Sigma-Aldrich, Madrid, Spain), was used for the daily mass calibration. Internal calibration was performed using a background ion coming from the GC-column bleed as lock mass (protonated molecule of octamethylcyclotetrasiloxane, *m/z* 297.0830).

Table 1SI. Structural information of the groups of steroids investigated

Compound	Ring A	Ring B	Ring C	Ring D
General Steroid Structure 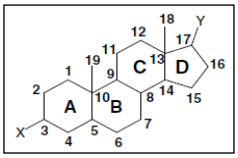				
Group I				
AED	Δ^4 ^{3}CO	-	-	^{17}CO
1-AED	Δ^1 ^{3}CO	-	-	^{17}CO
1-T	Δ^1 ^{3}CO	-	-	^{17}OH
4OH-AED	Δ^4 ^{3}CO ^{4}OH	-	-	^{17}CO
4OH-NAN	Δ^4 ^{3}CO ^{4}OH nor $^{19}CH_3$	-	-	^{17}CO
4OH-T	Δ^4 ^{3}CO ^{4}OH	-	-	^{17}OH
6OH-AED	Δ^4 ^{3}CO	^{6}OH	-	^{17}CO
6OXO-AED	Δ^4 ^{3}CO	^{6}CO	-	^{17}CO
BDmet	Δ^1 ^{3}CO	-	-	^{17}OH
DANmet	Δ^4 ^{3}CO	-	-	^{17}OH ^{17}C≡C

E	Δ^4 ^{3}CO	-	-	^{17}OH
FLU	Δ^4 ^{3}CO	^{9}F	^{11}OH	^{17}OH ^{17}CH$_3$
FLUmet	Δ^4 ^{3}CO	^{9}F	^{11}OH nor Δ^{13} ^{19}CH$_3$	^{17} CH$_3$ ^{17}CH$_3$
METH	Δ^1 ^{3}CO ^{1}CH$_3$	-	-	^{17}OH
1-MeT	Δ^1 ^{3}CO	-	-	^{17}OH ^{17}CH$_3$
MeT	Δ^4 ^{3}CO	-	-	^{17}OH ^{17}CH$_3$
MIB	Δ^4 ^{3}CO nor ^{19}CH$_3$	^{7}CH$_3$	-	^{17}OH ^{17}CH$_3$
OXY	Δ^4 ^{3}CO ^{4}OH	-	-	^{17}OH ^{17}CH$_3$
STEN	Δ^1 ^{2}CH$_3$ ^{3}CO	-	-	^{17}OH
T	Δ^4 ^{3}CO	-	-	^{17}OH
Group II				
1,4-AD	$\Delta^{1,4}$ ^{3}CO	-	-	^{17}CO
4,6-AD	Δ^4 ^{3}CO	Δ^6	-	^{17}CO
6OH-4Cl-MTD	$\Delta^{1,4}$ ^{3}CO ^{4}Cl	^{6}OH	-	^{17}OH ^{17}CH$_3$
6-T	Δ^4 ^{3}CO	Δ^6	-	^{17}OH
ATD	$\Delta^{1,4}$ ^{3}CO	Δ^6	-	^{17}CO
BD	$\Delta^{1,4}$ ^{3}CO	-	-	^{17}OH
epiMTD	$\Delta^{1,4}$ ^{3}CO	-	-	^{17}OH ^{17}CH$_3$
MTD	$\Delta^{1,4}$ ^{3}CO	-	-	^{17}OH ^{17}CH$_3$
MTDmet1	$\Delta^{1,4}$ ^{3}CO	^{6}OH	-	^{17}OH ^{17}CH$_3$
MDONE	Δ^4 ^{3}CO nor ^{19}CH$_3$	Δ^9	-	^{17}OH ^{17}CH$_3$
THG	Δ^4 ^{3}CO	Δ^9	Δ^{11}	^{13}CH$_2$CH$_3$
TREN	Δ^4 ^{3}CO nor ^{19}CH$_3$	Δ^9	Δ^{11}	^{17}OH
Group III				
11OH-Andros	^{3}OH, 5α-H	-	^{11}OH	^{17}CO
11OH-Etio	^{3}OH, 5β-H	-	^{11}OH	^{17}CO
Andros	^{3}OH, 5α-H	-	-	^{17}CO
CLOSmet1	Δ^4 ^{3}OH ^{4}Cl	-	-	^{17}CO

DHEA	^{3}OH	Δ^{5}	-	^{17}CO
DHT	^{3}CO, 5α-H	-	-	^{17}OH
DROSmet	^{2}CH$_3$, ^{3}OH, 5α-H	-	-	^{17}CO
Etio	^{3}OH, 5β-H	-	-	^{17}CO
MESTmet	^{1}CH$_3$ ^{3}OH, 5α-H	-	-	^{17}CO
METHmet	^{1}C=CH$_2$ ^{3}OH, 5α-H	-	-	^{17}CO
NANmet1	^{3}OH, 5α-H nor ^{19}CH$_3$	-	-	^{17}CO
NANmet2	^{3}OH, 5β-H nor ^{19}CH$_3$	-	-	^{17}CO
OXA	^{3}CO ^{2} –O–, 5α-H	-	-	^{17}OH ^{17}CH$_3$
Group IV				
16AOL	^{3}OH, 5α-H	-	-	Δ^{16}
5a3a-DIOL	^{3}OH, 5α-H	-	-	^{17}OH
5a3b-DIOL	^{3}OH, 5α-H	-	-	^{17}OH
5b3a-DIOL	^{3}OH, 5β-H	-	-	^{17}OH
BOLASmet	^{3}OH, 5β-H	^{7}CH$_3$	-	^{17}OH ^{17}CH$_3$
CALUSmet	^{3}OH, 5β-H	^{7}CH$_3$	-	^{17}OH ^{17}CH$_3$
MADOL	Δ^{2}, 5α-H	-	-	^{17}OH ^{17}CH$_3$
MTDmet3	Δ^{1}, ^{3}OH, 5β-H	-	-	^{17}OH ^{17}CH$_3$
MTDmet4	Δ^{1}, ^{3}OH, 5β-H	-	Δ^{13} nor^{18}CH$_3$	^{17}CH$_3$ ^{17}CH$_3$
METHASmet1	^{2}CH$_3$, ^{3}OH, 5α-H	-	-	^{17}OH ^{17}CH$_3$
MeTmet1	^{3}OH, 5α-H	-	-	^{17}OH ^{17}CH$_3$
MeTmet2	^{3}OH, 5β-H	-	-	^{17}OH ^{17}CH$_3$
NORBOLmet1	^{3}OH, 5α-H nor ^{19}CH$_3$	-	-	^{13}CH$_2$CH$_3$
NORBOLmet2	^{3}OH, 5β-H nor ^{19}CH$_3$	-	-	^{13}CH$_2$CH$_3$
NORETHANmet1	^{3}OH, 5β-H nor ^{19}CH$_3$	-	-	^{17}OH ^{17}CH$_2$CH$_3$

Figure 1SI. CID spectra at 20 and 30 eV of the $[M+H]^+$, $[M+H-H_2O]^+$ or $[M+H-2H_2O]^+$ of selected compounds of all the groups in the underivatized form

Underivatized		20 eV	30 eV
Group	*Example*		
Ia	T	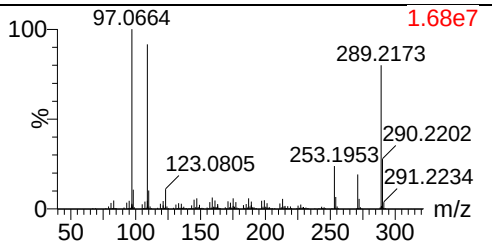	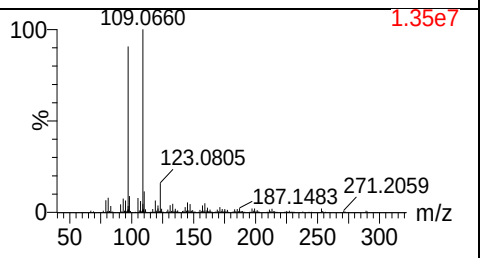
Ib	BDmet	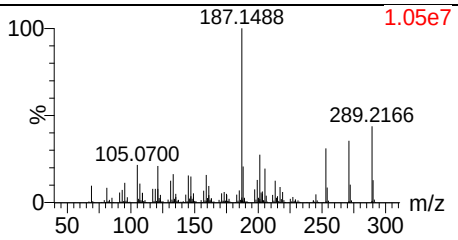	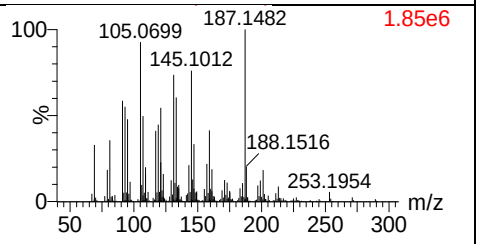
Ic	6OH-AED	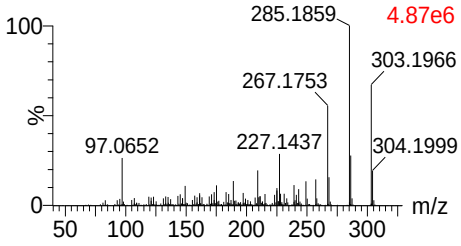	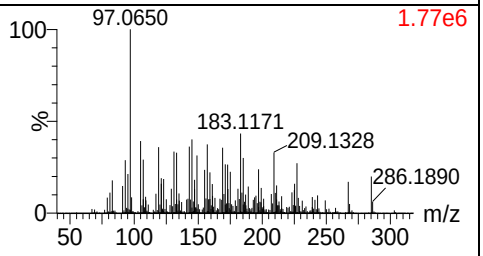
IIa	epiMTD	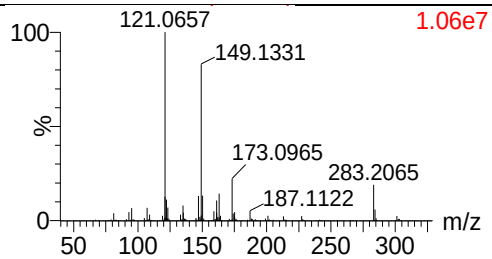	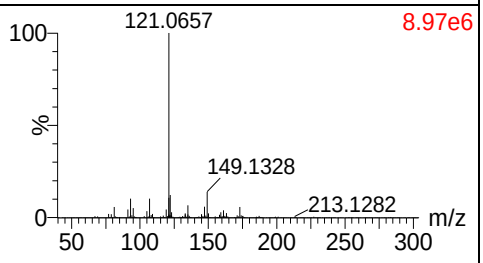
IIb	4,6-AED	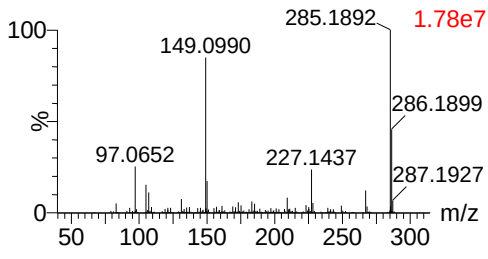	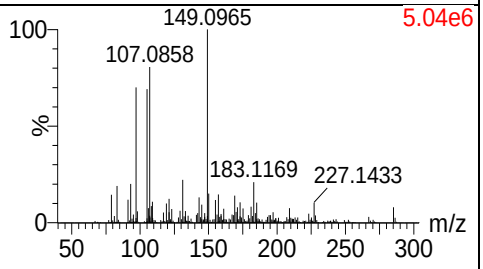

IIIa	DHT	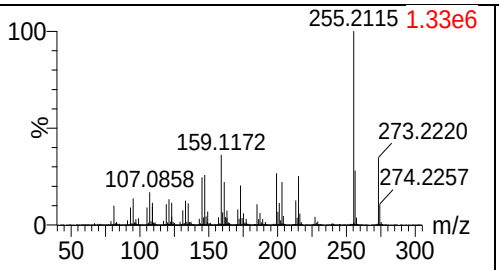	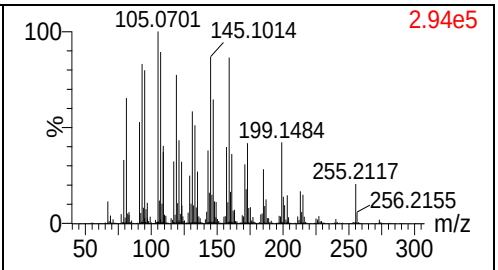
IIIb	Etio	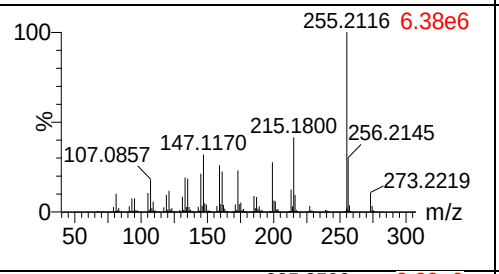	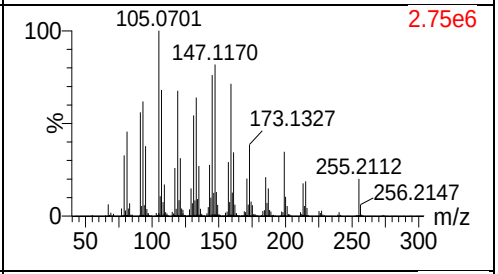
IV	CALUS met	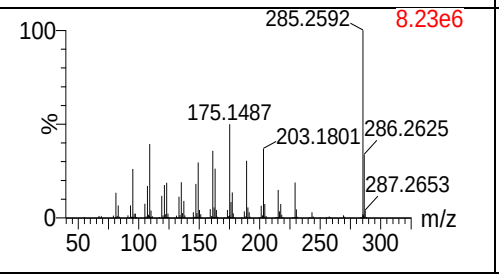	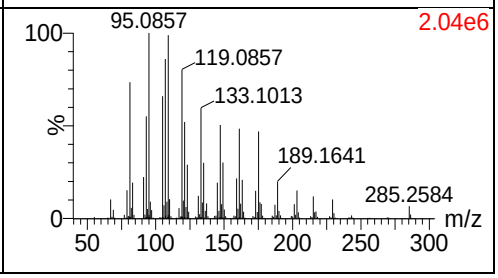

Figure 2SI. CID spectra at 20 and 30 eV of the $[M+H]^+$, $[M+H\text{-}TMSOH]^+$ or $[M+H\text{-}2TMSOH]^+$ of selected compounds of all the groups in the TMS-derivatized form

TMS-derivatized		20 eV	30 eV
Group	*Example*		
Ia	T	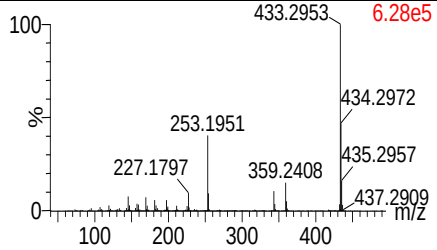	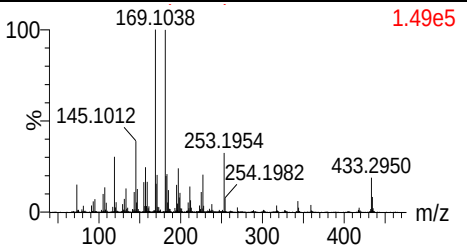
Ib	BDmet	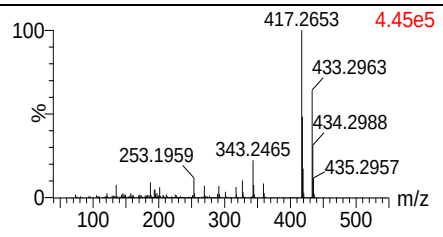	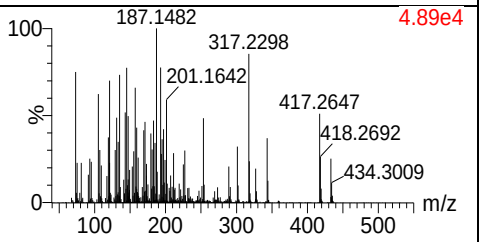
Ic	6OH-AED	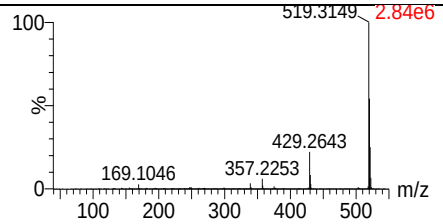	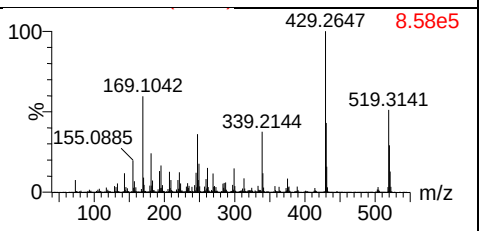
IIa	epiMTD	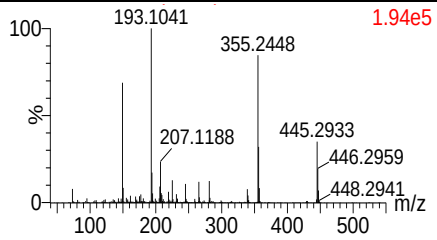	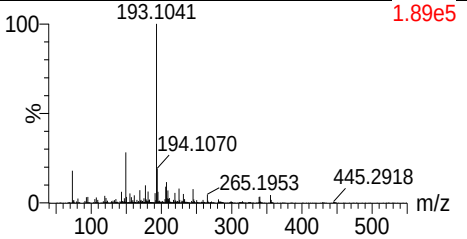
IIb	4,6-AED	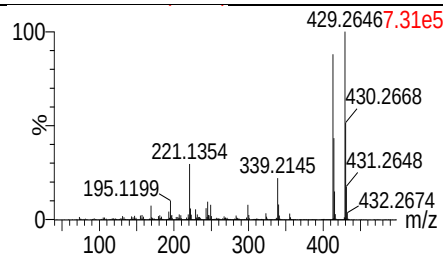	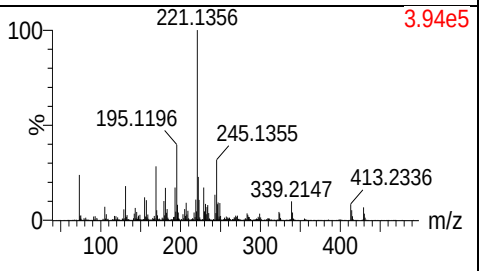

IIIa	DHT	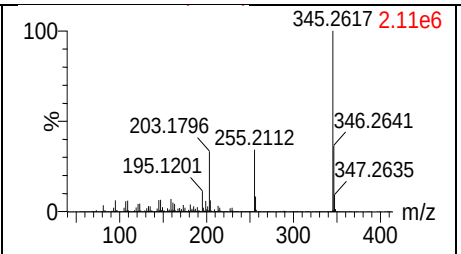	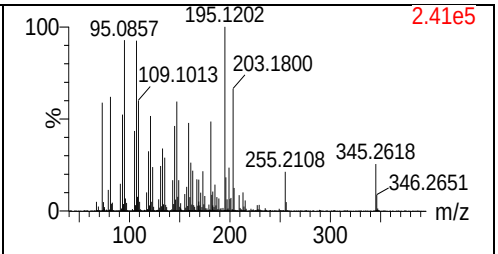
IIIb	Etio	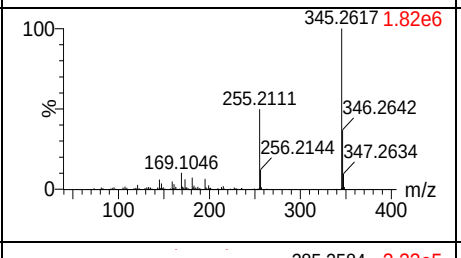	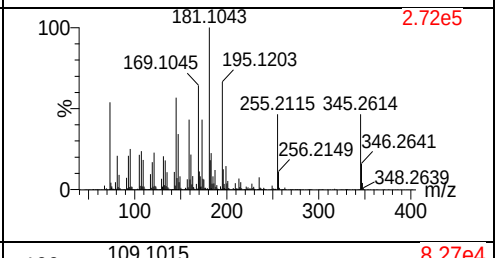
IV	CALUS met	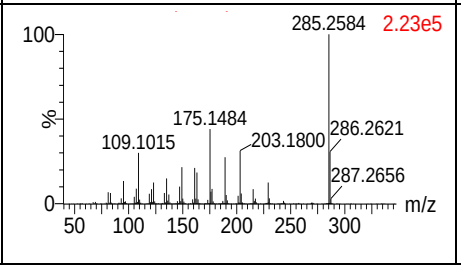	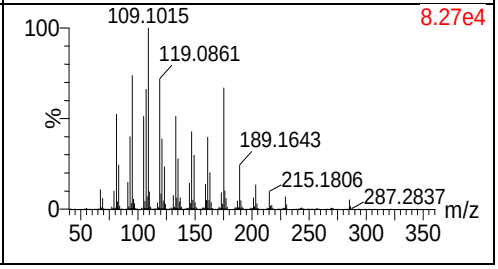

II.4. Artículo científico 3

Analytica Chimica Acta 906 (2016) 128–138

Contents lists available at ScienceDirect

Analytica Chimica Acta

journal homepage: www.elsevier.com/locate/aca

Potential of atmospheric pressure chemical ionization source in gas chromatography tandem mass spectrometry for the screening of urinary exogenous androgenic anabolic steroids

M. Raro [a], T. Portolés [a], E. Pitarch [a], J.V. Sancho [a], F. Hernández [a], L. Garrostas [b], J. Marcos [b, c], R. Ventura [b, c], J. Segura [b, c], O.J. Pozo [b, *]

[a] Research Institute for Pesticides and Water, University Jaume I, E-12071 Castellón, Spain
[b] Bioanalysis Research Group, IMIM, Hospital del Mar Medical Research Institute, Doctor Aiguader 88, 08003 Barcelona, Spain
[c] Department of Experimental and Health Sciencies, Universitat Pompeu Fabra, Doctor Aiguader 88, 08003 Barcelona, Spain

HIGHLIGHTS

- APCI source has been evaluated for the screening of 16 exogenous AAS in urine.
- Suitable precision was observed for APCI although lower than with EI.
- LODs for APCI were commonly lower.
- GC-APCI-MS/MS method increases the period in which the misuse of 4ClMTD is detected.
- APCI source is an adequate alternative to the traditional EI source in GC–MS.

GRAPHICAL ABSTRACT

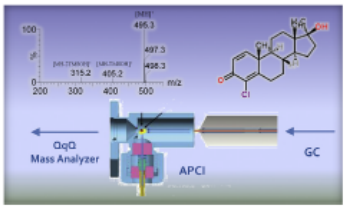

ARTICLE INFO

Article history:
Received 17 September 2015
Received in revised form
11 November 2015
Accepted 26 November 2015
Available online 17 December 2015

Keywords:
Anabolic androgenic steroids (AAS)
Atmospheric pressure chemical ionization (APCI)
Gas chromatography (GC)
Tandem mass spectrometry (MS/MS)
Triple quadrupole (QqQ)
Doping control analysis

ABSTRACT

The atmospheric pressure chemical ionization (APCI) source for gas chromatography-mass spectrometry analysis has been evaluated for the screening of 16 exogenous androgenic anabolic steroids (AAS) in urine. The sample treatment is based on the strategy currently applied in doping control laboratories i.e. enzymatic hydrolysis, liquid–liquid extraction (LLE) and derivatization to form the trimethylsilyl ether-trimethylsilyl *enol ether* (TMS) derivatives. These TMS derivatives are then analyzed by gas chromatography tandem mass spectrometry using a triple quadrupole instrument (GC-QqQ MS/MS) under selected reaction monitoring (SRM) mode. The APCI promotes soft ionization with very little fragmentation resulting, in most cases, in abundant $[M + H]^+$ or $[M + H\text{-}2TMSOH]^+$ ions, which can be chosen as precursor ions for the SRM transitions, improving in this way the selectivity and sensitivity of the method. Specificity of the transitions is also of great relevance, as the presence of endogenous compounds can affect the measurements when using the most abundant ions. The method has been qualitatively validated by spiking six different urine samples at two concentration levels each. Precision was generally satisfactory with RSD values below 25 and 15% at the low and high concentration level, respectively. Most the limits of detection (LOD) were below 0.5 ng mL^{-1}. Validation results were compared with the commonly used method based on the electron ionization (EI) source. EI analysis was found to be slightly more repeatable whereas lower LODs were found for APCI. In addition, the applicability of the developed method has been tested in samples collected after the administration of 4-

Potential of atmospheric pressure chemical ionization source in gas chromatography tandem mass spectrometry for the screening of urinary exogenous androgenic anabolic steroids

M. Raro[a], T. Portolés[a], E. Pitarch[a], J.V. Sancho[a], F. Hernández[a], L. Garrostas[b], J. Marcos[b, c], R. Ventura[b, c], J. Segura[b, c], O.J. Pozo[b]

a) Research Institute for Pesticides and Water, University Jaume I, E-12071 Castellón, Spain
b) Bioanalysis Research Group, IMIM, Hospital del Mar Medical Research Institute, Doctor Aiguader 88, 08003 Barcelona, Spain
c) Department of Experimental and Health Sciencies, Universitat Pompeu Fabra, Doctor Aiguader 88, 08003 Barcelona, Spain

Abstract

The atmospheric pressure chemical ionization (APCI) source for gas chromatography-mass spectrometry analysis has been evaluated for the screening of 16 exogenous androgenic anabolic steroids (AAS) in urine. The sample treatment is based on the strategy currently applied in doping control laboratories i.e. enzymatic hydrolysis, liquid–liquid extraction (LLE) and derivatization to form the trimethylsilyl ether-trimethylsilyl enol ether (TMS) derivatives. These TMS derivatives are then analyzed by gas chromatography tandem mass spectrometry using a triple quadrupole instrument (GC-QqQ MS/MS) under selected reaction monitoring (SRM) mode. The APCI promotes soft ionization with very little fragmentation resulting, in most cases, in abundant $[M + H]^+$ or $[M + H\text{-}2TMSOH]^+$ ions, which can be chosen as precursor ions for the SRM transitions, improving in this way the selectivity and sensitivity of the method. Specificity of the transitions is also of great relevance, as the presence of endogenous compounds can affect the measurements when using the most abundant ions. The method has been

qualitatively validated by spiking six different urine samples at two concentration levels each. Precision was generally satisfactory with RSD values below 25 and 15% at the low and high concentration level, respectively. Most the limits of detection (LOD) were below 0.5 ng mL^{-1}. Validation results were compared with the commonly used method based on the electron ionization (EI) source. EI analysis was found to be slightly more repeatable whereas lower LODs were found for APCI. In addition, the applicability of the developed method has been tested in samples collected after the administration of 4-chloromethandienone. The highest sensitivity of the APCI method for this compound, allowed to increase the period in which its administration can be detected.

1. Introduction

Since 2004, the World Anti-Doping Agency (WADA) publishes a list of prohibited substances and methods in sport which is yearly updated [1]. Among the groups of substances included in the list, androgenic anabolic steroids (AAS) are the most frequently reported ones [2]. AAS are mainly used due to their anabolic effects such as muscle and strength growth among others [3].

AAS are prohibited at all times i.e. in and out of competition. This prohibition makes that any evidence of AAS misuse (e.g. the mere presence of traces of the AAS and/or its metabolites) is sufficient for reporting an adverse analytical finding [4]. The detection of AAS misuse is a constant analytical challenge due to their low concentration in urine, the complexity of the matrix and the similarity between endogenous and exogenous AAS. Thus, sensitivity and selectivity of analytical methods are key factors and

requirements for AAS detection have evolved hand in hand with instrumental developments.

AAS have been traditionally determined by gas chromatography mass spectrometry (GC–MS) methods working in selected ion monitoring mode (SIM) using electron ionization (EI) sources [5]. After some preparation steps [6] i.e. hydrolysis with β-glucuronidase, liquid–liquid extraction and conversion of both hydroxyl and carbonyl function into the corresponding TMS ether/enol-TMS ethers, these methods allowed the detection of most of AAS metabolites at concentrations below 10 ng mL^{-1}. For this reason, the minimum required performance level (MRPL) for most AAS was set at 10 ng mL^{-1}. However, these methods failed for the detection of several AAS at the required MRPL, mainly those with difficulties in the derivatization step. Among them, stanozolol and AAS bearing a 4,9,11-triene nucleus like tetrahydrogestrinone (THG) [7].

The occurrence of high resolution mass spectrometry opened new possibilities for the detection of stanozolol [8], although the scenario drastically changed after the introduction of liquid chromatography tandem mass spectrometry (LC-MS(/MS)) in doping control laboratories [9] and [10]. Several methods have been developed for the LC-MS/MS detection of AAS with poor derivatization properties like stanozolol and THG [11], [12] and [13]. Thus, both GC–MS(/MS) and LC-MS(/MS) have been employed as complementary techniques in doping control laboratories in order to reach the required MRPLs. Qualitative methods for the detection of exogenous AAS in urine by LC-MS/MS with triple quadrupole (QqQ) analyzers and electrospray ionization source (ESI) [11] have been reported, as well as GC–MS/MS methods with EI [14] and [15] or chemical ionization (CI) sources [16].

In the last years, the commercialization of triple quadrupole instruments coupled to GC has allowed for increasing the sensitivity of the previous GC–MS methods. Thus, several GC-EI-MS/MS methods in selected reaction monitoring mode (SRM) have been published either for the detection of target analytes [14] and [15] or for metabolic studies [17], [18] and [19]. Nowadays, this technique has become the gold-standard in AAS analysis for doping control purposes. Due to the sensitivity improvement, the MRPL for AAS has been recently reduced to 2–5 ng mL^{-1} for most analytes [4]. This fact illustrates the impact of new analytical technologies in the detection of AAS. Therefore, it is valuable to test the performance of emerging analytical tools in this field.

As an alternative to EI, different "soft" ionization sources for GC have been tested for the detection of AAS in doping analysis, i.e. CI [16], heated nebulizer microchip atmospheric pressure photoionization (μAPPI) [20] and [21] or atmospheric pressure chemical ionization (APCI) [22] and [23]. The recently commercialized APCI source for GC represents an attractive alternative in several application fields [24], [25] and [26]. APCI promotes soft ionization for the generation of $[M + H]^+$ or $M^{+\cdot}$ ions as the base peak of the spectrum, by means of protonation or charge transfer mechanisms, deeper explained in literature [22] and [27]. This soft ionization presents an advantage in the selection of specific precursor ions in MS/MS based methods.

In the present work, the potential of APCI source using GC–MS/MS was evaluated for the development of a screening method for the detection of selected exogenous AAS in urine. After validation, the performance of the GC-APCI-MS/MS method has been compared with the conventional GC-EI-MS/MS, by analyzing a group of samples prepared under the same conditions. The applicability of the method was also evaluated in a set of

samples collected at different times after the administration of 4-chloromethandienone (4Cl-MTD).

2. Experimental

2.1. Chemical and reagents

The structures of the selected AAS are shown in Fig. 1. Boldenone (BD) was obtained from Sigma (St. Louis, MO, USA). 17β-hydroxy-5β-androstan-1-ene-3-one (Boldenone metabolite, BDmet), 17β-methyl-5β-androst-1-en-3α,17α-diol (Methandienone metabolite, MTDmet3), 1-testosterone (1-T), 5α-androstan-17α-methyl-3α,17β-diol (Methyltestosterone metabolite, MeTmet1), 5β-androstan-17α-methyl-3α,17β-diol (Methyltestosterone metabolite, MeTmet2), 5β-androstan-7β,17α-dimethyl-3α,17β-diol (Calusterone metabolite, CALUSmet), 17α-metyl-1-testosterone (Me-1-T), 5β-androstan-7α,17α-dimethyl-3α,17β-diol (Bolasterone metabolite, BOLASmet), 13β,17α-diethyl-5β-gonane-3α,17β-diol (Norbolethone metabolite, NORBOLmet2) 6β-hydroxy-4-chloromethandienone (6OH-4Cl-MTD) and 4-hydroxy-testosterone (4OH-T) were purchased from NMI (Pymble, Australia). Fluoxymesterone (FLU) was obtained from Steraloids (Newport, RI, USA). 5α-Androstan-2α,17α-dimethyl-3α,17β-diol (Methasterone metabolite, METHASmet) was a kind gift from the World Association of Anti-Doping Scientists (WAADS). Oxymesterone (OXY) and madol (MADOL) were provided by the Toronto Research Chemicals (Toronto, Canada).

AAS stock standard solutions at 10 and 100 μg mL^{-1} in methanol were stored at −20 °C. Working MIX solutions at appropriate concentration levels for validation were prepared in acetone and also stored at −20 °C, whereas

individual standard solutions were employed for the transition optimization step and for potential cross-talk evaluation.

β-glucuronidase solution (*Escherichia coli*, type K12) was purchased from Roche Diagnostics (Mannheim, Germany). Analytical grade potassium carbonate, potassium hydroxide pellets, sodium hydrogen phosphate, di-sodium hydrogen phosphate, *tert*-butyl-methyl ether and ammonium iodide were acquired from Merck (Darmstadt, Germany). The derivatization reagent preparation *N*-methyl-*N*-trimethylsilyl-trifluoroacetamide (MSTFA) was purchased from Karl Bucher Chemische Fabrik GmbH (Waldstetten, Germany) and 2-mercaptoethanol from Sigma–Aldrich (St Louis, MO, USA). Milli Q water was obtained using a Milli-Q purification system (Millipore Ibérica, Barcelona, Spain). Formic acid and ammonium formate (LC/MS grade), acetonitrile and methanol (LC gradient grade) were purchased from Merck (Darmstadt, Germany).

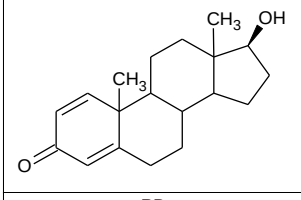	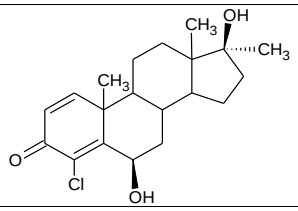	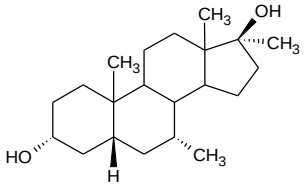
BD	6OH-4Cl-MTD	BOLASmet
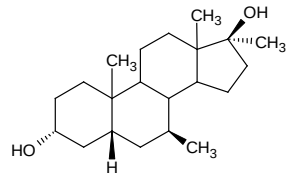	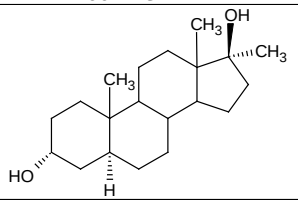	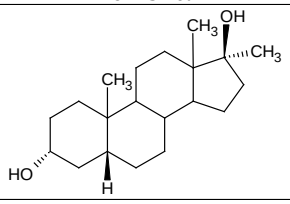
CALUSmet	MeTmet1	MeTmet2
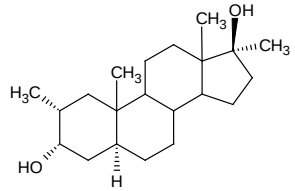	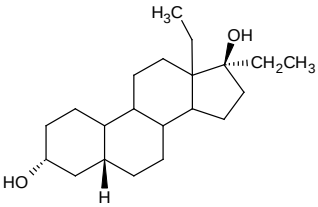	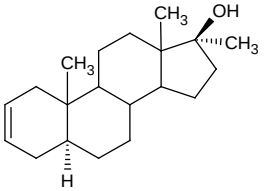
METHASmet	NORBOLmet2	MADOL
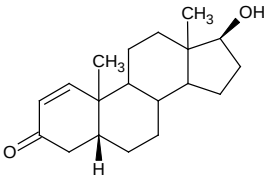	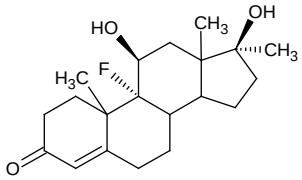	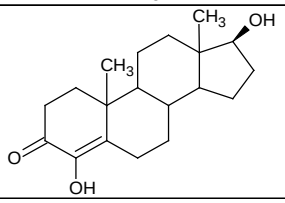
BDmet	FLU	4OH-T
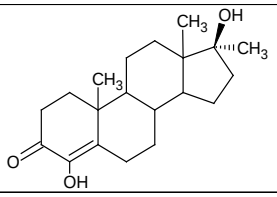	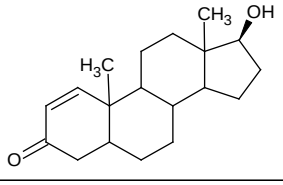	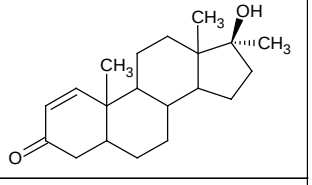
OXY	1-T	Me-1-T
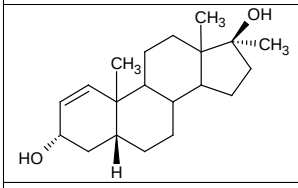		
MTDmet3		

Fig. 1. Structures of the selected analytes

2.2. Instrumentation

2.2.1. GC-APCI-MS/MS

An Agilent 7890A GC system (Palo Alto, CA, USA) equipped with an Agilent 7693 autosampler was coupled to a triple quadrupole mass spectrometer, Xevo TQ-S (Waters Corporation, Manchester, UK), using an APGC source, operating in APCI mode. The GC separation was performed using an HP Ultra 1 capillary column, (length 16 m × I.D. 0.20 mm × film thickness 0.11 μm). For the named as *gradient 1*, the oven was programmed as follows: 185 °C (0.5 min); 25 °C min^{-1} to 230 °C; 10 °C min^{-1} to 290 °C; 70 °C min^{-1} to 310 °C (2.5 min), being the total run time 11.6 min. G*radient 2* programme was: 180 °C (1 min); 3 °C min^{-1} to 230 °C; 40 °C min^{-1} to 310 °C (3 min), total run time 22.7 min. Split injections (ratio 1:10) of 2 μL using a straight deactivated liner with glass wool were carried out at 280 °C. Helium 99.999% (Carburos Metálicos, Spain) was used as carrier gas at 2 mL min^{-1}.

The interface temperature was set to 300 °C using N_2 as auxiliary gas at 250 L h^{-1}, make up gas at 300 mL min^{-1}, and cone gas at 170 L h^{-1}. The temperature in the source was set at 150 °C. The APCI corona pin was operated at 1.55 μA and a cone voltage of 20 V was selected. The water used as modifier when working under proton-transfer conditions was placed in an uncapped vial, which was located within a holder placed in the source door. For MS/MS measurement, argon 99.995% (Carburos Metálicos, Spain) was used as collision gas at a pressure of 4.15×10^{-3} mbar in the collision cell (Table 1).

2.2.2. GC-EI-MS/MS

For all EI experiments, a 7890A gas chromatograph equipped with a 7693 autosampler and coupled to a 7000A Series Triple Quadrupole GC/MS (Agilent Technologies) was employed. The same column and chromatographic conditions detailed in the APCI section (gradient 1) were used.

Nitrogen was used as collision gas at a flow rate of 1.5 mL min^{-1}, and helium (Abello-Linde) as a quenching gas at a flow rate of 2.25 mL min^{-1}. The electron impact source was kept at 230 °C and the quadrupoles at 150 °C.

2.3. Sample preparation

Urine samples were treated as previously described in literature [14] and [15]. Briefly, 25 µL of internal standard solution (methyltestosterone, 10 µg mL^{-1}) was added to 2.5 mL of urine. Then, the solution was hydrolyzed by the addition of 1 mL phosphate buffer (pH 7) and 30 µL of *β*-glucuronidase solution (55 °C, 1 h). After cooling at room temperature, 200 mg of $NaHCO_3/Na_2CO_3$ buffer (1:2; w/w) was added (pH 9.5). A LLE step was carried out by adding 6 mL of methyl tert-butyl ether (MTBE). After centrifugation (4350 rpm, 5 min), the organic phase was separated and evaporated to dryness (45 °C). Finally, in order to obtain the *enol-trimethylsylil* (TMS) derivatives of the analyte, 50 µL of a mixture of MSTFA/NH_4I/2-mercaptoethanol (1000/2/6; v/w/v) was added to the dry extract and then kept at 60 °C for 20 min.

2.4. Validation

Following the WADA criteria [4], the validation of the screening method was designed in order to confirm the suitability of the method to

detect half the MRPL of the compound. The method validation was performed using spot urine samples collected from six volunteers (three male and three female which did not take any steroid). Two spiking levels were selected taking into account the current MRPL for the compounds (Table 2). Low concentration levels (LCL) of 1 ng mL^{-1} and 2 ng mL^{-1}, and high concentration levels (HCL) of 10 ng mL^{-1} and 20 ng mL^{-1} were selected for AAS with MRPLs of 2 ng mL^{-1} and 5 ng mL^{-1}, respectively. In this sense, around 0.5xMRPL and 5xMRPL levels were assayed in both cases.

For the evaluation of the extraction recoveries of each analyte, six blank samples were spiked at the high concentration level and extracted. The same samples were extracted and spiked after the extraction. The extraction recovery was calculated by comparing peak areas for each analyte in both cases.

Relative standard deviation (RSD) of the ratio between the peak areas of each compound and the internal standard were calculated. Repeatability (expressed as RSD) for each analyte was evaluated at the two concentration levels tested.

Based on WADA suggestions [4], the limit of detection (LOD) for each analyte was estimated as the concentration that produced a peak signal of three times the background noise in the chromatogram at the lowest fortification level.

Selectivity was tested by analyzing 10 different blank urines and monitoring the absence of interferences with signal to noise (S/N) ratios above 3.

2.5. Application to real samples

To study the applicability of the validated method, samples from an excretion study of 4-chloromethandienone (4Cl-MTD) were analyzed. A single dose of 20 mg of 4Cl-MTD (oral Turinabol) was administrated to a male volunteer (49 years, 85 kg) and different urine samples at intervals of 0–4 h, 4–8 h, 8–12 h, 12–24 h, 24–36 h, 48–56 h and 72–84 h were collected.

The study was conducted in accordance with the Declaration of Helsinki. Subject signed an informed consent before participation. Treatment was well tolerated by the subjects and no serious adverse events were observed.

3. Results and discussion

3.1. Transition optimization

Two transitions were optimized for each compound to improve the reliability of the method. The first step was the acquisition of a full scan spectrum for each individual TMS-derivative standard. Once the main precursor ions were selected, $[M + H]^+$, $[M + H\text{-}TMSOH]^+$ or $[M + H\text{-}2TMSOH]^+$, depending on the structure of the steroid [21], product ion spectra were obtained at different collision energies (10, 20, 30 and 40 eV) (Figure S1, supplementary information). Based on this information, the largest number of possible optimized SRM transitions was preselected. Then, ten blank urine extracts and ten extracts spiked at the LCL were tested in order to choose the best transitions for each analyte in terms of sensitivity and specificity. Transitions showing the maximum S/N and the minimum influence of the background of the matrix interferences were selected.

For most analytes, the most sensitive transition was found to be specific enough since matrix interferences were not observed. Therefore, it was selected for detection of the compound in the screening. However, in some cases such as OXY, (Figure S2, supplementary information), the selected transition was not the most abundant (535.2 > 269.2), because of the presence of matrix interferences. Thus, a less sensitive but more specific transition was selected (535.2 > 389.5). In the case of NORBOLmet2 and BD in APCI, it was not possible to select any specific transition because of the presence of endogenous steroids with the same transitions at the same retention times under the selected conditions.

A list of the selected SRM transitions used in APCI, facing EI ones, is summarized in Table 1.

Table 1. Selected acquisition conditions for SRM method for GC-APCI-MS/MS and GC-EI-MS/MS.

Analyte	Derivative	Mw $[M+H]^+$	APCI			EI		
			RT (min)	Transition	CE (eV)	RT (min)	Transition	CE (eV)
MADOL	mono-O-TMS	361	3.96	271.1>105.1[a]	30	4.49	345.3>201.1	15
				271.1>90.9	30		345.3>255.1	15
BDmet	bis-O-TMS	433	4.27	433>417[a]	10	4.73	432.4>194.1	14
				433>187	20		432.4>206.1	14
MTDmet3	bis-O-TMS	449	4.27	269>201[a]	10	4.74	358.3>301.3	12
				269>105	30		358.3>196.1	12
1-T	bis-O-TMS	433	5.03	343.2>179.1[a]	20	5.61	432.4>194.1	15
				433.3>417	20		432.4>207.2	15
MeTmet2	bis-O-TMS	451	5.07	271.2>215.2[a]	10	5.64	270.2>213.2	15
				361.2>271.1	10		270.2>199.1	15
MeTmet1	bis-O-TMS	451	5.08	271.2>215.2[a]	20	5.64	255.2>199.1	25
				361.3>255.2	20		255.2>159.1	25
METHASmet	bis-O-TMS	465	5.25	285.2>229.2[a]	20	5.84	449.4>269.2	19
				375.3>245.2	20		449.4>213.2	19
BD	bis-O-TMS	431	5.29	341.2>193.1[a]	20	5.86	430.4>206.2	18
				431.3>193.1	20		430.4>191.2	30
CALUSmet	bis-O-TMS	465	5.32	285.3>109[a]	20	5.91	284.2>227.2	15
				285.3>175	20		374.3>269.2	13
BOLASmet	bis-O-TMS	465	5.49	285.2>175.1[a]	20	6.08	284.2>227.2	15
				375.2>245.2	20		284.2>269.2	15
Me-1-T	bis-O-TMS	447	5.52	357.2>179.2[a]	20	6.14	446.4>194.1	20
				447.3>431.3	20		446.4>143.1	20
NORBOLmet2	bis-O-TMS	465	5.97	375.3>285.2[a]	10	6.61	435.4>255.2	12
				375.3>231.2	20		435.4>345.3	12
4OH-T	tris-O-TMS	521	6.40	431.3>296.2[a]	30	7.08	520.4>147.1	33
				521.3>405.3	40		505.4>147.1	10
FLU	tris-O-TMS	553	6.82	463.3>297.4[a]	30	7.52	552.4>462.4	20
				553.3>353.4	20		552.4>319.3	20
OXY	tris-O-TMS	535	6.91	535.2>389.5[a]	20	7.62	534.4>429.4	30
				535.2>269.2	30		389.3286.2	30
6OH-4Cl-MTD	bis-O-TMS	495	7.25	495.1>315.1[a]	10	7.99	315.1>227.1	20
				495.1>155	40		315.1>241.1	15

[a] Most specific transition.

3.2. Method validation

Table 2 summarizes the results obtained for extraction recovery, repeatability and LOD by using GC-APCI-MS/MS. Suitable extraction recovery values between 67 and 89% were obtained in all cases except for Me-1-T (47%) and BDmet (53%).

Repeatability was evaluated by the RSD at both LCL and HCL (n = 6 for each level). Values between 3% and 30% were obtained confirming the satisfactory precision of the method. As expected, better repeatability was observed at the HCL, being in most cases below 15%, except for 6OH-4Cl-MTD (RSD 22%).

In terms of selectivity, no interferences were detected in the ten blank samples for the transitions selected for each compound. Regarding LOD, most of them were lower than 0.5 ng mL^{-1} and always below the established MRPL (Table 2). As stated in the previous section the main exceptions for this behaviour were NORBOLmet2 and BD, which were interfered by the presence of matrix components irrespective of the selected transition. Chromatographic separation was found to be critical for the proper validation of these compounds. The use of a longer gradient (gradient 2 in the experimental section) allowed for the discrimination between analytes and the matrix interferences (Figure S3, supplementary information). Using this gradient, all analytes were adequately validated. In order to isolate as much as possible the effect of the interface, results using gradient 1 will be discussed. Only in the case of NORBOLmet2 and BD results for gradient 2 are discussed.

Table 2.- Validation parameters obtained for extraction recovery (n=6), repeatability and LOD for APCI and EI analysis.

Analyte	Current MRPL (ng mL^{-1})	Extraction recovery (%)	LCL (ng mL^{-1})	Repeatability (%)		HCL (ng mL^{-1})	Repeatability (%)		LOD (ng mL^{-1})	
				APCI	EI		APCI	EI	APCI	EI
MADOL	5	75	2	10	1	20	6	0.3	1	1
BDmet	5	53	2	30	14	20	4.8	5.3	0.1	0.5
MTDmet3	2	70	1	5.3	1.2	10	4.6	0.5	0.3	0.3
1-T	5	79	2	4.2	2.5	20	14	0.5	0.3	2
MeTmet2	2	85	1	4.8	2.3	10	3.9	0.4	0.3	0.5
MeTmet1	2	83	1	12	2.7	10	6.3	1	0.5	0.5
METHASmet	5	78	2	24	8.5	20	9.1	2.3	1	0.3
BD*	5	89	2	3.8	2.5	20	5.9	2	0.1	1
CALUSmet	5	76	2	18	2.3	20	3.5	2	1	2
BOLASmet	5	80	2	23	5.2	20	6.8	1.6	0.1	1
Me-1-T	5	47	2	9.7	5.4	20	4.9	5.1	0.3	1
NORBOLmet2*	5	71	2	13	0.6	20	7.7	1.3	0.4	2
4OH-T	5	68	2	9.4	2.4	20	4.6	1.1	0.4	2
FLU	5	73	2	25	21	20	4	2.3	0.1	1
OXY	5	71	2	13	27	20	3	1.4	0.5	1
6OH-4Cl-MTD	2	86	1	3.2	4.2	10	22	0.3	0.2	1

* APCI values for BD and NORBOLmet2 were calculated using gradient 2 (see experimental section)

It is well-known that, differently to EI, atmospheric pressure ionization is more affected by matrix constituents that lead to possible matrix-induced suppression/enhancement of the analytes ionization. Since the main goal of the developed method was not quantification of the analytes but the detection/identification of all selected AAS at the LCL, this effect was not evaluated as that qualitative objective was satisfactorily reached independently on the matrix effects that might affect to ionization. However, matrix effect may be behind the higher RSD observed in APCI and it should be evaluated if the purpose of the analyses was quantification of analytes.

Fig. 2 shows typical chromatograms obtained for a blank urine sample compared with those of a sample spiked at the LCL.

Analyte	(a) Blank	(b) LCL
MADOL	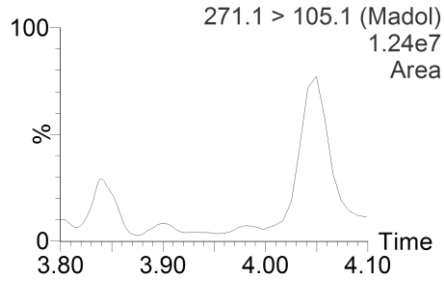	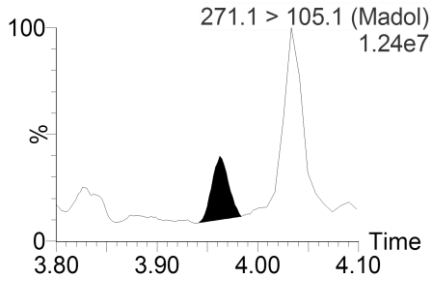
BDmet	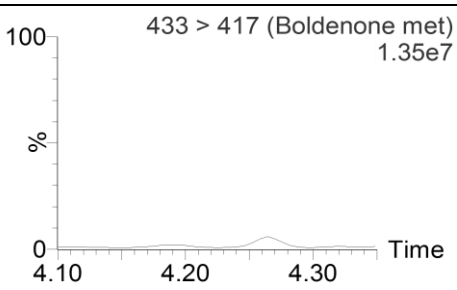	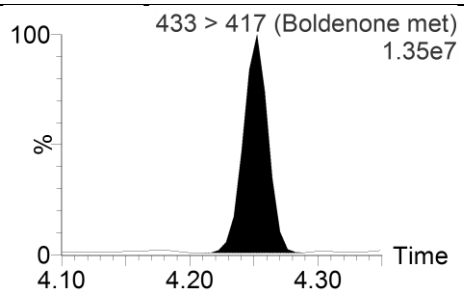
MTD met3	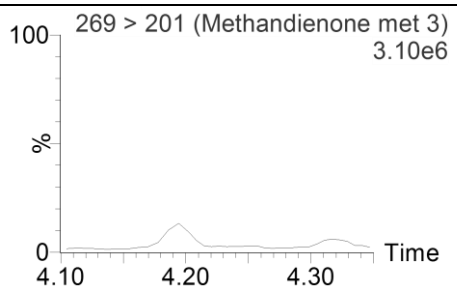	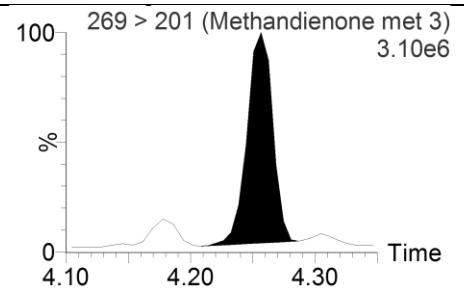

Fig. 2. APCI optimized transitions of selected AAS in (a) blank urine sample and (b) urine sample spiked at LCL.

1-T	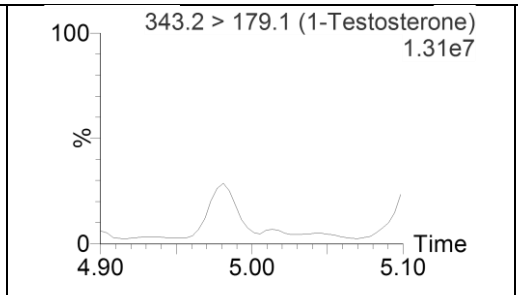	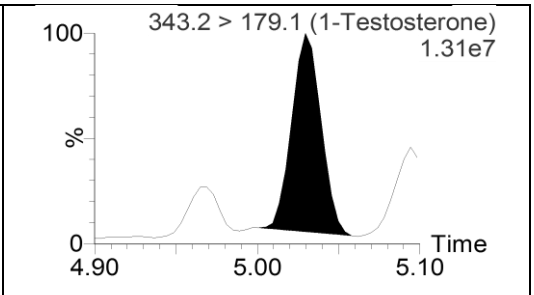
MeTmet2	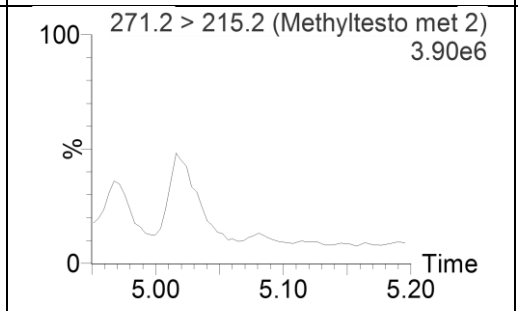	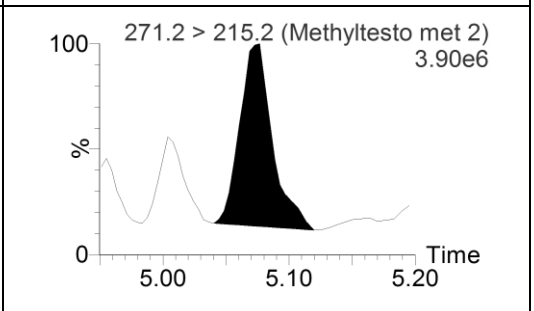
MeTmet1	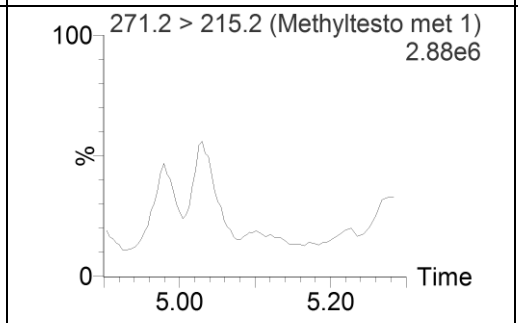	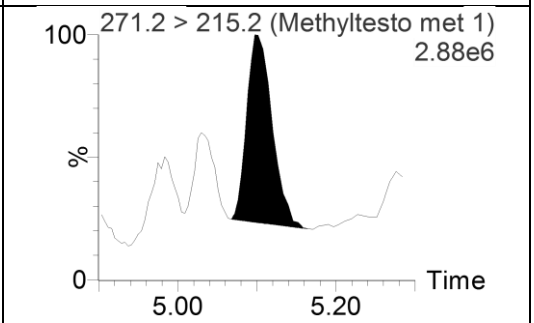
METHAS met	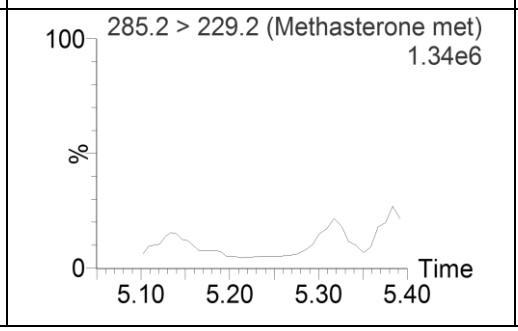	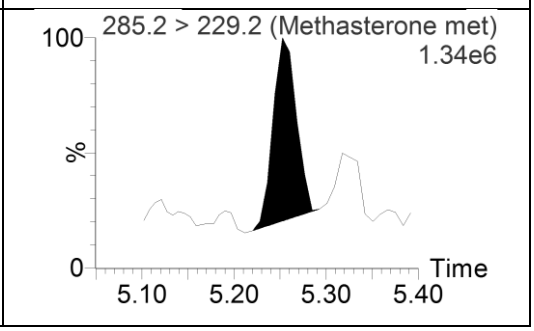

Fig. 2. (Cont)

CALUS met	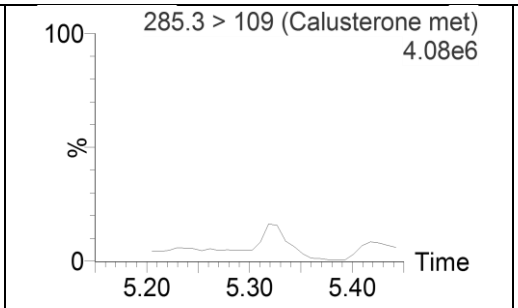	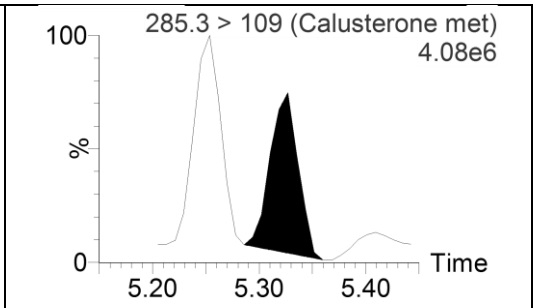
BOLAS met	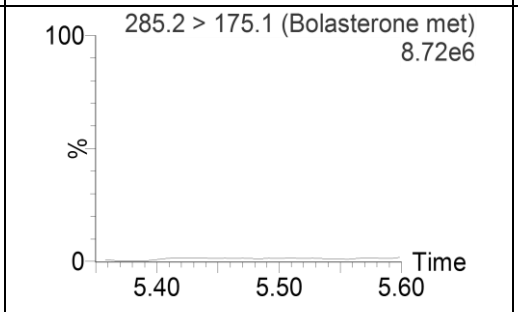	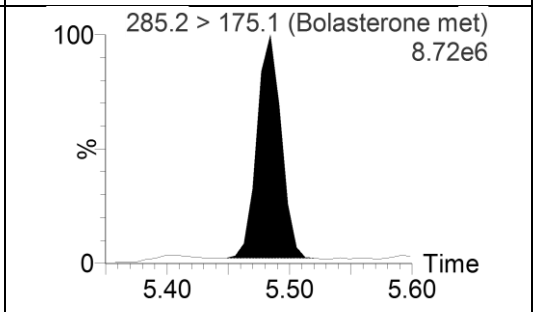
Me-1-T	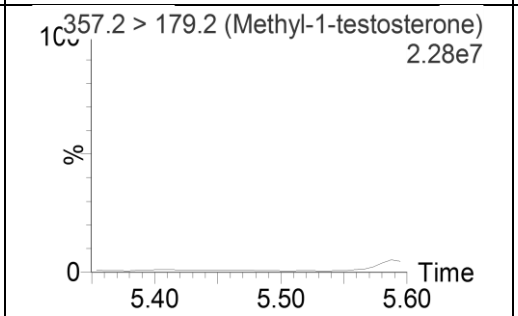	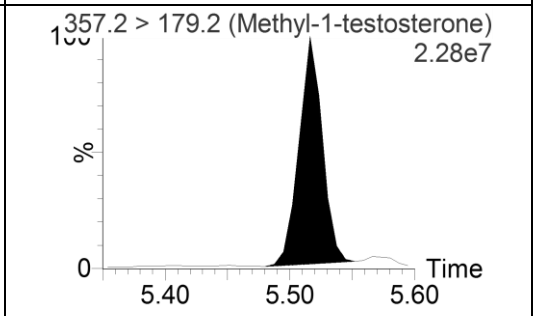
4OH-T	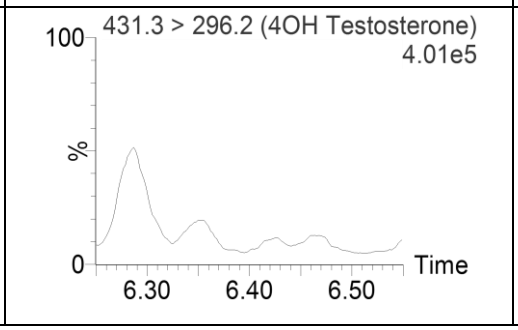	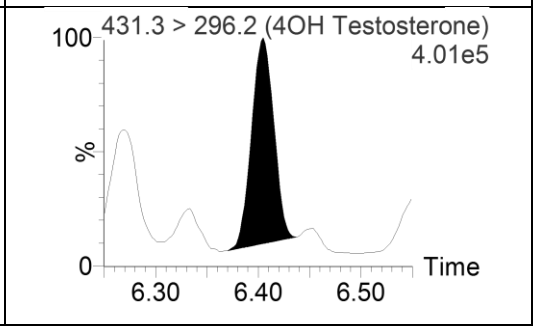

Fig 2. (Cont)

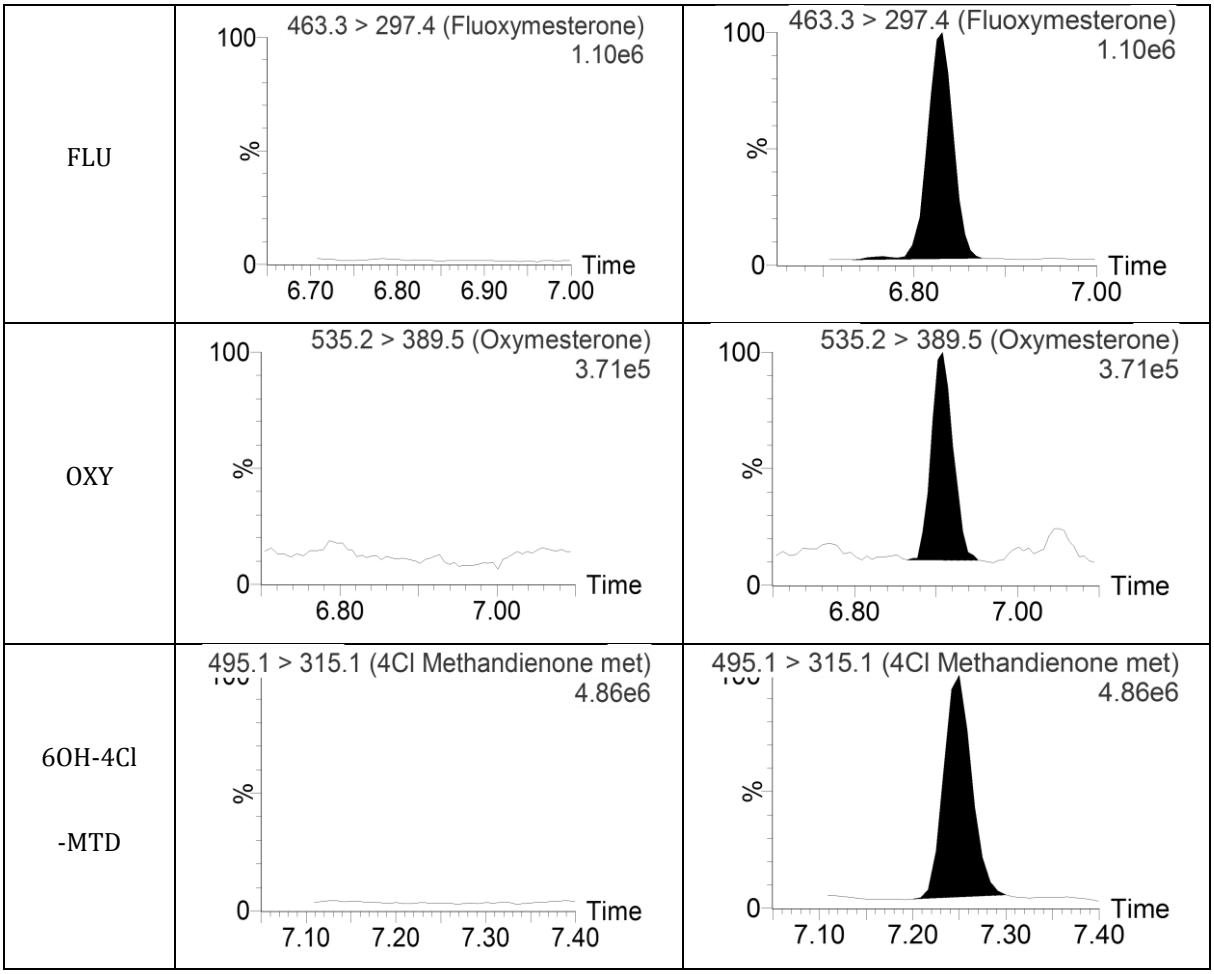

Fig 2. (Cont)

3.3. Comparison APCI vs EI

In order to evaluate the performance of the developed GC-APCI-MS/MS method, the validation results were compared with those obtained by GC-EI-MS/MS. All the factors involving the detection (urine used, extraction, derivatization, column and gradient of temperatures) were controlled in order to isolate as much as possible the effect of the ionization source. Ideally, both sources should be coupled to the same analyzer. Unfortunately, this ideal situation is currently not affordable, i.e. both interfaces are not

interchangeable, and, therefore, every source was coupled to a different QqQ analyzer. Thus, although the discussion will be focused on the effect of the interface, a potential influence of the specific analyzer on the results cannot be discarded.

Validation results for both methodologies are shown in Table 2. Regarding repeatability, in general, RSD values were lower for EI. At LCL, RSDs ranged from 0.6% to 14% in EI whereas in APCI increased up to 3.2–18%. At HCL, RSDs in the range 0.3–5% and 3–14% were obtained for EI and APCI, respectively. Some values higher than 20 were punctually obtained. Thus, although RSDs from both studies can be considered acceptable, a slightly better repeatability of the EI source was found in this study. The lower repeatability of APCI might be due either to factors affecting the ionization process such as the amount of water in the interface or to the potential matrix effect suffered by APCI.

Regarding sensitivity, the results largely depended on the MS behaviour of the steroid. Thus, analytes with an abundant $[M + H]^+$ in APCI BDmet, 1-T, Me-1-T, 4OH-T, FLU, 6OH-4Cl-MTD, BD and OXY exhibited LODs in the sub-ng/mL range (below 0.4 ng/mL) i.e. more than 10 times lower than the current MRPL for most AAS. For these AAS, LODs estimated for APCI were between 5 and 20 times lower than for EI (Fig. 3a), even in those cases in which an abundant $M^{+\cdot}$ was also present in EI.

Worse LODs (typically between 0.3 and 1 ng/mL) were obtained for AAS showing an abundant $[M + H\text{-}nTMSOH]^+$ in APCI (MADOL, MTDmet3, MeTmet1, CALUSmet, MeTmet2, METHASmet, NORBOLmet2 and BOLASmet). For these compounds, LODs using APCI were commonly in the same range as those obtained by EI (Table 2, Fig. 3b). The low specificity of the product ions can be behind this fact. After the in-source neutral loss of all TMS present in

the molecule (lost as TMSOH), the remained hydrocarbon skeleton was selected as precursor ion. Under these conditions the selection of a specific product ion was troublesome. Thus, most of the product ions obtained was not specific and both matrix interferences and high background decreased the sensitivity of the method. Only for BOLASmet, a specific product ion (*m/z* 175) could be obtained. In this case, the sensitivity was similar to those AAS exhibiting a $[M + H]^+$.

The selection of abundant and specific precursor ions was a key factor when aiming at the maximum sensitivity. In the light of obtained results, it is noteworthy to mention that the presence of $[M + H]^+$ in APCI led to the best results in terms of sensitivity. Future work in the search of diverse derivatizing agents that maximize the protonated molecule in APCI would be valuable.

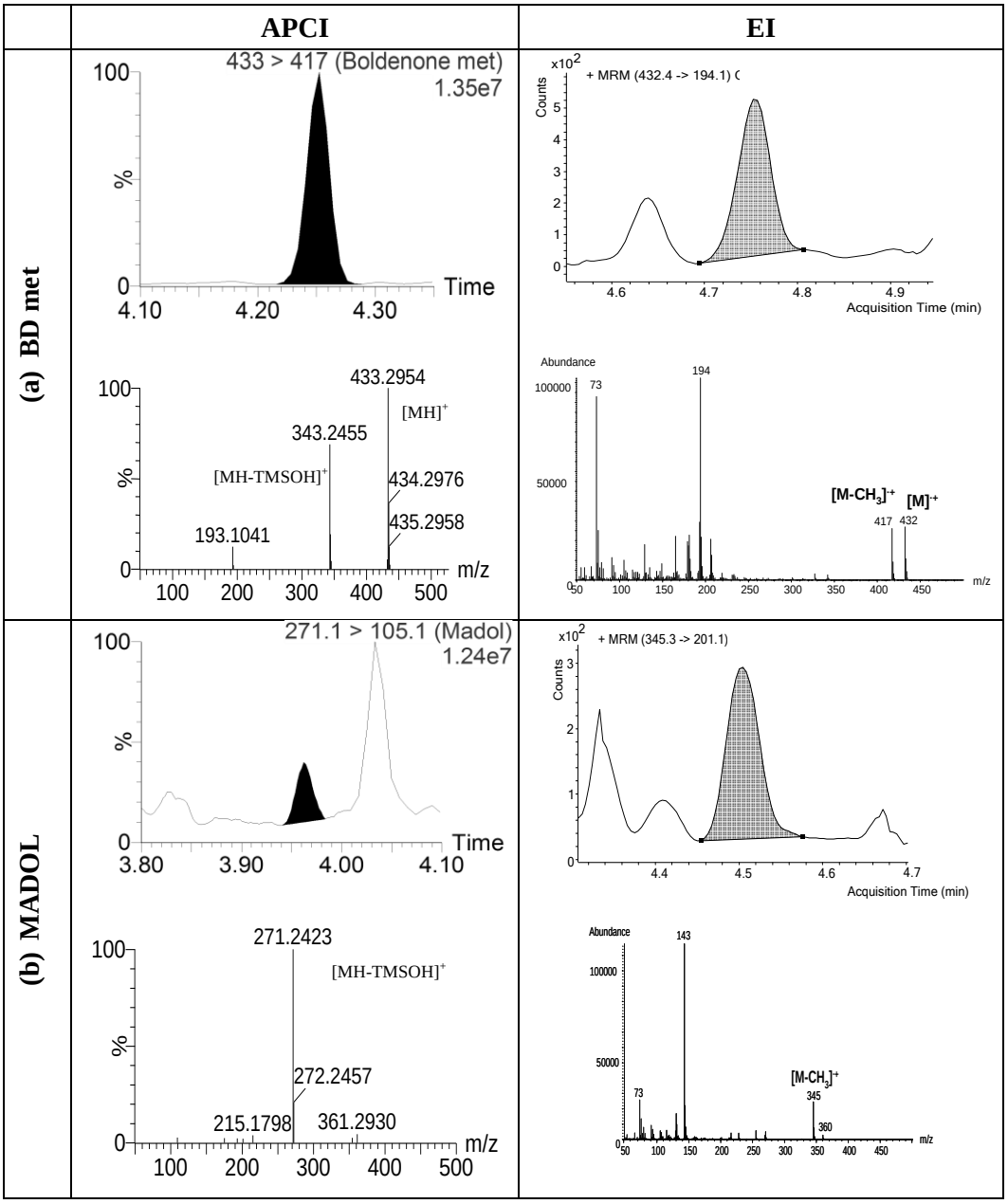

Fig. 3. Comparison between APCI and EI for selected compounds: (a) BDmet and (b) MADOL.

3.4. Application to real samples

To check the applicability of the developed methodology, samples collected after 4Cl-MTD administration were analyzed by GC-APCI-MS/MS and the results were compared with those obtained by GC-EI-MS/MS.

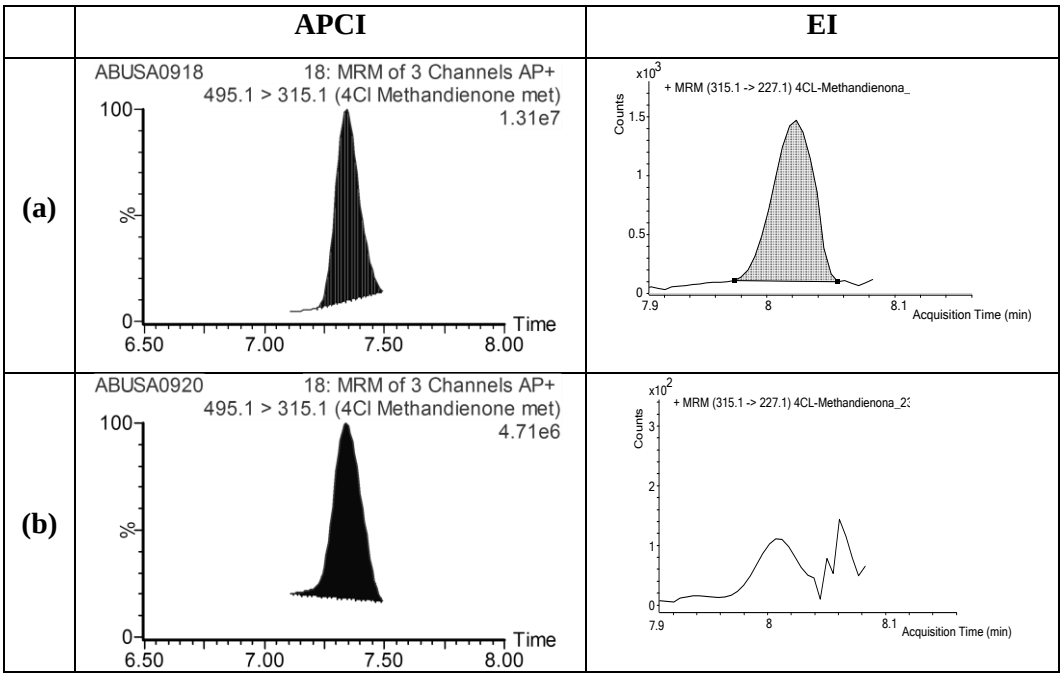

Fig. 4. Comparison between APCI and EI in urine samples collected after administration of 4Cl-MTD. Chromatograms of samples collected between (a) 24–36 h after administration and (b) 72–84 h after administration.

As expected, the main metabolite of 4-chloromethandienone (6OH-4Cl-MTD) was detected by both methods in the urines collected during the first hours after administration (Fig. 4a). Owing the better sensitivity provided by APCI, the misuse of 4Cl-MTD could be detected in samples in which the metabolite was undetectable by the commonly used GC-EI-MS/MS methods (Fig. 4b). Therefore, the period of time in which the misuse can be

detectable increased from 56 h to 84 h (the last sample collected) by using APCI. This fact illustrates the potential and future of this source in the detection of AAS misuse.

4. Conclusions

The suitability of GC-APCI-MS/MS for sensitive detection of AAS has been demonstrated by the validation of a method for the detection of 16 exogenous AAS in urine.

The present work illustrates the potential of the new APCI source as an adequate alternative to the traditional EI source in GC–MS methodologies. Due to the endogenous steroids present in urine, the selection of a specific transition has been found to be a key factor in the method development. Optimization of the chromatography was found to be critical for the correct detection of two of the analytes (BD and NORBOLmet2). Although suitable precision (RSD values below 25 and 15% at LCL and HCL, respectively) was obtained with the APCI method, it was slightly higher than the one obtained with EI.

Sensitivity was found to be higher with APCI for the majority of compounds tested, with LODs commonly lower than 0.5 ng mL^{-1}. These LODs are similar to the obtained with other soft ionization sources like CI [16]. The higher sensitivity obtained can be related with the abundance of a specific product ion. This, in around 50% of the analytes, the soft ionization of provided by the APCI source allowed for the selection of the $[M + H]^+$ as precursor ion. In the rest of analytes, ions resulting from one or two losses of TMSOH from the derivatizing reagent were selected as precursor. These ions

keep still the steroidal skeleton helping in the selection of specific product ions.

Anyway, the presence of an abundant $[M + H]^+$ in the mass spectra and its selection as precursor ion was found to be related with a higher sensitivity. Since the selected derivative (TMS) does not favor the protonation, the use of derivatives with higher proton affinity would theoretically improve the sensitivity of the method. Further research in order to investigate the applicability of other derivatizing agents able to generate specific fragments would be desirable.

The notable improvement in sensitivity provided by the use of APCI source in GC–MS/MS methods is of great relevance in doping control field, as revealed in the application of the method for the detection of 4-chloromethandienone misuse. Therefore, the use of GC-(APCI) MS/MS based methods could increase the period of time in which the misuse of the AAS can be detected, and opens interesting possibilities in the near future.

Acknowledgements

The authors acknowledge the financial support of the Ministry of Education and Science, Spain, in the project DEP2011-28573-C02-01/02. The authors from University Jaume I also acknowledge the support from Generalitat Valenciana (Research Group of Excellence Prometeo II/2014/023; ISIC EnviFood 2012/016). Authors are also grateful to the Serveis Centrals d'Instrumentació Científica (SCIC) of the University Jaume I for the use of GC–(APCI) (QqQ) MS/MS Xevo TQ-S. M. Raro is also grateful to the Ministry of Education and Science for her predoctoral grant. Spanish

Health National System is acknowledged for O. J. Pozo contract (MS10/00576).

References

[1] World Anti-Doping Agency. The 2014 Prohibited List. Available from: https://wada-main-prod.s3.amazonaws.com/resources/files/WADA-prohibited-list-2014-EN.pdf Last accessed 20.04.2015.

[2] World Anti-Doping Agency. Testing figures report 2013. https://wada-main-prod.s3.amazonaws.com/resources/files/WADA-2013-Anti-Doping-Testing-Figures-LABORATORY-REPORT.pdf Last accessed 22.06.2015.

[3] F. Hartgens, H. Kuipers, Effects of androgenic anabolic steroids in athletes, Sports Med. 34:8 (2004) 513-554.

[4] World Anti-Doping Agency. Technical Document – TD2014MRPL. https://wada-main-prod.s3.amazonaws.com/resources/files/WADA-TD2014MRPL-v1-Minimum-Required-Performance-Levels-EN.pdf Last accessed 22.06.2015.

[5] W. Van Thuyne, P. Van Eenoo, F. T Delbeke, Implementation of gas chromatography combined with simultaneously selected ion monitoring and full scan mass spectrometry in doping analysis, J Chromatogr A. 1210:2 (2008) 193-202.

[6] C. Gómez, O.J. Pozo, J. Marcos, J. Segura, R. Ventura, Alternative long-term markers for the detection of methyltestosterone misuse, Steroids 78 (2013) 44-52.

[7] E. M. Brun, R. Puchades, A. Maquieira, Analytical methods for anti-doping control in sport: anabolic steroids with 4,9,11-triene structure in urine, TRAC-Trend Anal Chem. 30:5 (2011) 771-783.

[8] W. Schänzer, P. Delahaut, H. Geyer, M. Machnik, S. Horning, Long-term detection and identification of metandienone and stanozolol abuse in athletes by gas chromatography-high-resolution mass spectrometry, J Chromatogr B. 687:1 (1996) 93-108.

[9] O. J. Pozo, P. Van Eenoo, K. Deventer, F. T. Delbeke, Detection and characterization of anabolic steroids in doping analysis by LC-MS, TRAC-Trend Anal Chem. 27:8 (2008) 657-671.

[10] M. Thevis, A. Thomas, V. Pop, W. Schänzer, Ultrahigh pressure liquid chromatography-(tandem) mass spectrometry in human sports drug testing: Possibilities and limitations, J Chromatogr A. 1292 (2013) 38-50.

[11] O. J. Pozo, P. Van Eenoo, K. Deventer, L. Lootens, S. Grimalt, J. V. Sancho, F. Hernández, P. Meuleman, G. Leroux-Roels, F. T. Delbeke, Detection and structural investigation of metabolites of stanozolol in human urine by liquid chromatography tandem mass spectrometry, Steroids 74 (2009) 837–852.

[12] M. Thevis, G. Fußhöller, H. Geyer, G. Rodchenkov, U. Mareck, G. Sigmund, A. Koch, A. Thomas, W. Schänzer, Detection of stanozolol and its major metabolites in human urine by liquid chromatography-tandem mass spectrometry, Chromatographia. 64:7-8 (2006) 441-446.

[13] D. H. Catlin, M. H. Sekera, B. D. Ahrens, B. Starcevic, Y.-C. Chang, C. K. Hatton, Tetrahydrogestrinone: discovery, synthesis, and detection in urine, Rapid Commun. Mass Spectrom. 18 (2004) 1245.

[14] P. Van Eenoo, W. Van Gansbeke, N. De Brabanter, K. Deventer, F. T. Delbeke, A fast, comprehensive screening method for doping agents in urine by gas chromatography-triple quadrupole mass spectrometry, J Chromatogr A. 1218:21 (2011) 3306-3316.

[15] M. A. Delgadillo, L. Garrostas, O. J. Pozo, R. Ventura, B. Velasco, J. Segura, J. Marcos, Sensitive and robust method for anabolic agents in human urine by gas chromatography–triple quadrupole mass spectrometry, J Chromatogr B. 897 (2012) 85-89.

[16] W. Van Gansbeke, M. Polet, F. Hooghe, C. Devos, Improved sensitivity by use of gas chromatography-positive chemical ionization triple quadrupole mass spectrometry for the analysis of drug related substances, J Chromatogr B. 1001 (2015) 221-240

[17] M. K. Parr, G. Fußhöller, N. Schlörer, G. Opfermann, T. Piper, G. Rodchenkov, W. Schänzer, Metabolism of androsta-1,4,6-triene-3,17-dione and detection by gas chromatography/mass spectrometry in doping control, Rapid Commun Mass Spectrom. 23 (2009) 207-218.

[18] G. de Albuquerque Cavalcanti, F. Dias Leal, B. Carius Garrido, M. Costa Padilha, F. Radler de Aquino Neto, Detection of designer steroid methylstenbolone in ‘‘nutritional supplement’’ using gas chromatography and tandem mass spectrometry: Elucidation of its urinary metabolites, Steroids 78 (2013) 228–233.

[19] T. Sobolevsky, G. Rodchenkov, Mass spectrometric description of novel oxymetholone and desoxymethyltestosterone metabolites identified in human urine and their importance for doping control, Drug Test Anal. 4:9 (2012) 682–691.

[20] L. Hintikka, M. Haapala, S. Franssilab, T. Kuuranne, A. Leinonen, R. Kostiainen, Feasibility of gas chromatography–microchip atmospheric pressure photoionization-mass spectrometry in analysis of anabolic steroids, J. Chromatogr A. 1217 (2010) 8290–8297.

[21] L. Hintikka, M. Haapala, T. Kuuranne, A. Leinonen, R. Kostiainen, Analysis of anabolic steroids in urine by gas chromatography–microchip atmospheric pressure photoionization-mass spectrometry with chlorobenzene as dopant, J. Chromatogr A. 1312 (2013) 111–117.

[22] M. Raro, T. Portolés, J. V. Sancho, E. Pitarch, F. Hernández, J. Marcos, R. Ventura, C. Gómez, J. Segura, O. J. Pozo, Mass spectrometric behavior of anabolic androgenic steroids using gas chromatography coupled to atmospheric pressure chemical ionization source. Part I: Ionization, J Mass Spectrom. 49:6 (2014) 509-521.

[23] D-X. Li, L. Gan, A. Bronja, O. J. Schmitz. Gas chromatography coupled to atmospheric pressure ionization mass spectrometry (GC-API-MS): Review, Anal Chim Acta (2015) 43-61

[24] T. Portolés, J. G. J. Mol, J. V. Sancho, F. J. López, F. Hernández, Validation of a qualitative screening method for pesticides in fruit and vegetables by gas chromatography quadrupole-time of flight mass spectrometry with atmospheric pressure chemical ionization, Anal Chim Acta 838 (2014) 76-85.

[25] C. Domeño, E. Canellas, P. Alfaro, A. Rodriguez-Lafuente, C. Nerin, Atmospheric pressure gas chromatography with quadrupole time of flight mass spectrometry for simultaneous detection and quantification of polycyclic aromatic hydrocarbons and nitro-polycyclic aromatic hydrocarbons in mosses, J Chromatogr A. 1252 (2012) 146-154.

[26] T. Bristow, M. Harrison, M. Sims, The application of gas chromatography/atmospheric pressure chemical ionisation time-of-flight mass spectrometry to impurity identification in pharmaceutical development, Rapid Commun Mass Spectrom. 24 (2010) 1673-1681.

[27] T. Portolés, J. V. Sancho, F. Hernández, A. Newton, P. Hancock, Potential of atmospheric pressure chemical ionization source in GC-QTOF MS for pesticide residue analysis, J Mass Spectrom. 45 (2010) 926-936.

SUPPLEMENTARY INFORMATION

Figure S1. Product ion spectra of the selected compounds at different collision energies

Compound	Product Ion Spectra 20/30 eV	Compound	Product Ion Spectra 20/30 eV
MADOL	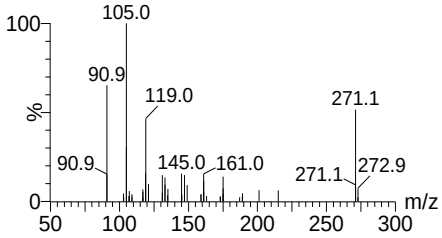	CALUS met	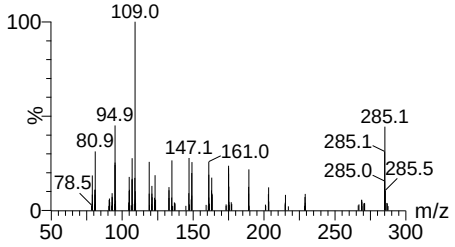
BDmet	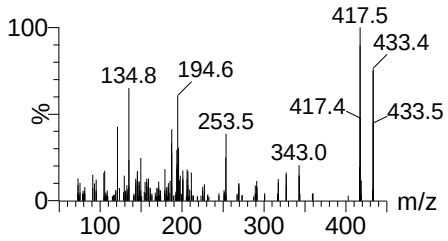	BOLAS met	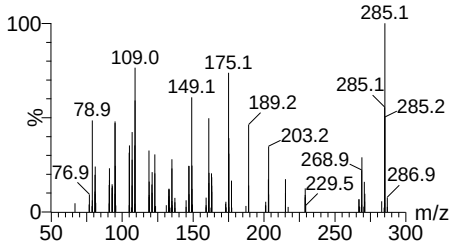
MTDmet3	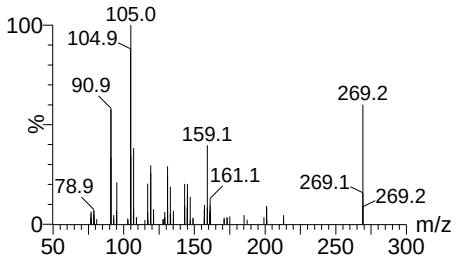	Me-1-T	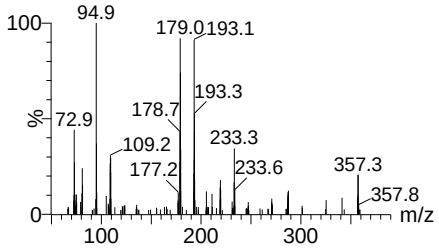
1-T	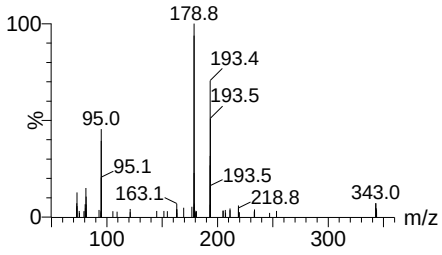	NORBOL met2	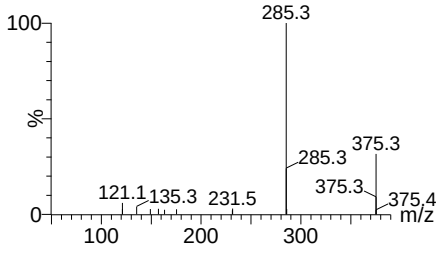

MeT met2	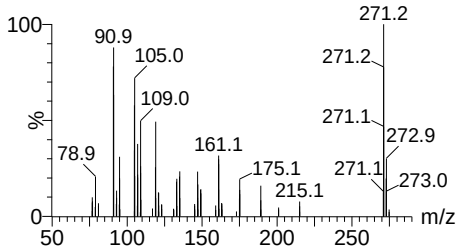	4OH-T	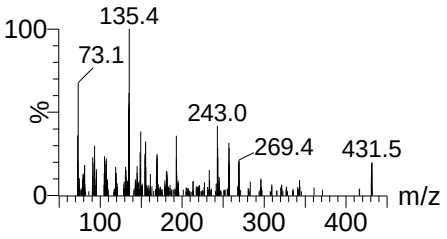
MeT met1	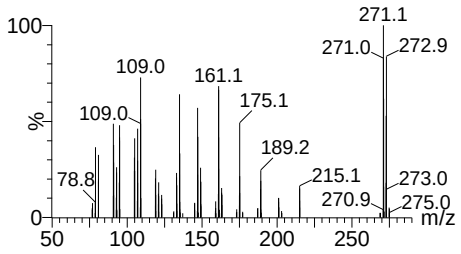	FLU	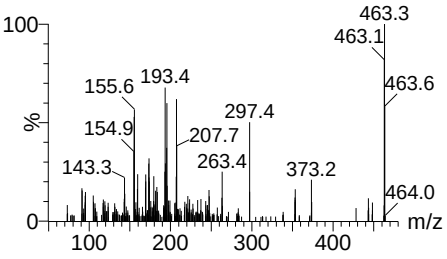
METHAS met	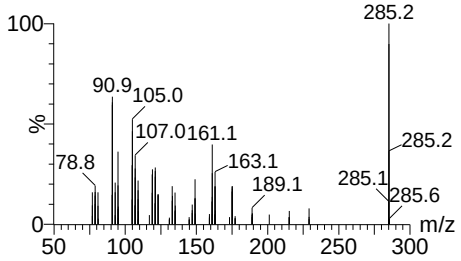	OXY	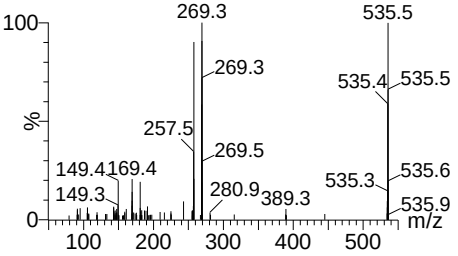
BD	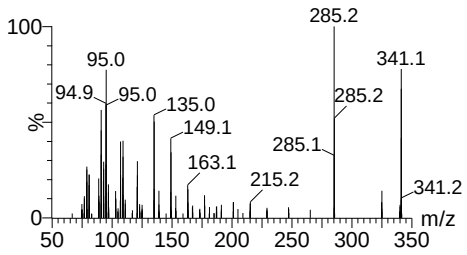	6OH- 4Cl-MTD	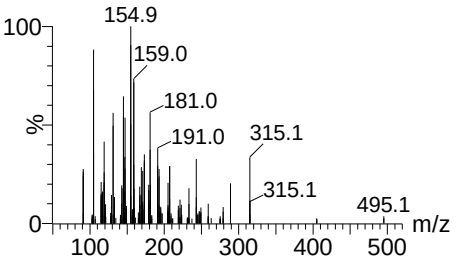

Figure S2. APCI transition optimization. OXY chromatograms from a) blank urine sample and b) urine sample spiked at LCL

	(a)	(b)
Sensitive transition	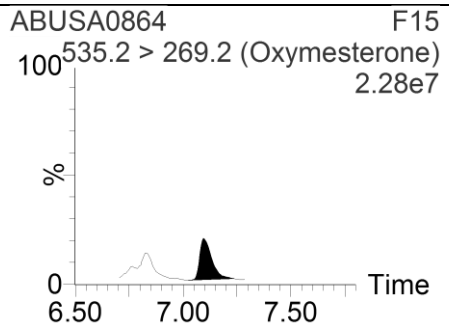	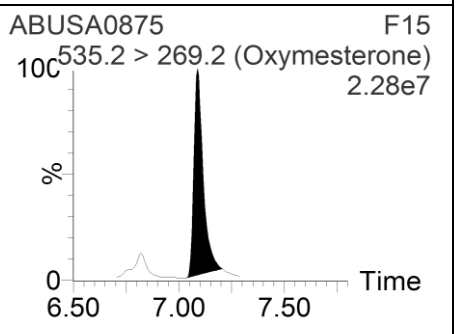
Specific transition	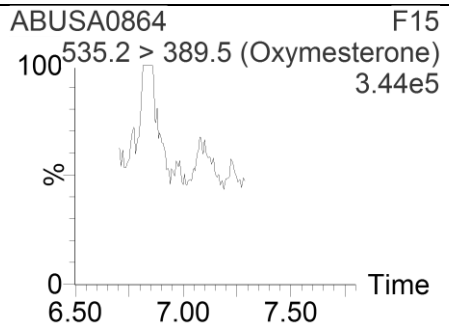	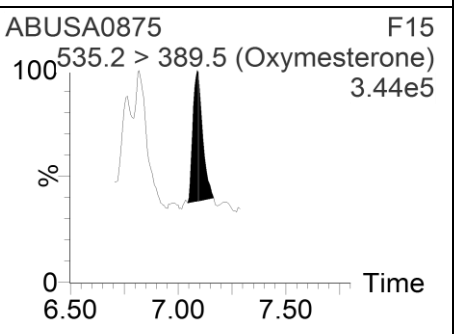

Figure S3.- Examples of transition selection for NorbolMet2 and BD

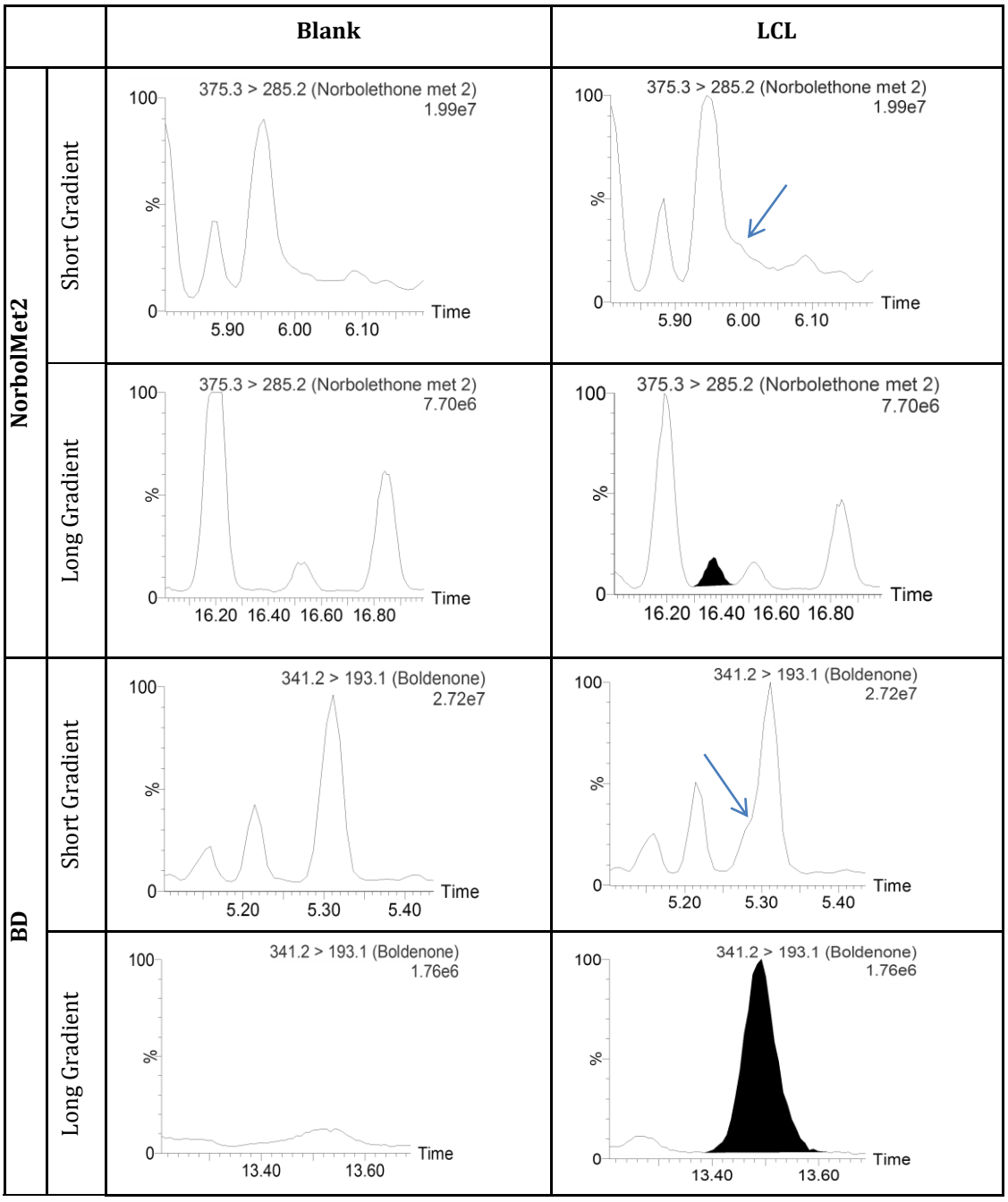

II.5. Discusión

Los trabajos presentados en los *artículos científicos 1, 2 y 3* tienen en común el uso de la fuente APCI para detectar AAS. Como se ha ido viendo a lo largo de las secciones teóricas de la introducción y de este capítulo, esta fuente es relativamente reciente para GC y su uso resulta novedoso para la determinación de este grupo de compuestos.

Por lo que respecta a los *trabajos científicos 1 y 2* se hizo uso del analizador de alta resolución QTOF para estudiar el comportamiento de ionización/fragmentación en masa exacta de un elevado número de AAS (60 analitos) e intentar establecer relaciones con sus estructuras. Por otra parte, en el *artículo científico 3*, se validó un método para la detección de AAS derivatizados con TMS en muestras de orina. En este caso, se incluyeron en el método un número más reducido de compuestos (16 analitos) mediante analizador QqQ.

Las condiciones cromatográficas utilizadas en los *trabajos 1 y 2* fueron diferentes con respecto al *trabajo 3* debido a los diferentes objetivos de los trabajos y las distintas matrices utilizados en ellos. Así, el objetivo de los *trabajos 1 y* 2 era el establecer relaciones Comportamiento MS-Estructura para los AAS mientras que el del *trabajo 3* era comparar el método APCI con un método establecido de EI en un laboratorio de rutina en la detección de AAS en orina. Por ese motivo, para los *trabajos 1 y 2* se inyectaron las muestras (patrones) con un gradiente de 20 minutos en *splitless,* modo de trabajo habitual para asegurar una buena sensibilidad de los compuestos, mientras que en el *tercer trabajo* las muestras se inyectaron con un gradiente más corto (10 min aprox.) y en *split*, para alargar la vida de las columnas en los análisis de rutina en matrices complejas como la orina.

En cuanto a la optimización de la interfase, algunas etapas son críticas para conseguir una sensibilidad y selectividad óptimas en la detección de esteroides por APCI. A continuación, se detallan las pruebas realizadas sobre la adición de agua en la fuente o la optimización del voltaje de cono. La intensidad de corriente aplicada a la aguja corona se optimiza siempre antes de empezar una secuencia. También se discutirán aspectos relevantes acerca del tratamiento de muestra realizado y la selección de transiciones llevada a cabo en el *tercer trabajo*.

ADICIÓN DE AGUA EN LA FUENTE

Como se comentó en la introducción de este capítulo y, tal como aparece también en el *artículo científico 1*, la adición de modificadores en la fuente como H_2O o MeOH puede favorecer mecanismos de protonación. Esto ocurre en el caso de analitos con tendencia a la protonación, generándose mayoritariamente el ion $[M+H]^+$ en lugar de dividirse la intensidad entre $M^{+\cdot}$ y $[M+H]^+$. Este comportamiento de transferencia protónica se explica porque el plasma de nitrógeno reacciona con el agua generándose protones que finalmente se transfieren a los analitos. En nuestro caso, se observó que los analitos estudiados tenían tendencia a protonarse, ya que debido a las trazas de vapor de agua en la fuente, en los espectros de masas ya se observaba el ion $[M+H]^+$ junto con el $M^{+\cdot}$. La adición de agua en la fuente se realizó mediante la introducción de un vial con una pequeña apertura en la parte superior, en un soporte diseñado especialmente para ello, posicionado en la puerta de la fuente APCI.

En la **figura II.3** se observan, a modo de ejemplo, cuatro situaciones para un compuesto seleccionado con elevada afinidad protónica (metandienona). Las **figuras II.3.c** y **II.3.d** muestran un espectro *Full Scan* en

masa exacta de la metandienona sin derivatizar (**figura II.3.a**), sin presencia de agua en la fuente (c) y con presencia de agua (d). Debido a la afinidad protónica de la metandienona (dada por la presencia de un carbonilo conjugado), en ambos casos sólo se observan los iones de *m/z* 301 y 283, que corresponden con $[M+H]^+$ y $[M+H-H_2O]^+$, si bien, la sensibilidad aumenta ligeramente en presencia de agua. Por otra parte, las **figuras II.3.e** y **II.3.f** corresponden a espectros de la la metandienona TMS-derivatizada (**figura II.3.b**) sin agua y en presencia de agua, respectivamente. La derivatización con TMS disminuye la afinidad protónica del carbonilo en C3. Por este motivo, tal y como se observa, en el caso de compuestos derivatizados, la abundancia del ión $[M+H]^+$ se vio favorecida en presencia de modificador. Si nos fijamos en la **figura II.3.f** aparece mayoritariamente el ion 445 ($[M+H]^+$), mientras que en la **figura II.3.e** (sin agua) también se observa el 444 ($M^{+\cdot}$).

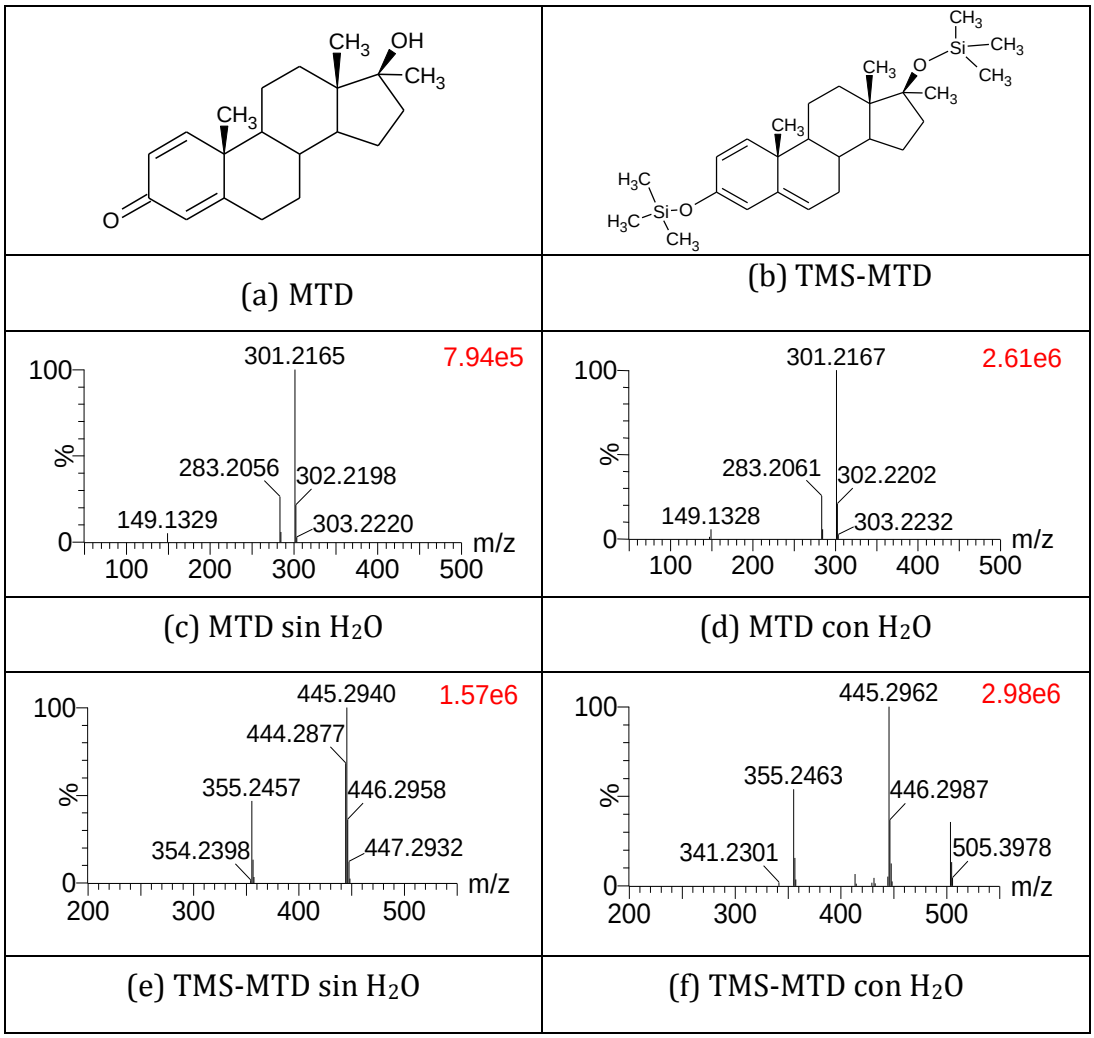

Figura II.3. Reacciones de ionización en APCI. Estructura: a) MTD, b) TMS-MTD. Espectro *Full Scan* TOFMS: c) MTD bajo condiciones de transferencia de N_2, d) MTD bajo condiciones de transferencia de protón, e) TMS-MTD bajo condiciones de transferencia de N_2, f) TMS-MTD bajo condiciones de transferencia de protón

Este comportamiento se observó, por lo general, para todos los compuestos, por lo que se decidió añadir el vial de agua como modificador en la fuente en todos los trabajos de estudio de AAS por GC-APCI.

OPTIMIZACIÓN DEL VOLTAJE DE CONO

Uno de los parámetros a considerar en la fuente APCI es la optimización del voltaje de cono. Este voltaje puede tener un efecto significativo en la fragmentación en la fuente (*in-source fragmentation*) ya que es el encargado de producir la transmisión de los iones generados en la fuente hacia el analizador de masas. Si es demasiado bajo, pueden perderse iones, mientras que si es un valor elevado pueden generarse las mencionadas fragmentaciones en la fuente. Se realizaron pruebas a distintos voltajes de cono (5, 10, 15, 20, 30 y 40 eV) tanto para compuestos no derivatizados como TMS-derivatizados con el objetivo de estudiar cambios en la fragmentación. Se observó que la intensidad de la molécula protonada no variaba significativamente, por lo que, se emplearon valores intermedios de 20 - 30 eV en todos los trabajos.

TRATAMIENTO DE MUESTRA

En la sección I.1.3.1 de la introducción general se describió el método analítico de rutina aplicado para la detección de agentes anabolizantes en orina por GC-MS. El procedimiento se muestra en la **figura I.2** de dicho apartado. El método conlleva diversos pasos para optimizar el comportamiento cromatográfico de los analitos, método ya aplicado y

establecido en los laboratorios de control del dopaje en análisis de rutina. A continuación, se muestra más en detalle este procedimiento.

El tratamiento de muestra incluye un primer paso de ***hidrólisis*** con *β-glucuronidasa* de *E. coli.* a pH 7 para liberar los esteroides que son excretados conjugados como glucurónidos. A continuación, los esteroides libres se ***extraen***, a pH 9.5 para eliminar posibles interferentes ácidos, con un disolvente apolar como el TBME y, una vez se encuentran en la fase orgánica, el disolvente se evapora. Estos pasos de hidrólisis y extracción se realizaron en el *trabajo científico 3* en el que se trataban muestras de orina.

El último paso para adecuar los analitos a la determinación por GC-MS es la ***derivatización*** con un agente sililante, para ello se requiere unas condiciones de ausencia total de humedad ya que los esteroides, una vez silanizados se pueden hidrolizar fácilmente en presencia de agua. Como se observa en la **figura II.4**, el derivatizante utilizado en los tres trabajos presentados, fue el MSTFA. Así, los grupos hidroxilo reaccionaron cuantitativamente dando derivados trimetilsililados estables, además de servir como disolvente adecuado para GC. Los hidroxilos secundarios también derivatizaron inmediatamente, aunque los terciarios, más impedidos estéricamente como los presentes en 17-metil-17β-hidroxi esteroides, necesitaron la presencia de un catalizador. Para ello, el trimetiliodosilano (TMIS) es muy eficaz, sirviendo también para derivatizar los grupos carbonilo, sililando tanto los grupos OH como los CO. Los grupos carbonilo se convierten en los enol-TMS derivados mediante el desplazamiento del equilibrio de la tautomería ceto-enólica. Como el TMIS no es fácil de manejar se recomienda el uso de NH_4I para generarlo *in situ*. Además, la adición de agentes reductores, como en nuestro caso el 2-mercaptoetanol, minimiza la

formación de yodo (proveniente de la oxidación del TMIS) y retrasa la degradación de la mezcla.

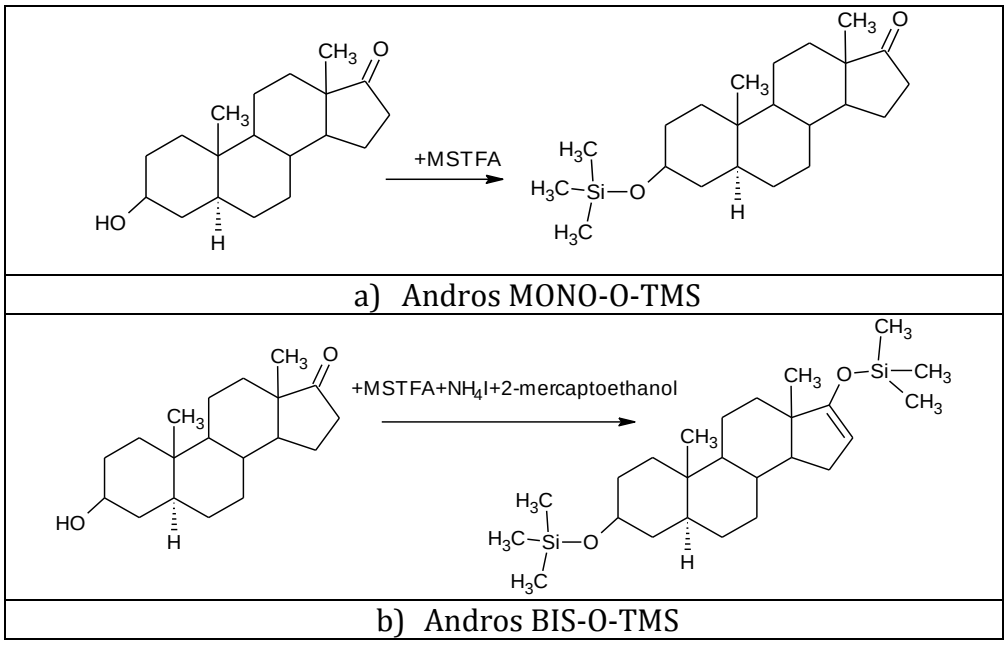

Figura II.4. Proceso de derivatización para a) MONO-O-Androsterona y la b) BIS-O-Androsterona

El rendimiento de derivatización puede ser crítico tanto en métodos cuantitativos como cualitativos. En este último caso, una derivatización incompleta puede ser la causa de no detectar algún analito incluso a concentraciones superiores al LOD. Teniendo en cuenta que el proceso de derivatización descrito depende, entre otras cosas, de los componentes de la matriz (sales, etc.), el rendimiento de derivatización debe controlarse en cada muestra. Con este propósito, se monitorizan en el método dos compuestos, uno correspondiente al producto de derivatización incompleta (e.g. androsterona-mono-O-TMS, **figura II.4.a**) y otro al de derivatización completa (e.g. androsterona-bis-O-TMS, **figura II.4.b**). La presencia del compuesto de derivatización incompleta debe ser residual. Una presencia

elevada es indicativa de una derivatización inadecuada y, por tanto, la muestra debe reanalizarse. Este aspecto se ha utilizado en el *artículo científico 3*, donde el objetivo fue validar cualitativamente 16 AAS. Para evaluar el proceso de derivatización, se añadieron las transiciones para Androsterona-mono-O-TMS (derivatización incompleta del AAS endógeno androsterona) y Androsterona-bis-O-TMS (derivatización completa). Como aproximación estándar en los laboratorios de control antidopaje, se consideró una ratio de áreas mono-TMS/bis-TMS superior al 5% como indicativa de una derivatización incompleta. En todas las muestras de validación y muestras reales analizadas se encontraron valores claramente inferiores al 5%. Se concluyó, por tanto, que el rendimiento de derivatización fue adecuado en todas las muestras analizadas. A modo de ejemplo, la **figura II.5** muestra los cromatogramas de las transiciones seleccionadas para el control de la derivatización en una muestra de validación. Se observa claramente la diferencia de áreas que confirma el buen rendimiento del proceso de derivatización en esta muestra.

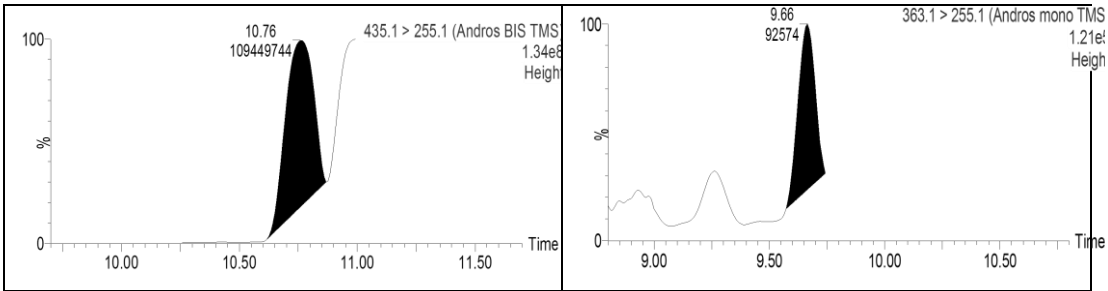

a) Andros BIS-O-TMS | b) Andros MONO-O-TMS

Figura II.5. Cromatogramas SRM en una muestra de validación para a) BIS-O-Androsterona y la b) MONO-O-Androsterona

SELECCIÓN DE TRANSICIONES ESPECÍFICAS (*Artículo científico 3*)

En el segundo trabajo de este capítulo acerca de la fragmentación de los esteroides, se observó en general, que todos presentaron patrones de fragmentación muy similares, compartiendo muchos de ellos iones producto comunes, sobre todo a altas energías de colisión (Ver tablas de iones producto del *artículo científico 2*).

Tal y como se detalla en el *artículo científico 3*, la selección de transiciones sensibles y, sobre todo, específicas para detectar AAS en orina es un paso complejo y crucial. La presencia de numerosos esteroides endógenos presentes en la orina dificulta la búsqueda de transiciones específicas, porque, en muchas ocasiones, se encuentran compuestos que coeluyen y que pueden compartir transiciones.

Con el objetivo de encontrar, para cada compuesto, las transiciones más sensibles y específicas, se evaluó un elevado número de ellas en extractos de matriz blanco, de matriz blanco fortificada a varios niveles y de patrón para elegir aquellas más sensibles pero menos interferidas. Primero se seleccionó el ión precursor más abundante en cada caso, $[M+H]^+$, $[M+H\text{-}TMSOH]^+$ o $[M+H\text{-}2TMSOH]^+$, dependiendo de la estructura del compuesto, tal y como se estudió en el *primer artículo científico*. A partir de estos iones se obtuvieron sus espectros de iones producto a diferentes energías de colisión, para, finalmente, seleccionar una lista de transiciones SRM (8-10 aproximadamente) para estudiarlas en la matriz.

En algunos casos no se pudieron obtener transiciones específicas con el gradiente de temperaturas aplicado, como fue el caso del metabolito 2 de la

norboletona y de la boldenona (NORBOLmet2 y BD). Este hecho se discute en la información suplementaria del tercer artículo, donde se detalla que con un gradiente de temperaturas más largo se consigue separar estos analitos de los interferentes endógenos.

A modo de ejemplo, en la **figura II.6** se muestra la selección de transiciones para el metabolito 3 de la metandienona (MTDmet3), presentándose las tres transiciones más sensibles.

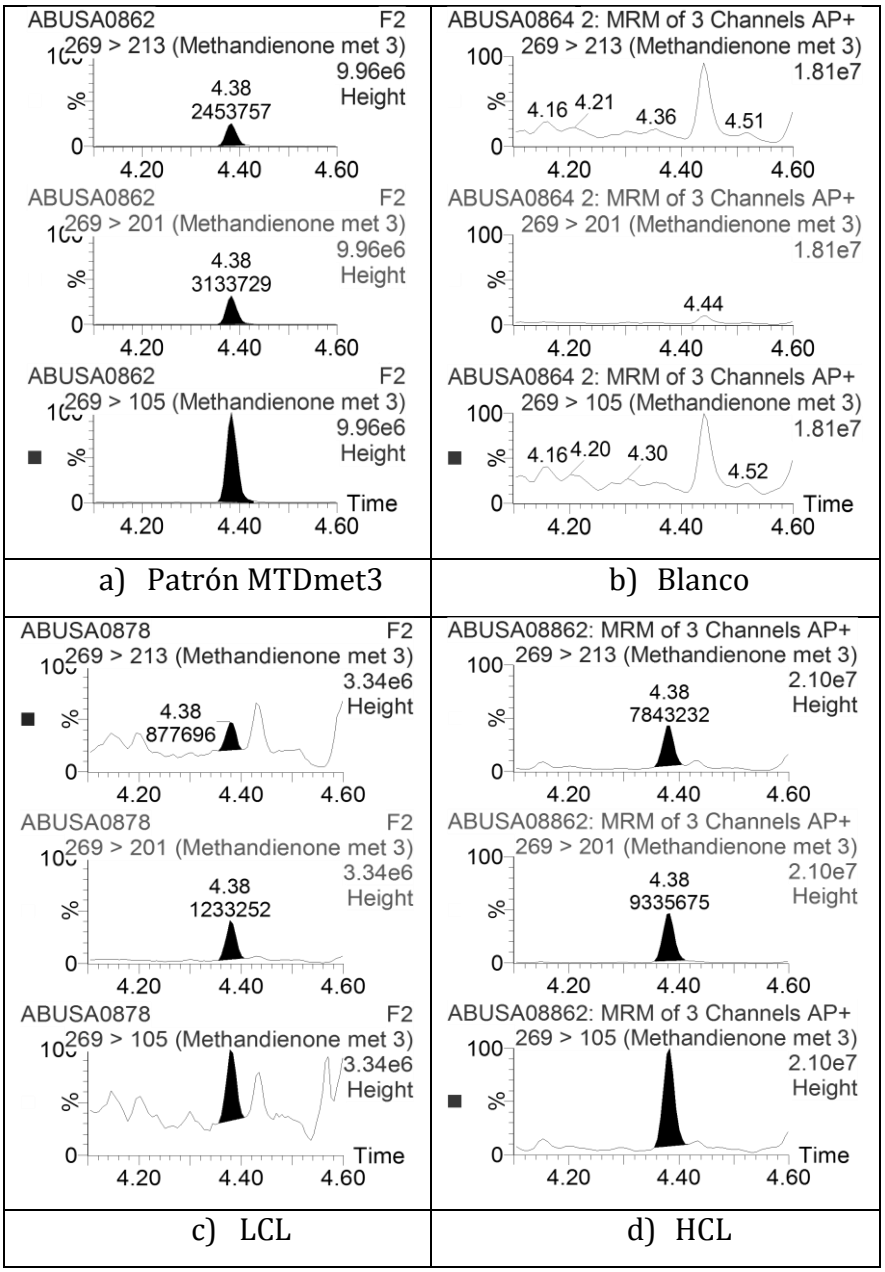

Figura II.6. Cromatogramas correspondientes a diferentes transiciones SRM para la MTDmet3 en a) patrón 100 ng/mL, b) muestra blanco, c) muestra al nivel bajo validado (LCL) (1 ng/mL) y d) muestra al nivel alto validado (HCL) (10 ng/mL)

Se observa que la transición más sensible es 269>105, seguida por 269>201. Sin embargo, la seleccionada para el *screening* fue esta última ya que está menos interferida por la matriz, demostrando la importancia de realizar este estudio de especificidad. Para la mayoría de compuestos, la transición más sensible fue también la más específica, seleccionando ésta para llevar a cabo el *screening*. El resto de transiciones pueden ser de utilidad para los posteriores estudios de confirmación.

En los trabajos expuestos en este capítulo, la fuente APCI se presenta como una potencial alternativa a la tradicional y robusta fuente de EI en el análisis de AAS por su ionización suave y universal. Este potencial queda de manifiesto en el tercer artículo presentado en este capítulo, donde se trata de comparar ambas fuentes intentando, en la medida de lo posible, que el resto de parámetros del proceso analítico fueran comunes.

Por otro lado y también mediante el uso de esta fuente, se ha comprobado que el comportamiento de ionización y fragmentación de este grupo de sustancias dopantes está estrechamente relacionado con su estructura, como queda reflejado en los *artículos 1 y 2*. Pese a la similitud entre los compuestos de una misma familia, se han establecido subgrupos de comportamiento común según parámetros estructurales, lo que puede ser de utilidad en el futuro para análisis no dirigidos de búsqueda de nuevos esteroides o sus metabolitos.

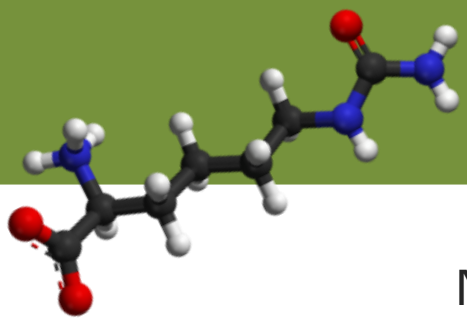

CAPÍTULO III

DETECCIÓN NO DIRIGIDA DE NUEVOS MARCADORES DEL ABUSO DE ESTEROIDES ANABOLIZANTES ANDROGÉNICOS Y OTROS AGENTES DOPANTES MEDIANTE HRMS(/MS) Y ESTRATEGIAS METABOLÓMICAS

III.1. Introducción

Los trabajos que abarca este tercer capítulo, tienen como denominador común las herramientas metabolómicas para la detección de marcadores del abuso de sustancias dopantes. Resumiendo la información descrita en la introducción general, a continuación se muestran en la **Tabla III.1** algunas definiciones relacionadas con la metabolómica (Dettmer *et al*., 2007).

Tabla III.1. Definiciones útiles relacionadas con las estrategias metabolómicas

Metabolito	Pequeñas moléculas que participan en reacciones metabólicas generales
Metaboloma	Conjunto de metabolitos de un organismo
Metabolic Profiling (Evaluación por perfil metabólico)	Análisis cuantitativo de un conjunto de metabolitos en una determinada ruta bioquímica o una clase específica de compuestos. Incluye el análisis *target*
Metabolic fingerprinting (Identificación mediante huella metabólica)	Estrategia *non target*, *screening* global para clasificar muestras basadas en patrones de los metabolitos o "huellas dactilares" que cambian en respuesta a enfermedad, perturbaciones medioambientales o genéticas con la finalidad de identificar los metabolitos discriminantes

En el caso de los trabajos que se presentan en este capítulo, la herramienta utilizada es la metabolómica no dirigida o *metabolic fingerprinting,* donde el objetivo es encontrar marcadores discriminantes entre muestras control y muestras de individuos que han consumido una determinada sustancia dopante.

Una de las principales tareas de los laboratorios de control antidopaje es la de detectar la presencia de marcadores del abuso a sustancias prohibidas en muestras recogidas de atletas. En este sentido, hay un

constante interés en el descubrimiento de marcadores adecuados para las sustancias prohibidas. La metabolómica y la búsqueda de nuevos biomarcadores pueden resultar de gran utilidad en este contexto. Así, uno de los principales fines de la metabolómica en este campo ha sido el desarrollo de métodos indirectos para la detección de sustancias difíciles de detectar mediante métodos convencionales, como por ejemplo la hormona de crecimiento (hGH). Existen trabajos reportados como el de Boyard-Kieken *et al*. de 2011 en el caso de caballos tratados con hormona de crecimiento (*recombinant equine Growth Hormone*, reGH). En el caso de animales, estas estrategias metabolómicas pueden aplicarse tanto en el campo del dopaje de animales de competición, como en el caso de ganado al que se administra hormonas u otras sustancias de forma ilegal para aumentar el crecimiento y mejorar su rendimiento comercial (Courant *et al*., 2009, Rijk *et al*., 2009, Regal *et al.,* 2011).

En humanos existen trabajos publicados con enfoques en el *profiling* de EAAS en orina (Boccard *et al*., 2011; Boccard *et al*., 2014), en los que se emplean instrumentos de alta resolución en modo de adquisición de espectro completo para diferenciar perfiles metabólicos antes y después de la administración de testosterona. Sin embargo, los resultados están filtrados por las masas y tiempos de retención de los metabolitos esperados, por lo que sigue siendo un análisis semidirigido. Aunque los análisis completamente no dirigidos o *non target* se han aplicado en la detección de rutas alteradas tras la administración de diversos agentes dopantes (Kiss *et al.*, 2013), su potencial en la búsqueda de marcadores sigue siendo un campo todavía por explorar.

Como se describe en la introducción general, los pasos que suelen incluirse en los trabajos de metabolómica son: un adecuado diseño experimental, toma y preparación de las muestras, análisis de las mismas y un posterior tratamiento de los datos. A continuación, se estudian y elucidan estructuralmente los marcadores, éste es uno de los pasos más relevantes dentro del análisis metabolómico no dirigido. Asimismo, habría que investigar el mecanismo que ha hecho destacar a dicho marcador, es decir, buscar una explicación biológica para afirmar que se trata de un buen marcador en un estudio en concreto. La selección del tratamiento de muestra, columnas, tratamiento de datos etc., está detallado en ambos artículos y será discutido en conjunto en el apartado III.4.

En este capítulo se evalúa la capacidad de las estrategias metabolómicas no dirigidas usando analizadores de alta resolución en el campo del análisis del control del dopaje. Se presentan dos trabajos, el primero de ellos (*artículo científico 4*) de búsqueda de marcadores del abuso de testosterona y el segundo (*artículo científico 5*) del abuso de hormona del crecimiento. En ambos casos la técnica analítica seleccionada fue UHPLC-HRMS(/MS).

III.2. Artículo científico 4

analytical chemistry

Article

pubs.acs.org/ac

Untargeted Metabolomics in Doping Control: Detection of New Markers of Testosterone Misuse by Ultrahigh Performance Liquid Chromatography Coupled to High-Resolution Mass Spectrometry

Montse Raro,[†] María Ibáñez,[†] Rubén Gil,[†] Andreu Fabregat,[‡] Eva Tudela,[§] Koen Deventer,[§] Rosa Ventura,[‡,∥] Jordi Segura,[‡,∥] Josep Marcos,[‡,∥] Aristotelis Kotronoulas,[‡,⊥] Jesús Joglar,[⊥] Magi Farré,[#] Sheng Yang,[○] Yanyi Xing,[○] Peter Van Eenoo,[#] Elena Pitarch,[†] Félix Hernández,[†] Juan Vicente Sancho,[†] and Oscar J. Pozo*[,‡]

[†]Research Institute for Pesticides and Water, University Jaume I, Av. Sos Baynat S/N, 12071 Castellón, Spain

[‡]Bioanalysis Research Group, IMIM, Hospital del Mar, Doctor Aiguader 88, 08003 Barcelona, Spain

[§]DoCoLab, Ghent University, Technologiepark 30, 9052, Zwijnaarde, Belgium

[∥]Department of Experimental and Health Sciences, Universitat Pompeu Fabra, Doctor Aiguader 88, 08003 Barcelona, Spain

[⊥]Department of Biological Chemistry and Molecular Modelling, Institute of Advanced Chemistry of Catalonia, Spanish Council for Scientific Research (IQAC−CSIC), Jordi Girona 18-26, 08034 Barcelona, Spain

[#]Human Pharmacology and Neurosciences Research Group, IMIM, Clinical Pharmacology Unit, Hospital Universitari Germnans Trias I Pujol-IGTP and Universitat Autònoma de Barcelona, Doctor Aiguader 88, 08003 Barcelona, Spain

[○]National Anti-Doping Laboratory, China Anti-Doping Agency, 1, An Ding Road, Beijing, 100029, China

Supporting Information

ABSTRACT: The use of untargeted metabolomics for the discovery of markers is a promising and virtually unexplored tool in the doping control field. Hybrid quadrupole time-of-flight (QTOF) and hybrid quadrupole Orbitrap (Q Exactive) mass spectrometers, coupled to ultrahigh pressure liquid chromatography, are excellent tools for this purpose. In the present work, QTOF and Q Exactive have been used to look for markers for testosterone cypionate misuse by means of untargeted metabolomics. Two different groups of urine samples were analyzed, collected before and after the intramuscular administration of testosterone cypionate. In order to avoid analyte losses in the sample treatment, samples were just 2-fold diluted with water and directly injected into the chromatographic system. Samples were analyzed in both positive and negative ionization modes. Data from both systems were treated under untargeted metabolomic strategies using XCMS application and multivariate analysis. Results from the two mass spectrometers differed in the number of detected features, but both led to the same potential marker for the particular testosterone ester misuse. The in-depth study of the MS and MS/MS behavior of this marker allowed for the establishment of 1-cyclopentenoylglycine as a feasible structure. The putative structure was confirmed by comparison with synthesized material. This potential marker seems to come from the metabolism of the cypionic acid release after hydrolysis of the administered ester. Its suitability for doping control has been evaluated.

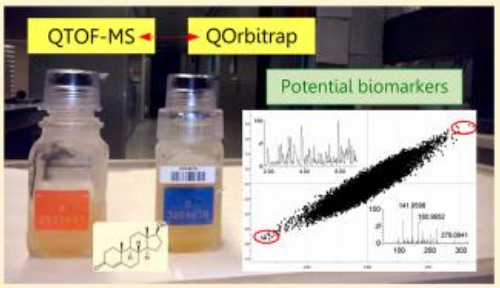

Untargeted Metabolomics in Doping Control: Detection of New Markers of Testosterone Misuse by Ultrahigh Performance Liquid Chromatography Coupled to High-Resolution Mass Spectrometry

Montse Raro[†], María Ibáñez[†], Rubén Gil[†], Andreu Fabregat[‡], Eva Tudela[§], Koen Deventer[§], Rosa Ventura[‡∥], Jordi Segura[‡∥], Josep Marcos[‡∥], Aristotelis Kotronoulas[‡⊥], Jesús Joglar[⊥], Magi Farré[#], Sheng Yang[○], Yanyi Xing[○], Peter Van Eenoo[#], Elena Pitarch[†], Félix Hernández[†], Juan Vicente Sancho[†], and Óscar J. Pozo[‡]

† Research Institute for Pesticides and Water, University Jaume I, Av. Sos Baynat S/N, 12071 Castellón, Spain

‡ Bioanalysis Research Group, IMIM, Hospital del Mar, Doctor Aiguader 88, 08003 Barcelona, Spain

§ DoCoLab, Ghent University, Technologiepark 30, 9052, Zwijnaarde, Belgium

∥ Department of Experimental and Health Sciences, Universitat Pompeu Fabra, Doctor Aiguader 88, 08003 Barcelona, Spain

⊥ Department of Biological Chemistry and Molecular Modelling, Institute of Advanced Chemistry of Catalonia, Spanish Council for Scientific Research (IQAC−CSIC), Jordi Girona 18-26, 08034 Barcelona, Spain

Human Pharmacology and Neurosciences Research Group, IMIM, Clinical Pharmacology Unit, Hospital Universitari Germnans Trias I Pujol-IGTP and Universitat Autònoma de Barcelona, Doctor Aiguader 88, 08003 Barcelona, Spain

○ National Anti-Doping Laboratory, China Anti-Doping Agency, 1, An Ding Road, Beijing, 100029, China

Abstract

The use of untargeted metabolomics for the discovery of markers is a promising and virtually unexplored tool in the doping control field. Hybrid quadrupole time-of-flight (QTOF) and hybrid quadrupole Orbitrap (Q Exactive) mass spectrometers, coupled to ultrahigh pressure liquid chromatography, are excellent tools for this purpose. In the present work, QTOF and Q Exactive have been used to look for markers for testosterone cypionate misuse by means of untargeted metabolomics. Two different groups of urine samples were analyzed, collected before and after the intramuscular administration of testosterone cypionate. In order to avoid analyte losses in the sample treatment, samples were just 2-fold diluted with water and directly injected into the chromatographic system. Samples were analyzed in both positive and negative ionization modes. Data from both systems were treated under untargeted metabolomic strategies using XCMS application and multivariate analysis. Results from the two mass spectrometers differed in the number of detected features, but both led to the same potential marker for the particular testosterone ester misuse. The in-depth study of the MS and MS/MS behavior of this marker allowed for the establishment of 1-cyclopentenoylglycine as a feasible structure. The putative structure was confirmed by comparison with synthesized material. This potential marker seems to come from the metabolism of the cypionic acid release after hydrolysis of the administered ester. Its suitability for doping control has been evaluated.

Introduction

Metabolomics is one of the most useful approaches for the discovery of new metabolites or markers. It consists of the comprehensive measurement of the low-molecular weight metabolites of a cell, tissue, or body fluid, resulting from metabolic processes in organisms (1). A large number of data is commonly obtained from analytical platforms based on mass spectrometry (MS) and nuclear magnetic resonance (NMR). The selection of the instrumentation is an important issue since it is a key factor regarding the number of peaks detected and their sensitivity/specificity. Because of their high resolution, mass accuracy, and full-spectrum acquisition capabilities, high-resolution (HR) mass analyzers such as Orbitrap, TOF, or hybrids analyzers like quadrupole-time-of-flight (QTOF) and quadrupole Orbitrap (Q Orbitrap) are adequate to develop metabolic profiling methods in complex biological matrixes such as urine (2-4). Profiling at metabolite levels or an individual's response to stimuli, environment, or drug treatment are well described (5), as well as other applications in food sciences (3, 6), plant metabolomics (7), and clinical research (8, 9) among others. However, its implementation in other fields such as doping control is rather limited.

The potential usefulness of metabolomics for doping control purposes is described in the literature (10-12), where it is illustrated that "omics" methods may be ideal platforms for the discovery of markers of the abuse of some prohibited substances or methods for which the direct detection presents difficulties. This is the case of endogenous anabolic androgenic steroids (EAAS) like testosterone (T).

EAAS are responsible for the largest number of adverse analytical findings reported by doping control laboratories (13). EAAS are naturally

present in humans; thus, the detection of the misuse of this group of compounds is a challenging task. Ratio between urinary T and epitestosterone (E), both excreted as glucuronides (T/E), was first used to distinguish between natural and administrated testosterone by Donike *et al.* in 1983 (14). This ratio provided a solution to screen for T misuse until it was found that people with a common deletion polymorphism in the UGT2B17 gene excreted low concentration of T, thus generating abnormally low T/E ratios even after testosterone administration (15, 16). Nowadays, the current strategy for the screening of EAAS is based on the quantification in every urine sample of the so-called steroid profile, i.e., seven markers related with T, and its inclusion in the Athlete Biological Passport (17) (ABP). The discovery of alternative markers which might complement the steroid profile is currently an active research topic in the doping control field. Several alternative T metabolites have been proposed for this purpose (18, 19). The application of target metabolomic approaches has been described as a useful tool for the selection of new markers (20, 21). Open detection methods, i.e., scan acquisition of the whole *m/z* range using high-resolution mass spectrometry have been used for the differentiation of the metabolic profiles before and after testosterone administration (12). However, the untargeted results were filtered by the expected *m/z* of T metabolites and only the expected ones (metabolites coming from known pathways such as hydroxylation, reduction, oxidation, and conjugation either with glucuronic acid or with sulfate) were considered for the ulterior statistical analysis. Although untargeted metabolomics has been used for the detection of pathways altered after the administration of different doping agents (22), its potential for the detection of alternative markers remains virtually unexplored in this field.

The goal of the present study is to evaluate the potential of untargeted metabolomics in the doping control field, analyzing the differences and similarities between two systems: UHPLC-QTOF and UHPLC-QOrbitrap. By means of a metabolomic approach and using these powerful analytical techniques, markers of T misuse after T cypionate administration were investigated. The experimental design aimed to detect those markers which can be detectable even several days after administration irrespective on the basal T/E values.

Materials and Methods

Reagents and Chemicals

For QTOF analysis, HPLC-grade water was obtained by purifying demineralized water in a Milli-Q plus system from Millipore (Bedford, MA). HPLC-grade methanol (MeOH), residue analysis grade acetone, sodium hydroxide (>99%), and formic acid (98–100%) were acquired from Scharlab (Barcelona, Spain). Leucine-enkephalin, used as the lock mass, was purchased from Sigma-Aldrich (St. Louis, MO).

In case of Q Orbitrap analysis, LC–MS grade methanol and LC–MS grade water were purchased from Biosolve (Valkenswaard, The Netherlands). Formic acid Optima LC/MS was purchased from Fischer Scientific (Loughborough, U.K.). Exactive Calibration Kit solutions employed were purchased from (Sigma-Aldrich, St. Louis, MO, and ABCR GmbH & Co. KG, Karlsruhe, Germany).

For the synthesis of the 1-cyclopentenoylglycine (1-CPG), 1-cyclopetenecarboxylic acid, glycine, benzyl chloroformate, triethylamine, and dimethyl sulfoxide (DMSO) were purchased from Sigma-Aldrich Química S.A. (Madrid, Spain) and trifluoroacetic acid (TFA) was purchased from Carlo Erba Reagents (Barcelona, Spain). Finally, deuterated methanol (CD3OD) used in the NMR experiments was purchased from Euriso Top (Saint-Aubin, France).

Instrumentation

Xevo G2 QTOF

The Acquity ultraperformance liquid chromatography system (Waters, Milford, MA) was interfaced to a Xevo G2 QTOF mass spectrometer (Waters Micromass, Manchester, U.K.) using an orthogonal Z-spray electrospray (ESI) interface. The chromatographic separation was performed using an Acquity UPLC BEH C18 column (1.7 μm, 2.1 mm × 100 mm) from Waters, using a flow rate of 0.3 mL/min. The mobile phases used were (A) H_2O and (B) MeOH, both with 0.01% (v/v) HCOOH. The percentage of MeOH was linearly increased as follows: 1 min, 2%; 3 min, 15%; 6 min, 50%; 9 min, 95%; 10 min, 95%; 10.01 min, 2%; and 12 min, 2%. The total run time was 12 min. The injection volume was 20 μL. Nitrogen (Praxair, Valencia, Spain) was used as both drying and nebulizig gas. The desolvation gas flow rate was set at 1000 L/h. The resolution of the TOF mass spectrometer was ∼20 000 at full width half-maximum (fwhm) at m/z 556. MS data were acquired over a m/z range of 50–1000 with a scan time of 0.4 s. Capillary voltages of 0.7 kV and 2.5 kV were used in positive and negative ionization modes, respectively. A cone voltage of 20 V was applied. Argon was used as collision gas

(99.995%, Praxair). The interface temperature was set to 550 °C and the source temperature to 130 °C. The column temperature was set to 40 °C and the autosampler to 5 °C. The same cone voltage and collision energy ramp was used for additional tandem MS (MS/MS) experiments.

Calibration of the mass-axis and automated accurate mass measurement are described in the Supporting Information (section S1).

Q-Exactive Orbitrap

The liquid chromatographic system was an Accela LC (Thermo Scientific, Bremen, Germany) equipped with degasser, Accela 1250 pump, autosampler at 7 °C, and a heated column compartment at 40 °C. The same column, injection volume, chromatographic conditions, mobile phases, flow rate, and gradient employed in the QTOF system were used in this instrument. The LC effluent was pumped to a Q-Exactive benchtop Orbitrap based mass spectrometer (Thermo Scientific, Bremen, Germany) operating in the positive/negative polarity switching mode and equipped with an ESI source. Nitrogen sheath gas flow rate and auxiliary gas were set at 50 and 20 (arbitrary units), respectively. The S-lens rf level was set at 100 (arbitrary units). The capillary temperature was 250 °C and the spray voltage 4 kV in both ion modes. The instrument operated in full spectrum acquisition from *m/z* 50 to 1000. The resolution was 35 000 (fwhm at *m/z* 200) with a scan time of 0.45 s in polarity switching mode. The automatic gain control (AGC) was 106. Data were acquired in centroid mode. The Q Orbitrap performance in both positive and negative ionization modes was evaluated daily and external calibration was daily done with Calibration Kit solutions.

Administration Study Samples

Eight healthy male volunteers were included in two T excretion studies (one performed in Spain and the other one in China). Four volunteers with T/E values between 1 and 3 (coming from the first study) and four volunteers with T/E values below 0.3 (coming from the second one) were selected. Four basal urine samples (first morning urine) were collected, three of them during the three consecutive days before the administration (− 72 h, − 48 h, and − 24 h) and the other one on the day of the administration (0 h). After the administration of a single dose of 100 mg of testosterone intramuscularly injected (Testex prolongatum, 1 vial of 2 mL containing 100 mg of testosterone cypionate, Desma Laboratorio Farmaceutico, Madrid, Spain), several samples were collected up to 15 days after administration. Samples were stored at −20 °C until the analysis.

Subjects signed an informed consent before participation. Both protocols were approved by the local Research Ethics Committees and authorized by the state authorities. Both studies were conducted in accordance with the Declaration of Helsinki and state laws concerning clinical trials. Treatment was well tolerated by the subjects and no serious adverse events were observed.

For the metabolomic study, urine samples before (4 samples) and after administration (7 samples collected on days 1, 2, 3, 4, 5, 7, and 9) were considered for the analysis. A total of 32 preadministration samples (4 per 8 volunteers) formed the group Control and 56 postadministration samples (7 per 8 volunteers) formed the group Treated.

General Strategy

The general 4-steps workflow followed during this work is described below and is summarized in Figure S1.

Sample Treatment and Injection

A volume of 500 µL of HPLC-grade water was added to the same volume of urine samples. The diluted extracts were directly injected into the UHPLC-QTOF and Q-Exactive MS systems in both positive and negative ionization modes. Samples were randomly injected in order to avoid that the results might be affected by the instrumental drift. Quality control (QC) samples were prepared by a pool of all the extracts in order to be a good representation of all the samples. First, 10 QCs were injected in order to stabilize the chromatographic system and then an additional QC sample was injected every 10 samples in order to check the stability and the robustness of the measurements. Gradient elution was optimized in the QTOF for both positive and negative ionization mode injections, focusing on a better separation of the visible peaks in the base peak ion (BPI) chromatograms.

Data Preprocessing and Multivariate Analysis

The raw data acquired by the UHPLC-QTOF MS with the MassLynx operating software (version 4.1, Waters) were converted to Common Data Format (CDF) files using the Databridge application (from MassLynx).

Raw data acquired by the UHPLC-QOrbitrap MS with Xcalibur 2.2 were initially separated into positive and negative files and then converted into CDF files using a conversion option provided within the Xcalibur software.

The CDF data from both instruments were preprocessed in the same way using the XCMS free software (23). First, a peak picking centWave method was used to locate mass traces, and then continuous wavelet transform (CWT) was applied to find chromatographic peaks (peak width = 5–20 s, S/N threshold = 10, ppm = 15). Then, a density grouping method was applied to align the retention times of peaks with the same exact mass in all samples. For this purpose, a cluster of "well behaved peaks", present in all samples with stable intensities, was used to correct the rest from an initial bandwidth of 5 to 1 s, after 4 iterations. The peak list provided by XCMS was normalized using the loess normalization method (24) and then imported into the EZinfo software (Umetrics, Umea, Sweden) for multivariate analysis. Principal component analysis (PCA), partial least squares-discriminant analysis (PLS-DA), and orthogonal partial least squares-discriminant analysis (OPLS-DA) were evaluated after unit variance (UV) scaling to look for the potential markers. In the OPLS-DA, samples belonging to control and treated classes were used for comparison.

Marker Selection

The S-Plots generated by OPLS-DA were studied in order to obtain a list of candidates. Points located at the top right or at the bottom left were studied in all cases, corresponding to the best markers which increase or decrease, respectively, after T administration. Feasibility of the candidates was evaluated based on their variable trend plots, adequate abundances, and peak shapes.

Marker Identification

In order to elucidate the structure of the potential marker, both MS and MS/MS spectra were studied. The molecular formula of the marker was

obtained by the use of the accurate mass measurements of the precursor ion. This information together with that obtained after collision-induced dissociation at different collision energies was used for establishing a feasible structure for the marker. Confirmation of the hypothesis was performed after synthesis of the proposed structure.

Synthesis of 1-Cyclopentenoylglycine (1-CPG)

For the synthesis of 1-CPG, 30 mg of 1-cyclopentenecarboxylic acid was dissolved in 0.5 mL of acetonitrile and 22 μL of triethylamine was added. The solution was cooled to 4 °C, and 50 μL of benzyl chloroformate was added. The reaction was left to proceed for 24 h under vigorous stirring at room temperature. After that, the solvents were removed under vacuum and the residue was dissolved in 0.5 mL of DMSO that contained 40 μL of triethylamine. Then, 30 mg of glycine dissolved in 0.5 mL of water was added and the reaction was left to proceed for 24 h at room temperature. The HPLC purification of the product is detailed in the Supporting Information (section S2). Finally, after solvent removal, 16 mg of product as white solid was obtained.

The characterization of the final product was performed by NMR on a Mercury 400 MHz spectrometer equipped with OneNMR ProTune system probe. The NMR experiments were performed in deuterated methanol (CD3OD), and chemical shifts are reported in ppm relative to the residual non deuterated methanol (δ = 3.31 ppm for ^{1}H NMR and δ = 49 ppm for ^{13}C NMR). ^{1}H NMR (400 MHz, CD_3OD) δ = 6.62 (m, ^{1}H), 3.95 (s, ^{2}H), 2.58 (ddq, J = 10.1, 4.5, 2.4 Hz, ^{2}H), 2.51 (ddq, J = 10.4, 5.1, 2.6 Hz, ^{2}H), 2.00 (p, J = 7.6 Hz, ^{2}H). ^{13}C

NMR (101 MHz, CD_3OD) δ = 175.68, 169.34, 139.80, 41.34, 31.87, 33.66, 23.87.

1-CPG and T/E Evaluation

In order to show the potential applicability of 1-CPG for doping control purposes, it was qualitatively determined in all samples collected from two volunteers, with basal T/E values of 2.9 and 0.15, respectively. The analysis was based on a 2-fold dilution of the sample with acetic acid 1 M and subsequent determination by LC–MS/MS with a triple quadrupole analyzer using the transition 170 → 95. All the details about this determination can be found in the Supporting Information (section S3). For comparison purposes, the common marker T/E was determined in the same samples by gas chromatography coupled to mass spectrometry (GC/MS) as described elsewhere (25).

Results and Discussion

Sample Treatment, Data Preprocessing, and Multivariate Analysis

A "Dilute-and-shoot" strategy was applied to the urine samples in order to minimize losses during sample preparation and because it is a low time-consuming (26).

Samples were divided into two groups. The first one (control) contained all samples collected before administration and the second one (treated) those collected after administration (from day 1 to day 9). In order

to extract those markers which allow for the detection of T misuse for long periods irrespective of the basal T/E values, neither the time after administration nor the basal T/E value were considered into the data analysis.

The obtained data were preprocessed by XCMS for automatic peak detection and retention time alignment, generating tables of possible markers for each sample given by *m/z* and retention time in seconds with the format *MxxxTxxx* (where *Mxxx* stands for *m/z* and *Txxx* for retention time). In the QTOF analysis, 9 889 and 11 910 unique peaks were found in positive and negative ionization modes, respectively, whereas these values decreased when using Q Orbitrap to 7 451 and 5 528, respectively. These features included isotopes, adducts and/or in-source fragments. The differences might be explained either by a potentially higher sensitivity of the QTOF or by the possible generation of a larger number of adducts/in-source fragments in the ESI interface of this analyzer.

XCMS data were first normalized to take into account the drift of the instrument as well as differences in urine concentration due to differences in the excreted volume. After loess normalization, intensities were more stable in the samples, in both positive and negative ionization modes, as it can be seen in Figure S2. These normalized data were then analyzed by PCA to have a nonsupervised visualization of the results (Figure S3).

The use of QCs in nontargeted metabolomics analysis can be considered equivalent to the use of standards in target analysis, and their importance is described in the literature (27, 28). The PCA analysis showed that QCs were just in the middle of the plot, which implies that they could be regarded as representative of all the samples. Additionally, discrimination

between samples before and after T cypionate administration was clearly observed in PCA for QTOF data (Figure S3).

The next step was the application of a PLS-DA, a supervised method that takes into account class information. Both instruments showed good discrimination of the groups (before and after T administration) irrespective of the ionization mode used (Figure S4).

Finally, an OPLS-DA was applied in order to enhance the differences between selected classes (control and treated). This algorithm is a powerful tool for the analysis of qualitative data structures. It consists in an extension of the previous PLS regression method which integrates an orthogonal signal correction filter (29). In the generated S-plots (Figure 1 for Q Orbitrap and Figure S5 for QTOF), points located at the top right square correspond to the features that increase after T administration whereas points at the bottom left square represent those that decrease after T administration.

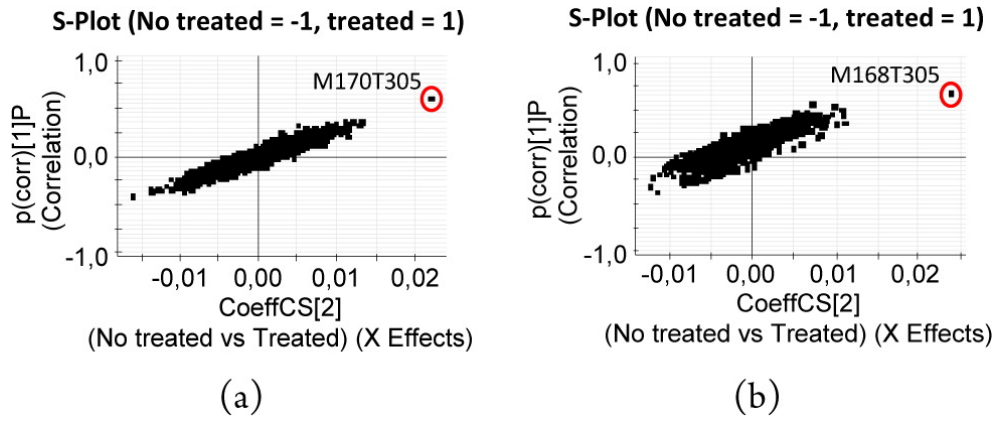

Figure 1. OPLS-DA S-Plot for Q Orbritrap in (a) positive ionization mode and (b) negative ionization mode. Significant markers (*m/z* and RT) are highlighted. See more information in Table 1.

Selection of the Marker

The list of the top five features for QTOF and Q Orbitrap of each ionization mode is shown in Table 1.

The variable trend plots of all the candidates that increased and decreased after T administration were evaluated. Variable trend plots from Q Orbitrap candidates M170T305 and M333T230 are shown in Figure S6, where it can be observed the different behavior of two candidates with p(corr) values of 0.60247 and 0.36836, respectively. Features with the highest p(corr) and with a suitable variable trend plot were selected as candidates.

Table 1. Best features obtained from OPLS-DA S-Plot, in QTOF and Q Orbitrap in both ionization modes

		Increase after T administration (right)		Decrease after T administration (left)	
		Marker	p(corr)	Marker	p(corr)
QTOF	POSITIVE	M95T295*	0,64951	M259T555	-0,43191
		M170T295*	0,62215	M228T456	-0,39339
		M951T542_1	0,4789	M511T554	-0,39040
		M994T542	0,47680	M227T456	-0,38987
		M951T542_2	0,47375	M283T274	-0,38928
	NEGATIVE	M249T380	0,78888	M192T217	-0,42053
		M168T295	0,77079	M422T355	-0,36789
		M369T381_1	0,74499	M286T422	-0,36677
		M367T381	0,53850	M457T544	-0,35284
		M371T381	0,38594	M451T448	-0,34879
Q Orbitrap	POSITIVE	M170T305*	0,60247	M265T42	-0,40982
		M333T230	0,36836	M127T59	-0,38174
		M114T238	0,35049	M132T73	-0,35674
		M183T31	0,34885	M138T107	-0,35498
		M85T39	0,34856	M328T358	-0,35203
	NEGATIVE	M168T305*	0,67447	M123T287	-0,38195
		M165T23	0,41701	M151T355	-0,36366
		M501T563	0,39021	M279T575	-0,35547
		M215T65	0,35798	M229T510	-0,33049
		M373T517	0,35584	M179T463	-0,33011

* denotes selected markers for study. M stands for *m/z* and T for retention time

Because of their low p(corr), none of the features that decreased after T administration was found to be a relevant candidate (Table 1). Regarding the features which increased after T cypionate administration, the use of Q Orbitrap revealed the presence of only one marker in each ionization mode whereas the use of QTOF was able to detect two and four markers in positive and negative modes, respectively. The two potential markers obtained by QTOF in positive ionization mode shared the same retention time (295 s) suggesting that both features were generated by the same compound. In negative ionization, the use of QTOF allowed for the detection of additional features with p(corr) values higher than 0.5 (Table 1).

These results illustrate that the larger number of features found by QTOF compared to Q Orbitrap seems to be related to both, a larger number of detected compounds and higher in-source fragmentation/adduct formation. Remarkably, the compound eluting at around 300 s was found by both instruments illustrating the suitability of both platforms for the detection of untargeted markers. This fact, together with the elevated p(corr), the adequate peak shape, and the suitable variable trend plot advised for the selection of this compound as a suitable marker. This marker was detected in both ionization modes with *m/z* 170 and *m/z* 168 in positive and negative modes, respectively. In the case of QTOF, the feature M95T295 was also observed. This feature could be explained as an in-source fragment generated from M170T295, considering the retention time match. This feature was not observed in the data obtained with the Q Orbitrap, most likely due to the different source designs.

Structural Elucidation of the Potential Marker

The first step for the structural elucidation was to establish the molecular formula of the marker. For this purpose, the exact masses of both protonated $[M+H]^+$ and deprotonated $[M-H]^-$ ions were extracted from the information processed by XCMS (Table 2). From the positive ionization data, an accurate mass of *m/z* 170.0818 was obtained for the marker, and $C_8H_{12}NO_3$ was established as possible elemental composition of $[M+H]^+$ (mass error 0 ppm). In negative mode, this marker showed an *m/z* 168.0657 corresponding to $C_8H_{10}NO_3$ (mass error of −2.4 ppm). All taken together allowed for the establishment of $C_8H_{11}NO_3$ as elemental composition for the marker. The ionization in both modes as $[M+H]^+$ and $[M-H]^-$ suggested the simultaneous presence of an acidic and a basic moiety in the molecule.

Table 2. Full Scan and Product Ion Scan information of the selected marker for QTOF

	Ionization	Marker	Accurate mass	Error (ppm)	Formula
Scan	ESI+	M170T295	170.0817	0	$C_8H_{12}NO_3$
	ESI-	M168T295	168.0657	-2.4	$C_8H_{10}NO_3$
	Ionization	Marker (CE eV)	Product ion *(m/z)*	Error (ppm)	Formula
Product ion scan	ESI+	M170T295 (20)	95.0493	-4.2	C_6H_7O
			67.0543	-4.5	C_5H_7
	ESI-	M168T295 (20)	124.0758	-3.2	$C_7H_{10}NO$
			96.0472	23.9	C_5H_6NO
			67.0547	-1.5	C_5H_7

As a second step for structural elucidation, MS/MS experiments were carried out at different collision energies in positive and negative ionization modes (Table 2). In positive, a predominant product ion at *m/z* 95.0493 was observed. This ion corresponded with the feature M95T295 observed in the

QTOF, thus confirming that it was produced by in-source fragmentation. The elemental composition of this ion was C_6H_7O (mass error −4.2 ppm); and therefore, it was formed after the neutral loss of $C_2H_5NO_2$. This formula matches with the amino acid glycine suggesting that the marker is a conjugate with glycine. This fact was in agreement with the ionization observed in both modes. The formula of the ion at *m/z* 95.0498 (C_6H_7O) had a double bond equivalent of 3.5 which is indicative of the presence of three unsaturations. When increasing the collision energy, an extra loss of CO was observed (*m/z* 67.0543, C_5H_7 mass error −4.5 ppm) suggesting the presence of a carbonyl group close to the glycine. The resultant ion (C_5H_7) had a double bond equivalent of 2.5 indicative of the presence of either two double bonds or a double bond and a ring. In the last case, a cyclopentene moiety was the most feasible structure for the formula C_5H_7 owing to the stability of the five-member ring structure.

In negative ionization mode, the product ion spectrum was dominated by a loss of CO_2 (*m/z* 124.0758, $C_7H_{10}NO$ mass error −3.2 ppm) (Table 2). These results were indicative of a carboxylic acid moiety. On the basis of this information, 1-CPG was postulated as a feasible structure for the selected marker.

Confirmation of the Proposed Structure

The confirmation of the proposed structure was made by comparison of the product ion spectra of the selected marker with the synthesized 1-CPG. The results are shown in Figure 2. The product ion scan spectra in both ionization modes and the retention times were identical. These results allowed for the ultimate confirmation of the identity of the marker.

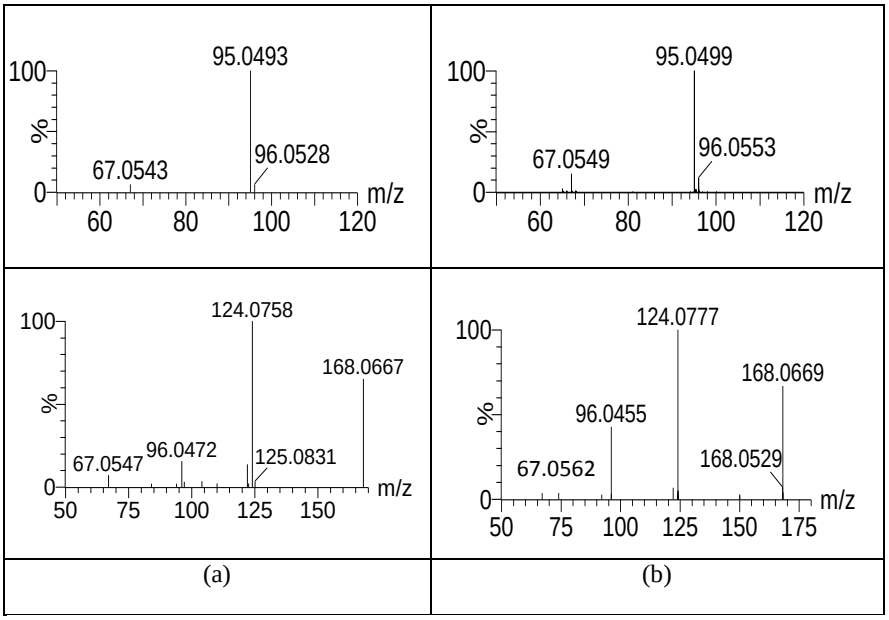

Figure 2. Product ion spectra in both positive (top) and negative (bottom) ionization mode for (a) urinary marker M170T295 and (b) synthesized 1-CPG.

Significance of the Marker and Potential Application

The pathway behind the occurrence of 1-CPG in urine after T cypionate injection was studied and a proposal for the formation of this marker is shown in Figure 3. As a first step, the hydrolysis of T cypionate releases free T and cypionic acid. Similar to fatty acids, cypionic acid might undergo β-oxidation as the main metabolic pathway (30). After activation, this pathway involves two main processes: first the formation of a conjugated double bond and second the oxidative breakdown of this double bond releasing acetyl-CoA. While linear fatty acids suffer sequential β-oxidation reactions until their total degradation, the second β-oxidation for cypionic acid is unable to produce acetyl-CoA due to its cyclic nature. Therefore, the degradation process is stopped after the formation of the second double bond. At this point, the 1-cyclopentenoyl-CoA formed is conjugated with

glycine. Conjugation with glycine is a common metabolic pathway preceding the urinary excretion of several acids like benzoic acid, 3-indoleacrylic acid, or acetylsalicylic acid (31, 32).

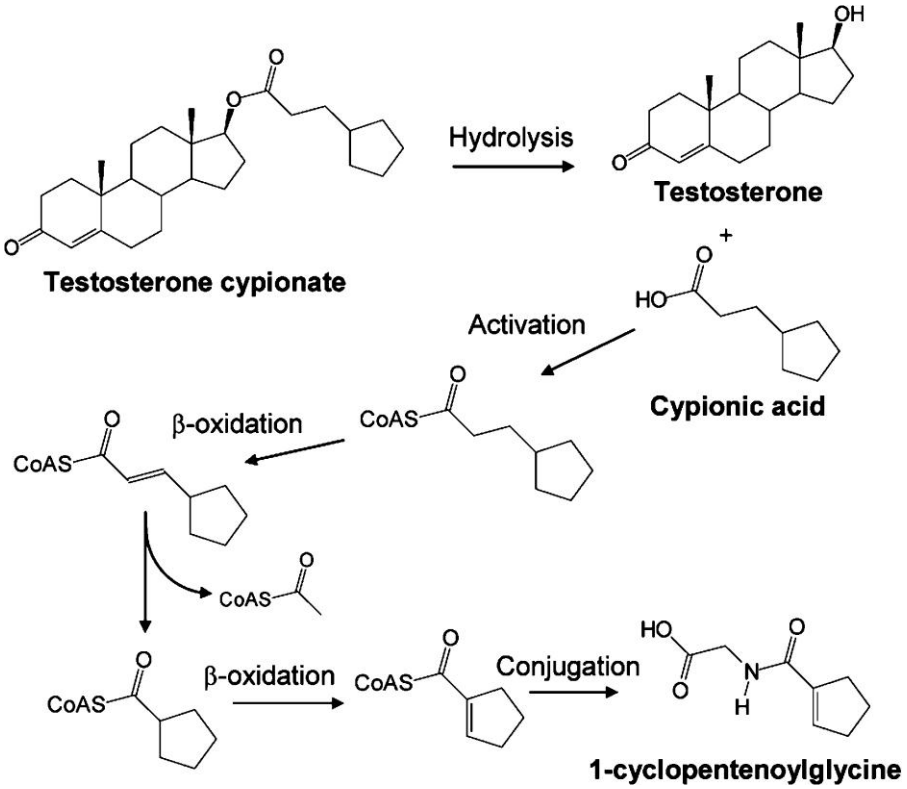

Figure 3. Proposed metabolic pathway involved in the urinary occurrence of 1-CPG after testosterone cypionate injection.

The potential usefulness of 1-CPG for T cypionate screening misuse was also evaluated and compared with the common marker T/E (Figure 4).

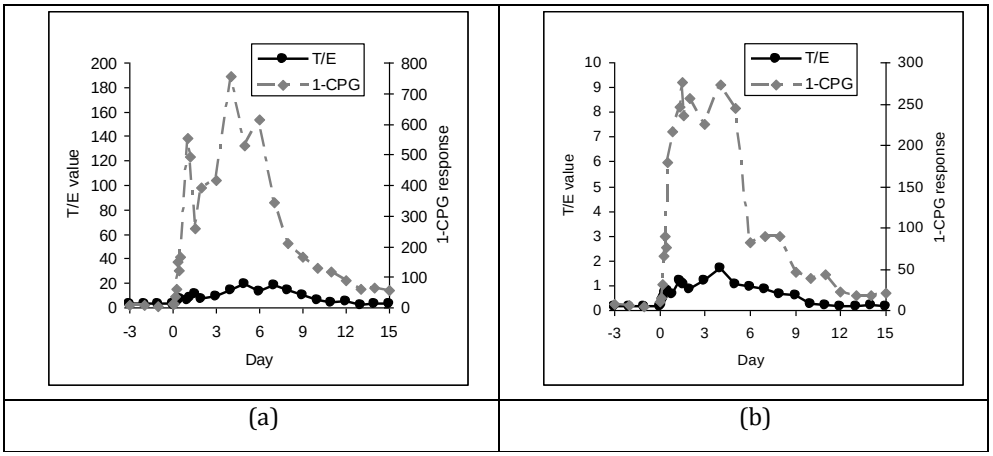

Figure 4. Comparison of the excretion profile of 1-CPG compared with T/E in (a) volunteer with basal T/E = 2.9 and (b) volunteer with basal T/E = 0.16.

The screening of T misuse by the detection of an exogenous compound has obvious advantages since the mere presence of the marker is sufficient to detect a suspicious sample. A small peak was found in every basal sample at the expected retention time (Figure S7). That opens the possibility for 1-CPG to be endogenous. Further research is needed to confirm the endogenous nature of the marker.

Results showed around 50-fold increase of 1-CPG after T administration (Figure 4 and Figure S2) which was substantially higher than the observed for T/E (7-fold). Since the metabolic pathway involved in the excretion of 1-CPG does not contain any glucuronidation step, the occurrence of this marker is irrespective of the polymorphism in the UGT2B17 gene affecting the T/E excretion. Therefore, similar differences were observed in both volunteers.

Whereas T/E was back to basal levels 10–11 days after administration, 1-CPG responses were still elevated in the last sample analyzed. Therefore, the use of 1-CPG improves the retrospectivity of the detection of T cypionate misuse. According to our data, the detection of urinary 1-CPG might be a suitable approach for the screening of T cypionate misuse.

However, the approach also shows limitations. The first one is the fact that other drugs are commercialized as cypionate esters and a similar pathway is expected to be present. Therefore, the urinary detection of 1-CPG is not specific of T cypionate misuse and its detection might be only useful as a screening strategy. A subsequent confirmation process via the currently applied gas chromatography combustion isotope ratio mass spectrometry (GC-C-IRMS) procedures is compulsory. This situation is comparable with the current strategy based on GC-MS(/MS) quantification of some EAAS for screening and ulterior confirmation by GC-C-IRMS. On the other hand, T is also commercialized as other esters, like undecanoate, decaoate, isocaproate, phenylpropionate, propionate, or enanthate and the approach will be not suitable to detect them. Despite some limitations, untargeted metabolomics appears as a suitable tool for the in-depth study of potential specific markers for other T preparations. The approach presented in this work is innovative and opens new possibilities in the field of doping control analysis. It might complement the current screening for T misuse or the direct detection of T esters which had been proposed long ago as a way to screen for T abuse (33, 34).

Conclusions

The usefulness of untargeted metabolomics for doping control analysis has been evaluated. The selection of an adequate procedure, that is, sample treatment, and analytical and data-treatment parameters, is of great importance in an untargeted strategy like that applied in this work. A key aspect of sample treatment is the absence of preconcentration and cleanup steps, which allows for the preservation of all analytes present in the sample. However, alternative markers at low concentration levels might be underestimated using this approach and they might be discovered only after previous preconcentration of the samples.

Urine samples collected before and after T administration were correctly separated by multivariate methods, giving as a result the same marker of T misuse using two HRMS analyzers. Both instruments seemed equally efficient for untargeted metabolomics and both were suitable for searching unknown compounds in the doping control field. These results evidenced the robustness of the methodology applied in the present work.

The strategy followed included the whole set of samples from all volunteers together and considered samples collected up to 9 days after T cypionate administration within the same group (treated). Thus, only those markers which are not affected by individual metabolism and which were still detectable after long periods are picked out. The satisfactory results of this study open novel alternatives in the data treatment for the discovery of new markers. On one hand, the comparison of samples of a single individual might lead to the discovery of new markers to be included in the ABP. On the other hand, a comparison between samples collected before and just after administration would also reveal markers for short-term administration. Additionally, it is worth noticing that the application of a similar approach to

samples collected after T administration in other forms (gel, oral) might reveal the presence of additional and suitable markers for the detection of this misuse.

This study confirms the suitability of state-of-the-art MS instrumentation for the development of untargeted metabolomics in doping control analysis. The developed approach allows for the detection of possible markers with the common bottleneck of the structure identification, a task that is facilitated by performing an in-depth study of the MS(/MS) fragmentation of the compound. Even so, there are still some challenges before the marker is ready for routine use. The most important is related to the specificity of the identified substance as a marker for the doping agent misuse. The concentration of the ideal marker should vary after the administration of the doping agent is irrespective of the administration form whereas it should remain constant under other hypothetical situations (including the administration of non-prohibited substances). More research is required to demonstrate the usefulness of the marker. Then, it might be added into current screening methods in order to minimize the resources used by the laboratories. The implementation of a new marker for doping control analysis implies a long way in which untargeted metabolomics might be seen as the first step.

Acknowledgements

The authors acknowledge the financial support of the Ministry of Education and Science, Spain (Project DEP2011-28573-C02-01/02) and WADA (Project 14A29OP). The authors from University Jaume I also acknowledge the support from Generalitat Valenciana (Research Group of Excellence Prometeo/2009/054; PrometeoII/2014/023; ISIC EnviFood 2012/016). M. Raro is also grateful to the Ministry of Economy and Competitiveness of Spain for her predoctoral grant and for the financial support for the research stay in Belgium. The Spanish Health National System is acknowledged for O. J. Pozo's contract (Grant MS10/00576).

References

1. Haring, R. J. Endocrinol. 2012, 215, 3– 16

2. Moco, S.; Bino, R. J.; De Vos, R. C. H.; Vervoort, J. TrAC, Trends Anal. Chem. 2007, 26, 855– 866

3. Díaz, R.; Pozo, O. J.; Sancho, J. V.; Hernández, F. Food Chem. 2014, 157, 84–93

4. Rijk, J. C. W.; Lommen, A.; Essers, M. L.; Groot, M. J.; Van Hende, J. M.; Doeswijk, T. G.; Nielen, M. W. F. Anal. Chem. 2009, 81, 6879– 6888

5. Roux, A.; Xu, Y.; Heilier, J.-F.; Olivier, M.-F.; Ezan, E.; Tabet, J.-C.; Junot, C. Anal. Chem. 2012, 84, 6429– 6437

6. Cevallos-Cevallos, J. M.; Reyes-de-Corcuera, J. I.; Etxeberria, E.; Danyluk, M. D.; Rodrick, G. E. Trends Food Sci. Technol. 2009, 20, 557– 566

7. Glauser, G.; Veyrat, N.; Rochat, B.; Wolfender, J.-L.; Turlings, T. C. J. J. Chromatogr A 2013, 1292, 151– 159

8. Mamas, M.; Dunn, W. B.; Neyses, L.; Goodacre, R. Arch. Toxicol. 2011, 85, 5–17

9. Armitage, E. G.; Rupérez, F. J.; Barbas, C. TrAC, Trends Anal. Chem. 2013, 52, 61– 73

10. Kiss, A.; Jacquet, A.-L.; Paisse, O.; Flament-Waton, M.-M.; de Ceaurriz, J.; Bordes, C.; Gauvrit, J.-Y.; Lantéri, P.; Cren-Olivé, C. Talanta 2011, 83, 1769–1773

11. Reichel, C. Forensic Sci. Int. 2011, 213, 20– 34

12. Boccard, J.; Badoud, F.; Jan, N.; Nicoli, R.; Schweizer, C.; Pralong, F.; Veuthey, J.-L.; Baume, N.; Rudaz, S.; Saugy, M. Bioanalysis 2014, 6 (19) 2523–2536

13. World Anti-Doping Agency. (2013) Antidoping testing figures-Sport Report, https://wada-main-prod.s3.amazonaws.com/resources/files/WADA-2013-Anti-Doping-Testing-Figures-LABORATORY-REPORT.pdf (accessed March 5, 2015).

14. Donike, M.; Bärwald, K.-R.; Klostermann, K.; Schänzer, W.; Zimmermann, J. Nachweis von exogem Testosteron. In Sport: Leistung und Gesundheit; Heck, H.; Hollmann, W.; Leisen, H.; Rots, R., Eds.; Deutscher Artze-Verlag: Köln, Germany, 1983; pp 293– 300.

15. Starcevic, B.; Butch, A. Clin. Chem. 2008, 54 (12) 1945– 1947

16. Kicman, A. T. Br. J. Pharmacol. 2008, 154 (3) 502– 521

17. Robinson, N.; Saugy, M.; Vernec, A.; Sottas, P.-E. Clin. Chem. 2011, 57 (6) 830– 832

18. Fabregat, A.; Pozo, O. J.; Marcos, J.; Segura, J.; Ventura, R. Anal. Chem. 2013, 85 (10) 5005– 5014

19. Fabregat, A.; Kotronoulas, A.; Marcos, J.; Joglar, J.; Alfonso, I.; Segura, J.; Ventura, R.; Pozo, O. J. Steroids 2013, 78 (3) 327– 336

20. Van Renterghem, P.; Van Eenoo, P.; Sottas, P. E.; Saugy, M.; Delbeke, F. Clin. Endocrinol. 2011, 75 (1) 134– 140

21. Van Renterghem, P.; Sottas, P. E.; Saugy, M.; Van Eenoo, P. Anal. Chim. Acta 2013, 768, 41– 48

22. Kiss, A.; Lucio, M.; Fildier, A.; Buisson, C.; Achmitt-Kopplin, P.; Cren-Olivé, C. PLoS One 2013, 8 (9) e74584

23. Scripps Centre for Metabolomics. XCMS Online, available from https://xcmsonline.scripps.edu/ Last accessed June 13, 2014.

24. Schmidt, M. T.; Handschuh, L.; Zyprych, J.; Szabelska, A.; Olejnik-Schmidt, A. K.; Siatkowski, I.; Figlerowicz, M. Acta Biochim. Pol. 2011, 58, 573– 580

25. Fabregat, A.; Marcos, J.; Garrostas, L.; Segura, J.; Pozo, O. J.; Ventura, R. J. Steroid Biochem. Mol. Biol. 2014, 139, 192– 200

26. Deventer, K.; Pozo, O. J.; Verstraete, A. G.; Van Eenoo, P. TrAC, Trends Anal. Chem. 2014, 55, 1– 13

27. Naz, S.; Vallejo, M.; García, A.; Barbas, C. J. Chromatogr A 2014, 1353, 99– 105

28. Dunn, W. B.; Wilson, I. D.; Nicholls, A. W.; Broadhurst, D. Bioanalysis 2012, 4, 2249– 2264

29. Boccard, J.; Rutledge, D. N. Anal. Chim. Acta 2013, 769, 30– 39

30. Schulz, H.; Kunau, W.-H. Trends Biochem. Sci. 1987, 12, 403– 406

31. Gregus, Z.; Fekete, T.; Halászi, E.; Klaassen, C. D. Drug Metab. Dispos. 1996, 24, 682– 688

32. Smith, H. G.; Smith, W. R. D.; Jepson, J. B.; Sorenson, K. Biochem. Pharmacol. 1970, 19, 1689– 1693

33. Shackleton, C. H.; Chuang, H.; Kim, J.; de la Torre, X.; Segura, J. Steroids 1997, 62, 523– 9

34. Peng, S. H.; Segura, J.; Farre, M.; González, J. C.; de la Torre, X. Steroids 2002, 67, 39– 50

SUPPORTING INFORMATION

EXPERIMENTAL

S1. QTOF calibration and lock mass

Calibration of the mass-axis from *m/z* 50 to 1000 was conducted daily with a 1:1 mixture of 0.05 M NaOH: 5% (v/v) HCOOH diluted (1:25) with water/acetonitrile (ACN) (20:80 v/v).

For automated accurate mass measurement, the lock-spray probe was employed, using as lockmass Leucine-Enkephalin (10 mg/L) in ACN:water (50:50) and 0.1% HCOOH, pumped at 20 µL/min through the lock-spray needle. $[M+H]^+$ (*m/z* 556.2771) and $[M-H]^-$ (*m/z* 554.2615), were used for recalibrating the mass axis in positive and negative ionization modes respectively.

S2. Purification of synthesized 1-CPG

For the purification of 1-CPG, the reaction's solution was directly injected to a semi-preparative HPLC (Waters Prep LC 4000 system) equipped with an Atlantis® dC18 OBDTM column (5 µm, 19 mm × 150 mm). The mobile phases used were (A): 0.01% trifluoroacetic acid (TFA) in H_2O and (B): 20:80:0.01, v/v/v ACN–H_2O–TFA and the selected gradient changed as follow: 0% B for 5 min, 0% to 35% B in 35 min.

S3. Determination of 1-CPG by LC-MS/MS

S3.1. Instrumentation

Chromatographic separation was performed by an Acquity UPLC instrument (Waters Associates, Milford, Massachusetts, USA). An Acquity UPLC® BEH C18 1.7 µm 2.1x100 mm column (Waters Associates) was used for the separation. Water (A) and methanol (B) both with 0.01 % HCOOH and 1 mM ammonium formate were selected as mobile phase solvents. During the gradient program used, the percentage of organic solvent changed as following: 0 min, 1%; 9 min, 30%; 10 min 95%; 11 min; 95%; 12 min 1%; 14 min; 1%. The injection volume was 10 µL and the flow rate 0.3 mL/min.

The detection was performed with a triple quadrupole (Quattro Premier XE, Waters) mass spectrometer equipped with an orthogonal Z-spray-electrospray ionization source (ESI). The desolvation gas flow was set to approximately 1200 L/h and the cone gas flow to 50 L/h. Nitrogen was used as drying and nebulising gas. A cone voltage of 15 V and a capillary voltage of 3.0 kV were used in positive ionization mode. The nitrogen desolvation temperature was set to 450 ºC and the source temperature to 120 ºC. The monitoring and quantification of 1-CPG was performed using the transition 170 → 95 with a collision energy of 10 eV.

S3.2. Sample preparation

A volume of 100 µL of urine was mixed with the same volume of acetic acid 1M. 10 µL of the diluted sample were directly injected into the LC-MS/MS system.

FIGURE S-1

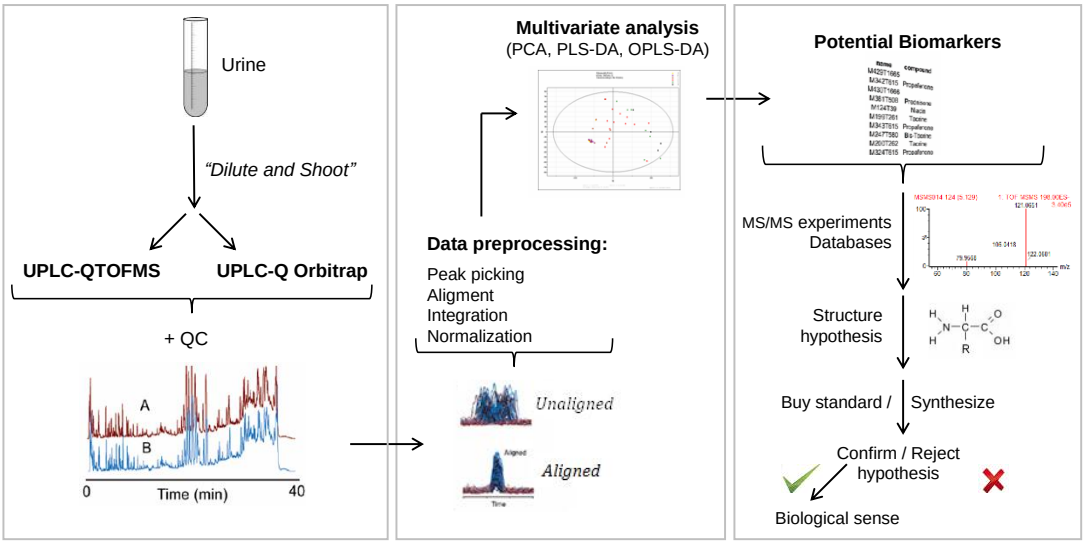

a) Analytical procedure b) Metabolomic approach c) Marker(s) elucidation

Simplified workflow of the employed strategy, schematized in three blocks: a) the analytical procedure applied, b) the metabolomic approach followed and c) the work carried out for the structural identification of the potential markers.

FIGURE S-2

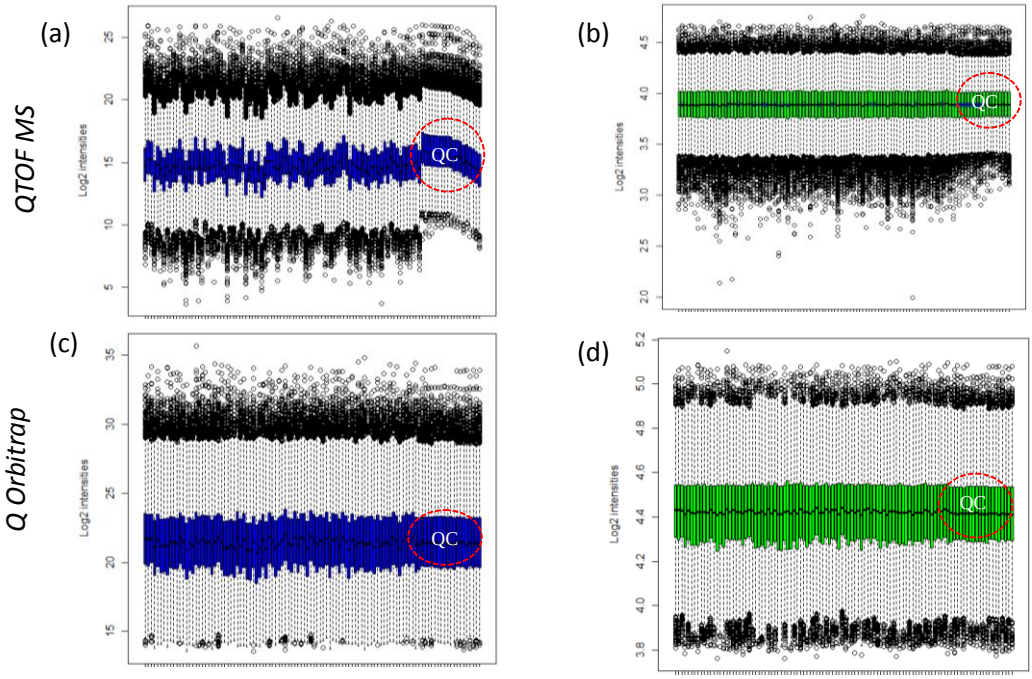

Box plots of the Log_2 of the intensities of the components of the different samples in positive mode a) QTOF MS data before normalization (blue), b) QTOF MS data after normalization (green), c) Q Orbitrap MS data before normalization (blue), d) Q Orbitrap MS data after normalization (green).

FIGURE S-3

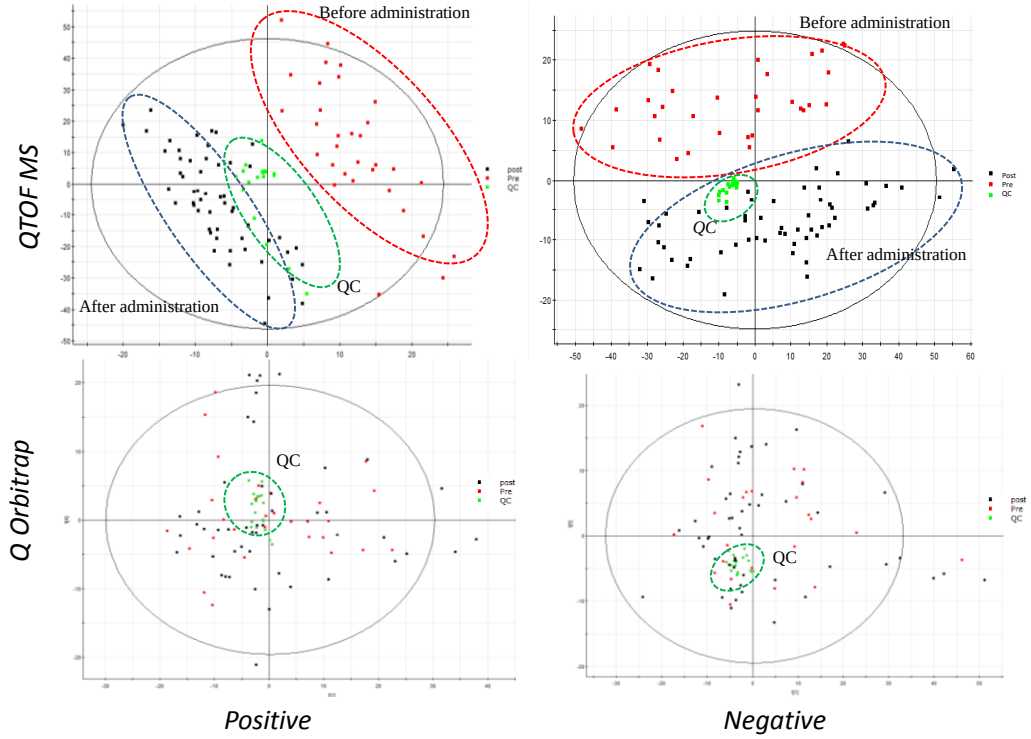

Principal Component Analysis (PCA) score plots from QTOF and Q Orbitrap MS in positive and negative ionization modes. Groups of samples before administration are highlighted in a red circle, samples after administration in blue and QC in green.

FIGURE S-4

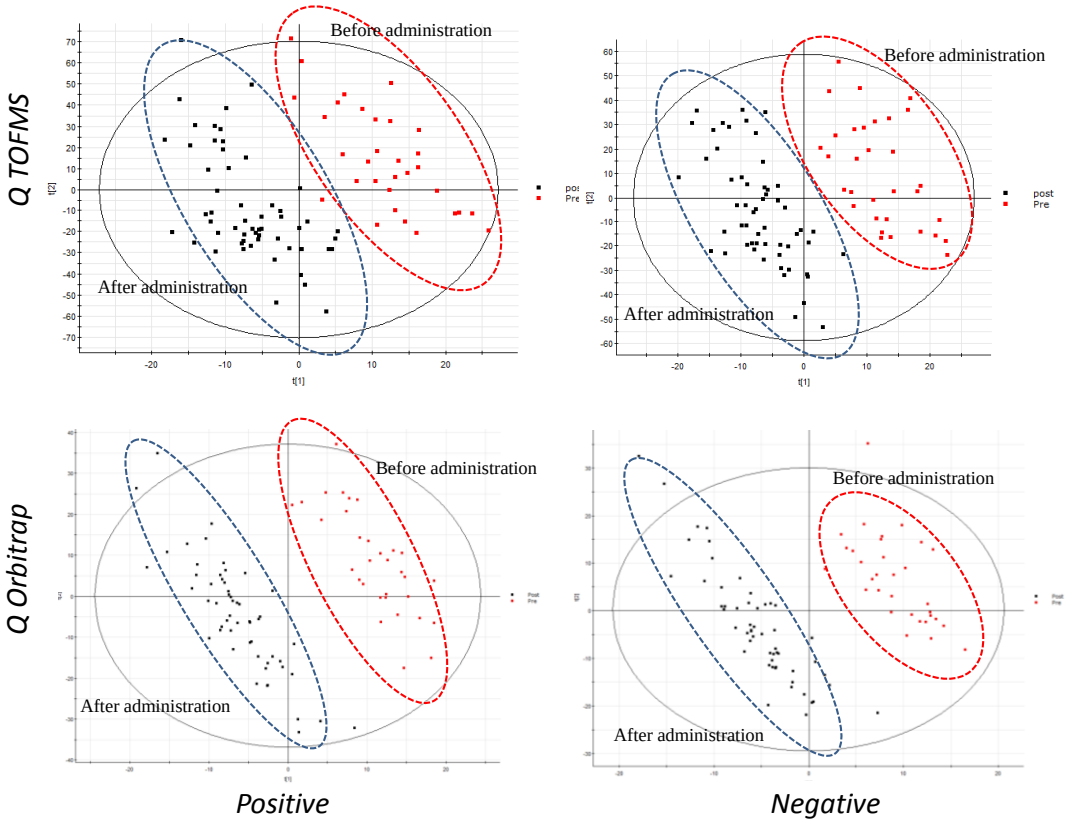

Partial Least Square Discriminant Analysis (PLS-DA) score plots from QTOF and Q Orbitrap MS in positive and negative ionization modes. Groups of samples before administration are highlighted in a red circle and samples after administration in blue.

FIGURE S-5

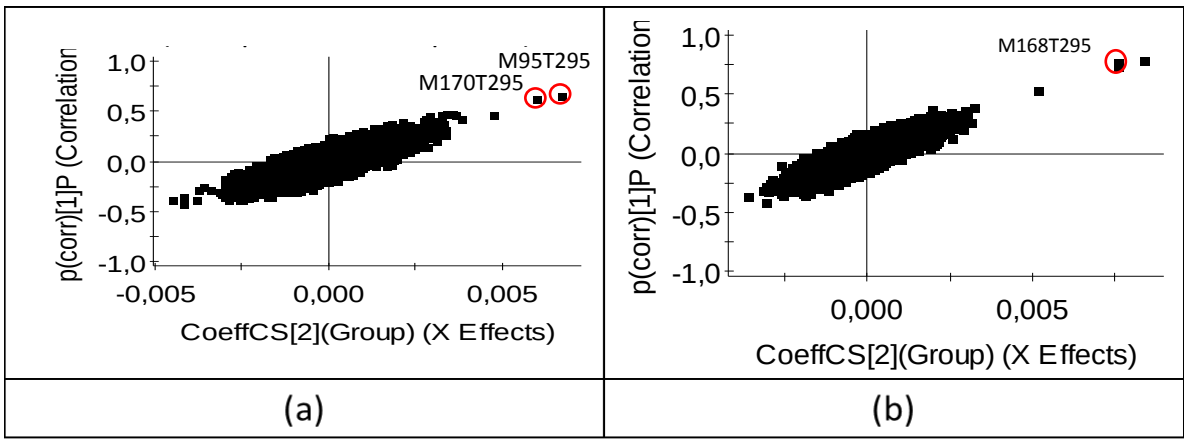

OPLS-DA S-Plot for QTOF MS in (a) positive ionization mode and (b) negative ionization mode. Significant markers (*m/z* and RT) are highlighted.

FIGURE S-6

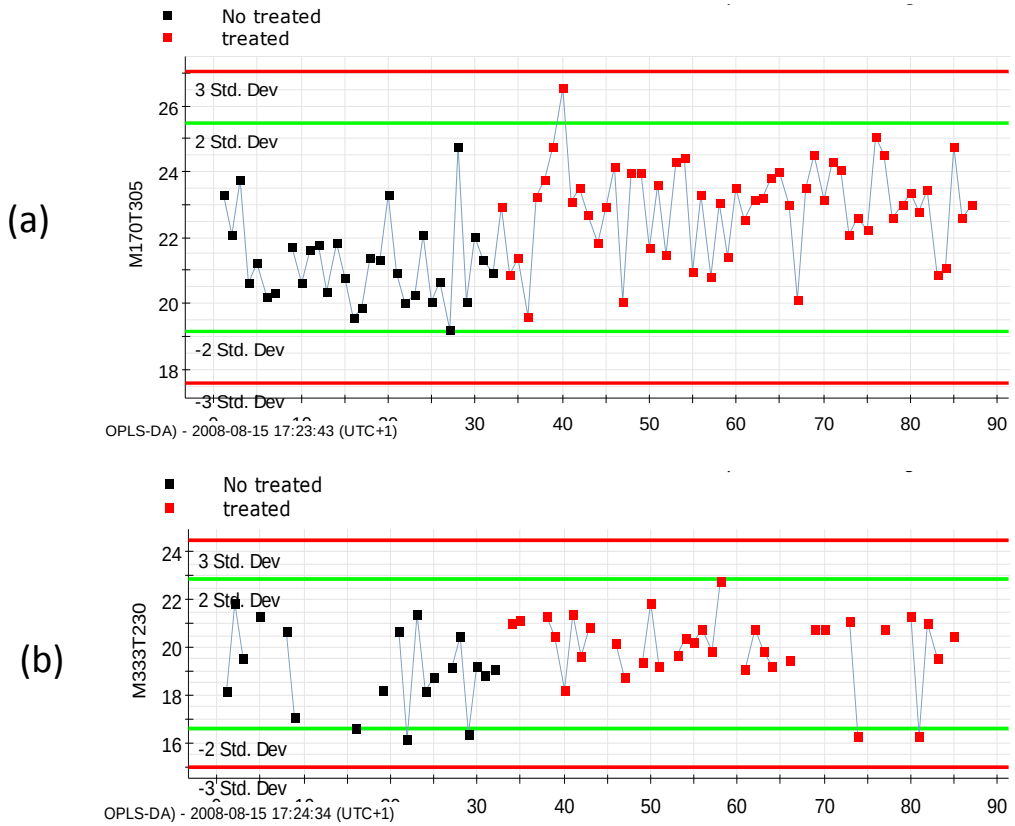

Variable trend plots from Q Orbitrap data. Features a) M170T305 and b) M333T230. Samples before administration are represented in black points whereas samples after administration are represented in red.

FIGURE S-7

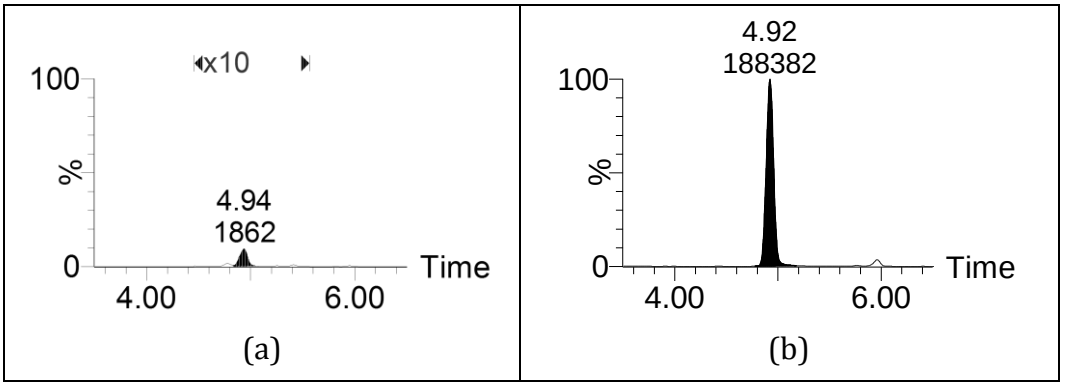

LC-MS/MS chromatograms for the determination of 1-CPG (a) sample collected 2 days before testosterone cypionate administration and (b) sample collected 8 days after testosterone cypionate administration.

III.3. Artículo científico 5

Evaluation of potential urinary markers for recombinant human growth hormone misuse by untargeted metabolomics

Montse Raro[a], Ramon Díaz[a], Juan Vicente Sancho[a], Elena Pitarch[a], Félix Hernández[a], Josep Marcos[b,c], Jordi Segura[b,d], Jaume Bosch[b], Beatriz G. de la Torre[d,e], Ricardo Gutiérrez-Gallego[b,f,g], Óscar J. Pozo[b]

[a]Research Institute for Pesticide and Water, University Jaume I, Av. Sos Baynat S/N, 12071 Castellón, Spain.

[b] Bioanalysis Research Group. IMIM, Hospital del Mar, Dr. Aiguader 88, 08003 Barcelona, Spain

[c] Toxicology Department, Labco Diagnostics, Verge de Guadalupe 18, 08950 Esplugues de Llobregat, Spain

[d] Bioanalysis Pharmacology and Proteomic Group, University Pompeu Fabra, Barcelona, Spain

[e] Catalysis and Peptide Research Unit, School of Health Sciences, University of KwaZulu-Natal, Durban 4001, South Africa

[f] Molecular Medicine Program, Department of Experimental and Health Sciences, Pompeu Fabra University, Dr. Aiguader 88, 08003 Barcelona, Spain

[g] Anapharm Europe, Encuny 22, 08038 Barcelona, Spain

ABSTRACT

Recombinant human growth hormone (rhGH) is an endogenous peptide that stimulates muscle mass growth and strength. Aside from its medical use, rhGH has been employed by some athletes and bodybuilders in order to have an unfair advantage. It is included in the World Anti-Doping Agency list of prohibited substances due to its adverse effects, although detection of illicit use remains challenging. Currently, there is no marker for the urinary screening of rhGH misuse. In the present work, hybrid quadrupole time of flight mass spectrometry coupled to ultra-high performance liquid chromatography has been used for the discovery of new biomarkers for the rhGH misuse. Using a dedicated excretion study, applied to 9 healthy volunteers, a total of 234 samples were examined using different sample treatments and chromatographic conditions. The data obtained after these orthogonal analytical processes were processed by means of untargeted metabolomic strategies, using XCMS application and multivariate analysis, to unveil biomarkers which enhanced differences between samples before and after rhGH administration. Two compounds were selected as candidate markers for rhGH urinary screening; one increased and the other decreased after the administration. A tentative identification was made for the two markers based on the evaluation of their MS/MS spectra. An eight carbon atoms carboxylic acid linked to glycine was proposed for the compound that increased its concentration after rhGH administration. Carnitine was proposed for the marker which suffered the opposite effect. Assingments for both compounds were confirmed by comparison with reference material. The usefulness of these markers for doping control analysis was evaluated. The ratio between both markers increased more than 140 fold 24 h after the last rhGH administration showing its potential application for the urinary screening of rhGH misuse. In this way, a new

strategy could be available in the near future for recombinant human growth hormone misuse in doping control laboratories.

Keywords: metabolomics, UHPLC-(Q)TOF MS, HILIC, recombinant human growth hormone, doping

1. INTRODUCTION

The human growth hormone (hGH) is a natural peptidic hormone family and its most abundant form consists in a polypeptide chain of 191 amino acids with a molecular weight of 22 kDa. It is secreted by the pituitary gland where it is regulated by two hypothalamic hormones; one which stimulates the secretion (growth hormone releasing hormone, GHRH) and other which inhibits secretion (somatostatin) (Ehrnborg et al. 2000). Additionally, hGH may be released by action of the natural peptide ghrelin when acting on the GHSR1a receptor (Kojima et al. 2001). In Thirty years ago, the recombinant form of hGH was developed by means of genetic engineering. This recombinant hGH (rhGH), with an identical sequence to the natural 22 kDa hormone, has been used with good results in patients which present GH deficiency (Saugy et al. 2006, Strobl and Thomas 1994). The rhGH administration has been proven to increase muscle mass, reduce fat mass and improve physiological functions (Powrie et al. 2007). Due to these anabolic properties, its misuse has been suspected in athletes and bodybuilders and so-called positive cases have been detected. This is of concern because of the undesirable effects on the sports ethics and also because the long-term administration may be dangerous to athletes health (Jenkins 1998; Holt 2013). The use of rhGH in sports was first prohibited by the International Olympic Committee (IOC) in 1989 and it currently appears

on the World Anti-Doping Agency list of banned substances (WADA, *Prohibited List 2016*).

The detection of exogenous rhGH administration is a challenge in sports. The routinary method called *Isoform Differential Immunoassays*, is used to distinguish between the proportions of hGH isoforms found under normal physiological conditions and those found after rhGH injection. The normal composition of hGH consists on a mixture of isoforms (18, 20, 22, glycosylated 23 18 kDa, deamidated variants, homo- and heteromultimeric variants, etc.) in different proportions (Baumann 2009), whereas rhGH is present only in the 22 kDa monomeric form. Thus, its administration causes an increase of the 22 kDa form and a time-dependent reduction of the others, altering the natural ratios (Wu 1999, WADA *Technical Document TD2015GH*, Bosch et al. 2012). This test was first introduced at the 2004 Summer Olympic Games held in Athens, Greece. Due to its short half-life, other strategies denoted as the indirect method have been developed. These indirect methods relies on the constantly increasing sensitivity and robustness of liquid chromatography tandem mass spectrometry techniques (LC-MS/MS) (Thevis and Schänzer, 2007; Thevis et al. 2011) or on the specific monitoring of secondary biomarkers like insuline-like growth factor 1 (IGF-1) or procollagen type III N-terminal propeptide (P-III-NP) (Bosch et al. 2012). However, all these approaches require invasive sampling strategies as they require blood/plasma to meet the required sensitivity. Although hGH in urine is found only in small quantities (less than 1% of what is encountered in circulation), the development of urine-based detection methods for hGH is starting to be explored (Saugy et al. 2006; WADA, *The human growth hormone*, Bosch et al. 2013), but currently there is no approved method for the screening of rhGH in urine.

In this context, metabolomic–based approaches seem to be promising not only in the research of the physiological effects related to rhGH administration but also in the detection of biomarkers for its misuse in sports. Metabolomics is becoming a very useful tool for the discovery of new metabolites/markers. It consists in the measurement of low-weight metabolites of a cell, tissue or body fluid, produced through metabolic processes in organisms (Haring 2012) and that are responsive to ingestion c.q. administration of a particular compound, or may be affected by pathological conditions. Metabolomic profiling has been used in a wide variety of applications deeply described in literature; e.g. profiling of individual's response to drug treatments (Roux et al. 2012), applications in food sciences (Díaz et al. 2014, Cevallos-Cevallos et al. 2009), in plant metabolomics (Glauser et al. 2013) and in clinical research (Mamas et al. 2011, Armitage et al. 2013). More recently, some studies have been directed towards doping control, showing that omics-based methods are ideal platforms for the discovery of biomarkers of abuse of different substances (Kiss et al. 2011, Kiss et al. 2013, Reichel 2011). A recent study carried out by our research group described the usefulness of untargeted metabolomics in the detection of alternative markers for testosterone misuse (Raro et al. 2015).

Due to their high resolution, mass accuracy and full-spectrum acquisition capabilities at high sensitivity, ultra-high performance liquid chromatography (UHPLC) combined with high resolution mass (HRMS) analyzers such as Orbitrap, TOF, hybrids quadrupole-time of flight (QTOF MS) or quadrupole-Orbitrap (Q Orbitrap) are very suitable to develop metabolic profiling methods of complex biological matrices like urine (Rijk et al. 2009).

In relation to GH, a limited number of studies have been carried out, but only focused on recombinant equine growth hormone (reGH) (Boyard-Kieken et al. 2011a, Boyard-Kieken et al. 2011b) applying metabolomic tools and LC-HRMS measurements. These studies compare, on one hand, different chromatographic columns and, on the other hand, different biological matrices, achieving for the identification of four endogenous markers (glucose, L-carnitine, acetylcarnithine and δ-12-prostaglandin-J2) for the detection of reGH misuse.

The aim of this investigation is explore the use of metabolomics for the fight against doping and bring the analytical strategies in this field for extremely complex category of protein and peptide hormones to a new level. We focused on the development of an analytical methodology for detecting rhGH abuse using urine, rather than blood and with a prolonged window of opportunity. For this purpose, state-of-the-art analytical techniques were used and data generated were treated with statistical multivariate analysis. In order to have a comprehensive overview of potential metabolites, the urine samples were analyzed using two complementary LC tools, reverse-phase liquid chromatography (RP-LC) and hydrophilic interaction liquid chromatography (HILIC). This strategy allows for the retention of analytes within a wide range of polarities (Spagou et al. 2010, Idborg et al. 2005).

2. MATERIALS AND METHODS

2.1. Reagents and chemicals

HPLC-grade water was obtained by purifying demineralised water in a Milli-Q plus system from Millipore (Bedford, MA, USA). HPLC-grade methanol (MeOH), Acetonitrile (ACN), sodium hydroxide (>99%), ammonium acetate

(NH_4Ac) and formic acid (98-100%) were acquired from Scharlab (Barcelona, Spain). Leucine-Enkephalin, used as the lock mass and carnitine were purchased from Sigma Aldrich (St. Louis, MO, USA).

For synthesis of the different octenoyl-glycine, glycine, 2-octenoic acid, 3-octenoic acid and 7-octenoic acid, Diisopropylethylamine (DIEA), diisopropylcarbodiimide (DIPCI) were obtained from Sigma-Aldrich. Fmoc-Gly-OH and 2-Chlorotrityl chloride resin (2-CTC resin) were from Iris-Biotech. Dichlormethane (DCM), Dimethylformamide (DMF), Trifluoroacetic acid (TFA) and Piperidine were purchased from Carlo Erba –SDS.

2.2. Instrumentation

Acquity ultra-performance liquid chromatography (UPLC) system (Waters, Milford, MA, USA) was interfaced to a Xevo G2 QTOF mass spectrometer (Waters Micromass, Manchester, UK) using an orthogonal Z-spray electrospray (ESI) interface. Two different chromatographic conditions (RPLC and HILIC) were used in this work. For RPLC, the chromatographic separation was performed using an Acquity UPLC BEH C18 column (1.7 µm, 2.1 x 100 mm) from Waters, using a flow rate of 0.5 mL/min. The mobile phases used were (A) H_2O and (B) MeOH, both with 0.01% (v/v) HCOOH. The percentage of MeOH was linearly increased as follows: 1 min, 2%; 3 min, 15%; 6 min, 50%; 9 min, 95%; 10 min, 95%; 10.01 min, 2% and 12 min, 2%. The total run time was 12 min and the injection volume was 20 µL. On the other hand, HILIC separation was performed using an Acquity UPLC BEH Amide column (1.7 µm, 2.1 x 100 mm) from Waters, using a flow rate of 0.3 mL/min. The mobile phases used were (A) 95% ACN 5% H2O NH_4Ac 10 mM and (B) H2O NH4Ac 10 mM. The percentage of phase B was linearly increased as follows: 1.5 min, 2%; 2.5 min, 15%; 6 min, 50%; 7.5 min, 75%;

7.51 min, 2% and 9.50 min, 2%. The total run time was 9.5 min and the injection volume was 20 µL.

Nitrogen (Praxair, Valencia, Spain) was used as both drying and nebulizing gas. The desolvation gas flow was set at 1000 L/h. The resolution of the TOF mass spectrometer was ~20,000 at full width half maximum (FWHM) at *m/z* 556. MS data were acquired over a *m/z* range of 50–1200 with a scan time of 0.3 s. Capillary voltages of 0.7 kV and 2.5 kV were used in positive and negative ionization modes, respectively. A cone voltage of 25 V was applied. Argon was used as collision gas (99.995%, Praxair). The desolvation temperature was set to 550 ºC and the source temperature to 120 ºC. The column temperature was set to 40 ºC and the sample compartment to 5 ºC. The same cone voltage and different collision energies (5, 10, 15, 20, 25, 30, 35, and 40 eV) were used for the additional MS/MS experiments.

Calibration of the mass-axis from m/z 50 to 1200 was conducted daily with a 1:1 mixture of 0.05 M NaOH: 5% (v/v) HCOOH diluted (1:25) with water/ACN (2:8 v/v).

For automated accurate mass measurement, the lock-spray probe was employed, using as lockmass Leucine-Enkephalin (2 mg/L) in ACN:water (1:1) and 0.1% HCOOH, pumped at 20 µL/min through the lock-spray needle. Parent ions of Leucine-Enkephalin, [M+H]+ (*m/z* 556.2771) and [M-H]- (*m/z* 554.2615), for positive and negative ionization modes respectively, were used for recalibrating the mass axis.

2.3. Administration study samples

The study was single blind and conducted according to the corresponding international ethics guidelines with permission obtained from

the Ethical Committee of Clinical Research (CEIC) from Parc Salut Mar (n◦ 2009/2510, CEIC-Parc Salut Mar, Barcelona, Spain) and volunteers gave written informed consent.

The study was performed with 9 healthy volunteers in a randomised and controlled fashion. rhGH was administered subcutaneously to 7 volunteers (Genotonorm®, Pfizer) 2 other volunteers were used as controls without drug treatment (blank subjects). The volunteers were recruited applying a number of selection criteria that included a history of normal growth and development and normal analytical values as well as exploratory complementary information performed prior to enrolling in the trial. The characteristics of demographic data were (mean ± SD), age 24.22 ± 2.22 years, weight 76.11 ± 6.07 kg, height 176.56 ± 6.74 cm and BMI 24.4 ± 1.40. Daily administrations of rhGH for 7 days with 0.026 mg /kg/day/person s.c. at 08.00 h in the morning were given and a wash out period of 4 days was included.

Samples were collected daily until nine days after the first administration. Additionally, two spot urine samples were collected 15 days and 21 days after the first administration. Samples were grouped in different classes, one class formed by the control samples and then, one class for each day after the administration. Control samples include samples from volunteers 4 and 7 as well as samples before administration of the rest of the volunteers. For the multivariate analysis, control group was confronted with each day group to obtain the potential markers, as explained below.

2.4. General strategy

A summary of the general workflow that has been followed in this work is shown in Figure 1. The proposed strategy can be divided in four steps:

2.4.1. Sample treatment and data acquisition

The first part consisted on sample treatment and data acquisition. For those samples analyzed under reversed phase conditions, 1 mL of HPLC-grade water was added to the same volume of the urine samples. They were mixed in Vortex for 30 seconds and then centrifuged at 12,000 rpm for 10 min. The supernatant was directly injected into the UHPLC-QTOF MS system in full scan mode under both positive and negative ionization modes. The same procedure was applied for samples injected under HILIC conditions but, in this case, the dilution was performed with ACN. Both groups of samples were randomly injected in order to avoid instrumental drift that could affect the results. Quality control samples (QC) were prepared by pooling identical volumes of all the samples. QCs were injected along the batch, every ten injections to compensate for potential variations in the retention times and responses of the analytes (Dunn et al. 2012) and initially to condition the system. Data was acquired using MassLynx operating software (version 4.1, Waters).

2.4.2. Data pre-processing and multivariate analysis

After acquisition, mass data were pre-processed and multivariate analysis was applied (Figure 1). The raw data (using both ionization modes and both chromatographic systems) were converted to .CDF format using the Databridge application (MassLynx).

The .CDF data were then pre-processed using the XCMS free software for automatic peak detection and retention time alignment (*Scripps Centre for Metabolomics. XCMS online*). A peak picking centWave method was used to locate the masses and continuous wavelet transform (CWT) was applied to find chromatographic peaks using the following parameters: peak width = 5-20 s, S/N threshold = 10, ppm = 15. Subsequently, a density grouping method was used to align retention times. The alignment of the peaks with the same exact mass in all samples was carried out using clusters of peaks that were present in almost all samples with stable intensities.

A table of detected features was generated for each sample defined as m/z (xxx) and retention time in seconds (yyy) with the format *MxxxTyyy*. Then, peak lists were normalized using Loess normalization method (Schmidt et al. 2011) and imported into the EZinfo software (Umetrics, Umea, Sweden) for multivariate analysis. Principal Component Analysis (PCA), Partial Least Squares Discriminant Analysis (PLS-DA) and Orthogonal Partial Least Squares Discriminant Analysis (OPLS-DA) were evaluated after unit variance (UV) scaling.

2.4.3. Marker selection

Results of the OPLS-DA were represented in an S-Plot. Features with a p(corr) > 0.5 were considered as potential markers. Candidates were selected in both upper-right and lower-left quadrants in order to have markers which increase (located in the upper-right quadrant) and decrease (located in the lower-left quadrant) after rhGH administration. A general study of these features regarding peak shape, intensity and factor of increase/decrease between pre and post-administration samples was performed and the results were taken into account for the selection of the marker.

2.4.4. Marker identification

In order to propose a feasible structure for the selected markers, the mass data obtained in full scan acquisition were carefully evaluated. Based on this information, the potential molecular formula of the marker was established. Afterwards, several product ion scans were performed. The molecular formula of each product ion was established and structural properties were associated with the ion/losses observed. A potential structure was proposed for each candidate.

The validity of the proposed structure was confirmed by comparison with commercial reference material when available. Alternatively, the alleged marker was synthesized and employed as reference material.

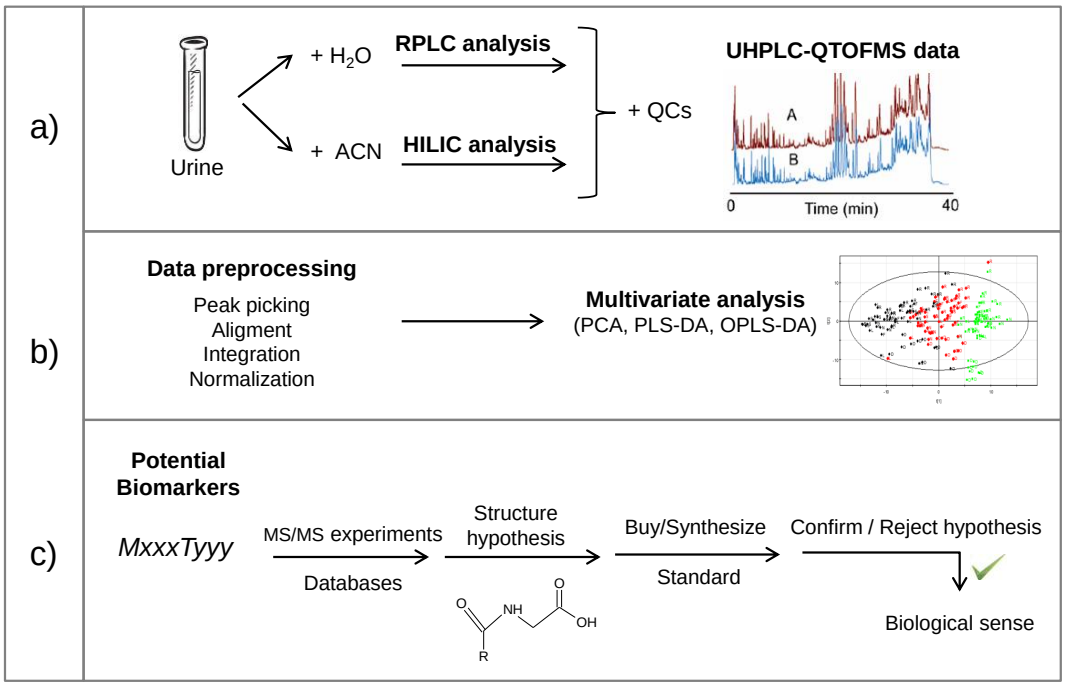

Fig 1. Simplified workflow of the suggested strategy, schematized in three blocks. a) The analytical procedure applied, b) the metabolomic approach followed and c) the work carried out for the structural identification of the potential biomarkers

2.5. Synthesis of different octenoyl-glycine

The general strategy for the synthesis of the different octenoyl-glycine is shown in Figure 2a. Briefly, 2-CTC resin (50 mg) was placed in a 5 mL polypropylene syringe fitted with a polyethylene filter disc. The resin was washed with DMF (3 × 2 mL, 1 min) followed by DCM (3 × 2 mL, 1 min). The coupling of Fmoc-Gly-OH (9 mg, 30 μmol) to the resin was performed in presence of excess of DIEA (30 μL, 180 μmol) dissolved in 0.5 mL DCM after 1 h reacting, MeOH (50 μL) was added for capping unreacted points and allow to react for 30 min, then the Fmoc-Gly-resin was washed with DCM (3 × 2 mL) and DMF (3 × 2 mL). Fmoc removal was carried out by 20% piperidine (2 × 10 min) and Gly-resin was divided in three equal parts. Then the corresponding octenoic acid was incorporated by mean of DIPCI (1:1, 10 equiv, 100 μmol) in DCM and allowed to react for 1 h. Then cleavage of the resin was performed in 2% TFA in DCM during 30 min. After filtration, the solvent was evaporated and the different octenoyl-Gly-OH derivatives were obtained in high purity. The structures of the synthesized material are given in the Figure 2b.

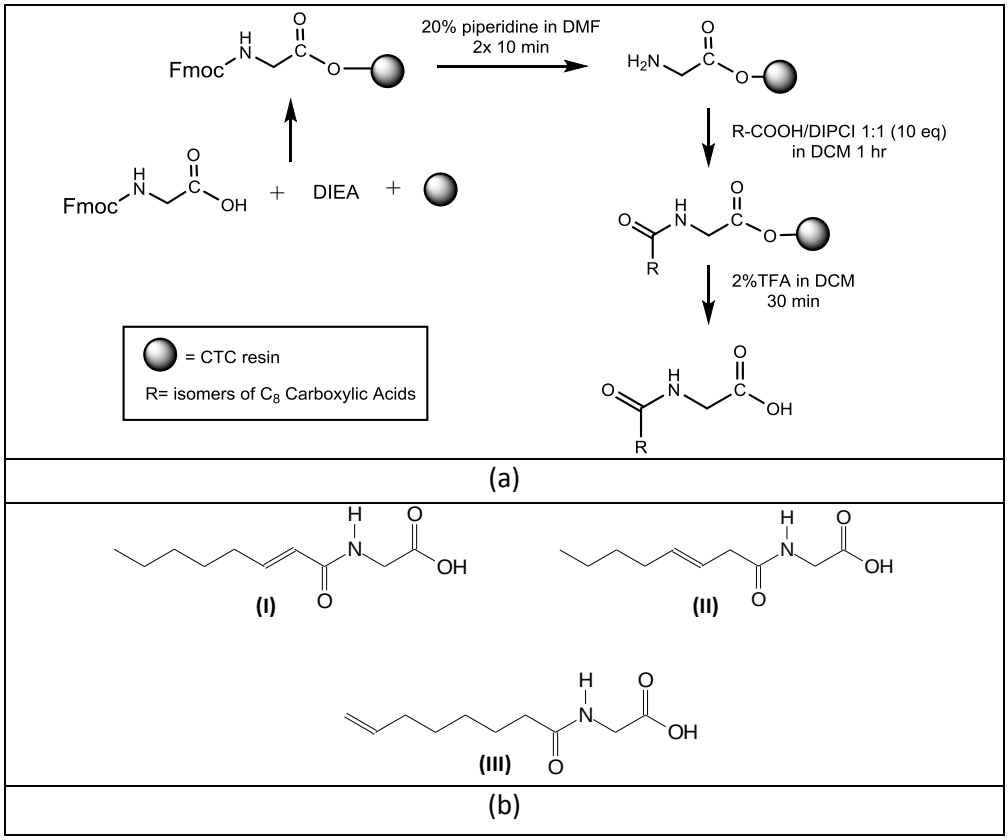

Fig 2. a) General scheme for the synthesis of octenoyl-glycine. b) Chemical structures of the synthesized material

3. RESULTS AND DISCUSSION

Sample treatment and liquid chromatography (LC) separation were scrutinized in order to maximize the number of detectable compounds. To this aim, samples were subjected to a simple treatment using a two-fold dilution with water or acetonitrile, and two complementary LC columns were used for either dilution to broaden the possibilities for better chromatographic retention of compounds of a wide range of polarities.

3.1. Sample treatment, data pre-processing and multivariate analysis

Two LC approaches based on different types of stationary phases were tested for all the samples: (i) RPLC, for detection of semi-polar and non-polar compounds and (ii) HILIC, for the most polar ones.

Urine samples were diluted 1:1 with water for RPLC analysis and with acetonitrile for HILIC, and then all samples were injected into the system in both positive and negative ionization modes (ESI+ and ESI–).

The obtained data were pre-processed by XCMS. More than 10,000 individual peaks in RPLC and around 3,000 individual peaks in HILIC were detected in each chromatogram. Data were first normalized to correct small variations between samples caused by the drift of the instrument or changes in urine concentration due to differences in the excreted volumes. The median intensities were more stable after applying the normalization (Figure S1, supplementary information), emphasizing the absolute requirement for data normalization prior to any further interpretation.

Once data were normalized, they were analyzed by Principal Component Analysis (PCA) for a non-supervised visualization of the results. An adequate behaviour of the QC samples was perfectly clustered in the center of the score plot, as a good representation of all the samples. Then, in order to extract the relevant information in the data, a supervised PLS-DA was applied employing the intake day as class information. At this point, a good separation between samples of different volunteers was achieved together with a good separation between control and post-administration samples. Results for PCA and PLS-DA, in negative ionization mode, for both type of analysis (RPLC and HILIC), are shown in Figures S2 and S3

(supplementary information). As it can be seen in the RPLC PCA (Figure S2a, colored by intake day and annotated by volunteer), the main variation in the model was explained by the differences between volunteers, which was reasonable and expected actually.

The last model applied was the Orthogonal Partial Least Square Discriminant Analysis (OPLS-DA), which allowed the identification of several peaks that were either elevated (upper right quadrants in S-Plots) or depressed (lower left quadrants in S-Plots) as a result of the rhGH administration. We confronted control class (samples collected before administration, excluding blank subjects) with the different days after administration to generate a series of S-Plots that helped us to find the best biomarkers. More relevant differences were obtained in the S-Plot *Control vs Day 8*. In Figure 3, the S-Plots obtained in negative and positive ionization modes after RPLC and HILIC analysis are shown.

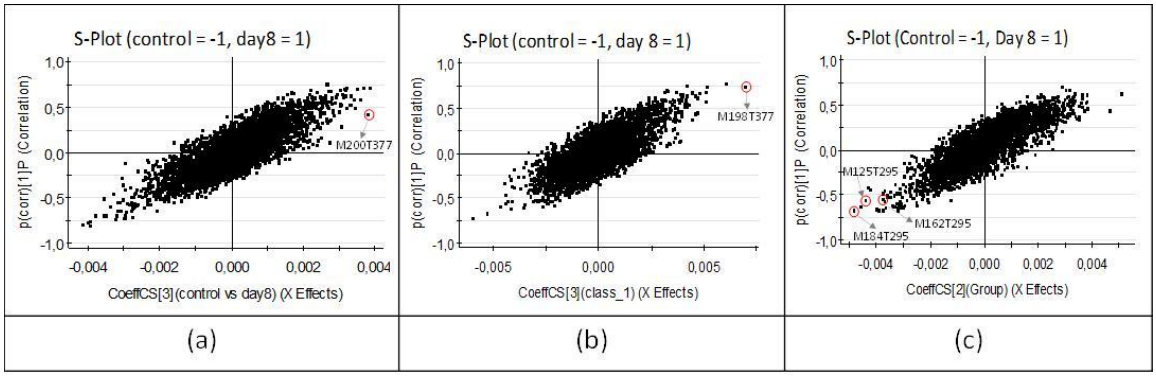

Fig 3. OPLS-DA S-Plot for RPLC samples in a) positive ionization mode, marker M200T377 is highlighted, b) negative ionization mode, marker M198T374 is highlighted and c) HILIC samples in positive ionization mode, markers M184T295, M162T295 and M125T295 are highlighted.

3.2. Selection of the markers

Among the 16546 features detected, 459 showed a p(corr) > 0.5 and, therefore, they were preselected as potential candidates. More in detail, RPLC analysis was able to find 122 and 85 features in the upper-right quadrant for ESI+ and ESI-, respectively. Additionally, 51 and 29 features with p(corr) > 0.5 were found in the lower-left quadrant in ESI+ and ESI- respectively. Regarding HILIC ESI+ analysis, 73 and 42 features were found in the upper-right and the lower-left quadrants respectively, whereas in ESI- 39 and 18 features were found in the upper-right and the lower-left quadrants respectively. Detailed information of these data is shown in supplementary information, Table S1.

One of the main bottlenecks of metabolomic approaches is the elucidation of the structure of the marker. The success of this step is directly related with the quantity and quality of structural information obtained for the marker. Therefore, the more abundant the MS information and the better quality thereof (e.g. accurate-mass full-spectrum data), the higher the chances of success in the marker elucidation step. Taking into account these considerations, potential candidates (p(corr) > 0.5) exhibiting several features (either in-source fragments or detected in both ionization modes) were selected as first options for subsequent structural elucidation.

In this particular study, the two most pronounced markers, one which increases after rhGH administration (located in the upper-right quadrant) and other which decreases (located in the lower-left quadrant) were selected. The reasons for this selection are detailed below.

The feature M198T374 (p(corr) = 0.7380) detected in RPLC negative mode was one with the highest p(corr) in the upper-right quadrant (Figure

3a). It also had a counterpart in positive ionization experiments (M200T377) which might correspond to the same marker. Although this feature showed lower p(corr) than M198T374 (p(corr) = 0.4256), it was found to be outside the cluster of data points (Figure 3b). The ionization in both positive and negative mode was considered a point in favor in order to obtain the largest amount of structural information which might eventually lead to its elucidation. Thus, this marker was selected as candidate which increases after rhGH administration.

Regarding the candidate that decreased after the administration, the feature labeled as M184T295 (p(corr) = -0.6706) detected in the HILIC ESI+ was one with the highest p(corr) in the lower left quadrant (Figure 3c). The features M162T295 (p(corr) = -0.5226) and M125T295 (p(corr) = -0.5631) were likely arise from the same compound (e.g. they might be adducts, in-source fragments, among others), since they shared the retention time. The presence of adducts and in-source fragments increased the chance of success in the elucidation. Therefore, it was selected as a candidate.

3.3. Structural elucidation

3.3.1. Marker M198T374/M200T377

Accurate mass of this marker could be extracted from the information obtained by XCMS. Masses of M198T374 in negative mode (*m/z* 198.1084 corresponding to a deprotonated formula of $C_{10}H_{16}NO_3$ with a mass error of -4.6 mDa) and M200T377 in positive mode (*m/z* 200.1325 corresponding to a protonated formula of $C_{10}H_{18}NO_3$ with a mass error of 3.8 mDa) indicated that this marker has a neutral molecular formula of $C_{10}H_{17}NO_3$. Additionally, both full scan and product ion scan spectra were acquired (Table 1).

Table 1. Full scan and product ion scan information of selected markers for RPLC and HILIC

	Analysis	Ionization	Marker	Accurate mass	Error (mDa)	Formula
Scan	RPLC	ESI+	M200T377	200.1325	3.8	$C_{10}H_{18}NO_3$
		ESI-	M198T374	198.1084	-4.6	$C_{10}H_{16}NO_3$
	HILIC	ESI+	M162T295	162.1147	1.7	$C_7H_6NO_3$
Product ion scan	RPLC	ESI+	M200T377	125.0992	2.6	$C_8H_{13}O$
				97.1006	-1.1	C_7H_{13}
				76.0397	-0.2	$C_2H_6NO_2$
		ESI-	M198T374	74.0238	-0.4	$C_2H_4NO_2$
	HILIC	ESI+	M162T295	103.0394	-0.1	$C_4H_7O_3$
				85.0290	0	$C_4H_5O_2$
				60.0782	-3.1	$C_3H_{10}N$

Product ion spectra for M198T374/M200T377 were acquired in both positive and negative ionization modes (Figure 4). The product ion spectrum in ESI- was dominated by the ion at *m/z* 74.0238, corresponding to a formula $C_2H_4NO_2$ (-0.4 mDa of error). In ESI+, a more complex spectrum was obtained. Besides the ion at *m/z* 76.0397 ($C_2H_6NO_2$, -0.2 mDa), a neutral loss of 75.0333 Da ($C_2H_5NO_2$, 1.3 mDa) and 27.0937 Da (CO, -0.3 mDa) were also observed. This fact suggested that the ionisable centre had a molecular weight of 75 Da, with a molecular formula of $C_2H_5NO_2$ and that it can be ionized in both positive and negative modes. Taking all information into consideration we postulated an amino acid as the most feasible structure for this part of the molecule. In particular, glycine matched with the experimental molecular formula.

The fragmentation in ESI+ mode also revealed structural information about the rest of the molecule. The neutral loss of CO suggested the presence of a carbonyl moiety linked to the glycine. This is in agreement with an amide group formed by conjugation of a carboxylic acid and a glycine. Several

carboxylic acids have been reported to be excreted in urine conjugated with glycine (Gregus et al. 1996, Smith et al. 1970).

Based on this information, a carboxylic acid linked to a glycine was postulated as feasible structure for M198T374/M200T377. Taking into account the molecular formula of the compound, it was proposed that the carboxylic acid contains eight carbon atoms and a single unsaturation.

In order to support the hypothesis, synthesis of Δ^2C8-Gly, Δ^3C8-Gly and Δ^7C8-Gly were performed (Figure 2) and these structures used as reference compounds. The MS/MS spectra in positive and negative ionization modes of the synthesized reference material (Figure 4), show that they share identical fragmentation with the marker M198T374/M200T377 (Figure 4), thus indicating that the structural identity of the marker is correct. Concretely, the spectrum corresponding with the authentic Δ^3C8-Gly and Δ^7C8-Gly showed the same product ions with very similar ion abundances that the urinary M198T374/M200T377. However, the retention times of these two compounds were, although similar, not exactly the same indicating that the specific localization of the unsaturated bond is different. Technically it is possible to obtain the precise M198T374/M200T377 structure by synthesizing more analogous compounds but the lack of other octenoyl acids from commercial sources rendered this option difficult at this stage. In any case, due to the almost identical product ion spectra, it is highly plausible to predict that the marker is an octenoyl-glycine (Δ^xC8-Gly).

	RT (min)	ESI+	ESI-
(a) Sample	7.70	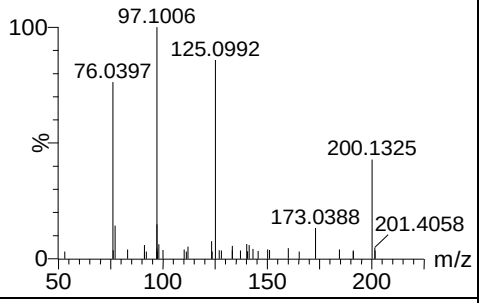	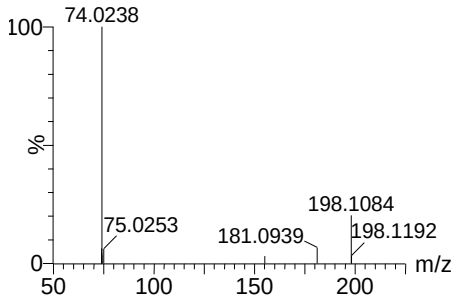
(b) Synthesized Δ^2C8-Gly	8.14	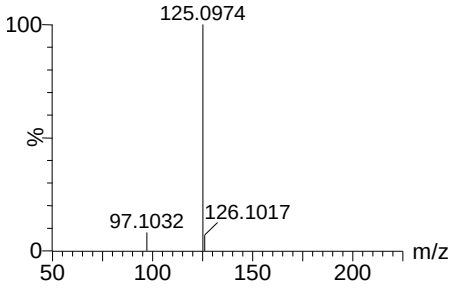	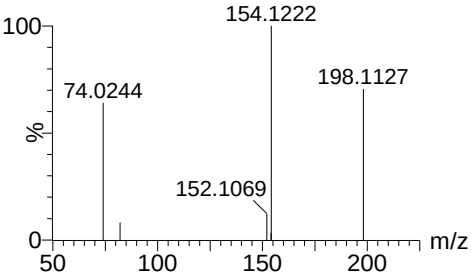
(c) Synthesized Δ^3C8-Gly	8.09	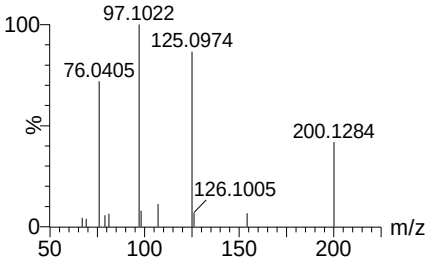	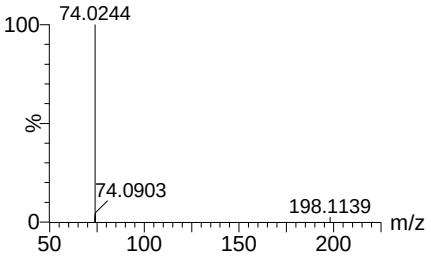
(d) Synthesized Δ^7C8-Gly	7.75	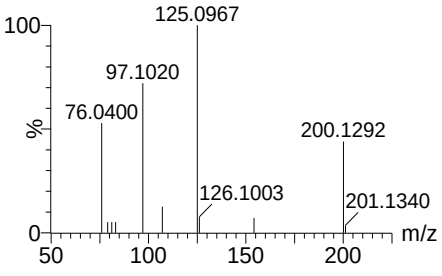	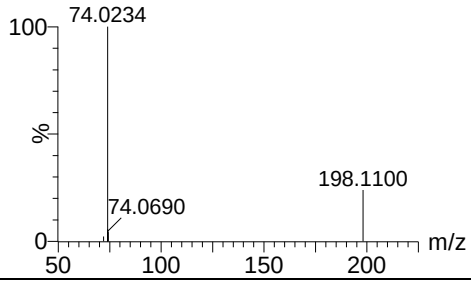

Fig 4. MS/MS spectra at 15 eV in positive and negative ionization modes of a) sample, b) synthesized Δ^2C8-Gly, c) synthesized Δ^3C8-Gly and d) synthesized Δ^7C8-Gly

3.3.2. Marker M184T295/M162T295/M125T295

The features M184T295, M162T295 and M125T295, located in the lower left quadrant, showed similar chromatographic behavior (retention time and peak shape). Therefore, it was considered that they belong to the same marker.

Accurate *m/z* values for M125T295, M162T295 and M184T295 were extracted from information provided by XCMS. Considering the potential adduct formation with alkali metals, $C_4H_6O_3Na$, $C_7H_{16}NO_3$ and $C_7H_{15}NO_3Na$ were found to be the most feasible molecular formulae for the ions at *m/z* 125.0217, 162.1125 and 184.0951 respectively. Based on this information, $C_7H_{15}NO_3$ was selected as the molecular formula for the marker M184T295/M162T295/M125T295 being the ions at *m/z* 162, 184 and 125 the $[M+H]^+$, $[M+Na]^+$ and a sodiated in-source fragment respectively.

The collision induced dissociation (CID) spectrum after selection of the ion *m/z* 162 as precursor ion (Figure 5), showed the presence of the ion at *m/z* 103.0375, coming from a neutral loss of 59.0753 (mass error 1.8 mDa). This neutral loss is related to the molecule trimethylamine, also present in the spectra as the protonated molecule (*m/z* 60.0782, mass error -3.1 mDa). The same loss is observed in Figure S4 (supplementary information) for the $[M+Na]^+$ at *m/z* 184, which suffers a neutral loss of triethylamine (59.0736, mass error 0.1 mDa) to obtain the ion at *m/z* 125.0216. This product ion corresponds to the in-source fragment found as the feature M125T295. Moreover, the presence of a hydroxyl group in the molecule was postulated by the neutral loss of a molecule of water (ion at *m/z* 85.0267, neutral loss of 18.0104 from 103.0375, mass error -0.2 mDa).

All together these data suggested that marker M184T295/M162T295/M125T295 had a charged trimethylammonium structure and a hydroxyl function. The presence of these moieties is in agreement with the fact that this compound is retained in the HILIC column i.e. it presents a high polarity.

Among trimethylammonium compounds, carnitine has the same molecular formula than M184T295/ M162T295/M125T295. Besides, carnitine has been identified as marker following administration of reGH in horses (Boyard-Kieken et al. 2011b) and it indicates, at least in part, a similar metabolic trajectory in different species. Therefore, carnitine was proposed as the structure for M184T295 M162T295//M125T295. The confirmation of the assignment for this marker was performed by comparing the accurate mass product ion spectra with the standard commercially available. Coincidence in retention time and fragmentation pattern is observed in Figure 5.

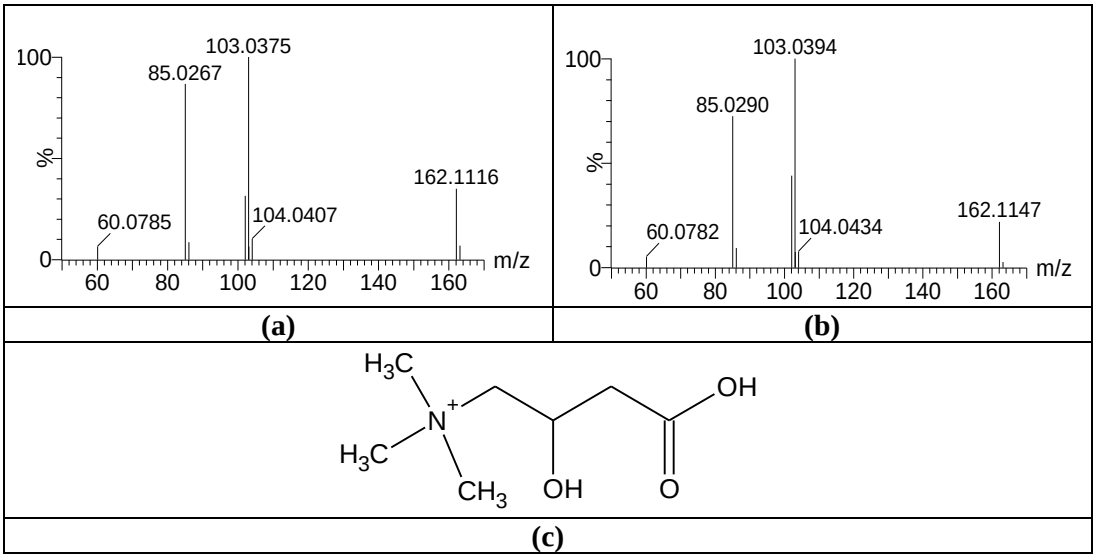

Fig 5. MS/MS spectra at 25 eV of a) carnitine standard and b) blank volunteer and c) carnitine structure

4. POTENTIAL USEFULNESS FOR DOPING CONTROL ANALYSIS

The potential usefulness of the two selected markers for the urinary screening of rhGH administration was evaluated. For this purpose, the peaks corresponding to both Δ^xC8-Gly and carnitine were integrated in all samples by XCMS and the resulting areas were plotted against time. As expected, the areas for the two selected markers showed opposite behavior after rhGH administration. The response for Δ^xC8-Gly increased during the treatment and contrarily, carnitine response increased during the first day of the treatment but then it started to decrease.

The juxtaposed behavior of the selected analytes advises to use the ratio between them in order to screen for rhGH administration. This ratio improved the discriminatory potency between pre and post-administration samples thus greatly facilitating the screening process for GH abuse. Additionally, the use of the ratio allowed for the correction of other factors like dilution of the urine, rendering the approach universal.

As an example, Figure 6 compares the evolution of the ratio Δ^xC8-Gly/carnitine between a volunteer after rhGH administration and other one taking placebo. At the maximum point, the Δ^xC8-Gly/carnitine value was more than 100 fold higher than the basal level. Due to the experimental design, the maximum point observed for some volunteers corresponded to the last sample collected in the administration week. Therefore, we cannot discard that the increase shown might continue being the maximum point underestimated in this study.

The large differences observed between pre and post-administration samples when using Δ^xC8-Gly/carnitine demonstrates the tremendous potential of urinary markers, more precisely the ratio between two or more,

for the detection of rhGH administration. It is much more defined and has a much longer detection window than the current strategies. However, this potential should be confirmed with additional analysis, and further research is needed for this purpose. In the case of Δ^xC8-Gly, the first compulsory step should be the complete elucidation of its actual structure. The location of the unsaturation in the molecule should be established. Then, since fatty acids degradation is the most feasible metabolic pathway behind this marker, its variation under different conditions e.g. diet, should be evaluated. Regarding carnitine, its use is not prohibited in sports and it is a common component in several supplements potentially used by the athletes. Additionally, urinary carnitine concentrations have been found to vary after exercise (Wall et al. 2011) putting some question marks to the use of carnitine as marker for doping purposes.

For these reasons, the variation (both the amount and the sign) of the ratio Δ^xC8-Gly/carnitine under different conditions such as diet, exercise or carnitine administration should be evaluated and compared with the obtained after rhGH administration. This comparison will provide the definitive data to include/discard this marker in future screening of rhGH in doping control analysis.

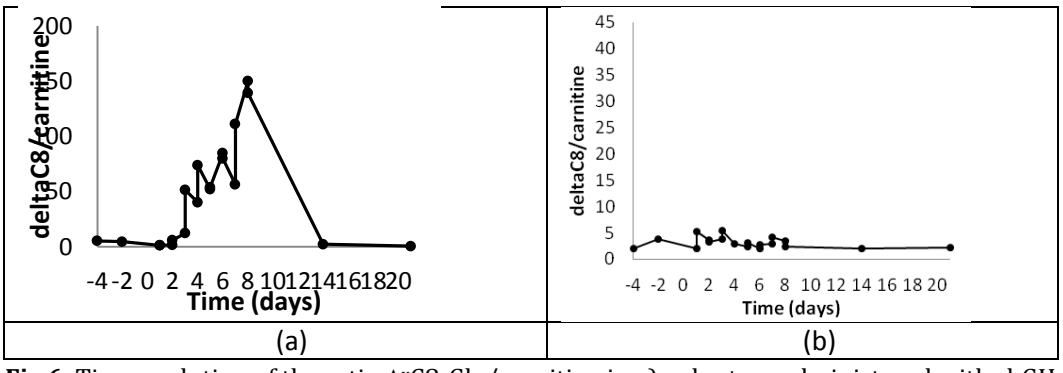

Fig 6. Time evolution of the ratio Δ^xC8-Gly/carnitine in a) volunteer administered with rhGH and b) control volunteer.

5. CONCLUSIONS

An untargeted metabolomic approach based on liquid chromatography (RPLC and HILIC) coupled to QTOF MS has been developed in order to shed light on the potential urinary screening of the rhGH abuse in sport.

The developed strategy allowed for the detection of more than 400 candidates which might be potential markers for the urinary screening of the misuse. Among them, two candidates were selected and assigned to octenoyl-glycine and carnitine.

As a result of this work, the use of □xC8-Gly/carnitine ratio for the urinary screening of rhGH administration in doping control is proposed as a promising approach. The high retrospectivity achieved and the fact that it can be measured with minimal sample preparation, by instruments available in antidoping laboratories make this approach potentially suitable for future rhGH screening. More research is needed in order to confirm this potential, focused on variations on diet or other external factors.

This study shows the usefulness of untargeted metabolomic approaches in doping control analysis. As a proof of concept, two of the potential markers were selected and elucidated. However, it is noticeable the large number of potential markers that offer alternative ways for the urinary screening of rhGH misuse. Further work, following similar strategies, will allow finding other options for the detection of rhGH misuse in sports.

6. ACKNOWLEDGEMENTS

The authors acknowledge the financial support of the Ministry of Education and Science, Spain, in the project DEP2011-28573-C02/01/02 and the World Anti-Doping Agency (WADA). The authors from University Jaume I also acknowledge the support from Generalitat Valenciana (Research Group of Excellence Prometeo/2009/054; PrometeoII/2014/023; ISIC EnviFood 2012/016). Authors are very grateful to David Andreu for the helpful discussions about the synthesis of reference materials. M. Raro is also grateful to the Ministry of Economy and Competitiveness of Spain for her predoctoral grant. Spanish Health National System is acknowledged for O. J. Pozo contract (MS10/00576).

7. REFERENCES

Armitage E. G., Rupérez F. J., Barbas C. (2013). Metabolomics of diet-related diseases using mass spectrometry. Review. *Trends in Analytical Chemistry*, 52, 61-73

Baumann G. P. (2009). Growth hormone isoforms. *Growth Horm & IGF Research*, 19 (4), 333-340

Bosh J., Duch-Sanmartín G., Segura J., Gutiérrez-Gallego R. (2012). Tracking growth hormone abuse in sport: Performance of marker proteins in a controlled setting. *Analytica Chimica Acta*, 745, 118-123

Bosch J., Luchini A., Pichini S., Tamburro D., Fredolini C., Liotta L., Petricoin E., Pacifici R., Facchiano F., Segura J., Garaci E., Gutiérrez-Gallego R. (2013). Analysis of urinary human growth hormone (hGH) using hydrogel nanoparticles and isoform differential immunoassays after short recombinant hGH treatment: preliminary results. *Journal of Pharmaceutical and Biomedical Analysis*, 85, 194-197

Boyard-Kieken F., Pinel G., Antignac J-P., Paris A-C., Garcia P., Popot M-A., et al. (2011a). Generation and processing of urinary and plasmatic metabolomic fingerprints to reveal an illegal administration of recombinant equine growth hormone from LC-HRMS measurements. *Metabolomics*, 7, 84-93

Boyard-Kieken F., Dervilly-Pinel G., Garcia P., Paris A-C., Popot M-A., le Bizec B., et al. (2011b). Comparison of different liquid chromatography stationary phases in LC-HRMS metabolomics for the detection of recombinant growth hormone doping control. *Journal of Separation Science*, 34, 3493-3501

Cevallos-Cevallos J. M., Reyes-de-Corcuera J. I., Etxeberria E., Danyluk M. D., Rodrick G. E. (2009). Metabolomic analysis in food science: a review. *Trends in Food Science and Technology*, 20, 557-566

Díaz R., Pozo O. J., Sancho J. V., Hernández F. (2014). Metabolomic approaches for orange origin discrimination by ultra high liquid chromatography coupled to quadrupole time-of-flight mass spectrometry. *Food Chemistry*, 157, 84-93

Dunn W. B., Wilson I. D., Nicholls A. W., Broadhurst D. (2012). The importance of experimental design and QC samples in large-scale and MS-driven untargeted metabolomic studies of humans. *Bioanalysis*, 18, 2249-2264

Ehrnborg C., Bengtsson B. A., Rosén T. (2000). Growth hormone abuse. *Best Practice & Research Clinical Endocrinology & Metabolism*, 14 (1), 71-77

Glauser G., Veyrat N., Rochat B., Wolfender J-L, Turlings T. C. J. (2013). Ultra-high pressure liquid chromatography-mass spectrometry for plant metabolomics: A systematic comparison of high-resolution quadrupole-time-of-flight and single stage Orbitrap mass spectrometry. *Journal of Chromatography A*, 1292, 151-159

Gregus Z., Fekete T., Halászi E., Klaassen C. D. (1996) Lipoic acid impairs glycine conjugation of benzoic acid and renal excretion of benzoylglycine. *Drug Metabolism and Disposition*, 24, 682-688.

Haring R. (2012). Perspectives for metabolomics in testosterone replacement therapy. *Journal of Endocrinology*, 215, 3-16

Holt R. I. G. (2013). Detecting growth hormone abuse in athletes. *Indian Journal of Endochrinology and Metabolism*. Vol 7. Supplement 1. doi: 10.4103/2230 8210.119494

Idborg H., Zamani L.,. Edlund P. O, Schuppe-Koistinen I., Jacobsson S.P. (2005). Metabolic fingerprinting of rat urine by LC/MS: Part 1. Analysis by hydrophilic interaction liquid chromatography–electrospray ionization mass spectrometry. *Journal of Chromatography B*, 828 (1), 9-13

Jenkins P. (1998). Cancer in acromegaly. *Trends in Endocrinology & Metabolism*, 9, 360-366

Kiss A., Jacquet A-L., Paisse O., Flament-Waton M-M., de Ceaurriz J., Bordes C., et al. (2011). Urinary signature of anabolic steroids and glucocorticoids in humans by LC-MS. *Talanta*, 83, 1769-1773

Kiss A., Lucio M., Fildier A., Buisson C., Achmitt-Kopplin P., Cren-Olivé C. (2013). Doping control using high and ultra-high resolution mass spectrometry based non-targeted metabolomics- A case of study of salbutamol and budesonide abuse. *Plos One*, 8 (9), 1-13

Kojima M, Hosoda H, Matsuo H, Kangawa K. (2001). Ghrelin: discovery of the natural endogenous ligand for the growth hormone secretagogue receptor. *Trends Endocrinology Metabolism*, 12 (3), 118-22.

Mamas M., Dunn W. B., Neyses L., Goodacre R. (2011). The role of metabolites and metabolomics in clinically applicable biomarkers of disease. *Archives of Toxicology*, 85, 5-17

Powrie J. K., Bassett E. E., Rosen T., Jørgensen J. O., Napoli R., Sacca L. et al. (2007). Detection of growth hormone abuse in sport. *Growth hormone & IGF research*, 17 (3), 220-226

Raro M., Ibáñez M., Gi R., Fabregat A., Tudela E., Deventer K., Ventura R., et al. (2015).Untargeted Metabolomics in Doping Control: Detection of New Markers of Testosterone Misuse by Ultrahigh Performance Liquid Chromatography Coupled to High-Resolution Mass Spectrometry. *Analytical Chemistry*, 2015 87 (16), 8373-8380

Reichel C. (2011). OMICS-strategies and methods in the fight against doping. *Forensic Science International*, 213, 20-34

Rijk J. C. W., Lommen A., Essers M. L., Groot M. J., Van Hende J. M., Doeswijk T. G., et al. (2009). Metabolomics approach to anabolic steroid urine profiling of bovines treated with prohormones. *Analytical Chemistry*, 81, 6879-6888

Roux A., Xu Y., Heilier J-F., Olivier M-F., Ezan E., Tabet J-C., et al. (2012). Annotation of the human adult urinary metabolome and metabolite identification using ultra high performance liquid chromatography coupled to a linear quadrupole ion trap-orbitrap mass spectrometer. *Analytical Chemistry*, 84, 6429-6437

Saugy M., Robinson N., Saudan C., Baume N., Avois L., Mangin P. (2006). Human growth hormone doping in sport. British Journal of Sports Medicine, 40, Suppl I. doi: 10.1136/bjsm.2006.027573

Schmidt M. T., Handschuh L., Zyprych J., Szabelska A., Olejnik-Schmidt A. K., Siatkowski I., et al. (2011). Impact of DNA microarray data transformation on gene expression analysis-comparison of two normalization methods. *Acta Biochimica Polonica*, 58, 573-580

Scripps Centre for Metabolomics: XCMS Online. https://xcmsonline.scripps.edu/ Accessed 19 August 2014

Smith H. G.; Smith W. R. D.; Jepson J. B.; Sorenson K. (1970). The metabolism and excretion of indolylacrylic acid in the rat. *Biochemical Pharmacology*, 19, 1689-1693.

Spagou K., Wilson I. D., Masson P., Theodoridis G., Raikos N., Coen M., et al. (2010). HILIC-UPLC-MS for exploratory urinary metabolic profiling in toxicological studies. *Analytical Chemistry*, 83 (1), 382-390

Strobl J. S., Thomas M. J. (1994). Human growth hormone. *Pharmacology Reviews*, 46 (1), 1-34

Thevis M., Schänzer W. (2007). Current role of LC–MS (/MS) in doping control. *Analytical and Bioanalytical Chemistry*, 388 (7), 1351-1358

Thevis M., Thomas A., Schänzer W. (2011). Doping control analysis of selected peptide hormones using LC–MS (/MS). *Forensic Science International*, 213 (1), 35-41

Wall B. T., Stephens F. B., Constantin-Teodosiu D., Marimuthu K., Macdonald I. A, Greenhaff P. L. (2011). Chronic oral ingestion of L-carnitine and carbohydrate increases muscle carnitine content and alters muscle fuel metabolism during exercise in humans. *Journal of Physiology*, 589, 963–973

World Anti-Doping Agency. The 2016 Prohibited List. https://wada-main-prod.s3.amazonaws.com/resources/files/wada-2016-prohibited-list-en.pdf. Accessed 08 February 2016.

World Anti-Doping Agency. The Human Growth Hormone. https://www.wada-ama.org/en/questions-answers/human-growth-hormone. Accessed 18 August 2014.

World Anti-Doping Agency. Technical Document – TD2015GH. https://wada-main-prod.s3.amazonaws.com/resources/files/wada_td2015gh_hgh_isoform_diff_immunoassays_en.pdf.Accessed 14 October 2015

Wu Z., Bidlingmaier M., Dall R., Strasburger C.J. (1999) Detection of doping with human growth hormone. *The Lancet*, 353, 895

SUPPLEMENTARY INFORMATION

Fig s1. Box plots of the log_2 intensities of the different samples in RPLC data before normalization and after normalization in positive and negative ionization modes.

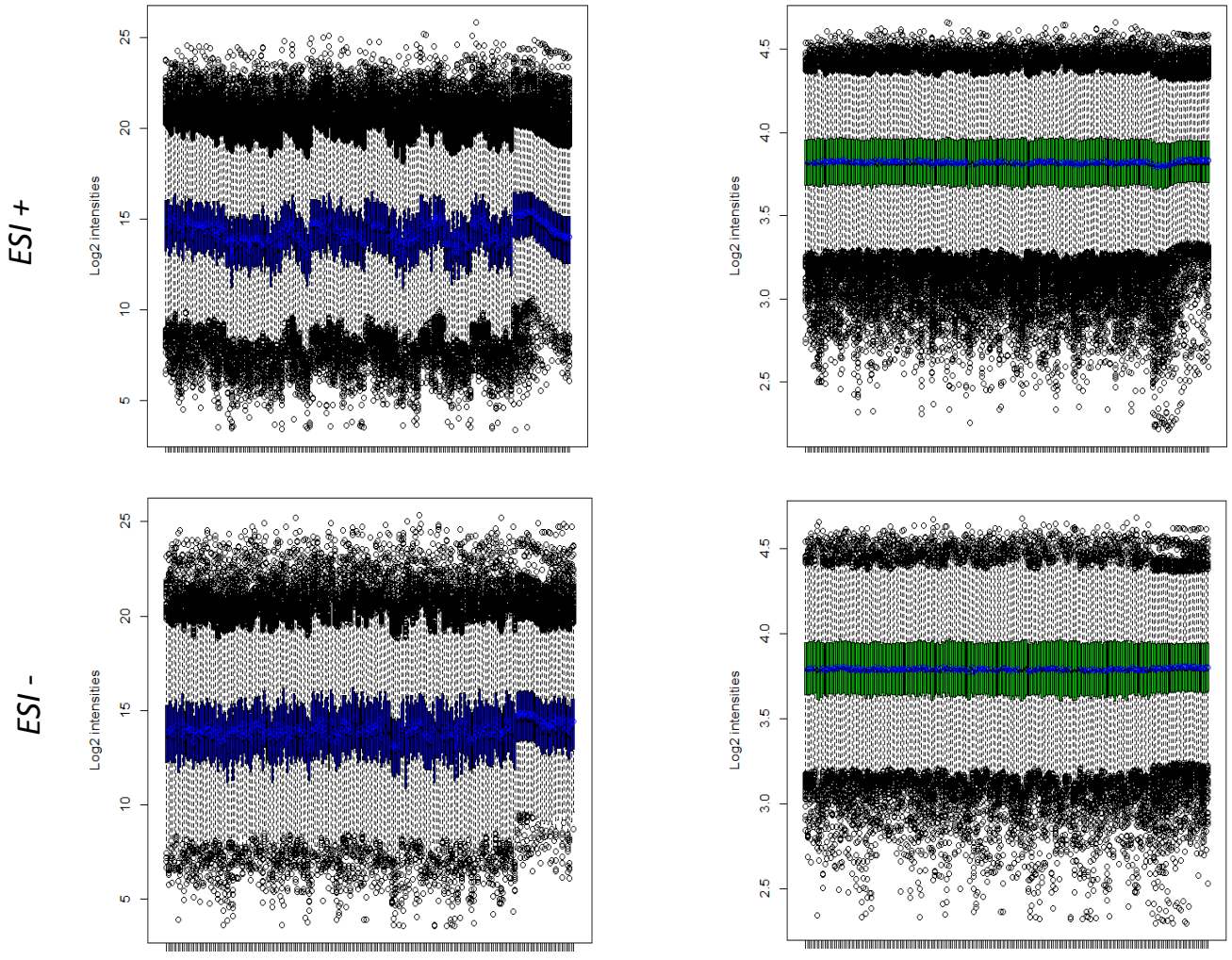

Fig s2. Score plots of RPLC data in negative ionization mode a) PCA with highlighted QCs, b) PLS-DA score plot separated by days and c) PLS-DA score plot separated by days excluding blank volunteers.

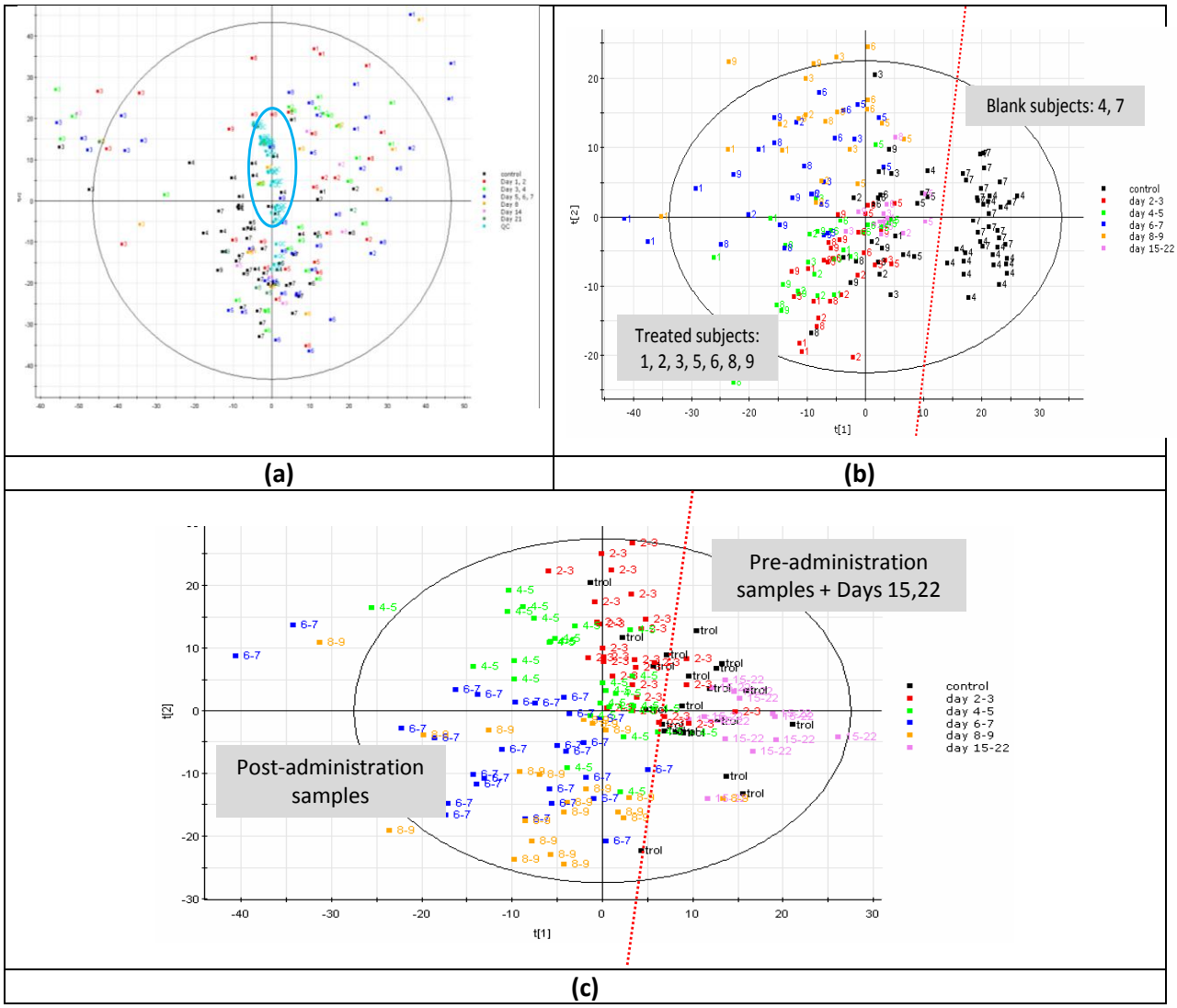

Fig s3. Score plots of HILIC data in positive ionization mode a) PCA with highlighted QCs, b) PLS-DA score plot separated by days

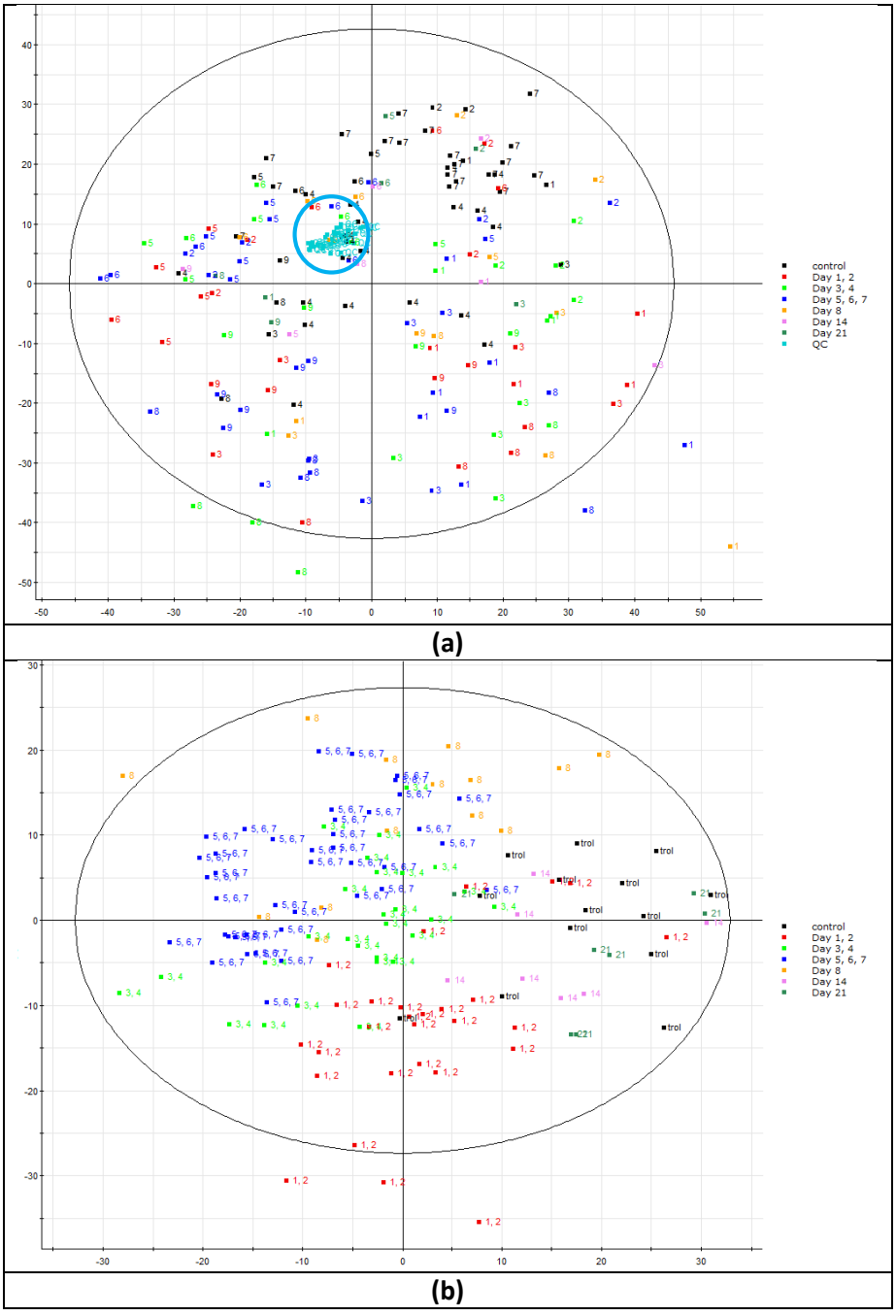

Fig s4. Accurate MS/MS spectra at 20 eV of marker M184T295 in positive ionization mode.

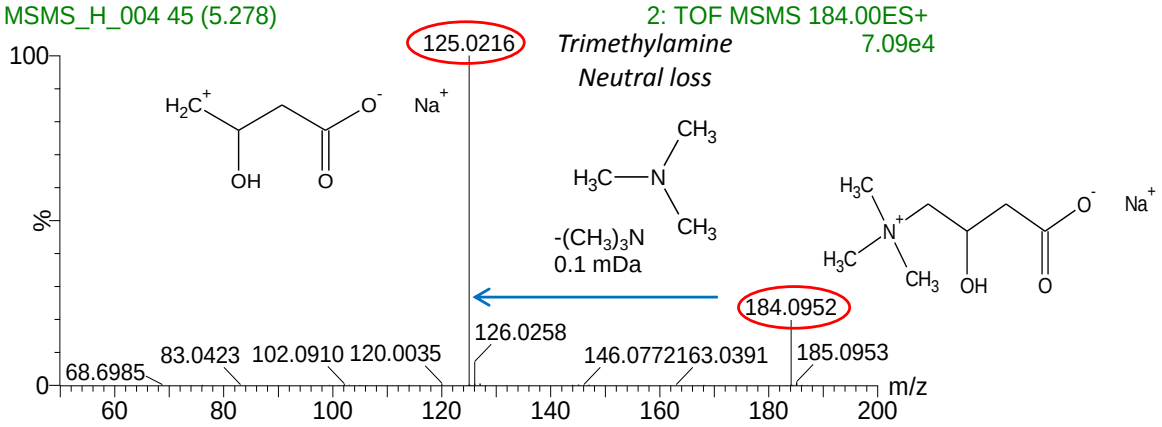

Table S1. Candidates with p>0.5 and statistical relevance obtained from OPLS-DA S-Plot, in both ionization modes, for RPLC and HILIC data

HILIC								C18							
ESI +				ESI -				ESI +				ESI -			
upper-right quadrant		lower-left quadrant		upper-right quadrant		lower-left quadrant		upper-right quadrant		lower-left quadrant		upper-right quadrant		lower-left quadrant	
Primary ID	p(corr)	Primary ID	p(corr)	Primary ID	p(corr)	Primary ID	p(corr)	Primary ID	p(corr)	Primary ID	p(corr)	Primary ID	p(corr)	Primary ID	p(corr)
M325T400	0,6936	M246T194	-0,6755	M223T66	0,7785	M256T350	-0,6688	M454T232	0,7538	M170T272	-0,8130	M633T356	0,7721	M412T60	-0,7207
M626T392	0,663	M163T264	-0,6711	M224T66	0,732	M545T288	-0,6192	M318T288	0,7535	M320T272	-0,7989	M441T416	0,7427	M852T420	-0,6779
M627T392_1	0,6599	M184T295	-0,6706	M317T386	0,6935	M393T289	-0,6087	M344T233	0,7112	M298T297	-0,7717	M198T374	0,7380	M714T378	-0,6253
M627T392_2	0,6585	M233T202	-0,6694	M225T82	0,6826	M341T349	-0,5814	M719T238_1	0,7095	M321T272	-0,7656	M557T292	0,7343	M479T517	-0,6083
M719T391_1	0,6205	M232T194	-0,6589	M299T235	0,6814	M302T345	-0,5743	M719T238_2	0,7043	M219T68	-0,7397	M384T378	0,7028	M431T500	-0,5962
M151T246	0,6178	M146T230	-0,6517	M760T421_1	0,6570	M173T69	-0,5704	M727T226_2	0,7019	M278T446	-0,7220	M588T358	0,6872	M456T76	-0,5941
M736T416	0,6079	M164T263	-0,6512	M722T422	0,6421	M357T288	-0,5665	M727T226_1	0,7008	M260T76	-0,7192	M586T364	0,6747	M595T464	-0,5861
M719T391_2	0,6078	M85T228	-0,6484	M760T421_2	0,6384	M231T61	-0,5587	M720T238	0,6989	M277T446	-0,7147	M921T384	0,6726	M513T375	-0,5701
M241T388	0,6055	M205T228	-0,6435	M223T94	0,6356	M665T296	-0,5391	M728T225	0,6910	M294T446	-0,7026	M826T380	0,6716	M611T455	-0,5608
M610T368_1	0,6029	M246T70	-0,6375	M269T62	0,6181	M529T296	-0,5369	M219T467	0,6816	M338T273	-0,7021	M891T421	0,6716	M854T417	-0,5596
M327T400	0,6016	M185T295	-0,6371	M845T375	0,6172	M255T352	-0,5363	M455T232	0,6793	M305T337	-0,6977	M185T266	0,6613	M350T403	-0,5571
M204T348	0,6012	M206T228	-0,6353	M415T386	0,6104	M182T135	-0,5347	M618T239	0,6782	M276T247	-0,6959	M825T380	0,6573	M909T464	-0,5563
M326T400	0,5960	M147T238	-0,6340	M177T308	0,5993	M165T73	-0,5299	M1068T232	0,6687	M280T248	-0,6924	M927T417	0,6538	M512T455	-0,5404
M719T416_2	0,5956	M205T236	-0,6221	M313T308	0,5970	M263T317	-0,5289	M190T232	0,6641	M184T397	-0,6547	M385T412	0,6497	M1108T409	-0,537
M161T60	0,5919	M145T228	-0,6214	M632T389	0,5934	M159T318	-0,5285	M331T402	0,6591	M274T177	-0,6514	M339T349	0,6385	M411T517	-0,5369
M598T389	0,5905	M260T224	-0,6177	M198T58	0,5919	M232T61	-0,5198	M317T409	0,6501	M296T207	-0,6503	M921T420	0,6359	M165T99	-0,5352
M691T392_1	0,5885	M146T238	-0,6063	M609T292	0,5844	M235T289	-0,5080	M330T402	0,6443	M169T273	-0,6463	M442T416	0,6297	M293T429	-0,5345
M712T416	0,5880	M206T236	-0,60329	M425T396	0,5755	M113T307	-0,5050	M1005T256_2	0,6364	M258T411	-0,6431	M836T380	0,6119	M197T62	-0,5315
M628T393	0,5864	M85T236	-0,6019	M257T371	0,5742			M763T288_1	0,6338	M317T433	-0,6268	M249T353	0,6089	M910T464	-0,5308
M203T64	0,5845	M246T140	-0,59754	M215T246	0,5658			M277T285	0,6318	M310T243	-0,6145	M835T380	0,6069	M166T99	-0,5301
M465T390	0,5841	M246T164	-0,5987	M1140T421_2	0,5487			M483T503	0,6294	M218T100	-0,6124	M209T251	0,6062	M863T464	-0,5291

Table S1 (cont.). Candidates with p>0.5 and statistical relevance obtained from OPLS-DA S-Plot, in both ionization modes for RPLC and HILIC data

M761T415_1	0,5808	M145T236	-0,5839	M1152T422_1	0,5469			M10990T292	0,6256	M274T137	-0,6087	M795T465	0,5995	M412T517	-0,526					
M859T393	0,5805	M217T219	-0,5814	M225T137	0,5448			M799T298	0,6253	M291T207	-0,6003	M385T360	0,5979	M514T375	-0,5239					
M827T374_1	0,5730	M160T197	-0,5799	M223T116	0,5333			M607T237	0,6243	M277T218	-0,5922	M541T434	0,5959	M864T464	-0,5207					
M724T421	0,5693	M261T231	-0,5770	M537T246	0,5310			M720T242	0,6136	M230T295	-0,5808	M439T394	0,5930	M511T455	-0,5205					
M421T385	0,5685	M246T179	-0,5738	M290T367	0,5277			M598T224	0,6136	M274T297	-0,5769	M208T258	0,5929	M375T542	-0,518					
M720T416	0,5650	M192T272	-0,56457	M1140T421_1	0,5262			M466T231	0,6121	M218T71	-0,5756	M614T366	0,5902	M254T180	-0,5146					
M761T415_2	0,5638	M125T295	-0,5631	M760T397	0,5259			M201T377	0,6120	M162T55	-0,5727	M666T465	0,5884	M881T504	-0,5052					
M720T391	0,56251	M142T214	-0,5569	M223T82	0,5259			M1005T256_1	0,6046	M261T77	-0,5720	M384T412	0,5878	M622T220	-0,5010					
M288T50	0,5582	M246T201	-0,5536	M329T58	0,5186			M262T294	0,6001	M317T300	-0,5719	M234T328	0,5872							
M725T421_1	0,5553	M277T49	-0,5515	M341T308	0,5157			M356T467	0,5993	M284T323	-0,5685	M493T432	0,5847							
M599T389	0,5518	M233T172	-0,5489	M225T128	0,5115			M319T288	0,5988	M198T252	-0,5650	M494T432	0,5843							
M549T393	0,5511	M541T309	-0,5475	M224T81	0,5064			M627T245	0,5947	M277T432	-0,5577	M248T355	0,5779							
M578T392	0,5495	M218T203	-0,5312	M579T462	0,5066			M264T318	0,5944	M275T137	-0,5553	M926T417	0,5763							
M762T420_3	0,5466	M407T228	-0,5302	M763T385	0,5056			M379T426	0,5929	M356T435	-0,5532	M405T293	0,5733							
M300T52	0,54610	M260T232	-0,5264	M387T307	0,5044			M429T465	0,5912	M276T152	-0,5519	M334T465	0,5699							
M725T421_2	0,5459	M233T153	-0,5263	M348T298	0,5035			M284T463	0,5891	M334T407	-0,5511	M831T416	0,5680							
M76T220	0,5447	M162T295	-0,5226	M319T308	0,5017			M827T292_2	0,5883	M285T323	-0,5414	M386T381	0,5679							
M618T385	0,5431	M233T214	-0,5148	M323T401	0,5005			M1089T292_2	0,5867	M1100T423	-0,5303	M312T237	0,5674							
M281T387	0,5420	M121T272	-0,5133					M161T334	0,5863	M345T375	-0,5301	M316T333	0,5673							
M663T389	0,5406	M142T132	-0,5111					M755T302	0,5839	M344T376	-0,5286	M508T422	0,5653							
M307T400	0,5389	M257T246	-0,5038					M259T285	0,5836	M345T432	-0,5282	M665T465	0,5615							
M570T392_1	0,5386							M422T293	0,5811	M167T93	-0,5274	M376T489	0,5599							
M550T393_1	0,5358							M288T291	0,5804	M310T403	-0,5269	M371T429	0,5570							
M200T59	0,5349							M398T369	0,5778	M275T177	-0,5178	M290T280	0,5527							
M694T419_2	0,5338							M565T298	0,5776	M199T66	-0,5131	M328T223	0,5470							
M309T397	0,5320							M217T455	0,5765	M403T307	-0,5121	M727T356	0,5472							
M190T366	0,5310							M498T445	0,5698	M276T220	-0,5070	M333T465	0,5469							

Table S1 (cont.). Candidates with p>0.5 and statistical relevance obtained from OPLS-DA S-Plot, in both ionization modes for RPLC and HILIC data

M316T236	0,5278				M1086T222_2	0,5666	M286T207	-0,5067	M479T445	0,5437			
M827T374_2	0,5245				M392T440	0,5652	M330T410	-0,5050	M315T369	0,5405			
M130T76	0,5245				M817T272_2	0,5626	M366T387	-0,5020	M265T352	0,5394			
M115T254	0,5237				M176T251	0,5621			M243T482	0,5391			
M113T267	0,5232				M371T474	0,5613			M331T475	0,5382			
M662T389_1	0,5220				M619T239	0,5609			M792T379	0,5370			
M428T301	0,5200				M258T427	0,5579			M300T326	0,5370			
M763T375_1	0,5195				M222T218	0,5578			M480T446	0,5364			
M645T392	0,5183				M721T242_1	0,5578			M253T424	0,5356			
M736T417	0,5177				M162T333	0,5554			M823T380	0,5349			
M737T416	0,5176				M10887T222	0,5533			M300T454	0,5332			
M662T389_2	0,5163				M764T288	0,5533			M257T498	0,5318			
M694T419_1	0,5136				M295T397	0,5525			M10841433	0,5258			
M77T221	0,5127				M526T424	0,5502			M348T199	0,5237			
M336T249	0,5117				M626T217	0,5501			M365T85	0,5234			
M579T392	0,5110				M296T268	0,549			M657T223	0,5215			
M422T385	0,5082				M798T297	0,5490			M472T522	0,52139			
M113T254	0,5082				M817T272_1	0,5479			M348T406	0,5206			
M741T420	0,5081				M870T226_1	0,5473			M861T415	0,5193			
M638T392_1	0,5054				M283T296	0,5464			M542T434	0,5186			
M610T368_2	0,50411				M755T301	0,5460			M10877433	0,5183			
M861T418	0,5038				M925T256	0,5457			M615T366	0,5143			
M479T394	0,5035				M827T292_1	0,5441			M790T378	0,5116			
M634T254	0,5027				M10867222_1	0,5436			M789T378	0,5112			
M719T416_1	0,5006				M214T408	0,5434			M432T465	0,5092			
					M627T217_2	0,5433			M664T465	0,5074			
					M203T350	0,5432			M537T378	0,5070			
					M763T288_2	0,5427			M460T298	0,5061			

Table S1 (cont.). Candidates with p>0.5 and statistical relevance obtained from OPLS-DA S-Plot, in both ionization modes for RPLC and HILIC data

| | | |

Table S1 (cont.). Candidates with p>0.5 and statistical relevance obtained from OPLS-DA S-Plot, in both ionization modes for RPLC and HILIC data

| | | |

III.4. Discusión

En la introducción general (Capítulo I) se trató la importancia del correcto diseño experimental, toma, conservación y preparación de las muestras, del tratamiento de las mismas y de las técnicas analíticas utilizadas en metabolómica. De la misma forma, el tratamiento de datos es también un paso crítico para el éxito de este tipo de trabajos. El conjunto de datos obtenido es muy complejo y necesita de un tratamiento correcto que logre llegar a los marcadores adecuados, así como su elucidación y explicación biológica.

En este apartado se van a discutir los pasos realizados dentro del proceso analítico en los trabajos de metabolómica presentados en este capítulo, los *artículos científicos 4 y 5*. Para ello, se seguirá el mismo esquema que en el apartado I.3.2 de la introducción general.

1) Diseño experimental

En ambos trabajos presentados se optó por seguir una estrategia de metabolómica *untargeted* o no dirigida, donde no se realiza ninguna selección previa de los compuestos a analizar. El análisis no dirigido pretende obtener información de la muestra sin información previa. Esta estrategia es la más común y tiene ventajas e inconvenientes, pero debe adecuarse al estudio en cuestión que se vaya a realizar. En nuestro caso, se pretendía buscar cualquier metabolito que se viera alterado frente al abuso de testosterona (*artículo científico 4*) o rhGH (*artículo científico 5*). Al no disponerse de información previa ni aplicarse ningún filtro en la búsqueda, cualquier compuesto podía ser un buen candidato, obviamente, siempre y cuando fuera correctamente detectado mediante las técnicas analíticas seleccionadas. Sin

embargo, esta estrategia presenta dos desventajas principales (i) la necesidad de elucidar los compuestos que se veían exaltados por el análisis multivariante y (ii) establecer su origen biológico.

En este punto, se decidió estudiar aquellos marcadores que en la estadística se encontraran por encima de un valor arbitrario de p(corr) = 0.5. El p(corr) o *variable confidence* fluctúa entre 0 y 1, aportando más confianza cuanto más cercano sea este valor a 1. En el caso de obtenerse muchos marcadores por encima de este umbral, como ocurría en determinados casos, se empezó a estudiar por los que tenían el valor más alto o los que presentaban *Variable Trend Plot* más interesantes (ver ejemplo Figura S6, *artículo científico 4*).

Una de los puntos críticos al aplicar la metabolómica untargeted es asegurar que los compuestos detectados son marcadores del proceso seleccionado. La concentración de metabolitos en una muestra biológica puede verse afectada por factores como la variabilidad inter-individual, el ritmo circadiano o la posible degradación. Por este motivo, la selección, toma y conservación de las muestras son pasos esenciales dentro del proceso analítico. Así, se debe asegurar que las muestras son representativas de la población de estudio. En los trabajos que nos ocupan, las muestras correspondían a individuos diferentes, recogidas a diferentes horas tras la administración de las sustancias dopantes y, también, previas a la administración muestras control). En el caso de la testosterona, para mayor representatividad, las muestras provenían de individuos con diferentes niveles basales T/E (asiáticos y caucásicos).

2) Tratamiento de muestra

Es necesario que el tratamiento de muestra en metabolómica no dirigida donde, por lo general, el número de muestras es elevado, sea realizado aleatoriamente, y, además, sea el más simple posible con el fin de minimizar las pérdidas de metabolitos durante el proceso. En el caso de la rhGH, algunas muestras presentaban un residuo insoluble, por lo que el tratamiento llevado a cabo fue dilución con agua (o ACN para HILIC) seguida de centrifugación, para inyectar el sobrenadante y, así, evitar problemas de obturación en el sistema. En el caso de la testosterona, las muestras eran más limpias y se decidió realizar un *Dilute and shoot* para agilizar el tratamiento de muestra y evitar, todavía más, posibles pérdidas de compuestos durante el proceso.

La centrifugación de las orinas realizadas para la rhGH (*artículo científico 5*) puede producir pérdidas de alguno de los metabolitos. Con el fin de evaluar este aspecto se aplicó una liofilialización de las muestras previa a la centrifugación (Kim et al., 2008).

El tratamiento de muestra que se siguió fue el que se muestra en la **figura III.1**. Se llevó a cabo la extracción del residuo seco con una mezcla DCM:MeOH para aumentar la extracción de potenciales componentes más apolares cuya pérdida parcial en la centrifugación es más factible.

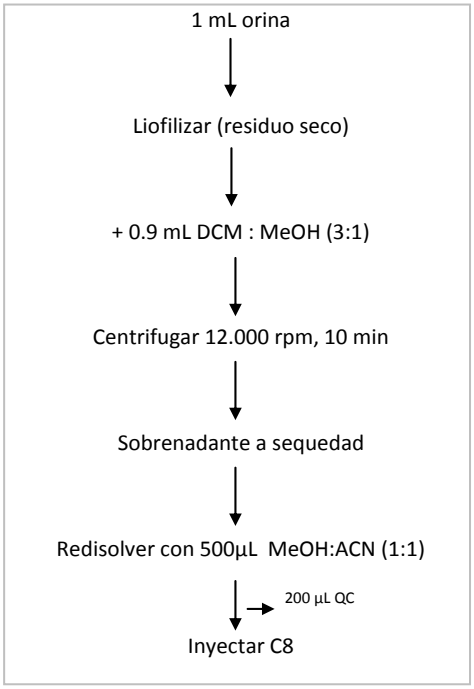

Figura III.1 Tratamiento de muestra propuesto para las muestras de rhGH

Las muestras se inyectaron en una columna C8. De esta manera se podrían cromatografiar posibles fosfolípidos u otros compuestos más apolares presentes en el residuo insoluble de la orina, ya que presenta una menor retención que las convecionales C18. Se optimizó el tratamiento de muestra y la cromatografía. Se hicieron pruebas con diversos gradientes y fases móviles para finalmente inyectarlo con el siguiente: *A: H_2O 0.1 %HCOOH, B: MeOH 0.1%HCOOH (25% → 75% B). E*n la **figura III. 2** se muestra como ejemplo la diferencia entre una muestra liofilizada y una centrifugada.

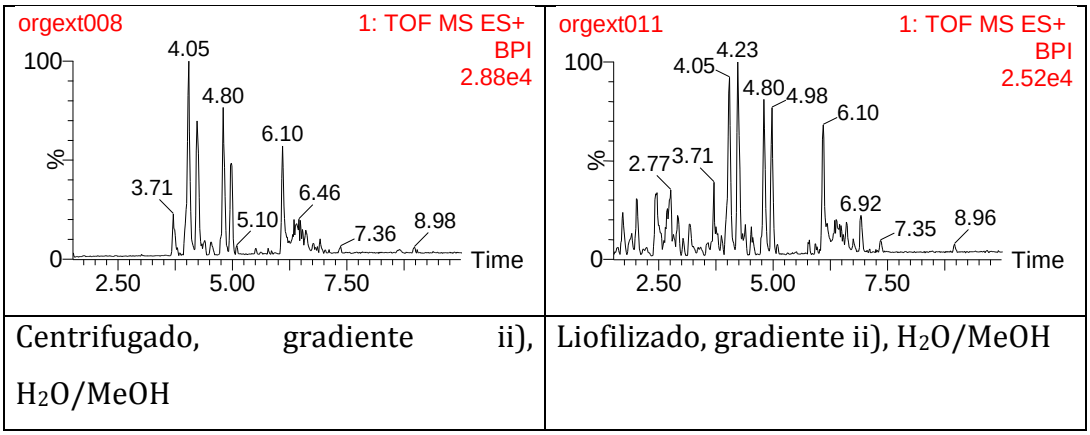

Centrifugado, gradiente ii), H_2O/MeOH	Liofilizado, gradiente ii), H_2O/MeOH

Figura III.2. Muestras de rhGH inyectadas en columna C8. a) Tratamiento de muestra mediante centrifugación, b) Tratamiento de muestra mediante liofilización

Como puede verse en la figura III.2, aunque en las muestras liofilizadas se detectó un número de compuestos ligeramente mayor, no se observaron grandes diferencias.

Se estudiaron los marcadores obtenidos en el proceso en el que se incluia la liofilización y se observó que este análisis conducía a los mismos marcadores obtenidos con la columna C18 y orina centrifugada, presentados en el *artículo científico 5*. En modo de ionización positiva, se encontraron los iones marcadores M125T254, M200T254 y M222T254, que se explican como la molécula protonada M200T254, un fragmento M125T254 y el aducto $[M+Na]^+$ M222T254 de un mismo compuesto, respectivamente. En modo de ionización negativa, se observó el ión marcador M198T254, que se justifica como el $[M-H]^-$ del mismo compuesto que se observaba en positivo. Tras comprobar las masas exactas y sus espectros, se concluyó que se trataba del mismo marcador que el presentado en RP con columna C18, la octenoil-glicina (Δ^xC8-Gly).

3) Análisis de las muestras

A diferencia del capítulo II, en estos trabajos se ha hecho uso de la cromatografía de líquidos en lugar de la cromatografía de gases, ya que resulta más adecuada tanto para compuestos de polaridad media-alta, poco volátiles y térmicamente lábiles como para la matriz de estudio, orina. Se eligió la **LC** debido a su mayor universalidad y simplicidad en el tratamiento de muestra (no requiere de la etapa de derivatización), así como por su adecuación a los metabolitos esperados (polares). Así mismo, permite un fácil acoplamiento a analizadores de masas de amplio rango, interesante en estudios metabolómicos donde el rango de masa de los metabolitos a detectar debe ser lo más amplio posible.

En el caso de la rhGH se inyectaron las muestras tanto en **columnas** RP como HILIC, para que el alcance del *screening* fuera mayor. Por lo que respecta a la testosterona sólo se inyectaron en RP, ya que en este estudio la complejidad estaba en inyectar las muestras con dos analizadores diferentes. En ambos casos y con todas las columnas estudiadas, las muestras se inyectaron en modo de ionización positivo y negativo. Mientras que con la columna RP se cromatografían compuestos de polaridad media-alta, con la columna HILIC se detectan compuestos muy polares, como aminoácidos o péptidos pequeños.

Las fases móviles, modificadores y gradiente fueron optimizados de forma que se observara el mayor número posible de picos a lo largo del cromatograma BPI (Base Peak Ion chromatogram). El BPI representa la intensidad del pico más intenso en cada punto del análisis, por lo que es similar al TIC pero visualmente más limpio. En este caso, al tratarse de tabajos no dirigidos o *untargeted* no se pueden optimizar los parámetros dirigidos a un compuesto o grupo de compuestos conocidos, como ocurre en

los trabajos *target* como los expuestos en el capítulo anterior. En la **figura III.3** se observa un ejemplo de rhGH en columna RP y modo de ionización negativo.

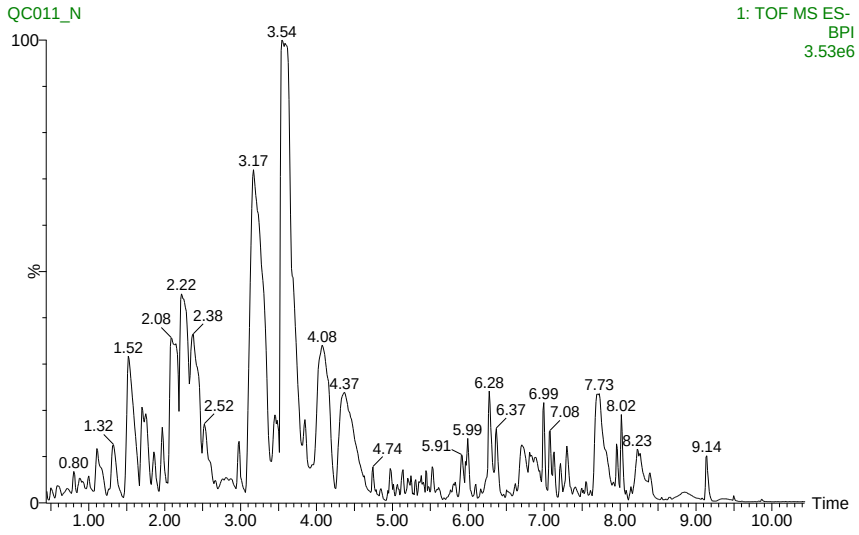

Figura III.3 Ejemplo de un Base Peak Ion chromatogram (BPI) de una muestra QC inyectada en columna RP en modo de ionización negativo

La **fase móvil** utilizada en RP en ambos casos fue la misma, H_2O/MeOH con 0.01%(v/v) de ácido fórmico (HCOOH) como modificador. Los **modificadores** en LC sirven para regular el pH, facilitando en muchos casos la cromatografía. Además, mejoran la ionización facilitando la formación de iones protonados $[M+H]^+$, que pueden aumentar la sensibilidad. En el caso de HILIC para el estudio de rhGH, la fase móvil empleada fue ACN/H_2O con acetato amónico (NH_4Ac, 10mM) como modificador para mejorar la cromatografía en la medida de lo posible, ya que estas columnas retienen mejor los compuestos en presencia de altas concentraciones de sales.

Se realizaron pruebas con dos columnas HILIC distintas, BEH HILIC y BEH Amide, con distintos gradientes, distintas fases móviles y porcentajes. También se evaluó si mejoraba la adición o no de HCOOH. Las fases móviles óptimas fueron (A) 95% ACN 5% H_2O NH_4Ac 10mM y (B) H_2O NH_4Ac 10mM; con el gradiente en porcentaje de variación de B: 1.5 min, 2%; 2.5 min, 15%; 6 min, 50%; 7.5 min, 75%; 7.51 min, 2% and 9.50 min, 2%; utilizando una columna Acquity UPLC BEH Amide (1.7 µm, 2.1 x 100 mm). A continuación, se muestra un cromatograma BPI con el gradiente optimizado para HILIC (**figura III.4**).

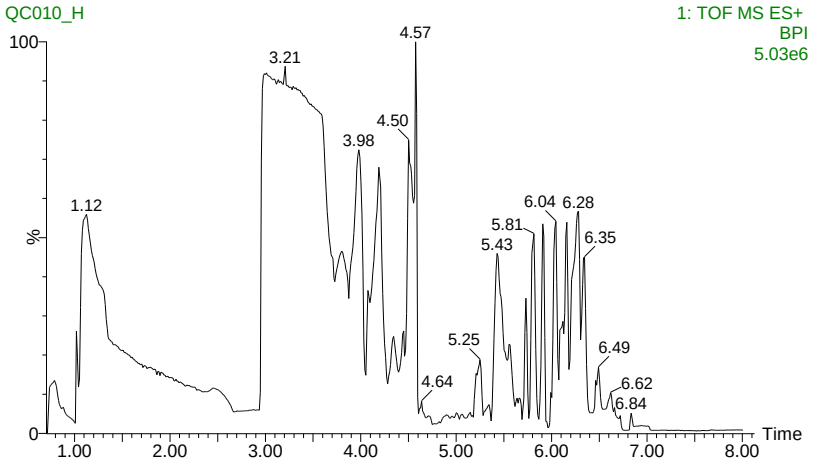

Figura III.4 Ejemplo de un Base Peak Ion chromatogram (BPI) de una muestra QC inyectada en columna HILIC en modo de ionización positivo

Siguiendo con la parte instrumental del proceso analítico, la **fuente** seleccionada fue la de ESI. Esta es la fuente más utilizada en LC-MS, adecuada para analitos polares proporcionado la molécula protonada $[M+H]^+$, desprotonada $[M-H]^-$ o formando aductos.

En cuanto a los **analizadores** seleccionados, como ya se comentó, fueron analizadores de alta resolución, QTOF y (Q)Orbitrap (en el caso de la testosterona). En el caso de trabajos de metabolómica no dirigida, la metodología debe cumplir requisitos como presentar un amplio rango de aplicación, adecuada sensibilidad y proporcionar información estructural útil. Estos requisitos se consiguen con los analizadores mencionados, ya que se detecta un número elevado de compuestos y, gracias a la masa exacta, se pueden llegar a elucidar los compuestos de interés. Entrando más en detalle en estos aspectos, vemos, en el *artículo científico 4* acerca de la testosterona, que en el QTOF se obtienen del orden de 10000-12000 picos (ESI positivo y negativo, respectivamente), mientras que en el QOrbitrap 5500-7500 (ESI negativo y positivo, respectivamente). Estos picos incluyen isótopos, aductos o fragmentos en la fuente (*in-source fragments*). Estas diferencias pueden deberse a una mayor sensibilidad por parte del QTOF, una mayor generación de aductos o *in-source fragments* por parte de la fuente ESI del QTOF, o por una combinación de ambos factores. A la vista del marcador obtenido en el caso de la testosterona, la hipótesis de la mayor generación de fragmentos en la fuente ESI del QTOF resulta más plausible, ya que en este caso se obtiene también como ión marcador M95T295, fragmento en la fuente del marcador M170T295, mientras que en las inyecciones del QOrbitrap sólo se observa el compuesto padre.

Referente a los modos de trabajo llevados a cabo en QTOF y el Q Orbitrap, fueron modo SCAN (MS^E/AIF) y modo MS/MS. El primero nos proporciona una adquisición del espectro completo en un amplio rango de m/z y mayor sensibilidad. Por su parte, el modo MS/MS es menos sensible pero nos permite aislar *m/z* consiguiendo una mayor especificidad, y aportando información estructural útil.

Los parámetros relevantes a la hora de comparar los analizadores de masa son el poder de resolución, la exactitud de masa, la sensibilidad y la especificidad. El poder de resolución se define como la capacidad de un analizador de masas de distinguir entre dos iones de *m/z* próximas. Se trata de un parámetro crucial a la hora de asegurar una buena exactitud de masas en muestras muy complejas. Por otro lado, la exactitud de masa mide la capacidad de ofrecer un valor de *m/z* muy cercano al valor real. Para conseguir una exactitud de masa robusta se requiere un poder de resolución adecuado así como una correcta calibración del eje de masas. Cuanto mayor sea la exactitud de masa con mayor seguridad podremos confirmar la identidad de un analito, facilitando la labor de elucidación

Se podría concluir que la técnica UHPLC-ESI-HRMS es la más apropiada para estudios metabolómicos abiertos, ya que (i) mediante la cromatografía de líquidos se evita la pérdida de compuestos con tratamiento de muestra *dilute and shoot*, (ii) gracias a la resolución cromatográfica del UHPLC se pueden separar potenciales compuestos isobáricos, (iiI) la fuente ESI se ionizan compuestos de un amplio rango de polaridades y pesos moleculares y (iv) utilizando analizadores de alta resolución, se obtiene información estructural en masa exacta de gran utilidad a la hora de elucidar los marcadores. Si por el contrario, se planteara un estudio de metabolómica dirigida, la selección de la

técnica se decantaría por instrumentos de triple cuadrupolo, mucho más adecuados para análisis *target,* en términos de sensibilidad y especificidad.

4) Tratamiento de datos

Como se comentó en la introducción, el software empleado para el **pre-tratamiento de los datos** en los trabajos presentados en este capítulo fue el paquete de R, XCMS. Mediante este paquete se lleva a cabo el *Peak Picking*, la alineación de los tiempos de retención y la integración de los picos. En la **figura III.5** se muestran los parámetros empleados en cada paso dentro del software *R* con el paquete *XCMS.* Dentro del primer paso (*peak picking*), el parámetro *Peakwidth* (5, 20) establece en segundos la anchura mínima esperada (5 segundos) y máxima (20 segundos) de los picos del cromatograma. Con la variable *Prefilter* (3,1000) se indica que para considerar un pico como tal, al menos 3 de sus puntos deben tener una señal mayor o igual a 1000 cuentas. *Snthresh* (10) indica la mínima relación señal/ruido que se establece para definir un pico. Y finalmente *ppm* es el máximo error de masa aceptado a lo largo del pico para asignar a un único ión como responsable de la aparición de ese pico. Típicamente se emplea 3 veces el error de masa del analizador utilizado. En este caso, fue menor para el QOrbitrap (5ppm) que para los análisis por QTOF (10-15ppm). Finalmente, para todos los iones que generan picos cromatográficos, sus correspondientes áreas de pico son integradas.

El siguiente paso es agrupar los picos alineando los tiempos de retención ya que pueden variar ligeramente entre muestras o a lo largo de la secuencia de análisis por efecto de la matriz sobre la separación cromatográfica. Para ello se emplea la función *group*, variando el *band width* (bw) o la anchura en la que los picos pueden moverse desde unos 5-10 s iniciales hasta un

alineamiento (mediante la función *retcor*) inferior a 1 segundo en los tiempos de retención. Para ello se aplica un valor *missing* de 10, que indica el número de muestras en el que permitimos que no esté el compuesto para utilizarlo en el alineamiento de los tiempos de retención. Por último, se integran las muestras en las que no se ve pico o se ve por debajo de los requisitos para evitar que haya iones sin área de pico asignada (*fillPeaks*). Finalmente, se generan las tablas Excel que, a continuación, se normalizan y a las que se aplica el posterior análisis multivariante.

La metodología para la **normalización** de los datos aplicada se basó en la mediana de la respuesta de todos los metabolitos detectados. Mediante un algoritmo iterativo (*Loess Normalization*) se consigue igualar la mediana de la señal de todos los metabolitos en las diferentes muestras. En algunos casos puede resultar necesaria y en otros no. En ambos trabajos se aplicó este proceso con buenos resultados, tal y como se muestra en las figuras correspondientes de *Supplementary Information* en cada caso.

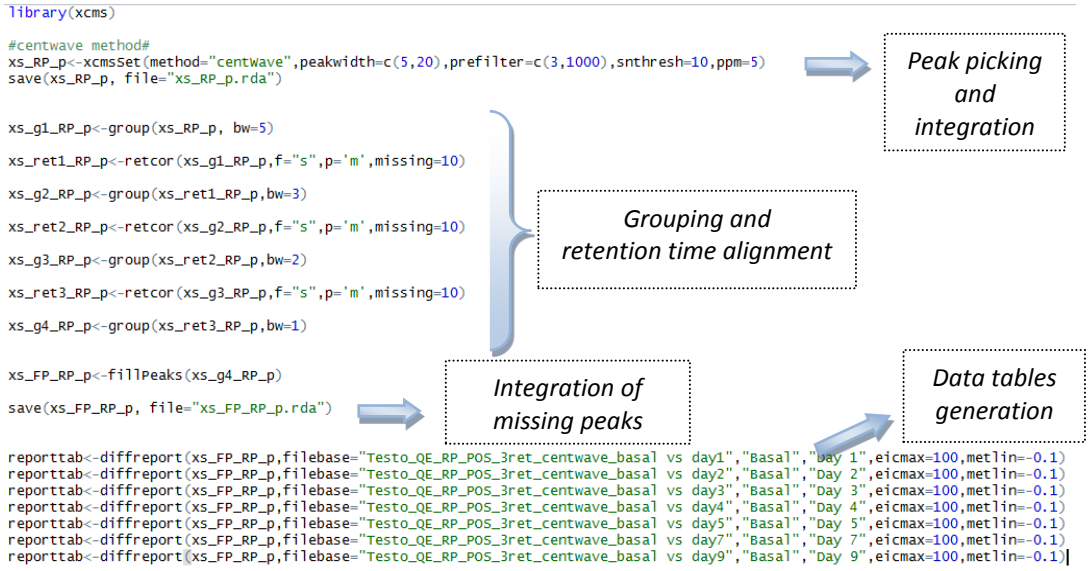

Figura III.5 Parámetros utilizados en el *script* de trabajo en *R*. Ejemplo del estudio de testosterona en QOrbitrap, (RP_ESI positivo)

Una vez realizada la normalización, se genera una tabla de datos aplicando logaritmos en base 2 a las intensidades, de manera que la escala numérica que alimenta al análisis multivariante se reduce. Este proceso evita que picos de gran intensidad encubran picos de menor escala pero de igual importancia. El análisis multivariante (sobre todo el PCA) reduce la dimensionalidad de los datos intentando explicar el máximo de varianza del conjunto, pero mira desviaciones estándar no relativas, por lo que aquellas variables que se encuentren a mayor escala tendrán una mayor varianza e influirán en mayor medida en la creación del modelo estadístico. Con el mismo objetivo, la aproximación Varianza Unitaria (*Unit Variance*) aplicada por el *software* en estos trabajos, permite minimizar este efecto, dando el mismo peso a todas las variables.

En cuanto al **análisis multivariante**, se ha llevado a cabo mediante el software *EZInfo* (Umetrics, Umea, Sweden), y el procedimiento que se siguió

también fue equivalente en ambos trabajos, el de la rhGH y el de la testosterona. Es destacable la importancia de los QC en estos estudios. Estas muestras QC son una mezcla de todas las muestras del estudio y se inyectan diez al principio de la secuencia y uno cada diez muestras, con el fin primero de estabilizar el sistema cromatográfico y después de comprobar la estabilidad y robustez de las medidas a lo largo de la secuencia de análisis. Esto se comprueba mediante un análisis por PCA, donde se observa que estas muestras estén lo más centradas y juntas posible. En la Figura S3 (*Supporting Information*) del *artículo científico 4* de este capítulo o las figuras S2 y S3 del *artículo científico 5*, se puede apreciar como los QC de estos estudios en los correspondientes PCA, siempre se encuentran relativamente centrados y juntos.

Como se indica en la introducción general (I.3.2), los siguientes pasos en el análisis multivariante son el PLS-DA y el OPLS-DA, análisis discriminantes. En el primero se indican las clases en las que se pueden agrupar las muestras para trabajar con ellas, por ejemplo "día", "voluntario"... En el OPLS-DA (ortogonal) se enfrentan dos grupos de muestras dentro de esas clases. En nuestro caso, lo más útil es enfrentar "muestras previas a la administración" frente a "muestras posteriores a la administración" ya sea agrupando días posteriores a la administración como hicimos en el caso de la testosterona o frente a un día en concreto donde la respuesta de los marcadores fuera mayor, como ocurrió en el caso de la rhGH. El S-Plot que se genera en este punto está formado por todos los compuestos y, en los extremos, encontramos los compuestos que mejor explican la separación de estos grupos. En la **figura III.6** se muestra un ejemplo de S-Plot.

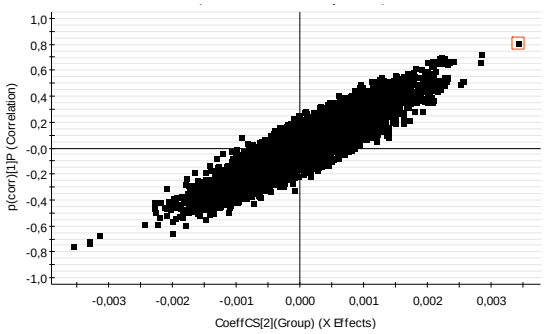

Figura III.6 S-Plot obtenido en el análisis C8, ESI negativo. Marcador M198T254 destacado en rojo

El siguiente paso es estudiar los máximos candidatos, de mayor a menor p(corr) y teniendo en cuenta su tendencia en el *Variable Trend Plot*, así como su forma cromatográfica, etc. En la **figura III.7** se muestra el *Variable Trend Plot* para el marcador obtenido en RP para la rhGH (*artículo científico 5*), donde se ve una tendencia diferente entre muestras control y tras la administración de rhGH.

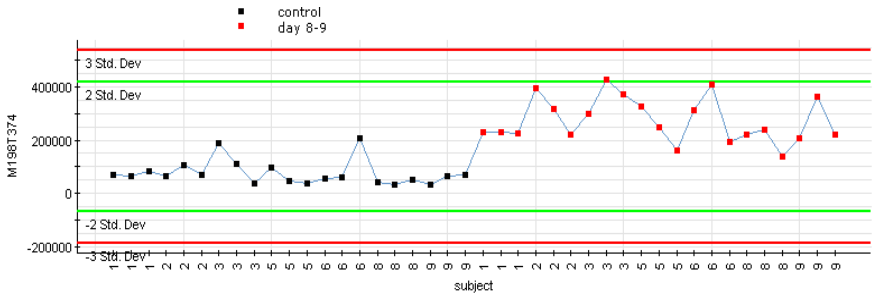

Figura III.7. *Variable Trend Plot* del marcador M198T374 de la rhGH (RP, ESI negativo)

Siguiendo con éste marcador como ejemplo, ya que en negativo seleccionamos el marcador M198T374, es por elloque también buscamos y seleccionamos en positivo el marcador M200T374, aunque estuviera un poco por debajo del umbral marcado de p(corr)=0.5. El hecho de que sea un

compuesto que ionice en modo positivo y negativo es, por tanto, de ayuda para la siguiente etapa, la **elucidación** de los marcadores. Éste paso, realizado en ambos artículos científicos, es crucial en el proceso analítico en metabolómica. Para ello, a partir de sus masas exactas se realizaron experiencias de MS/MS con el objetivo de estudiar los iones producto y poder establecer relaciones que nos llevaran hasta su estructura. Como se encuentra detallado en los artículos, una vez se disponía de una hipótesis se sintetizaron los compuestos o se compraron los patrones, si éstos estaban disponibles comercialmente, como fue el caso de la carnitina. A continuación se compararon los espectros de iones producto y los tiempos de retención para confirmar la identidad de los marcadores. En el caso del marcador M198T374 resulta necesario más trabajo de síntesis para determinar qué compuesto es exactamente, sabiendo que es una octenoil-glicina (Δ^xC8-Gly) pero con el ácido octenoico sin confirmar estructuralmente.

Finalmente, se intenta dar una **explicación biológica** a cada uno de los marcadores seleccionados, este paso es crucial a la hora de entender qué mecanismo ha hecho destacar a dichos marcadores. En el caso de rhGH, el marcador obtenido por RP, la octenoil-glicina (Δ^xC8-Gly), podría tener sentido, ya que, tal como ha sido reportado, diversos ácidos carboxílicos son excretados conjugados con glicina (Gregus *et al.*, 1996). Por otro lado, el marcador obtenido por HILIC, la carnitina, ha sido reportado previamente como marcador de administración de reGH en caballos (Boyard-Kieken *et al.*, 2011).

El marcador obtenido en el caso del estudio de la testosterona fue el 1-ciclopentenoil glicina, que proviene de la parte del cipionato con el que está combinada la testosterona cuando se aplica de forma inyectada, por lo que este marcador también tiene una clara explicación. No obstante, para incluir

estos marcadores en un *screening* de rutina de un laboratorio antidopaje todavía se requiere de trabajo y estudio de los marcadores y de su potencial, así como descartar que puedan venir de otras vías que no sea la administración de la sustancia dopante en cuestión.

CAPÍTULO IV

DISCUSIÓN GENERAL

Discusión General

Como se ha ido viendo a lo largo de los capítulos previos, en la presente Tesis Doctoral se fusionan dos grandes campos, la **química analítica** y el **control del dopaje**. En los trabajos presentados en los Capítulos II y III, se ha tratado de evaluar el potencial de diversas técnicas analíticas de vanguardia (como la fuente APCI), así como diferentes estrategias de tratamiento de datos y búsqueda de marcadores (estrategias metabolómicas), con el fin de mejorar la detección de sustancias preocupantes dentro del control del dopaje.

Los laboratorios de control del dopaje se enfrentan a menudo a la necesidad de una elevada sensibilidad en sus métodos de análisis, así como al reto de diferenciar entre compuestos endógenos y exógenos y a la posibilidad de la existencia de compuestos dopantes desconocidos de similar estructura en las muestras. Debido a todo esto, se requiere instrumentación analítica avanzada que permita detectar sustancias prohibidas con la máxima sensibilidad y especificidad posibles, así como descubrir nuevas sustancias o metabolitos.

En nuestro caso, se han estudiado diferentes familias de compuestos problemáticos por diferentes motivos. Por una parte, los AAS forman el grupo de sustancias dopantes con un número más elevado de casos positivos reportados por los laboratorios. La dificultad en su análisis radica, por ejemplo, en la similitud entre compuestos exógenos y endógenos (presentes naturalmente en la orina), así como en la baja concentración a la que se puedan encontrar transcurrido un tiempo desde su ingesta en la orina. El objetivo de los dos primeros trabajos ha sido la evaluación del comportamiento de ionización y fragmentación de estos compuestos

mediante la fuente APCI para GC (Capítulo II, *artículos científicos 1 y 2*), para relacionarlo con sus estructuras y poder mejorar, en la medida de lo posible, la sensibilidad y/o selectividad, a la hora de trabajar en modo SRM (Capítulo II, *artículo científico 3)*. La información obtenida de estos trabajos puede ser de utilidad en el campo del control del dopaje a la hora de buscar o identificar compuestos o metabolitos desconocidos que pudieran ser mejores marcadores del abuso que el mismo compuesto ingerido. Ligando ambos Capítulos, I y II, cabe destacar el *artículo científico 4* que también se focaliza en un esteroide. En este caso, se pretendía buscar marcadores del abuso de testosterona exógena gracias a un estudio de excreción en el que participaron tanto individuos caucásicos como asiáticos. Las muestras se analizaron mediante LC acoplada a analizadores de alta resolución y aplicando estrategias metabolómicas.

En el *artículo científico 5*, la sustancia dopante a estudiar también fue un compuesto endógeno, como la hormona del crecimiento. El problema en su detección viene dado por su corta vida media, su baja concentración y secuencia idéntica de aminoácidos entre la hormona recombinante y la natural. Además, las metodologías disponibles actualmente se basan en la detección en muestras de sangre, con la complicación que esto conlleva respecto a la toma de muestra. El objetivo de este trabajo (al igual que en el mencionado anteriormente) consistía en buscar marcadores de abuso, provenientes de cambios en el metabolismo desencadenados por el consumo de rhGH, es decir, compuestos que se vieran alterados bien aumentando o bien disminuyendo su concentración y que pudieran resultar mejores marcadores que la propia rhGH. Como ya se ha mencionado, pero es importante destacar, tras encontrar y elucidar marcadores del abuso de una sustancia dopante mediante herramientas metabolómicas *untargeted*, es necesario estudiar su significado biológico, así como la idoneidad y aplicabilidad de los marcadores encontrados dentro del campo del control del dopaje.

Como visión global, a lo largo de los artículos científicos presentados en la presente Tesis Doctoral, se ha trabajado con diversos compuestos como son los AAS o la rhGH, de manera dirigida mediante métodos SRM y no dirigida gracias a estrategias metabolómicas. Se han utilizado técnicas analíticas de cromatografía de gases y de líquidos, comparando la detección de analitos derivatizados y sin derivatizar. Asimismo, se ha hecho uso de distintos analizadores, de baja resolución (QqQ) o de alta resolución (QTOF y QOrbitrap), dependiendo del objetivo del trabajo en cada caso. Finalmente, en el caso de GC, se han comparado distintas fuentes de ionización (EI vs. APCI).

La novedad de la aplicación de la fuente APCI para detección de esteroides, así como el uso de la metabolómica *untargeted,* abre nuevas vías de investigación en un campo que trabaja de la mano de los nuevos avances analíticos con el fin de acabar con el fraude en el deporte, siempre presente y en continuo desarrollo.

CAPÍTULO V

CONCLUSIONES

Conclusiones

Las líneas de investigación llevadas a cabo durante el desarrollo de esta Tesis Doctoral han permitido evaluar el potencial de la instrumentación analítica más reciente aplicada al campo del control del dopaje. Las **conclusiones principales** son: la fuente APCI para cromatografía de gases es una buena alternativa para el estudio y detección de esteroides anabolizantes androgénicos y la cromatografía de líquidos acoplada a analizadores de alta resolución, junto con las estrategias metabolómicas, constituyen herramientas útiles a la hora de detectar marcadores desconocidos del abuso de sustancias dopantes.

De los trabajos expuestos se pueden extraer una serie de **conclusiones específicas** que se detallan a continuación:

- El estudio del comportamiento de ionización y fragmentación de un elevado número de AAS mediante la fuente APCI ha permitido establecer relaciones entre dicho comportamiento y sus estructuras. Esto supone un avance en el conocimiento de esta familia de compuestos pudiendo resultar de utilidad a la hora de elucidar metabolitos desconocidos, relacionando patrones de ionización/fragmentación con sus estructuras.
- La adición de agua en la fuente APCI favorece la reacción de transferencia de protones generando, mayoritariamente en el caso de AAS, las especies protonadas, tanto para compuestos derivatizados como sin derivatizar.
- La similitud estructural dentro del grupo de los AAS y la existencia de interferentes esteroidales endógenos, dificulta la selección de transiciones específicas a la hora de trabajar en modo SRM.

- La fuente APCI se presenta como una alternativa adecuada a la fuente EI para la determinación de AAS en orina, en términos de precisión y sensibilidad. El aumento notable de sensibilidad puede ser de gran importancia en casos como el de la 4-cloro-metandienona, en el cual se amplía la ventana de detección temporal respecto a los análisis por EI.
- El uso de LC-HRMS junto con estrategias metabolómicas se presenta como una herramienta prometedora a la hora de buscar, de forma no dirigida, marcadores derivados del abuso de sustancias dopantes, sobre todo para compuestos endógenos.
- La selección de un adecuado tratamiento de muestra, condiciones cromatográficas y espectrométricas, así como un apropiado tratamiento de datos, es de gran importancia para obtener resultados de alta calidad en trabajos de metabolómica.
- A la hora de incorporar un marcador en los análisis de rutina en los laboratorios de control del dopaje, éste debe superar una serie de pasos previos, como que su exaltación o disminución pueda ser explicada biológicamente, o demostrar su idoneidad como marcador de una sustancia en concreto. La metabolómica en la búsqueda y la espectrometría de masas en la elucidación de los marcadores, son tan sólo el primer paso a la hora de conseguir establecer como válido un marcador dentro del análisis de control del dopaje.

CHAPTER V

CONCLUSIONS

Conclusions

The lines of research carried out in the development of this Doctoral Thesis, allowed for the evaluation of the potential of the recent analytical instrumentation in application to the doping control field. The **main conclusion** are: APCI source for GC is an adequate alternative for the study and detection of anabolic androgenic steroids and, liquid chromatography coupled to high resolution analyzers together with metabolomic strategies, are useful tools for the detection of unknown markers of the misuse of prohibited substances.

A series of **specific conclusions** are also extracted and they are detailed below:

- The study of ionization and fragmentation of a high number of AAS by means of APCI source has allowed establishing relationships between that behavior and their structures. This fact presents an advance in the knowledge of this family of compounds and it can be useful for the elucidation of unknown metabolites, making relations between ionization/fragmentation patterns and their structures.
- The addition of water to the APCI source favors the proton transfer reaction generating, mainly, protonated AAS species, for derivatized and underivatized compounds.
- Structural similarities of the compounds of the group of AAS and the existence of endogenous steroidal interferences complicate the selection of specific transitions working in SRM mode.
- APCI source is presented as an appropriate alternative to EI source for the determination of AAS in urine, in terms of precision and

sensitivity. The noticeable increase of sensitivity can be of great relevance in some cases such as for 4-chloro-methandienone. For this compound, the detection time window is increased in comparison to EI analysis.

- Use of LC-HRMS and metabolomic strategies is presented as a promising tool for searching unknown markers derived from prohibited substances in sport; specially, for endogenous substances.
- The selection of an adequate sample treatment, chromatographic and MS conditions, as well as, an appropriate data treatment is of great relevance to obtain high-quality results in metabolomic works.
- To incorporate a selected marker into the routine analysis of the doping control laboratories, the marker should be appropriate for a determined substance. That is, it should have a biological explanation. For this reason, the selected marker should pass a series of tests. Metabolomics for the search and mass spectrometry for the elucidation of the markers are only the first steps in order to achieve the goal of incorporating a marker into the doping control analysis.

CAPÍTULO VI

BIBLIOGRAFÍA

Aguilera R., Catlin D. H., Becchi M., Phillips A., Wang C., Swerdloff R. S., Pope H. G, Hatton C. K. (1999) "Screening urine for exogenous testosterone by isotope ratio mass spectrometric analysis of one pregnanediol and two androstanediols". Journal of Chromatography B, 727: 95–105

Ardrey B. (2003) "Liquid Chromatography-Mass Spectrometry: An introduction". Analytical Techniques in the Sciences. ISBN: 0-471-49801-7

Armitage E. G., Rupérez F. J., Barbas C. (2013) "Review: Metabolomics of diet-related diseases using mass spectrometry". Trends in Analytical Chemistry, 52: 61-73

Ayotte C., Goudreault D., Charlebois A. (1996) "Testing for natural and synthetic anabolic agents in human urine". Journal of Chromatography B, 687: 3-25

Barceló D. (1996) "Applications of LC-MS in environmental chemistry". Journal of Chromatography Library. Volume 59. ISBN: 0-444-82067-1

Beckett A. H., Cowan D. A. (1976) "Misuse of drugs in sport". British Journal of Sports Medicine, 12: 185-194

Boccard J., Badoud F., Grata E., Ouertani S., Hanafi M., Mazerolles G., Lantéri P., Veuthey J-L., Saugy M., Rudaz S. (2011) "A steroidomic approach for biomarkers discovery in doping control". Forensic Science International, 213: 85-94

Boccard J., Rutledge D. N. (2013) "A consensus orthogonal partial least squares discriminant analysis (OPLS-DA) strategy for multiblock Omics data fusion". Analytica Chimica Acta, 769: 30-39

Boccard J., Badoud F., Jan N., Nicoli R., Schweizer C., Pralong F., Veuthey J-L., Baume N., Rudaz S., Saugy M. (2014) "Untargeted profiling of urinary steroid metabolites after testosterone ingestion: opening new perspectives for antidoping testing" Bioanalysis, 6(19): 2523-2536

Bosch J., Such-Sanmartín G., Segura J., Gutiérrez-Gallego R. (2012) " Tracking gowth hormone abuse in sport: Performance of marker proteins in a controlled setting". Analytica Chimica Acta, 754: 118-123

Botrè T, Pavan A. (2008) "Enhancement drugs and the athlete". Neurologic Clinics, 26: 149-167

Boyard-Kieken F., Dervilly-Pinel G., Garcia P., Paris A-C., Popot M-A., Le Bizec B., Bonnaire Y. (2011) "Comparison of different liquid chromatography stationary phases in LC-HRMS metabolomics for the detection of recombinant growth hormone doping control". Journal of Separation Science, 34: 3493-3501

Brereton, R. G. (2003) "Chemometrics: Data Analysis for the Laboratory and Chemical Plant". John Wiley & Sons. ISBN 0-471-48977-8

Brooks R. V., R. G. Firth, Sumner N. A. (1975) "Detection of anabolic steroids by radioimmunoassay". British Journal of Sports Medicine, 9: 89-92

Brun E. M., Puchades R., Maquieira A. (2011) "Analytical methods for anti-doping control in sport: anabolic steroids with 4,9,11-triene structure in urine".Trends in Analytical Chemistry, 30(5): 771-783

Catlin D. H., Kammerer R. C., Hatton C. K., Sekera M. H., Merdink J. L. (1987) "Analytical chemistry at the games of the XXIIIrd Olympiad in Los Ángeles". Clinical chemistry, 33: 319-327

Cawley A. T., Trout G. J., Kazlauskas R., Howe C. J., Georde A. V. (2009) "Carbon isotope ratio (δ13C) values of urinary steroids for doping control in sport". Steroids, 74: 379-392

Courant F., Pinel G., Bichon E., Monteau F., Antignac J-P., Le Bizec B. (2009) "Development of a metabolomic approach based on liquid chromatography-high resolution mass spectrometry to screen for clenbuterol abuse in calves". Analyst, 134: 1637-1646

Cubbon S., Antonio C., Wilson J., Thomas-Oates J. (2010) "Metabolomic Applications of HILIC-LC-MS". Mass Spectrometry Reviews, 29: 671-684

Dass C. (2007) "Fundamentals of Contemporary Mass Spectrometry". Wiley-Interscience Series on Mass Spectrometry. ISBN: 978-0-471-68229-5

Delbeke F.T. (2000) "From amanita muscaria to somatotropine: the doping story". Biology of Sport, 17(2): 81-86.

Dettmer K., Aronov P. A., Hammock B. D. (2007) "Mass spectrometry-based metabolomics". Mass Spectrometry Reviews, 26: 51-78

Deventer K., Pozo O. J., Verstraete A. G., Van Eenoo P. (2014) "Dilute-and-shoot-liquid chromatography-mass spectrometry for urine analysis in doping control and analytical toxicology". Trends in Analytical Chemistry, 55: 1-13

Díaz R., Pozo O. J., Sancho J. V., Hernández F. (2014) "Metabolomic approaches for Orange origin discrimination by ultra-high performance líquid chromatography coupled to quadrupole time-of-flight mass spectrometry". Food Chemistry, 157: 84-93

Donike M. (1969) "N-Methyl-N-trimethylsilyl-trifluoroacetamid, ein neues silylierungs mittel aus der reihe der silylierten amide". Journal of Chromatography, 42: 103-104

Donike M., Bärwald K-R., Klostermann K., Schänzer W., Zimmermann J. (1983) "Nachweis von exogem testosterone" (Detection of exogenous testosterone). Editors: Heck H., Hollmann W., Leisen H., Rots R. Testosterone in sport: leistung und gesundheit 1983:293-300

Dunn W. B., Ellis D. I. (2005) "Metabolomics: Current analytical platforms and methodologies". Trends in Analytical Chemistry, 24 (4) 285-294

Erotokritou-Mulligan I., Guha N., Stow M., Eryl Bassett E., Bartlett C., Cowan D. A., Sönksen P. H., Holt R. I. G (2012) "The development of decision limits for the implementation of the GH-2000 detection methodology using current commercial insulin-like growth factor-I and amino-terminal pro-peptide of type III collagen assays". Growth Hormone & IGF Research, 22: 53-58

Fabregat A., Pozo O. J., Marcos J., Segura J., Ventura R. (2013) "Use of LC-MS/MS for the Open Detection of Steroid Metabolites Conjugated with Glucuronic Acid". Analytical Chemistry, 85(10): 5005–5014

Geraline C. L., Erinoff L. (1990) "Anabolic Steroid Abuse". National Institute on Drug Abuse. Research Monograph, 102.

Geyer H., Schänzer W., Thevis M. (2014) "Anabolic agents: recent strategies for their detection and protection from inadvert doping". British Journal of Sports Medicine, 48:820–826.

Gómez C., Fabregat A., Pozo O. J., Marcos J., Segura J., Ventura R. (2013) "Analytical strategies based on mass spectrometric techniques for the study of steroid metabolism". Steroids, 78(12-13): 1245–1253

Gregus Z., Fekete T., Halászi E., Klaassen C. D. (1996) "Lipoic acid impairs glycine conjugation of benzoic acid and renal excretion of benzoylglycine". Drug Metabolism and Disposition, 24, 682-688

Grob R. L., Barry E. F. (2004) "Modern practice of gas chromatography". Wiley-Interscience, John Wiley & Sons, Inc., NY. ISBN: 978-0-471-22983-4

Hartgens F., Kuipers H. (2004) "Effects of androgenic-anabolic steroids in athletes". Sports Medicine, 34:8, 513-554

Hemmersbach P. (2008) "History of mass spectrometry at the Olympic Games". Journal of Mass Spectrometry, 43:839-853

Hübschmann H-J. (2001) "Handbook of GC-MS. Fundamentals and Applications". Wiley-VCH. ISBN: 3-527-30170-4

Horning E. C., Carroll D. I., Dzidic I., Haegele K. D., Lin S-N., Oertli C. U., Stillwell R. N. (1977) "Development and use of analytical systems based on mass spectrometry". Clinical Chemistry, 23(1): 13-21

Idborg-Bjorkman H., Edlund P. O., Kvalheim O. M. Schuppe-Koistinen I., Jacobsson S. P. (2003) "Screening of biomarkers in rat urine using LC/electrospray ionization-MS and two-way data analysis". Analytical Chemistry, 75: 4784-4792

Kuhn C. M. (2002) "Anabolic Steroids". Recent Progress in Hormone Research, 57:411-434

Kieken F., Pinel G., Antignac J-P., Paris A-C., García P., Popot M-A., Grall M., Mercadier V., Toutain P. L., Bonnaire Y., Le Bizec B. (2011) " Generation and processing of urinary and plasmatic metabolomic fingerprints to reveal an illegal administration of recombinant equine human growth hormone from LC-HRMS measurements". Metabolomics, 7: 84-93

Kim H., Ahna E., Hee Moon M. (2008) "Profiling of human urinary phospholipids by nanoflow liquid chromatography/tandem mass spectrometry". Analyst, 133, 1656-1663

Kiss A., Lucio M., Fildier A., Buisson C., Achmitt-Kopplin P., Cren-Olivé C. (2013) "Doping Control Using High and Ultra-High Resolution Mass Spectrometry Based Non-Targeted Metabolomics. A Case Study of Salbutamol and Budesonide Abuse" Plos One, 8(9): 1-13.

Kniess A., Ziegler E., Thieme D., Müller R. K. (2013) "Intra-individual variation of GH-dependent markers in athletes: Comparison of population based and individual thresholds for detection of GH abuse in sports". Journal of Pharmaceutical and Biomedical Analysis, 84: 201– 208

Kochakian C. D. (1976) "Anabolic-Androgenic Steroids". Springer-Verlag. Berlin

Kremenik M., Onodera S., Nagao M., Yuzuki O., Yonetani S. (2006) "A historical timeline of doping in the Olympics (Part 1 1896-1968)". Kawasaki Journal of Medical Welfare, 12: 19-28.

Li D-X., Gan L., Bronja A., Schmitz O. J. (2015) "Gas chromatography coupled to atmospheric pressure ionization mass spectrometry (GC-API-MS): Review". Analytica Chimica Acta, 891: 43-61

Lu X., Zhao X., Bai C., Zhao C., Lu G., Xu G. (2008) "LC-MS-based metabonomics analysis". Journal of Chromatography B, 866: 64-76

Ma Y-C., Kim H-Y. (1997) "Determination of Steroids by Liquid Chromatography/Mass Spectrometry". Journal of American Society of Mass Spectrometry, 8: 1010-1020

Makarov A. (2000) "Electrostatic axially harmonic orbital trapping: A high performance technique of mass analysis". Analytical Chemistry, 72: 1156-1162

Makarov A., Denisov E., Kholomeev A., Balschun, Lange O., Strupat K., Horning S. (2006). "Performance evaluation of a hybrid linear ion trap/Orbitrap mass spectrometer". Analytical Chemistry, 78: 2113-2120

Maravelias C., Dona A., Stefanidou M., Spiliopoulou C. (2005) "Adverse effects of anabolic steroids in athletes. A constant threat". Toxicology Letters, 158: 167-175

Meier-Augenstein W. (1999) "Applied gas chromatography coupled to isotope ratio mass spectrometry". Journal of Chromatography A, 842: 351–371

Moco S., Bino R. J., De Vos R. C. H., Vervoort J. (2007) "Metabolomics technologies and metabolite identification". Trends in Analytical Chemistry, 26: 855-865

Niessen W. M. A. (2007) "Liquid Chromatography-Mass Spectrometry". Chromatographic Science Series, 97

Park J., Park S., Lho D., Choo H. P., Chung B., Yoon C., Min H., Choi M. J. (1990) "Drug testong at the 10th Asian Games and the 24th Seoul Olympic Games". Journal of Analytical Toxicology, 14: 66-72

Parr M. K., Schänzer W. (2010) "Detection of misuse of steroids in doping control". Journal of Steroid Biochemistry and Molecular Biology, 121: 528-537

Pong Law K., Pin Lim Y. (2013) "Recent advances in mass spectrometry:data independent analysis and hyper reaction monitoring". Expert Reviews of Proteomics, 10(6): 551-566

Portolés T., Sancho J. V., Hernández F., Newton A., Hancock P. (2010) "Potential of atmospheric pressure chemical ionization source in GC QTOF MS for pesticide residue analysis". Journal of Mass Spectrometry, 45: 926-936

Portolés T., Cherta L., Beltrán J., Hernández F. (2012) "Improved gas chromatography tandem mass spectrometry determination of pesticide residues making use of atmospheric pressure chemical ionization". Journal of Chromatography A, 1260: 183-192

Pozo O. J., Van Eenoo P., Deventer K., Delbeke F. T. (2007) "Development and vadation of a qualitative screening method for the detection of exogenous anabolic steroids in urine by liquid chromatography-tandem mass spectrometry". Analytical Bioanalytical Chemistry, 389: 1209-1224

Pozo O. J., Van Thuyne W., Deventer K., Van Eenoo P., Delbeke F. T. (2008a) "Elucidation of urinary metabolites of fluoxymesterone by liquid chromatography-tandem mass spectrometry and gas chromatography-mass spectrometry" Journal of Mass Spectrometry, 43: 394–408

Pozo O. J., Van Eenoo P., Deventer K., Delbeke F. T. (2008b) "Detection and characterization of anabolic steroids in doping analysis by LC-MS". Trends in Analytical Chemistry, 27: 657-671

Pozo O. J., Marcos J., Ventura R., Fabregat A., Segura J. (2010) "Testosterone metabolism revisited: discovery of new metabolites". Analytical and Bioanalytical Chemistry, 398: 1759-1770

Rahmanian M. S., Thomson D. L., Melrose P. A. (1997) "Immunocytochemical localization of prolactin and growth hormone in the equine pituitary". Journal of Animal Science, 75: 3010-3018

R. Paquete estadístico. Disponible desde; http://www.r-project.org/. Último acceso (17.03.2015)

Regal P., Anizan S., Antignac J-P., Le Bizec B, Cepeda A., Fente C. (2011) "Metabolomic approach based on liquid chromatography coupled to high resolution mass spectrometry to screen for the ilegal use of stradiol and progesterone in cattle". Analytica Chimica Acta, 700: 16-25

Reichel C. (2011) “OMICS-strategies and methods in the fight against doping”. Forensic Science International, 213: 20-34

Rijk J. C. W., Lommen A., Essers M. L., Groot M. J., Van Hende J. M., Doeswijk T. G., Nielen W. F. (2009) “Metabolomic approach to anabolic steroid urine profiling of bovines treated with prohormones”. Analytical Chemistry, 81: 6879-6888

Robinson N., Saugy M., Vernec A., Sottas P-E. (2011) “The Athlete Biological Passport: An Effective Tool in the Fight against Doping”. Clinical Chemistry 57:6, 830-832

Saugy M., Robinson N., Saudan C., Baume N., Avois L., Mangin P. (2006) “Human growth hormone doping in sport”. British Journal of Sports Medicine, 40: i35-i39

Schänzer W. (1996) “Metabolism of anabolic androgenic steroids”. Clinical Chemistry, 42(7): 1001-1020

Scott R. P. W. Principles and Practices of Chromatography. Chrom-Ed Book Series. 2003.

Sjöqvist F., Garle M., Rane A. (2008) “Use of doping agents, particularly anabolic steroids, in sports and society”. The Lancet, 371: 1872-82

Smith C. A., Want J., O'Maille G., Abagyan R., Siuzdak G. (2006) "XCMS: Processing mass spectrometry data for metabolite profiling using nonlinear peak aliment, matching and identification". Analitycal Chemistry, 78: 779-787

Spyridaki M. H., Kiousi P., Vonaparti A., Valavani P., Zonaras V., Zahariou M., Sianos E., Tsoupras G., C. Georgakopoulos C. (2006) "Doping control analysis in human urine by liquid chromatography–electrospray ionization ion trap mass spectrometry for the Olympic Games Athens 2004: Determination of corticosteroids and quantification of ephedrines, salbutamol and morphine". Analytica Chimica Acta, 573–574: 242–249

Tautenhahn R., Christoph B., Neumann S. (2008) "Highly sensitive feature detection for high resolution LC/MS". BMC Bioinformatics, 9: 504

Thevis M., Geyer H., Mareck U., Schänzer W. (2005) "Screening for unknown synthetic steroids in human urine by liquid chromatography-tandem mass spectrometry". Journal of Mass Spectrometry, 40: 955-962

Thevis M., Schänzer W. (2007a) "Current role of LC-MS(/MS) in doping control". Analytical Bioanalytical Chemistry, 388: 1351-1358

Thevis M., Schänzer W. (2007b) "Mass spectrometry in sports drug testing: structure characterization and analytical assays". Mass Spectrometry Reviews, 26: 79-107

Thevis M., Kuuranne T., Geyer H., Schänzer W. (2013) "Annual banned-substance review: analytical approaches in human sports drug testing". Drug Testing and Analysis, 5: 1-19

Thieme D., Anielski P., Grosse J., Sachs H., Mueller R.K. (2003) "Identification of anabolic steroids in serum, urine, sweat and hair. Comparison of metabolic patterns". Analytica Chimica Acta, 483: 299-306

Todd T. (1987) "Anabolic Steroids: The Gremlins of Sport". Journal of Sport History.

Tolstikov V. V., Fiehn O. (2002) "Analysis of highly polar compounds of plan origin: Combination of hydrophilic interaction chromatography and electrospray ion trap mass spectrometry". Analytical Biochemistry, 301: 298-307

Van Renterghem P., Van Eenoo P., Geyer H., Schänzer W., Frans T. Delbeke F. T. (2010) "Reference ranges for urinary concentrations and ratios of endogenous steroids, which can be used as markers for steroid misuse, in a Caucasian population of athletes". Steroids, 75(2): 154–163

Van Renterghem P., Polet M., Brooker L., Van Gansbeke W., Van Eenoo P. (2012) "Development of a GC/C/IRMS method – Confirmation of a novel steroid profiling approach in doping control". Steroids, 77: 1050-1060

WADA. Statistics 2014. Antidoping testing figures sport report. Dsiponible desde: *https://wada-main-prod.s3.amazonaws.com/wada_2014_anti-doping-testing-figures_full-report_en.pdf*. (Último acceso 22.02.2016)

WADA. Minumun Required Performance Levels 2014. Disponible desde: *https://www.wada-ama.org/en/files/wada-td2014mrpl-v1-minimum-required-performance-levels-enpdf* (último acceso 15.12.2014)

WADA. Technical Document TD 2014 EEAS. Disponible desde: *https://wada-main-prod.s3.amazonaws.com/resources/files/wada-td2014eaas-v2-endogenous-anabolic-androgenic-steroids-measurement-and-reporting-en_0.pdf* (último acceso 16.12.2014)

WADA. The 2016 prohibited list. Disponible desde: *https://wada-main-prod.s3.amazonaws.com/resources/files/wada-2016-prohibited-list-en.pdf* (último acceso 22.02.2016)

WADA. The Code. Disponible desde: *https://wada-main-prod.s3.amazonaws.com/resources/files/wada-2015-world-anti-doping-code.pdf* (último acceso 22.02.2016)

XCMS software. Disponible desde *http://www.bioconductor.org/packages/release/bioc/html/xcms.html.* Último acceso (17.03.2015)

Artículos científicos que componen la Tesis Doctoral

Artículo científico 1

Mass spectrometric behavior of anabolic androgenic steroids using gas chromatography coupled to atmospheric pressure chemical ionization source: Part I

M. Raro, T. Portolés, J. V. Sancho, E. Pitarch, F. Hernández, J. Marcos, R. Ventura, C. Gómez, J. Segura, O. J. Pozo

Journal of Mass Spectrometry, ***2014***, 49, 509-521

Artículo científico 2

Mass spectrometric behavior of anabolic androgenic steroids using gas chromatography coupled to atmospheric pressure chemical ionization source: Part II

M. Raro, T. Portolés, J. V. Sancho, E. Pitarch, F. Hernández, J. Marcos, R. Ventura, C. Gómez, J. Segura, O. J. Pozo

Journal of Mass Spectrometry, ***2016*** *(In process)*

Artículo científico 3

Potential of atmospheric pressure chemical ionization source in gas chromatography tandem mass spectrometry for the screening of urinary exogenous androgenic anabolic steroids

M. Raro, T. Portolés, E. Pitarch, J. V. Sancho, F. Hernández, L. Garrostas, J. Marcos, R. Ventura, J. Segura, O. J. Pozo

Analytica Chimica Acta, ***2016***, 906, 128-138

Artículo científico 4

Untargeted metabolomics in doping control: Detection of new markers of testosterone misuse by ultra-high performance liquid chromatography coupled to high resolution mass spectrometry.

M. Raro, M. Ibáñez, R. Gil, A. Fabregat, E. Tudela, K. Deventer, R. Ventura, J. Segura, J. Marcos, A. Kotronoulas, J. Joglar, M. Farré, S. Yang, Y. Xing, P. van Eenoo, E. Pitarch, F. Hernández, J. V. Sancho, O. J. Pozo

Analytical Chemistry, ***2015***, 87, 8373-8380

Artículo científico 5

Evaluation of potential urinary markers for recombinant human growth hormone misuse by untargeted metabolomics

M. Raro, R. Díaz, J. V. Sancho, E. Pitarch, F. Hernández, J. Marcos, J. Segura, J. Bosch, B. G. de la Torre, R. Gutiérrez-Gallego, O. J. Pozo

Metabolomics, ***2016***, *(Submitted)*

Sugerencias para futuros trabajos

A raíz de las conclusiones expuestas previamente, se pone de manifiesto el potencial de diversas técnicas analíticas y metabolómicas en aplicación al campo del control del dopaje. Visto esto, a continuación se detallan posibles líneas de trabajo a realizar en un futuro:

- Llevar a cabo una validación mediante GC-APCI-MS/MS para un mayor número de AAS, ampliando el trabajo presentado en el artículo científico 3 y prestando especial atención en el paso de selección de transiciones específicas y sensibles. Comparar resultados con los obtenidos mediante la fuente EI utilizada tradicionalmente en análisis de rutina. Además, incluir sustancias de otras clases.
- Continuar con estudios *semitarget,* preliminares, llevados a cabo con muestras de 4Cl-MTD donde se trata de detectar metabolitos conocidos o desconocidos mediante modo de trabajo Precursor Ion Scan, gracias a fragmentos comunes de los esteroides (*m/z* 77, 91 y 105).
- Aplicar estrategia Precursor Ion Scan en estudios de excreción de diferentes AAS.
- Dentro de los trabajos de metabolómica presentados en el Capítulo III, elucidar compuestos diferentes a los propuestos y estudiar su idoneidad como marcadores de abuso testosterona y hormona del crecimiento.
- Elucidar por completo la estructura de la octenoil-glicina propuesta como marcador de rhGH, averiguando la posición exacta del doble enlace o si la estructura presenta ramificaciones.

- Estudiar la idoneidad del resto de marcadores propuestos para rhGH y testosterona, para determinar si podrían ser incorporados en la rutina de *screening* de los análisis de control del dopaje.
- Aplicar análisis LC-HRMS y metabolómica en la búsqueda de marcadores del abuso de otros compuestos de interés en el control del dopaje.

Suggestions for future works

From the conclusions previously exposed, the potential of some analytical and metabolomic techniques applied to the doping control field, is demonstrated. Possible future lines of research are detailed below:

- To carry out a validation by GC-APCI-MS/MS for a higher number of AAS, to expand the work presented in scientific paper 3, paying special attention to the selection of specific and sensitive transitions. To compare the results with the ones obtained by EI source, commonly used in routine analysis. Besides, to include other substances from other classes.
- To continue with semitarget preliminary studies carried out with 4Cl-MTD in order to detect known and unknown markers by Precursor Ion Scan working mode, thanks to the common ions *m/z* 77, 91 and 105.
- To apply Precursor Ion Scan strategy to excretion studies of different AAS.
- In the metabolomic works presented in Chapter III, to elucidate different compounds and to study their suitability as markers of testosterone and growth hormone misuse.
- To elucidate octenoyl-glycine structure, proposed as marker of rhGH, to figure out the exact position of the double bond or if the structure contains branches.
- To study the suitability of the other proposed markers for rhGH and testosterone to determine if they could be incorporated into the routine screening of doping control.
- To apply LC-HRMS and metabolomics in the search of markers of the misuse of other compounds of interest in the doping control field.